ISSN 1341-3643

国立環境研究所研究報告書　第151号

Research Report from the National Institute for Environmental Studies, Japan, No. 151, 2000

R－151－2000

Proceedings of the Japan-China Joint Workshop on the Cooperative Study of the Marine Environment

—Environmental Capacity and Effects of Pollutants on Marine Ecosystem in the East China Sea—

18-19 March 1999
Shiba Park Hotel,Tokyo, Japan

Edited by Masataka Watanabe and Mingyuan Zhu
1999
National Institute for Environmental Studies

Proceedings of

Japan - China Joint Workshop

on the Cooperative Study of the Marine Environment

—ENVIRONMENT CAPACITY AND EFFECTS OF POLLUTANTS
ON MARINE ECOSYSTEM IN THE EAST CHINA SEA—

1998, Tokyo, Japan

Origanized by
National Institute for Environmental Studies (NIES), Japan
State Oceanic Administration (SOA), China

Sponsored by:
Environment Agency of Japan

THE JAPAN – CHINA JOINT WORKSHOP ON THE COOPERATIVE STUDY OF THE MARINE ENVIRONMENT

—ENVIRONMENT CAPACITY AND EFFECTS OF POLLUTANTS ON MARINE ECOSYSTEM IN THE EAST CHINA SEA—

March 18 –19, 1998, Tokyo, Japan

Sponsored by:

Environment Agency of Japan

Organized by:

National Institute for Environmental Studies(NIES), Japan
State Oceanic Administration (SOA), China

Organizing Committee:

Japan : Masataka Watanabe
Makoto Watanabe
Shogo Murakami
Hiroshi Koshikawa
Yoshiki Saito
Kazumaro Okamura

China : Shouben Lu
Youfen Lhang
Xiaoli Fan
Mingyuan Zhu
Huaiyang Zhou
Xiulin Wang

Published by:

National Institute for Environmental Studies(NIES), Japan

Proceedings Editor:

Masataka Watanabe (NIES) and Mingyuan Zhu (SOA)

Preface

The Changjiang River is the major source of freshwater, sediments and nutrients that flow into the East China Sea and the northeastern Pacific Ocean, which is one of the most productive oceanic shelves in the world in terms of biodiversity and standing stocks. Human activity in the Changjiang catchment area, including industrialization, agriculture and water-resource development, such as the construction of the Three Gorges Dam, may affect the aquatic, elemental and energy cycles of the catchment area. Ultimately, the supply of freshwater, sediment and nutrients to the East China Sea will be altered and, therefore, the structure and function of the East China Sea ecosystem may be affected.

After extensive discussion between the National Institute for Environmental Studies (NIES) and the State Oceanic Administration (SOA) of China, it was agreed that a collaborative research project on 'Environmental loading from river inputs and their effects on the marine ecosystem in specified areas of the East China Sea' would be established, and the agreement between the two agencies was signed on 18 March 1997. The objective of the project is to provide a scientific basis for management measures to protect the environment and resources of the East China Sea, through research such as on the evaluation of environmental capacity for pollution and the prediction of its effects on the ecosystem of the East China Sea.

Primary production is high in spring and autumn in the East China Sea. A field survey and mesocosm experiments were conducted during 10 to 20 October 1997 and 14 May to 3 June 1998. The Chinese research vessel 'Haijian 49' (1000 gross tons) was used and the following research institutes participated in the cruises: NIES; Geological Survey of Japan; Seikai National Fisheries Research Institute; National Research Institute of Aquaculture; First Institute of Oceanography, SOA; Second Institute of Oceanography, SOA; East Sea Branch, SOA; and the Ocean University of Qingdao.

The field survey area and location of the mesocosm experiment are shown in Fig. 1. The study area is controlled by two water masses, diluted water from the Changjiang River and offshore water of the East China Sea. NOAA AVHRR data during the project's two cruises in 1997 and 1998 indicated that highly turbid water from the Changjiang River was spread along the coast of China(Fig.2); the field survey area was located around the frontal zone of these two water masses. The physical characteristics of the Changjiang estuary have been elucidated through field survey, such as horizontal and vertical distributions of temperature, salinity, nutrients, trace metal and biodiversity.

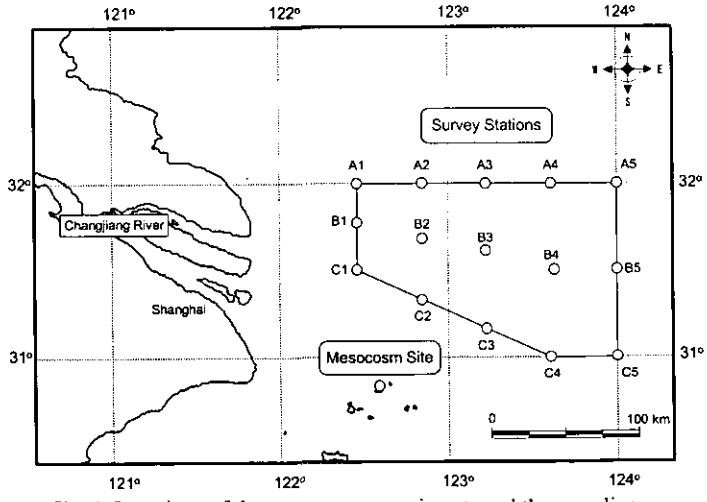

Fig. 1. Locations of the mesocosm experiments and the sampling stations for the field survey.

Mesocosms, which are useful tools for investigating the response of an ecosystem to nutrients and pollution loading, were installed near Liuhuashaw - Huanaoshan; they

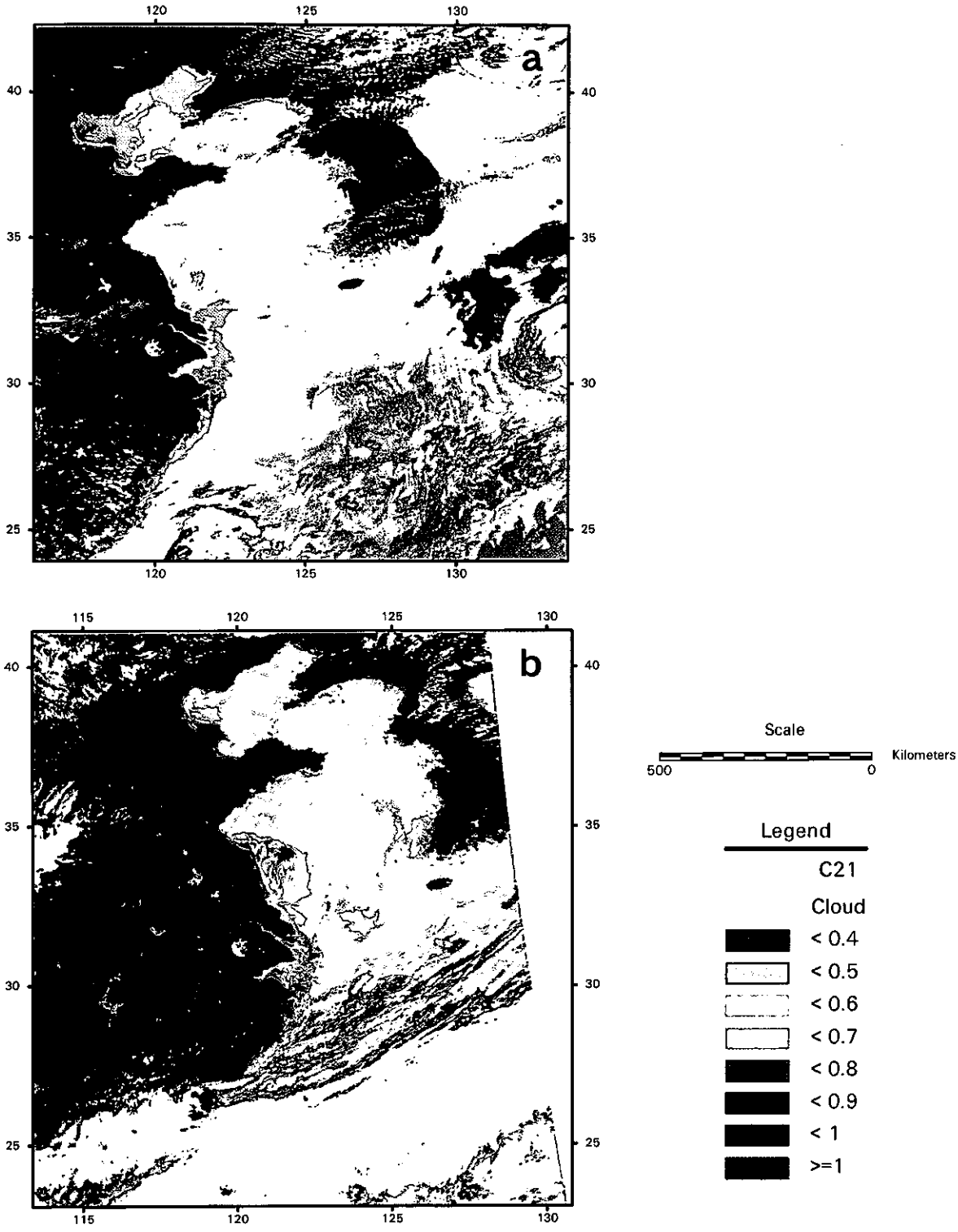

Fig. 2 a) Distribution of turbidity during the cruise in 1997 in the East China Sea
(NOAA AVHRR Data, Oct. 17, 1997)
b) Distribution of turbidity during the cruise in 1998 in the East China Sea
(NOAA AVHRR Data, May. 26, 1998)

were developed by NIES and are made of ethylenevinylacetate reinforced with a polyester grid. They are extremely strong, flexible and translucent, with no elution from the surface, and are 5 m deep and 3 m in diameter, with a volume of about 25 m^3 (Fig. 2). Phosphate, the limiting nutrient, was enriched in these experiments and aspects of the mesocosm ecosystem response were analyzed, including nutrient dynamics, succession of plankton groups, bacterial abundance, and the inorganic and organic carbon cycle through autotrophic and heterotrophic pathways. It is important that the ecosystem model should include both the autotrophic and heterotrophic pathways in order to predict the effects of environmental loading from river input on the marine ecosystem of the East China Sea.

An increase in oil pollution was observed from sediment analysis; thus, oil enrichment in a mesocosm was also conducted during the 1998 research to understand the effect of oil on marine ecosystems.

Sediment traps were installed near the mesocosm experimental site as well as in the field survey area. Sediment core samples were also obtained in order to analyze the long-term change in biogeochemical processes in the Changjiang Estuary.

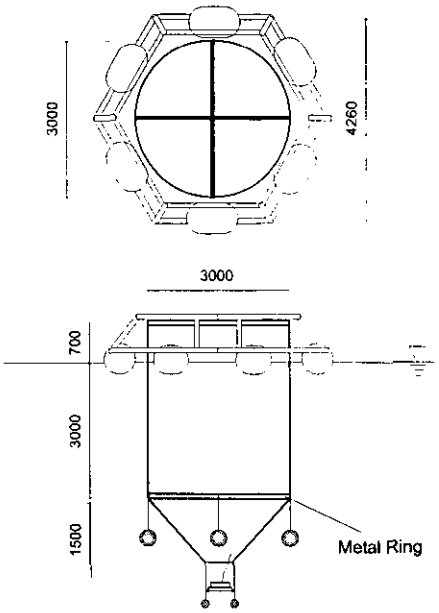

Fig.3. Schematic illustration of the mesocosm

During the cooperative study, the analytical methods and results were intercalibrated between Japanese and Chinese laboratories in order to guarantee accuracy, reliability and comparability of the data. It is very important to emphasize that during the field surveys mutual understanding and close cooperation between the scientists of the two countries were established. During the project, three Chinese scientists stayed for periods of 7 to 12 months in NIES and 10 Chinese scientists visited NIES and the Geological Survey of Japan for scientific research and exchange of views on the research program.

We would like to express our great appreciation to the Environment Agency of Japan and to SOA for their great support to our study; and to all the crew members of the 'Haijian 49' of the East Sea Branch, SOA, who provided efficient working conditions during the field survey and mesocosm experiments. Our special thanks should be given to Mr. Hironori Hamanaka, Director General, Department of Global Environment, Environment Agency of Japan and Mr. Yu Yuancheng, former Director General, Department of International Cooperation, SOA, who showed deep understanding of this joint project and was dedicated to establishing a collaborative study between our two countries. Without his efforts this project would not have come to fruition. Finally, our thanks go to all the scientists, both of Japan and China, for their hard work and friendly cooperation during this joint study. On the whole, the project has been very successful in establishing a solid foundation of scientific achievement and friendship between our two countries.

Masataka WATANABE (National Institute for Environmental Studies)
Mingyuan ZHU (First Institute of Oceanography, SOA)

Table of Contents

General Session

EFFECT OF OIL POLLUTION ON MARINE PELAGIC ECOSYSTEM : A MESOCOSM STUDY

Mingyuan ZHU[1], Shang CHEN[1], Ruixiang LI[1], Xueyuan MU[1], Ruihua LU[1], Baohua LI[1], Xiaoyong SHI[2], Xiuling WANG[2], Zhiling LIU[3] and Jinghui WANG[4]

[1]Division of Marine Biology, First Institute of Oceanography, State Oceanic Administration
(3A Hongdaozhi Road, Qingdao, 266003, China)
[2] School of Chemistry and Chemical engeering, Ocean University of Qingdao
(5 Yushang Road, Qingdao,266003, China)
[3] Second Institute of Oceanography, State Oceanic Administration
(No. 9 Xixihexia Road, Hangzhou, 310012, China)
[4] Environment monitor center, East China Sea Branch, State Oceanic Administration
(Dong Tang road 630, Shanghai, 200137, China)

The mesocosm experiments to exam the impact of water-soluble oil on plankton were conducted near Changjiang River Estuary in May 1998. Dinoflagellate, *Prorocentrum dentatum*, was the dominant species during the experiment. Adding oil did not cause obvious increase of the phytoplankton stock, but the primary productivity, assimilation number of photosynthesis and zooplankton are quite sensitive to oil pollution. To some extent, adding oil benefits the micro-phytoplankton (>20μm), inhibits the growth of nano-phytoplankton (2~20μm) and does not effect significantly to the pico-phytoplankton (<2 μm). During the experiment, bacteria productivity as well as the sinking rate of particulate matter and phytoplankton increased.

Key Words: *Changjiang River Estuary, mesocosm experiment, oil pollution, marine pelagic ecosystem*

1.INTRODUCTION

Oil pollution is becoming a serious threat to marine ecosystem in coastal region and river estuary. It seems more serious near port and oil field. Oil pollution will have acute and long-term effects on the marine ecosystem. Aquaculture industry often suffers heavy economical loss when oil spill happens. Many researches attempt to deal with the problem[1), 2), 3), 4)]. In Changjiang River estuary, the oil pollution becomes the important environmental problem because of the busy ship transportation. To understand the impact of oil pollution on ecosystem and estimate the carrying capacity of oil in Changjiang River Estuary ecosystem, the Chinese and Japanese scientists jointly conducted the mesocosm experiment and field survey during May 1998. So far, only a few researches were focused on the problem of oil pollution in Changjiang River Estuary and East China Sea. The purposes of this paper were (1). Address the comprehensive responses of marine pelagic ecosystem after adding oil, (2). Distinguish the potential difference of behavior of ecosystem in mesocosms with oil pollution and without pollution

2. MATERIALS AND METHODS

(1) Site and time of the experiment

The oil polluted mesocosm experiment was conducted for seven days from 26 May (day 0) to 1 June (day 6) 1998 at the Luhuashan region near the Changjiang River Estuary (Fig.1).

(2) Installing of mesocosms

The mesocosm made of ethylenevinylacetate reinforced with a polyester grid was provided by National Institute for Environmental Studies, Japan (Fig.2). Two mesocosms were used in the experiment, one was

treated with oil, while the other as the control. One mesocosm can fill 25m^3 seawater (3-m diameter and 4.5-m depth). There is a round opening with 30-cm diameter at the bottom of mesocosm. The seawater entered the mesocosm through this opening by putting down the mesocosm slowly into the seawater. When the water surface in mesocosm reached the same water level as the outside, the opening was closed. This installing process does not significantly disturb the vertical structure of water and does not harm the structure of community.

On 26, when finishing installing of mesocosms, the same amount of phosphate was added into the oil mesocosm and control mesocosm, to stimulate the growth of phytoplankton. The phosphate reached about 1.5 μmol·l^{-1}. On 28, 1 ton seawater with saturated water-soluble diesel were added into the oil mesocosm by siphon.

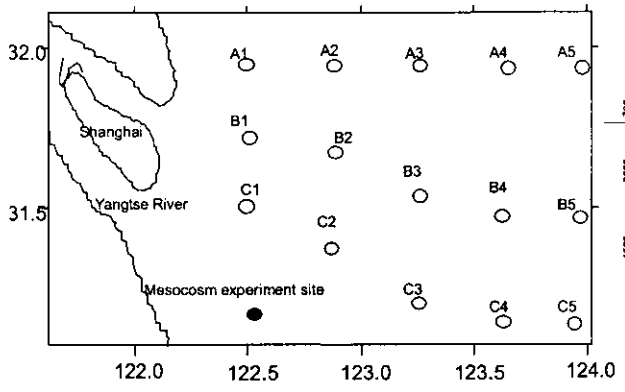

Fig.1 Stations of mesocosm experiments and field survey

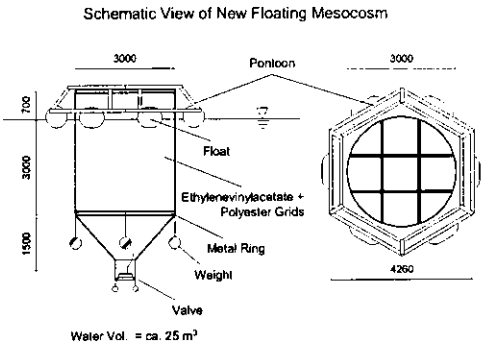

Fig.2 View of mesocosms

(3) Sampling and analysis

The seawater was sampled at 1-m depth in mesocosm during 8:30 to 9:30 every morning. The environmental parameters (temperature, salinity, dissolved oxygen, NO_3, NO_2, NH_4, PO_4, SiO_3, total particulate matter, particulate organic matter, particulate organic carbon, particulate organic nitrogen) and biological parameters (Chl-a, primary production, phytoplankton and zooplankton abundance, bacterial abundance and production) were determined following the method in Specification for Oceanographic Survey.

To measure the sinking fluxes of phytoplankton, TPM, POM, POC and PON, two sediment traps were deployed in mesocosms. The trap is a plastic cylinder with 50-cm height and 10-cm diameter.

3.RESULTS AND DISCUSSIONS

(1) Nutrients and oil

In natural seawater, dissolved inorganic phosphate was about 0.3 μmol/l in May. On second day after adding phosphate, the phosphate in oil mesocosm decreased to 1.02 μmol·l^{-1}, however the phosphate in C-mesocosm decreased to 0.549 μmol·l^{-1} (Table 1). The concentration of phosphate declined to about 0.3 μmol·l^{-1} during the later period of the experiment. Dissolved inorganic nitrogen (DIN) decreased obviously, from the initial 14.6 μmol·l^{-1} to 0.59 μmol·l^{-1}. As NO_3 was the main form of DIN, it decreased from 12.9 to 0.1 μmol·l^{-1}, while NO_2 and NH_4 did not show obvious change. The dissolved silicate did not decrease because the dominant species of phytoplankton did not uptake silicate.

The oil concentration averaged 35-63ppb in the natural seawater. After adding the oil, the oil reached 1847.60ppb in oil mesocosm, then it declined slowly and was 1287.7ppb on 1 June (Fig.3, Table1). The decrease of oil may result mainly from the bacterial decomposition. In control mesocosm, the oil had no obvious change.

(2)Plankton

a) Chl-a

The initial concentration of Chl-a was 7.953 $\mu g \cdot l^{-1}$ in oil mesocosm and 14.381 $\mu g \cdot l^{-1}$ in the control

Table1 Variation of nutrients in oil mesocosm and control mesocosm

	DIP		DIN		NO2		NO3		NH4		Si		Oil	
Date	C-meso	Oil-meso	C-meso	Oil-meso	C-meso	Oil-meso	C-meso	Oil-meso	C-meso	Oil-meso	C-meso	O-meso	C-meso	O-meso
5.26	0.337	0.376	10.189	14.603	0.760	0.775	8.350	12.946	1.160	0.882	22.414	22.205		
5.27	0.549	1.015	10.202	8.394	0.679	0.666	7.864	7.148	1.578	0.580	19.586	19.744	63.09	35.19
5.28	0.337	0.490	1.561	6.578	0.595	0.607	0.175	5.299	0.974	0.673	18.853	16.130	54.21	1870.60
5.29	0.347	0.347	2.537	5.280	0.411	0.651	0.365	2.611	1.578	2.018	17.701	16.130	52.76	1561.89
5.30	0.297	0.282	1.027	1.437	0.461	0.461	0.100	0.100	0.835	1.021	16.444	15.921	64.44	1404.80
5.31	0.337	0.337	0.957	0.726	0.526	0.532	0.100	0.100	0.766	0.534	18.382	16.968	100.50	1308.43
6.1	0.332	0.332	2.580	0.590	0.607	0.511	0.100	0.100	2.366	0.441	19.115	18.644	80.01	1287.70

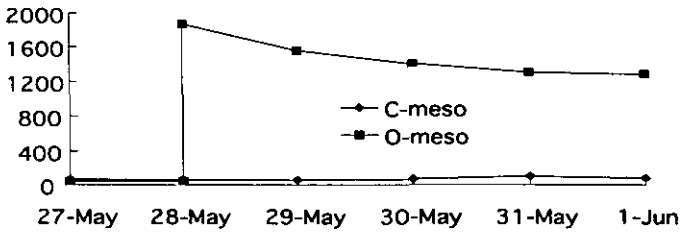

Fig.3 Variation of Oil(ppb) in mesocosms

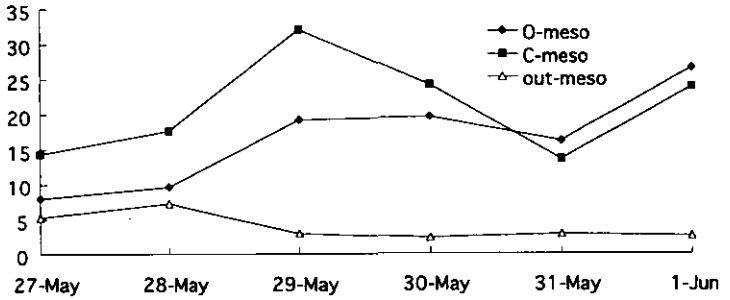

Fig.4 Chla(ug/l) in O-meso, C-meso and natural seawater

mesocosm. Chl-a in C-mesocosm increased then declined, and it increased in Oil-mesocosm (Fig.4). This showed oil pollution delayed the increase of Chl-a in a short time. The Chl-a in natural seawater varied from 2.3 to 7.3 $\mu g.l^{-1}$.

Fig.5 and Fig.6 showed that the smaller-than-20-μm phytoplankton make the main contribution to total Chl-a of phytoplankton in May, because the small-sized dinoflagellete was the dominant species. But the adding oil may inhibit the growth of nano-phytoplankton, rather than micro-phytoplankton. In Oil mesocosm, the proportion of >20 μm group increased from 6% on 27 May to 17% on 1 June, while the 2-20 μm group decreased from 47% to 38% and the GF/F-2 μm group had not obvious change (Fig.7). In Control mesocosm, there was no obvious variation for different size-fraction Chla (Fig.5).

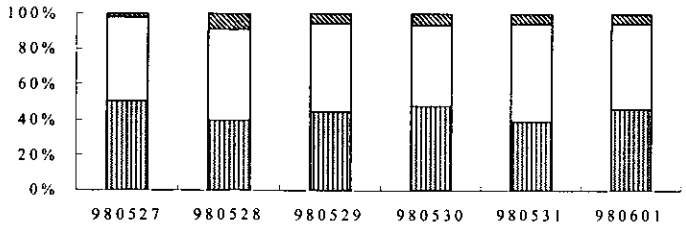

Fig.5 Change of size fraction of Chla in Control meso

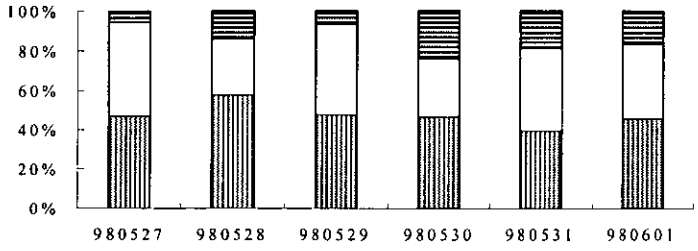

Fig.6 Change of size fraction of Chla in Oil-mesocosm

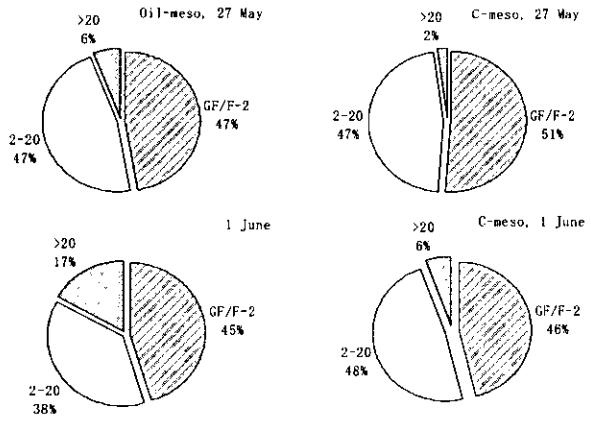

Fig.7 Variation of the different size-fraction Chl-a in oil mesocosm and control

b) Primary production and assimilation number

Adding oil may impact the photosynthesis process and decreased the primary production of phytoplankton. On 28 May, the primary productivity at 100% relative light intensity was 57.96 $mgC.m^{-3}.h^{-1}$ in oil mesocosm and 52.18 $mgC.m^{-3}.h^{-1}$ in control, but it became 44.65 $mgC.m^{3}.h^{-1}$and 94.63 $mgC.m^{3}.h^{-1}$ respectively on 29 May. Compared to the increase of primary productivity in control, the primary production at surface layer in oil mesocosm was impaired severely. However the primary production at low light level was not impaired severely by oil pollution, and still kept increasing for one day after adding oil (Table 2).

The assimilation number of photosynthesis indicates the effect of oil on primary production better than primary productivity. After adding oil, assimilation number at the 100% and 50% light intensities decreased from 28 May to 29 May. At the same time in control mesocosm, the assimilation number at 100% and 50% light intensities increased (Table 3). From 28 to 29, the assimilation number at 100% light intensity decreased 62%, that at 50% light intensity decreased 31% and that at 30% light intensity decreased 28%. At different light level, the effect of oil on assimilation number is different.

Table2. Primary productivity ($mgC.m^3.h^{-1}$) at the different light intensities in oil mesocosm and control mesocosm

	100%		50%		30%	
Date	O-meso	C-meso	O-meso	C-meso	O-meso	C-meso
980526	34.04	46.29				
980527	36.05	61.02	45.70	71.37	30.68	59.52
980528	57.96	52.18	30.60	48.93	22.20	37.15
980529	44.65	94.63	42.36	88.60	31.82	47.87
980530	18.17	64.20	51.67	63.58	51.53	63.53
980531	17.71	35.33	31.93	35.79	31.65	29.04
980601	44.46	31.59	18.24	22.22	4.82	11.93

c) Phytoplankton species composition

In May, the dinoflagellate was the dominant species rather than diatom. In control mesocosm, cell number of dinoflagellate was much higher than that of diatom. In oil mesocosm, however, diatom grew faster than dinoflagellate and cell number of diatom exceeded that of dinoflagellate on 30 May(Fig.8). The *Prorocentrum dentatum* was the dominant species in dinoflagellete while *Skeletonema costatum* was the dominant species in diatom. The dinoflagellate was more sensitive to oil pollution than diatom (Fig.9 & Fig.10).

Table 3. The assimilation number of photosynthesis ($mgC.mgchl\text{-}a^{-1}.h^{-1}$) at the different light intensities in oil mesocosm and control

	100%		50%		30%	
Date	O-meso	C-meso	O-meso	C-meso	O-meso	C-meso
980526	4.75	4.3				
980527	4.50	4.24	5.75	4.96	3.86	4.14
980528	6.06	2.65	3.20	2.49	2.32	1.89
980529	2.32	2.96	2.20	2.77	1.66	1.49
980530	0.86	2.66	2.46	2.63	2.45	2.63
980531	0.96	2.60	1.80	2.63	1.78	2.13
980601	1.67	1.33	0.69	0.93	0.18	0.50

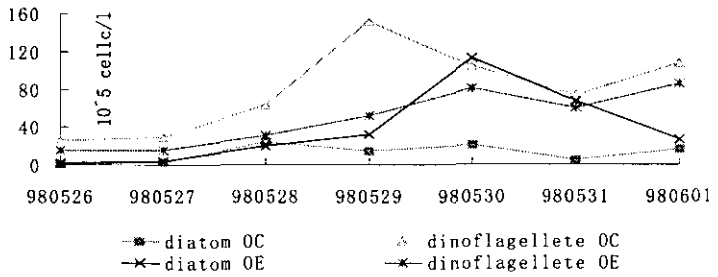

Fig.8 Variation of dominant species in oil-mesocosm and control. (OC: control mesocosm, OE: oil mesocosm)

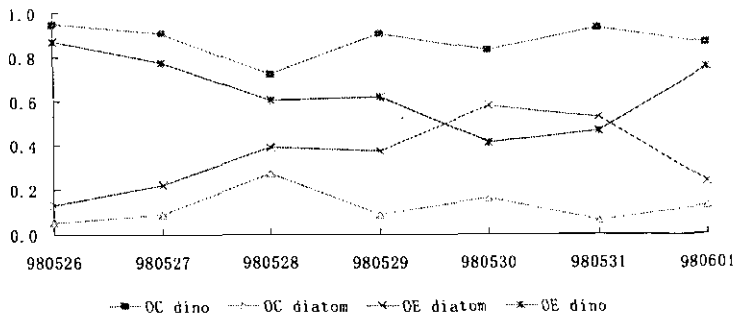

Fig.9 Proportion of dominant group in oil-mesocosm and control. (OC: in control mesocosm, OE: in oil mesocosm, dino: dinoflagellate)

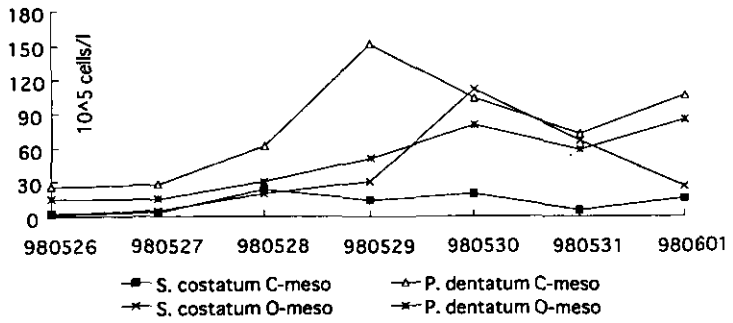

Fig.10 Variation of dominant species in oil-mesocosm and control

d) Zooplankton

Noctiluca scintillans was the dominant species in both oil mesocosm and in control (Fig.10), it declined sharply on the second day after adding oil. The density of zooplankton decreased after adding oil,which was different from phytoplankton (Fig.11) and the species number of zooplankton also declined (Fig.12). This showed that the zooplankton was more sensitive to oil pollution than phytoplankton. In both mesocosm, the density and species number of zooplankton bigger than the 100 μm increased while that from 20 to 100 μm decreased(Fig.13).

e) Bacterial number and productivity

After adding oil, both the bacterial number and productivity increased (Fig.14). Oil may stimulate the growth of heterotrophic bacteria.

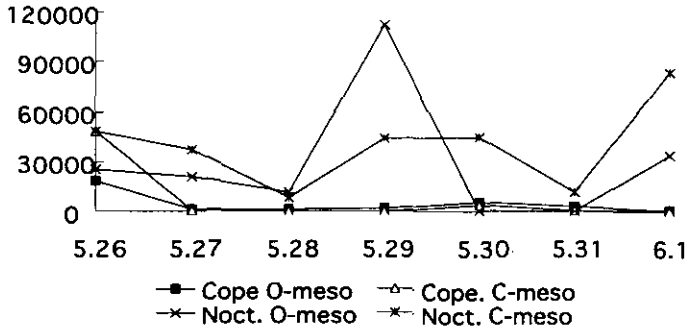

Fig.11 Dominant species of zooplankton in control and oil mesocosm
(unit: ind.m $^{-3}$, Cope: *Copepodite nauplius*, Noct. *Noctiluca scintillans*)

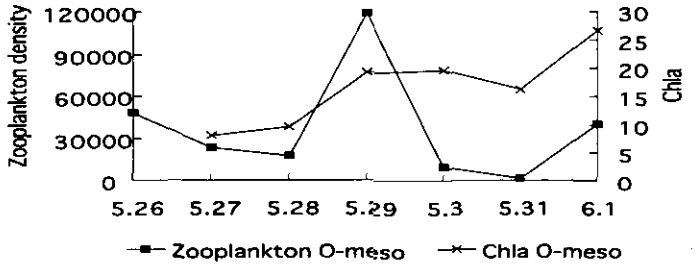

Fig.12 Zooplankton density (ind.l^{-1}) and phytoplankton biomass (mg Chla.l^{-1}) in oil enriched mesocosm

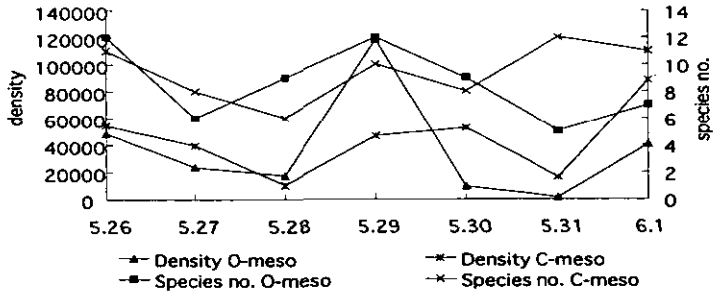

Fig.13 Species number and density of zooplankton in oil mesocosm and control

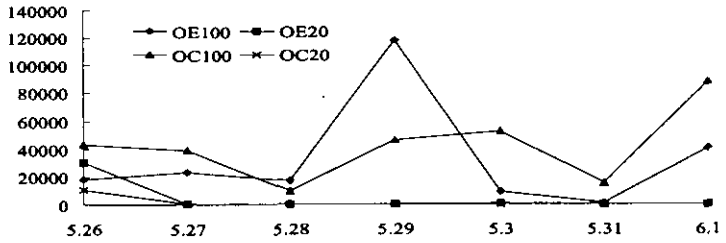

Fig.14 Zooplankton at the different size fraction in oil mesocosm and control. (Unit:ind.l^{-1}, OE100 and OE20: >100μm, 20-100μm in oil mesocosm, OC100 and OC20: >100μm, 20-100μm in control)

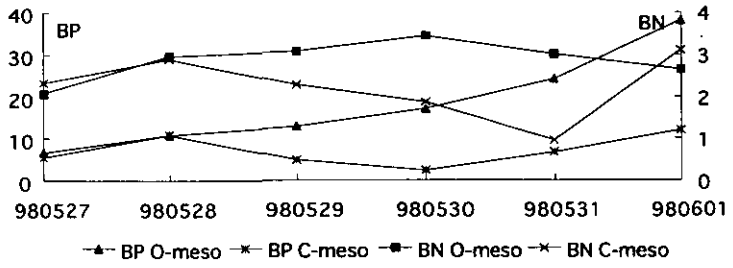

Fig.15 Bacterial density(10^5cells/l and productivity(μ gC/l/h) in oil mesocosm and control. BP: Bacterial productivity, BN: Bacterial density

(3) Suspended particulate matter

Particulate organic matter (POM) increased from 5.73mg/l to 10.47mg/l, TPM(total particulate matter) also increased, and the proportion of POM to TPM increased from 26% in the beginning period to 38% at the end (Fig.15). The same variation happened in the control mesocosm. The TPM and POM were more in control than oil mesocosm. Particulate organic carbon (POC) also was more in control than that in oil mesocosm (Fig.16). POC increased from 1000.5 μ g/l to 4028.0 μ g/l in oil mesocosm, while from 1497 μ g/l to 4587 μ g/l in control. Particulate organic nitrogen (PON) in oil mesocosm increased from 149.0 μ g/l to 375.5 μ g/l (Fig.17). The variation of TPM, POM, POC and PON showed the increase of phytoplankton in mesocosm.

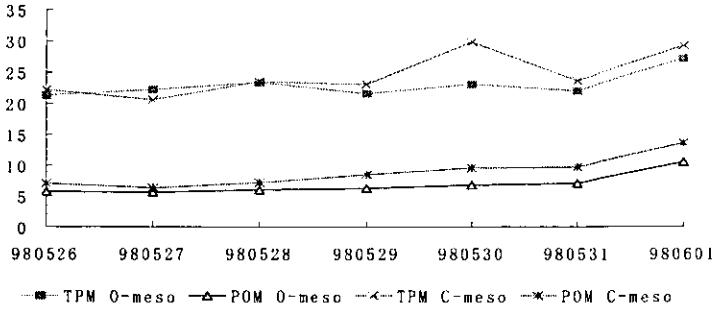

Fig.16 TPM and POM in oil mesocosm and control

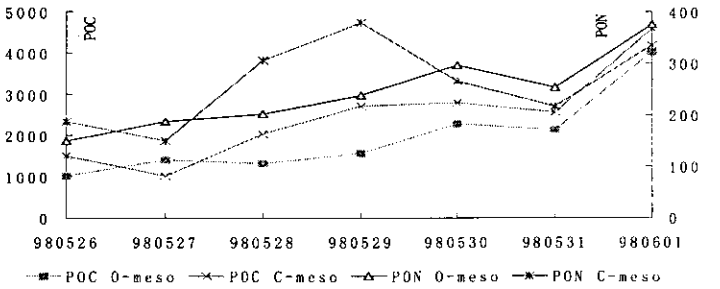

Fig.17 POC and PON in oil mesocosm and control

(4) Sinking fluxes of phytoplankton and suspended particulate matter

In both oil mesocosm and control mesocosm, the sinking flux of phytoplankton increased (Fig.18). In Oil mesocosm, the sinking fluxes was higher than that in control, and it increased from 6.56 gChla.m^{-2}.d^{-1} to 137.23 gChla.m^{-2}.d^{-1}. The average sinking fluxes of phytoplankton is 44.58 gChla.m^{-2}.d^{-1} in oil mesocosm and 35.70 gChla.m^{-2}.d^{-1} in control (Table 4).

The sinking fluxes of POM and TPM increased in both mesocosms; both TPM and POM sunk more in control than in oil mesocosm. The sinking flux of POM in oil mesocosm increased from the initial value of 8.48 g. m^{-2}. d^{-1} to 38.58 g. m^{-2}. d^{-1},and from 5.48 g. m^{-2}. d^{-1} to 68.37 g. m^{-2}. d^{-1} in control mesocosm (Fig.19). The average sinking fluxes of TPM, POM, POC and PON were higher in oil mesocosm than those in control (Table 4).

Table 4. Average sinking fluxes of suspended particulate matter (g.m^2.d^-1) and phytoplankton (g Chla/m^2/d) in oil mesocosm and control

	TPM	POM	POC	PON	phytoplankton
O-meso	64.30	9.29	2.65	0.35	44.58
C-meso	75.28	28.60	8.26	0.75	35. 70

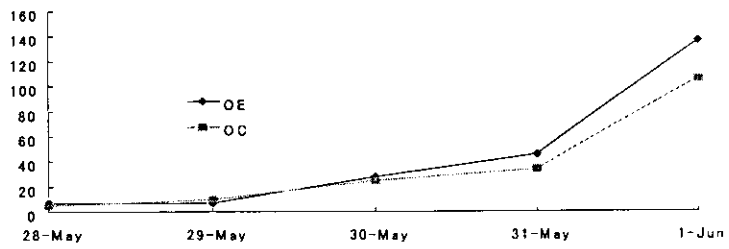

Fig.18 Sinking fluxes(gChla/m^2/d) of phytoplankton in oil enriched experiment

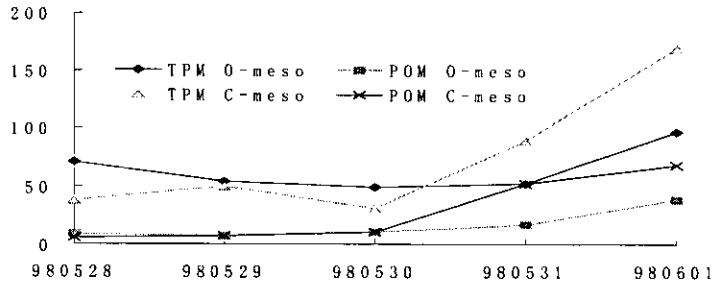

Fig.19 Sinking flux (g. m^{-2}. d^{-1}) of POM and TPM in oil mesocosm and control

5.CONCLUSIONS

(1) The primary productivity, assimilation number of photosynthesis and zooplankton are sensitive to oil pollution.

(2) To some extent, oil pollution increased the percentage of micro-phytoplankton (>20μm), while that of nano-phytoplankton (2-20μm) decreased and that of pico-phytoplankton had no change (GF/F-2 μm).

(3) In oil mesocosm, the sinking fluxes of POC and PON and phytoplankton averaged 2.65 $g.m^{-2}.d^{-1}$, 0.35 $g.m^{-2}.d^{-1}$ and 44.58 g Chla $.m^{-2}.d^{-1}$ respectively. The variation of POC, PON, POM and TPM in mesocosm was mainly attributed to the change of phytoplankton.

ACKNOWLEDGEMENT: Thanks to Drs. J. K. Xu and H. Koshikawa for their friendly help. We also thank to Mrs. Fan Xiaoli, Mr. Zhang Youfeng and Dr. Watanabe for their contribution to the mesocosm experiments and field survey. The research project was also funded by Natural Science Foundation of China (No. 49876030).

REFERENCES

1) Cai, Zhiping, Wu, Jingping: The bacterial degradation to oil and chemical dispersant in marine mesocosm experiments, *Acta Oceanologiga Sinica,* 14(5): 107-777, 1992
2) Lee, R. F., Takahashi, M, and Beers, J.: Short term effect of oil on plankton in controlled ecosystem, *Proceeding of the Conference on Assessment of Ecological Impacts of Oil Spills,* American Institute of Biological Sciences, Arlington, VA, 634-650,1978.
3) Parsons, T. R., Harrison, P. J. et. al.: An experimental marine ecosystem response to crude oil and corexit 9572- part2. Biological effects, Marine Environmental Research, 6:265-275,1984
4) Roy, S, Siron, R and Pelletier, E.: Comparison of radiocarbon uptake and DCMU-fluorescence techniques in evaluating dispersed oil effects on phytoplankton photosynthetic activity, *Water Research,* 25(10): 1249-1254, 1991
5) Shen, Liangfu, Huang, B., and Zhu, Ling: mesocosm experiments to study the effect of Bohai crude oil on the phytoplankton community in Yellow Sea and Bohai Sea, *Acta Oceanologiga Sinica,* 8(6): 729-735, 1986.
6) Siron, R, Pelletier, E and Roy, S: Effects of dispersed and absorbed crude oil on microalgal bacterial community of cold seawater, *Ecotoxicology,* 5(4): 229-251, 1996
7) Siron, R, Pelletier, E.: Oil biodegradation in cold seawater-A mesocosm study, *Proceedings of the twentieth annual toxicity workshop,* pp.117-136,1994.
8) Stewart, P.S., Tedaldi, D. J., Lewis, A. R., Goldman, E.: Biodegradation rates of crude oil in seawater, *Water Environmental Research,* 65(7): 845-848, 1993.
9) Zhuang, Dongfa, Wu, Jingshang, Lin, Yi, and Cai, Zhiping: The fate of crude oil dispersed by dispersant of corexit 9572 in marine mesocosm ecosystem, *Acta Oceanologiga Sinica.* 19(1): 43-49, 1997
10) Zhou, Zhongcheng, Ni, Chunzhi, Cai, Zhiping and Zhen, Huoshui: Mesocosm experiments on oil pollution in marine ecosystem: 1. Ecological distribution of decomposing bacteria, *Acta Oceanologiga Sinica,* 11(3): 341-348, 1989.

RESPONSE OF PHYTOPLANKTON TO PHOSPHATE ENRICHMENT IN MESOCOSM EXPERIMENTS

Ruixiang LI[1], Mingyuan ZHU[1], Shang CHEN[1], Xueyuan MU[1], Ruihua LU[1] and Baohua LI[1]

([1]Division of Marine Biology, First Institute of Oceanography, SOA,
3A Hongdaozhi Road, Qingdao, 266003, China)

The mesocosm experiments were conducted near Yangtse River Estuary during October 1997 and May 1998. In October, After adding phosphate, the DIP reached 3.25 μmol/l in phosphate enriched mesocosm and the atomic ratio of N to P reached 5.6. The diatom increased quickly to the peak at the fifth day and *Skeletonema costatum* was the dominant species during the experiment. In May, after adding phosphate, the DIP increased to 1.72 μmol/l and the ratio of N to P became 9.2. *Prorocentrum dentatum* kept dominant during experiment but *S. costatum* increased quicklier and also become dominant species in the later of experiment.

Keywords: *mesocosm experiment, phosphate eutrophication, phytoplankton bloom, Yangtse River Estuary*

1.INTRODUCTION

Eutrophication refers to the enrichment of the nutrients (usually dissolved inorganic nitrogen, phosphate and silicate) in the ecosystem and the changes of the ecosystem thereby. Serious eutrophication in the coastal waters was due to the rapid development of coastal industries and aquaculture. Eutrophication has led to elevation of phytoplankton biomass and primary productivity directly, thereafter affects species composition of the zooplankton, and changes the benthic communities. Research conducted in Long Island, USA showed that eutrophication may change the energy flow through planktonic food web, especially increase the energy flux in the microbial loop and decrease the food supplement for fish[1]. In China, Zou (1983)[2] and Lin (1997)[3] studied the relationship between eutrophication and red tide and proposed some chemical and biological indicators to assess the eutrophication.

An effective method to study the response of marine ecosystem on eutrophication is the enclosure experiment. Compared with lab experiment, the conditions in the mesocosm are quite similar to the nature environment, and there is no water exchange between the inside and outside of the mesocosm. Hence the ecological processes in the mesocosm ecosystem are simplified, become easy to be measured (Takahashi 1990)[4].

In 1961, Strickland and Torhune first studied the biological and chemical changes during phytoplankton blooms by a 6-m-diameter mesocosm in Canada. From then on, many mesocosm experiments were carried out. In the 1970's, NSF of USA funded a 6-year project "Controlled Ecosystem Pollution Experiment (CEPEX)" and obtained a lot of data on the impacts of various pollutants on the planktonic ecosystem. During 1983-1987, China and Canada jointly conducted a project on the marine enclosed ecosystem experiment (MEEE) in Xiamen coastal water (Wong and Harrison, 1992)[5]. In the paper, we will present the results from mesocosm experiments conducted in the area off Yangtse River Estuary.

2.MATERIALS AND METHODS

(1) Mesocosm device

The devices of mesocosm was provided by National Institute for Environmental Studies, Japan. The mesocosm bag was made of the ethylenevinylacetate and polyester grid (Fig.1).

(2) Site and time of the experiment

The experiments were carried out near the Huaniaoshan region off the Yangtse River Estuary from 10 to 17 October 1997 and 18 to 26 May 1998(Fig.2).

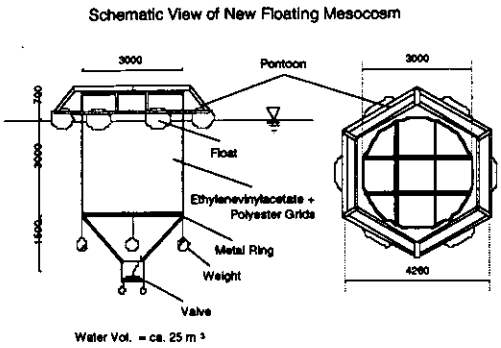

Fig.1 View of mesocosms

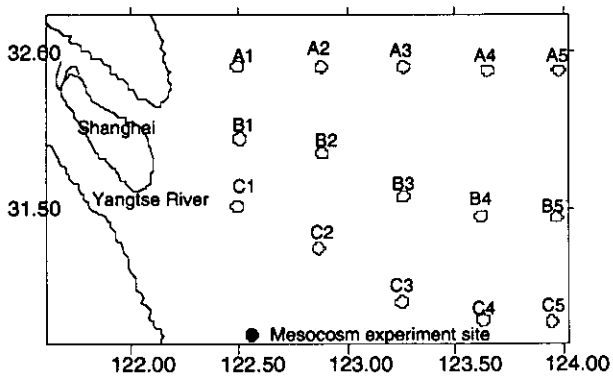

Fig.2 Stations of mesocosm experiments and field survey

(3) Sampling and analysis

The two mesocosms was set up every time, one for adding phosphate another one for control. According to the initial concentration of dissolved inorganic nitrate and phosphate. The 3 μmol/l phosphate was planned to add into the P-mesocosm in October, and 2 μmol/l phosphate in May. For simpility, The phosphate enriched mesocosm was called P-mesocosm, while the control mesocosm was called C-mesocsom. From the second day on, seawater sample was collected at near 9:00 every morning at one-meter depth. The concentration of nutrients were determined according the methods in " Specification for Oceanographic Survey of China" and chlorophyll a was measured by Turner Design fluorometer. The phytoplankton sample was fixed with 5% formalin in October and Lug's iodic solution in May about 48 hours. The sample was identified and counted by an inverted microscope at laboratory. Primary productivity was measured by ^{14}C method.

3.RESULTS AND DISCUSSIONS

(1) The physical and chemical environment in mesocosms

The seawater temperature and salinity were different between the two experiments. In October 1997, the temperature ranged from 22.67~23.3°C. The average temperature was 3.6 °C higher in October than May 1998. The range of salinity in October was 24.9~26.5‰. Its average value was 2.78 ‰ lower than May. There was no significant difference between the water temperature in the mesocosms and natural seawater. The salinity in the mesocosm changed a little during the experiment, Because there was no water exchange.

The nutrient changed greatly during the experiment. In October, the dissolved inorganic nitrogen, phosphate and silicate in seawater outside of the mesocosm were 23.9, 0.75 and 20.5 $\mu mol \cdot l^{-1}$ respectively, which indicated the obvious eutrophication in Yangtse River Estuary. The DIN in natural seawater was quite high during whole experiment, and more than above 10 $\mu mol \cdot l^{-1}$ (Fig.3). The dissolved inorganic silicate varied in 15.5~30.7 $\mu mol \cdot l^{-1}$ and DIP was 0.23-0.78 $\mu mol \cdot l^{-1}$. The N/P ratio was 46.6. When DIP fell to

minimum on 13 October, phosphate, other than nitrogen, might be the limiting element for phytoplankton growth in seawater.

From Fig.4, we can see that the initial concentration of DIN was 18.15 μmol·l^{-1} in mesocosm, the concentration of phosphate amounted to 3.25 μmol·l^{-1} after adding phosphate, and the N/P ratio became 5.58. Because of the fast uptake of phytoplankton, the concentration of DIN and DIP and Si decreased quickly. The phytoplankton reached the peak when the nutrients decreased to the minimum level.

The nutrients content in May 1998 were lower than October. In C-mesocosm (Fig.5), the nitrogen decreased slightly. While the silicate first dropped down then showed slight increase at the later period of the experiment, which may be attributed to the decomposition of dead diatom. The phosphate concentration was lower, ranged between 0.307~0.406 μmol·l^{-1}, and the N/P ratio decreased from 49.8 at the beginning to 21.1 at the end of the experiment. In P-mesocosm (Fig.6), the DIP was 1.723 μmol·l^{-1} after adding phosphate and N/P ratio became 9.2. This led to the fast growth of phytoplankton and the depletion of nutrients. Nitrogen decreased from 16 to 2 μmol·l^{-1} and phosphate declined to its initial value before adding phosphate. However, silicate fell down slowly from 20.48 μmol·l^{-1} to 15.083 μmol·l^{-1}, which was similar to that in C-mesocosm.

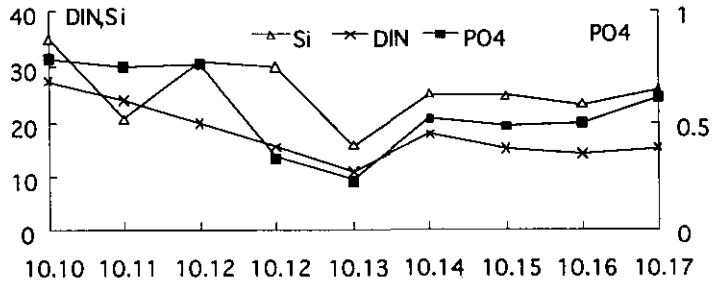

Fig. 3 Nutrients in natural seawater(unit: μmol/l)

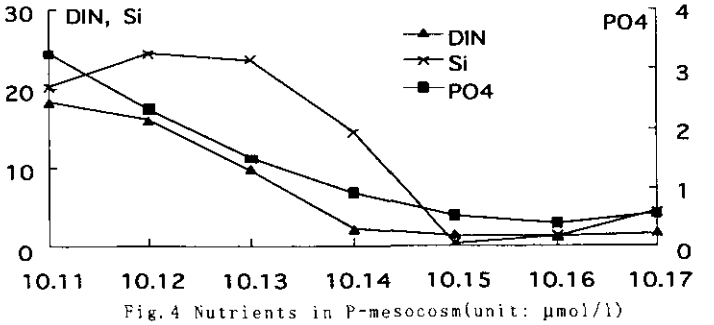

Fig. 4 Nutrients in P-mesocosm(unit: μmol/l)

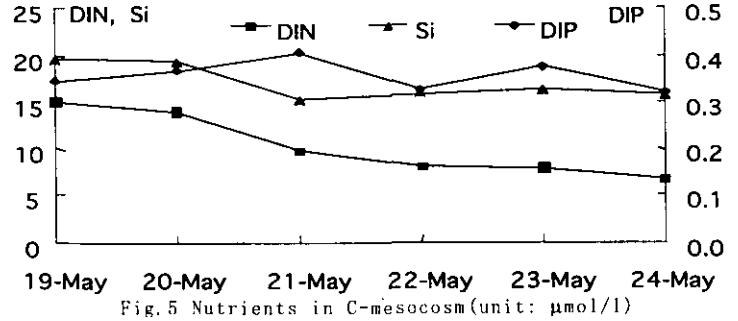

Fig. 5 Nutrients in C-mesocosm(unit: μmol/l)

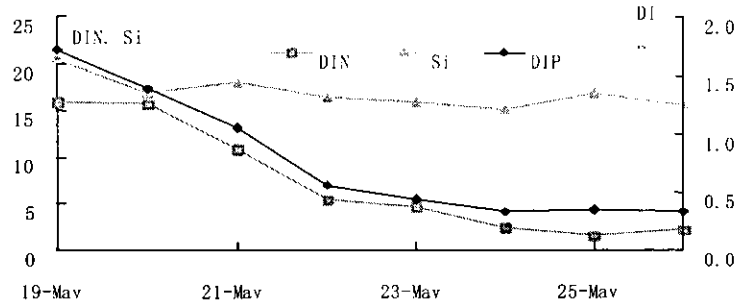

Fig. 6 Nutrinets in P-mesocosm (unit: umol/l)

(2) Density of the phytoplankton, chlorophyll a and primary productivity

The phytoplankton was abundant in seawater near Huaniaoshan Island in October 1997. The initial density on 10 October was 1.72×10^6 cells·l^{-1}. Golden-brown water mass was seen once, indicating there were algal bloom in natural seawater. The phytoplankton reached the peak at 13 Oct, when N, P, and Si declined to the minimum values (Fig. 7). From 16 to 17 October, although the nutrients in seawater increased, the cell number of phytoplankton was still low. In P-mesocosm, the initial density of phytoplankton was 2.54×10^6 cells·l^{-1}. It increased fast after adding phosphate and reached the highest value of 2.93×10^7 cells·l^{-1} on the 5th day, which was 11.5 times of the initial density. The change of Chla was linearly correlative to the cell number of phytoplankton, the correlative coefficient was 0.979 (Fig. 8). Chla reached 74.89 μg·l^{-1} on the 5th day, was 5 times more than its initial value. The primary productivity reached its peak on the 4th day, then decreased one day earlier than the cell number and Chla. When phytoplankton reached its peak, P, N, and Si fell to 0.53, 1.46, and 0.53 μmol·l^{-1} respectively. On the 6th day, the cell number of phytoplankton decreased suddenly and water became clear, the algal bloom disappeared. Nitrogen and silicate may play important role in disappearance of this bloom in mesocosm.

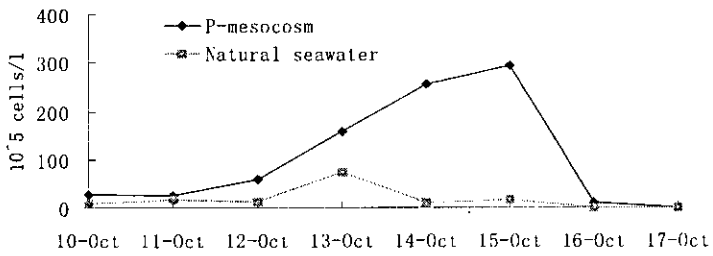

Fig. 7 phytoplankton in P-mesocosm and natural seawater in October

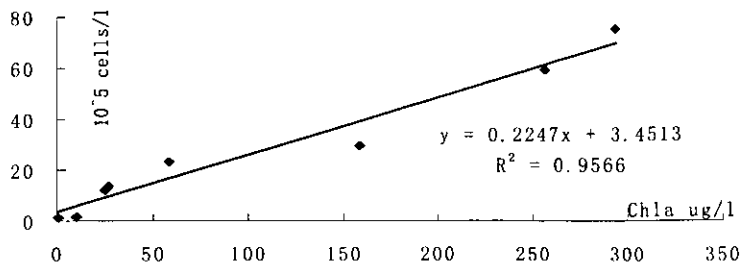

Fig. 8 Corelationship between the phytoplankton density and Chla in P-mesocosm in October

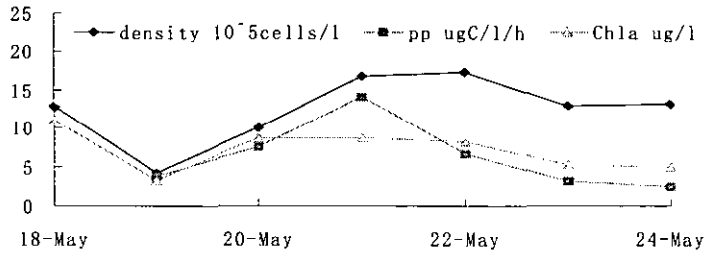

Fig. 9 phytoplankton density, Chla and primary productivity in control mesocosm in May

In May of 1998, the density of phytoplankton was less than that in October 1997. In control, phytoplankton grew slowly, and reached the peak on the 4th day with the value of 1.73×10^6 cells·l^{-1}(Fig.9), which was only 4 times than its initial density. The peaks of primary productivity and Chla came one day earlier than that of cell number, and their peak values were 3.7 and 2.7 times of the their initial values respectively. Nitrogen and silicate decreased during the growth of phytoplankton. However, when phytoplankton reached the peak, nitrogen and silicate were still high. They may not be the limiting factor for phytoplankton. The phosphate may be the limiting factor for phytoplankton. In P-mesocosm, the growth period of phytoplankton was longer than October experiment (Fig.10). The cell number was 72.3 times more than the initial density, while Chla was

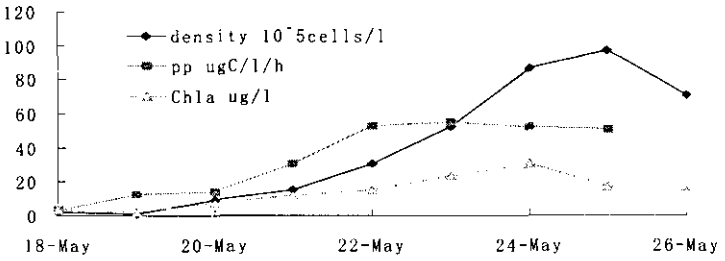

Fig. 10 Change of phytoplankton density, Chla and primary productivity in P-mesocosm in May

decreasing range of silicate was small and its lowest value was still more than 15 μmol·l^{-1}. From the change of nutrients, the two experiment results showed that phosphate enrichment quickened the reproduction of phytoplankton and its uptake to nitrogen. Nitrogen took an important role in ending bloom.

(3) The alternation of dominant species of phytoplankton

The dominant species was *Skeletonema costatum* in October. The bloom dominated by this species often breaks out in the Yangtse River Estuary and coastal areas near Zhejiang province[6]. The density of *Skeletonema costatum* in mesocosm and natural seawater were 2.38×10^6 cells.l^{-1} and 7.29×10^5 cells.l^{-1} at the beginning of experiment, and accounted for 88.2% and 84.5% of phytoplankton respectively. After adding phosphate, this diatom increased quickly and reached 2.93×10^7 cells.l^{-1} on 5th day and accounted for 99.9% of the phytoplankton. Then its cell number decreased sharply and down to 1.5×10^4 cells.l^{-1} on 7th day, and its proportion in phytoplankton was less than 20%. The second dominant species was *Thalassiosra* spp., its density sometimes exceeded to 4×10^5 cells.l^{-1}. It accounted for about 10% of the total in natural seawater. But in phosphate enriched mesocosm, its initial density was 1.93×10^5 cells.l^{-1} and also decreased during experiment. This species disappeared almost after 6th day (Fig.11). However, *Peridinium* sp. and *Alexandrum* sp. of dinoflagellete increased rapidly to become the dominant in the later of experiment.

Prorocentrum dentatum and *Skeletonema costatum* were dominant species in May of 1998. The initial densities of *Prorocentrum dentatum* were 3.78×10^5 cells.l^{-1} and 1.92×10^5 cells.l^{-1} in control and phosphate

enriched mesocosm respectively, and accounted for 88% and 86% of the total respectively. In control mesocosm, this species reached the peak on 4th day and was 4.5 times of initial density and accounted for 99% of the total. After 4th day this dinoflagellete declined slightly. The peak of *Skeletonema costatum* appeared one day earlier than that of *Prorocentrun dentatum*. Its peak value was 2 times more than its initial density (Fig.12). It can be seen that the phosphate-scarce condition obviously limits the growth of *Skeletonema costatum*. In mesocosm added phosphate, *Skeletonema costatum* increased and became the first dominant species (accounted for 56.9% of the total) and was 149 times of its initial density when phytoplankton reached the peak. *Prorocentrun dentatum* accounted for 40.5% of the total and increased 45 times than its initial density. The decreasing rate of *Skeletonema costatum* was bigger than *Prorocentrun dentatum* after the peak of phytoplankton (Fig.13). The cell number of other species was always low due to the suppressing from the two dominant species

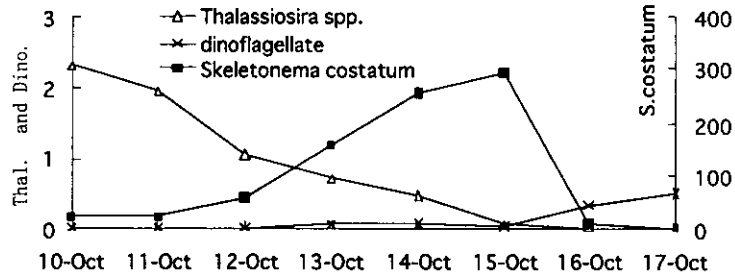

Fig. 11 Change of dominant species in P-mesocosm in October(10^5cells/l)

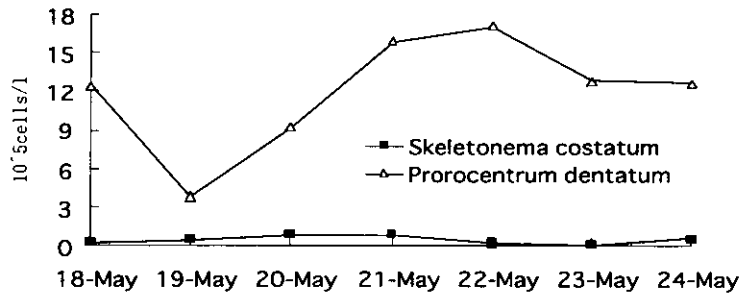

Fig. 12 Change of dominant species in control mesocosm in May

(4) The change of species diversity and evenness of phytoplankton

The species diversity index and evenness index reflect the homogeneous level of inter-species individual distribution and are also the useful ecological indicators reflecting the environment conditions. Generally, the diversity and evenness indexes of the phytoplankton in open sea are higher than that in coastal region, and higher in normal situation than during red tide. Lin et.al.(1997)[3] suggested the critical values of species diversity (H') and evenness(J) of phytoplankton to assess the outbreak of red tide, i.e. H'= 1.0, J=0.2. According to the standard, the red tide appeared in the two experiments. The dominant species in October 1997 was single, so the diversity and evenness indexes were very low, ranging from 0.216 to 1.304 and from 0.111 to 0.7 in natural seawater respectively. In P-mesocosm, H' and J decreased with the development of red tide (Fig.14) and were only 0.008 and 0.003 at 5th day respectively, meanwhile the cell number of *Skeletonema costatum* was the highest. In the end of the experiment, the dominant species replaced and species number increased, H' and J rose to the highest value (1.567 and 0.503 respectively).

There were two dominant species in May 1998. H' and J were a little higher than that in October. In control mesocosm, the two indexes ranged from 0.10 to 0.41 and 0.033 to 0.21 respectively. The replacement of dominant species caused H' and J changed in P-mesocosm. (Fig15)

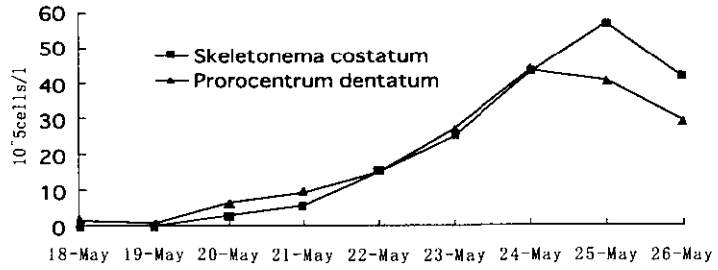

Fig. 13 Change of dominant species in P-mesocosm in May

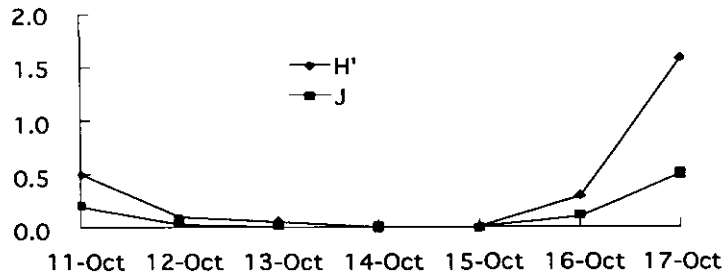

Fig. 14 Diversity index(H') and evenness index(J) of phytoplankton in P-mesocosm in Oct.

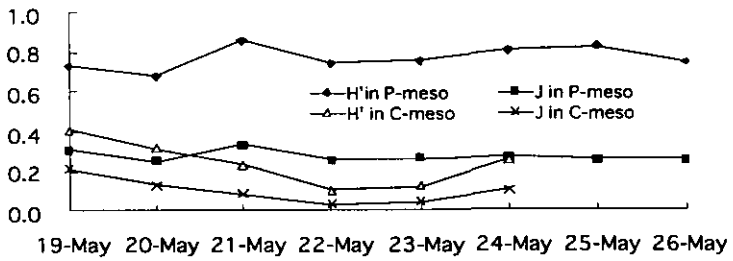

Fig. 15 Species diversity and evenness of phytoplankton in May

(5) Reproduction rate of dominant species of phytoplankton, *Skeletonema costatum* and *Prorocentrun dentatum*, and their absorption to phosphate.

In natural seawater, the reproduction rate of phytoplankton is affected by many factors, e.g. temperature, salinity, light and nutrients as well as feeding by other organism, behavior of phytoplankton: death and sinking. Suppose that the sinking and death of phytoplankton are neglected, and the feeding by other organisms was also omitted, according to the following formula, the reproductive rate of phytoplankton was calculated.

$$u=K'/\log 2,$$
$$K'=(\log Nt-\log No)/t$$

Here u means the reproduction rate of phytoplankton, No and Nt refer to the initial cell density and the cell density after t days.

Table1 Reproduction rate of dominant species in mesocosms

Species	Month	C-mesocosm	P-mesocosm
Skeletonema costatum.	October		0.993
	May	0.482	1.202
Prorocentrun dentatum	May	0.720	1.103

From the table 1 we may see that *Prorocentrun dentatum* reproduce faster than *Skeletonema costatum* under the low phosphate condition. However in the phosphate-enriched condition, *Skeletonema costatum* reproduced faster than *Prorocentrun dentatum*. Chen (1990)[7] also found the reproduction rate of the diatom was higher than that of dinoflagellete in laboratory.

The uptake rate of phytoplankton to phosphate maximizes at the 2nd and 3rd day, and became low in later period of experiment because of the low nutrients. The maximum uptake rate was 6.542×10^{-9} μmol.cell^{-1}.h^{-1} in October in P-mesocosm experiment and 1.513×10^{-8} μmol.cell^{-1}.h^{-1} in May in P-mesocosm experiment. The difference of the absorption rate in two seasons might be resulted from the different species composition of plankton.

4.CONCLUSION

(1). Phytoplankton bloom broke out in the mesocosm experiments by adding phosphate in October and May. They were called as *Skeletonema costatum* bloom in October and *Prorocentrun dentatum* and *Skeletonema costatum* bloom in May. The shortage of dissolved inorganic nitrogen caused the disappearance of two blooms.

(2). When one population becomes absolutely dominant species, the species diversity and evenness of phytoplankton community was low. On 4th day of October experiment, the diversity and evenness minimized 0.008 and 0.003 respectively, when *Skeletonema costatum* reached the peak. After the *Skeletonema costatum* died extensively, the diversity and evenness increased to 1.576 and 0.503 respectively. In May, there were two dominant species in mesocosm, in later period of experiment, the *Skeletonema costatum* became the first dominant species instead of the *Prorocentrun dentatum*. The diversity and evenness of phytoplankton were higher in May than that in October.

(3). The average and maximum reproduction rates of the diatom, *Skeletonema costatum*, were 0.993 d^{-1} and 1.419 d^{-1} in P-mesocosm in October. In May, the average reproduction rates of this diatom were 0.482 d^{-1} in control and 1.202 d^{-1} in P-mesocosm. Meanwhile, the average reproduction rates of the dinoflagellete, *Prorocentrun dentatum*, were 0.72 d^{-1} in control and 1.103 d^{-1} in P-mesocosm. This dinoflagellete reproduces faster than the diatom under the oligotrophic condition, and easily adapts to the oligotrophic condition. However in the phosphate-enriched condition, this diatom reproduces faster than dinoflagellete.

(4). The maximum absorption rate of phytoplankton in P-mesocosm experiment was 6.542×10^{-9} μmol.cell^{-1}.h^{-1} in October and 1.513×10^{-8} μmol.cell^{-1}.h^{-1} in May. The difference of the uptake rate in two seasons might be resulted from the different species composition of plankton.

REFERENCES

1) Capriulo, G. M.: Alteration of the planktonic food web of Long Island Sound due to eutrophication. Final report grant report to CTDEP Long Island Sound research fund. 1996
2) Zou, J. Z., Dong, L. P. And Qen, B. P.: The preminiary study of eutrophication and red tide in Bohai Bay, *J. Marine Environment Science*. 2(2): 41-55, 1983 (in Chinese)
3) Lin, Y. S., Zhou, X. P., Qiu D. Q., and Zhou J. M.: The application of the diversity index in precasting red tide, *A study on eutrophication and red tide in the offshore area*, Zhu M. Y. Eds., Ocean press, Beijing, pp 25-29, 1997 (in Chinese with English abstract)
4) Takahashi, M.: Pelagic mesocosm: 1. Food chain analysis, *Enclosed experimental marine ecosystem: A review and recommendations*. Lalli eds. pp:61-80, 1990
5) Wong, C. S. and Harrison P. J.: Marine ecosystem enclosed experiments. IDRC. Ottawa CA, 1992
6) Hong, J. C., Huang, X. Q. and Jiang, X. S.: Inverstigation report on the *Skeletonema costatum* red tide in Changjian River Estuary, *J. Oceanologia et Limnologia Sinica*, 25(2): 179-184, 1994 (in Chinese with English abstract)
7) Chen, C. M., Bao, G. G. And Wu, X. D.: Relationship between the different forms, concentration of nutrients and the conpetition and growth of phytoplankton. 1. Effect of phosphous, *Marine environmental science*, 9(1): 6-12, 1990 (in Chinese)

RESPONSE OF ZOOPLANKTON POPULATIONS TO PETROLEUM HYDROCARBON AND PHOSPHATE ENRICHMENT IN MESOCOSM

Jinhui WANG, Weifei, WANG, Zhennan WU, Youfen ZHANG

Environment monitor center, East China Sea Branch, State Oceanic Administration
(Dong Tang road 630, Shanghai, 200137, China)

Fluctuations in zooplankton abundance and species composition are described for oil contaminated experiment and phosphate enrichment experiments conducted in two mesocosm on October 1997 and May 1998. The major phenomenon in both phosphate enrichment experiments (1997 and 1998) was a steadily increase in the abundance of zooplankton in concordance with the increase in abundance of phytoplankton and bacteria. The additive petroleum hydrocarbon caused a major change in the ecology of the mesocosm which resulted in a depression of ciliate, zooflagellate and some copepods.

Key words: *zooplankton, petroleum hydrocarbon, phosphate enrichment, mesocosm*

1.INTRODUCTION

In changjiang estuary, the inappropriate agricultural using fertilizer caused surplus nitrogen divulging into east china sea, moreover, the surface of continent and shelf along changjiang river lack phosphate comparatively[5) 13)], causing high ratio of N:P in the estuary water in which phosphate controls alga growth [19)]. In East china sea, nitrogen, phosphate and oil constitute major pollutants, recently the content of phosphate has the tendency of increase which is up to 84% higher than normal standard in 1997. Enrichment of N and P together or solely can cause bloom and red tide in natural conditions[11)], 6 different scale harmful algae bloom outbreak in East China sea in 1998 which may be caused by enrichment of N, P and other pollutants. In nutrient enriched marine ecosystem, conditions necessary for red tides outbreaks are multitude such as optimum temperature, salinity, water exchange, diel vertical migration, light intensity, predator etc[21)]. Fluctuations in these properties represent an index of the biological response of the ecosystem to physical forcing, these patterns are an important aspect of ecosystem structure because environmental perturbations may affect the outcome of biological interactions between populations[9)].

Zooplankton act a pivotal role as intermediaries between alternative carbon sources and higher consumers such as fish. As the idealistic media to research pressure reaction in ecosystem according to marine environment changes, zooplankton is one focus of GLOBEC and the fluctuation of which is one idealistic parameter to monitor kinetics of ecosystem. Zooplankton can modify the P supply to phytoplankton in two ways: they act as P sinks by incorporating P and as P sources by regenerating P[18)]. Abundant phytoplankton provide foods for generation of zooplankton and in contrary zooplankton grazing limit the growth of phytoplankton. Besides opposite environmental factors, zooplankton density on the early stage contribute to inhibit spring bloom and red tide outbreak and intrigue the shift of dominant species[20)], on the other hand, neither food availability nor transport processes can alone or together account for distribution and migration patterns in plankton. Mortality risk is a major factor that governs habitat choice and vertical migration behavior in zooplankton. Previous researchers have reported both negative and positive correlations between zooplankton abundance and algal biomass and productivity[17)] attributing this phenomenon to the compensatory processes of nutrient regeneration and grazing loss through their effects on algal nutrient status and size distribution.

P or N enrichment mostly increasing phytoplankton biomass and primary production is certified in many districts all over the world[24)]. P enrichment experiments were conducted on October 1997 and May 1998 to learn the effects of nutrient enrichment on plankton ecosystem, in this paper, zooplankton abundance is

related algal biomass and productivity in the context of nutrient availability.

Previous research activities related to oil pollution in recent years focus on acute and chronic effects of petroleum and specific petroleum hydrocarbons on ecosystems. Crude oil could cause a major change in the ecology of ecosystem which resulted in large numbers of bacteria and zooflagellates, but a depression of all other zooplankton,[12] other research had similar results which inhibited the growth of diatoms and copepods, but stimulated planktonic bacteria, choanoflagellates and tintinnid ciliates[10], but whether the dissolved fraction of oil or spill affect plankton ecosystem is hard to determine[16], although most samples appear to be contaminated by hydrocarbons. One fleck is apparent that the samples are more easily contaminated by oil if crude oil or feul is used, so the dissolved fraction of oil was made to add into mesocosm.

Most of Chinese ships use No.0 diesel oil as supply, the oil contaminants in the region of east china sea studied in Chinese – Japanese cooperation project are mainly from petroleum wastewater discharged by ships and input from Changjiang river etc. Therefore, petroleum hydrocarbon of No.0 diesel oil was added to one mesocosm on East China Sea, the following mainly discuss the impact on zooplankton.

2. MATERIALS AND METHODS

Mesocosm experiments were conducted at anchor place off the LUHUA island in east china sea from 10 October to 17 October 1997and from 18 May to 1 June 1998. The sea around this island is the interactive center of different current which has complex physichemical character, and outbreak of red tides (especially Noctiluca scintillans and Skeletonema costatum) have frequently been observed in the past decades. Mesocosm used in 1997 and that in 1998 are very similar except some improvements, no inflow or outflow occurred across the boundary of the enclosure. In October 1997,the phosphate in enrichment mesocosm was adjusted from 0.78umol/L to 3.25umol/L. At midnight of 18 may 1998, 2 umol/l phosphate was added into P enrichment enclosure, 1.5 umol/l phosphate and 1800ppb petroleum hydrocarbon were added separately into oil polluted enclosure at midnight of 26 May 1998 and 28 May 1998. Different sampling tubes and mesh nets were adopted in oil polluted mesocosm and controlled mesocosm to eliminate the contamination of the sample. Sample water (10 liters) was passed through two zooplankton nets(100um mesh and 20um mesh) in order, and net samples were fixed with 8% formalin immediately after collection to identify and enumerate zooplankton.

3.RESULTS

(1) P enrichment experiments

On 1997, the zooplankton population exhibited a progressive increase during both control and enrichment experiments (Fig 1). The initial abundance of zooplamkton in the P enrichment experiment was approximately twice that in the control, although sea water were input simultaneously. In general, patterns of zooplankton abundance were similar in both experiments, but abundance of the control rise more dramatically on the developing stage mainly contributing to microzooplankton (size between 20-100um) partly because of the high initial abundance comparing to that of macrozooplankton(size >100 um). Zooplankton abundance at the end of P enrichment experiment was up to 5 times it's initial level.

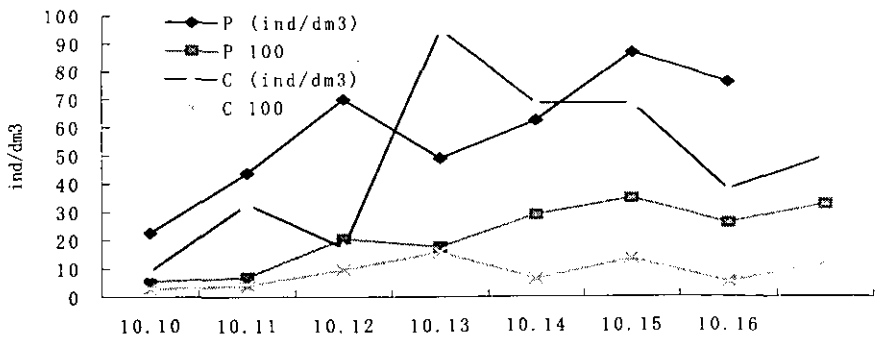

Fig 1 Abundance of zooplankton fluctuation in control and P enrichment Experiment, October 1997(P: P enrichment, C: control)

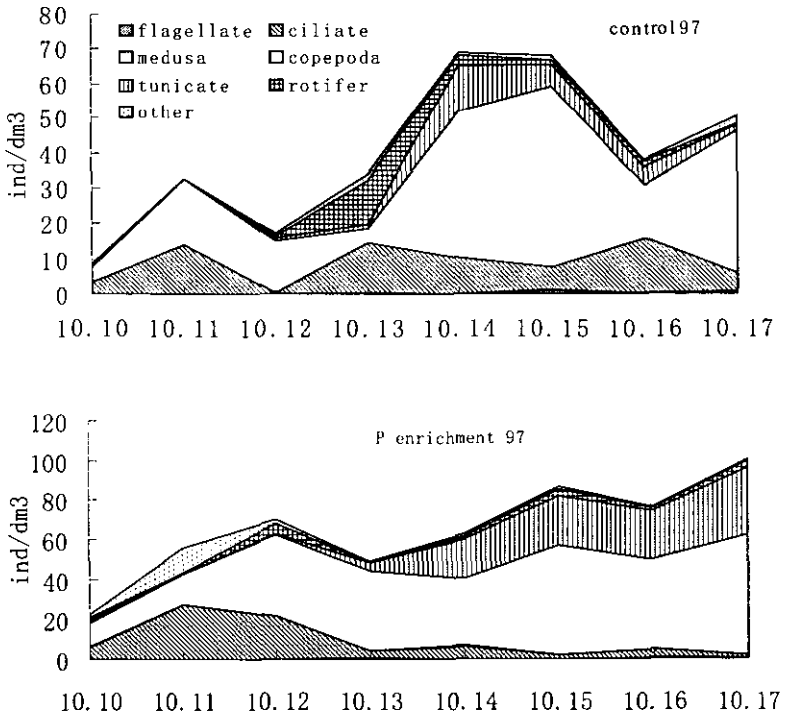

Fig 2 Composition of zooplanktonin in control and P enrichment during experiment, October 1997

Copepod, ciliate, tunicata appeared as the first, second and third dominance in most samples during the 1997 experiments.(Fig2). In control, copepod dominated ciliate and some other groups while in P enrichment mesocosm the dominant population shifted from ciliate to copepod in 12 October. After the depression of the ciliate, the abundance of tunicata increased dramatically and soon became the second dominance. In P enrichment enclosure, the abundance of larvae showed a progressive increase during the experiment and the ciliate had the tendency to decline after the second experimental day's dominant (27.2ind/dm3) , unlike the control experiment where larvae declined after peaked on 13 October (63ind/dm3) and the ciliate shows no regularity on the abundance. The larvae of copepod and tunicata composed most of the larva and the number of copepodite naupplius increased sharply It must be pointed out that the copepod was more abundance in P enrichment enclosure than in control, ostracod, chaetognatha and medusa were only found in some samples with low abundance.

On May 1998, patterns of zooplankton abundance were very similar from 18 May to 24May in both control and P enrichment enclosure (Fig 3). First day maintaining stable with slight increase due to adapt to new environment in control, however, progressive decrease to a stable condition (115.4ind/dm3 I) had been found after adding phosphate, then increase moderately till the end. An apparent increase in the total number of zooplankton in P

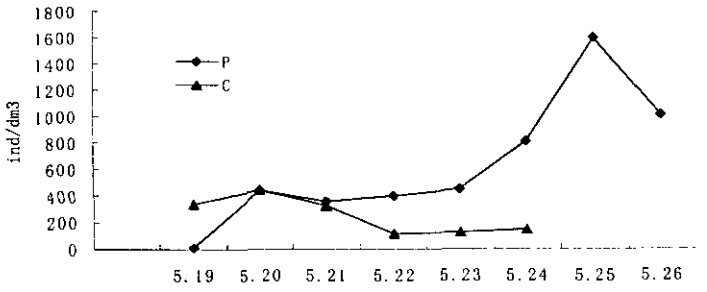

Fig3 Total number of zooplankton fluctuation in P enrichment and control, May 1998

enrichment mesocosm can be found except sharp decrease at the last day which is roughly 186 times it's initial abundance. On the peak the total number of zooplankton in P enrichment was about 1600ind/dm3. In concord with 1997's experiment, microzooplankton (size between 20 and 100um) constituted most all of population with macrozooplankton subsidiary.

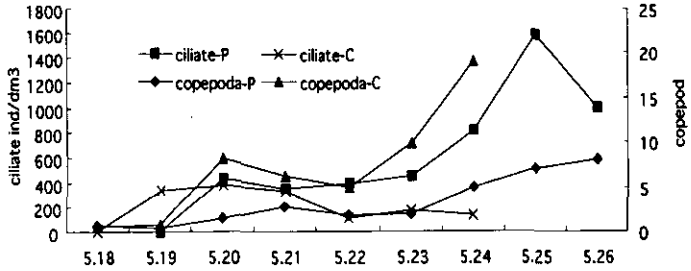

Fig 4 The fluctuation of dominant group (ciliate and copepod) in control and P enrichment Experiment, May 1998

Dominant groups during experiment in both control and enrichment enclosure were ciliate. The ciliate in both mesocosm composed most of the zooplankton and increased dramatically after the bloom of *Prorocentrum dentatum* and *Skeletonema costatum* in P enrichment whereas decrease slightly in control. The number of copepod increased in both container but more violently in control (Fig 4). The copepodite nauplius abundance increased slightly and constituted most of the larva, the group showed moderately stableness indicating that bloom induced by P enrichment had no apparent effect on the copepodite larvae. Tintinnopsis was the major species in ciliate. The Corycaeus dahil, Corycaeus gibbulus and Paracalanus parvus contributed most of the increase in the group copepod. It is very strange that N. sintillans was not found in the first 2 days, one day after enrichment, N.scintillans emerged (12 ind/dm3in P enrichment and 5.2 ind/dm3 in control) but decline soon. Another doubtful matter is the exceptional high abundance of larvae on 24 May in control. It should be emphasized that the density of zooplankton in 1998 experiment was higher than that of 1997 due to seasonal variations. Copepoda nauplius were dominance in larvae group. Oithina.sp , Microsetella norvegica were also recorded, but never composed a significant portion of the samples, unlike the 1997 P enrichment experiment where they comprised a significant proportion of the zooplankton.

(2) Oil enrichment experiments

The zooplankton population showed the tendency of increase in control and decrease in oil enrichment (Fig5). In the first two days when the dissolved fraction of oil had not been added but mediate phosphate had been added to oil mesocosm, zooplankton abundance increased slightly but declined (approximately 1/5 at the end that uncontaminated) after dissolved fraction of oil was added into mesocosm. In both container, the microplankton (size between 20 and 100 um) dominated the zooplankton and determined the fluctuation of zooplankton.

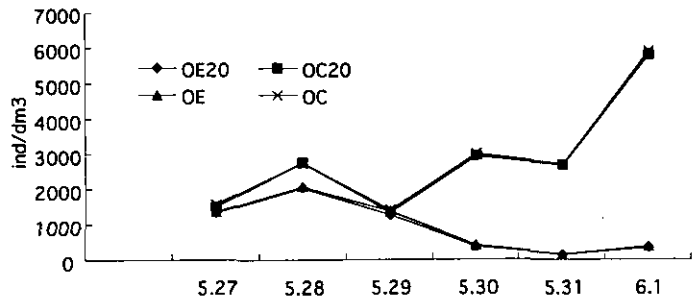

Fig 5 The total number of zooplankton in control and oil enrichment experiment, May/June 1998

Dominant species on both control and oil mesocosm was *Tintinnopsis* sp.(cf.*beroidea*) which declined after oil contamination and propagated in control which only dealt with P enrichment.(Fig 6) While other groups such as copepod, cladocera, never superceded ciliate although their abundance was not low,

compared with the control, the copepod in oil enrichment increased slightly during 2days after oil addition and then declined which seemed affected by oil contamination. In oil enrichment mesocosm, the abundance

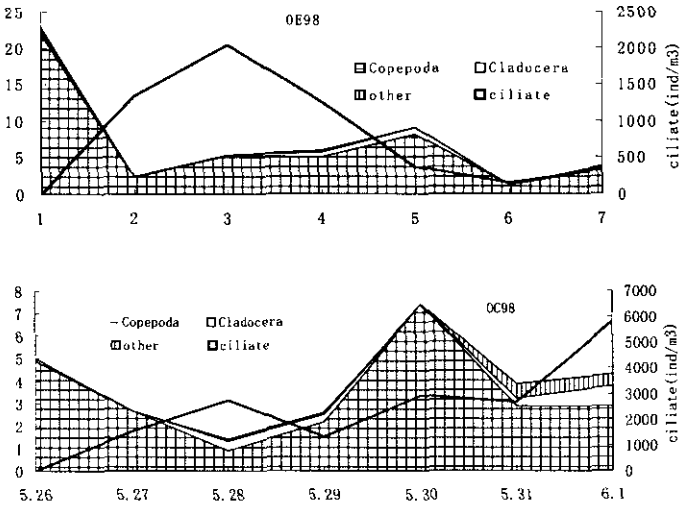

Fig 6 Composition of zooplankton in control and enrichment mesocosm during the oil enrichment experiment, May/June 1998

of N.scintillans varied dramatically during experiments in which declined to 1/10 its initial abundance after oil enrichment while maintained stable in control. The number of larvae decreased sharply during P enrichment and continued to decline after oil enrichment. Copepodite nauplius constituted an extremely substantial part of larvae in both mesocosm which coincided with corycaeus gibbulus showing sensitive to oil enrichment than other species.

(3) Diversity

Zooplankton diversity (Shannon-weaver, 1963) during 1997 P enrichment experiment was highest at a range of values between 2.4 and 3.6 (Fig 7), which was interpreted in terms of relative maturity and stability of the community. Lower variety was found during 1998 P enrichment and oil enrichment experiments. The diversity in 1997 was more stable although some decline was found in both control and enrichment experiment, thus can be assumed as representative of normal conditions. In 1998 P enrichment experiment, diversity value varied from 0.22 to 1.91 and 0.5 to 1.5 in control and enrichment respectively, keeping similar pattern variation. In oil enrichment experiment, the diversity of oil polluted mesocosm maintained more stable although had the tendency to decrease. The low diversity value in 1998 attributed to the absolute dominance of ciliate indicating interspecies homogeneity. It is interesting that the diversity in oil enrichment remain higher value than that in control during experiment because of the greater number of ciliate, indicating higher heterogeneity in oil enrichment mesocosm.

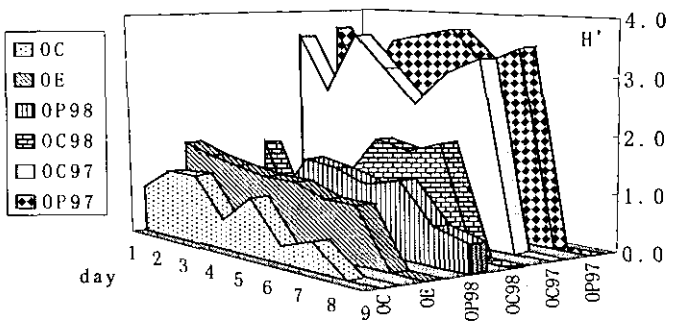

Fig7. Time serial changes in total diversity of zooplankton

4. DISCOURSSION

(1)P enrichment experiment

The mesocosm systems (P enrichment and control) described in this paper coincide in their hydrography, the temperature, DO, salinity and turbidity showed little variation during the experiment and no apparent divergence between P enrichment and control mesocosm. So the affection of physical environment on zooplankton can be ignored. The interactions between environmental heterogeneity and the population dynamics of zooplankton are acknowledged to be complex. Preliminary consideration of the changes in concentration of the more common species suggested water temperature[6] and general food availability may have been paramount; however, J.M.Thompson [7]considered neither of these factors was continuously or simultaneously limiting the development of all populations. The total Chl-a increased progressively during experiments except the first day's decline due to impound into the enclosure and sediment of some inactive phytoplankton. All most of this chlorophyll was between 2um and 20um, and therefore directly available to copepods as food. POC values within P enrichment exceeded that within control indicate phytoplankton in P enrichment multiplied fast than in control. P enrichment caused phytoplankton bloom and consequentially depressed after day five in 1997 autumn experiment but no depression found in 1998 spring experiment. The high POC and PON values indicate the prevalence of detritus in enclosure. Detritus may be important in the nutrition of copepods[1] , and the associated bacterial cells may enhance the nutritional value of detrital particles occurred via intermediary organisms such as prorozoa than directly from detrital particle uptake[26] .

In 1997 P enrichment experiment, the ciliate depression after peaking (27.2ind/dm3) at 11 October indicate some other environmental pressure existed after phytoplankton bloom in base of abundant food supply, or copepods and tunicate predate pressure coerced this group to depress. In some factorial

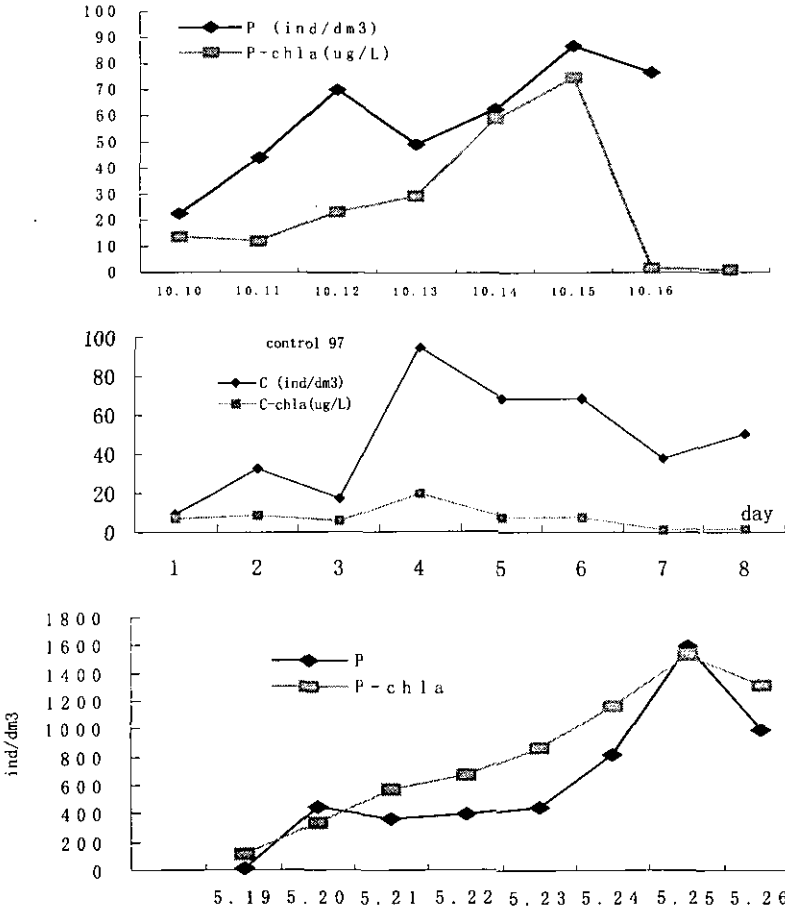

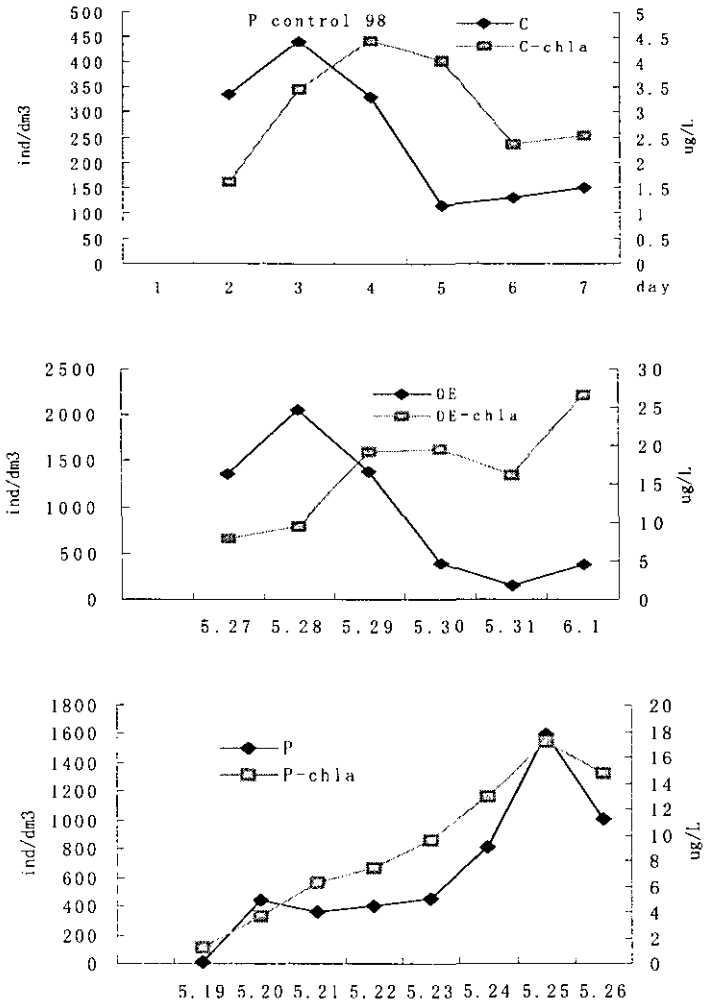

Fig 8 The fluctuation of zooplankton abundance according with Chl-a in 1997, 1998 P enrichment experiment and 1998 oil enrichment experiment.

experiments[20], the top-down effects of zooplankton was usually stronger than nutrient additions in determining final densities of protozoa. The zooplankton abundance fluctuation coincided with that of pytoplankton and a lag phase existed indicating that the food somewhat determine zooplankton multiply and growth(Fig 8). The diel vertical migration of phytoplankton affected the migration of zooplankton, apparent accumulation of zooplankton attracted to the high phytoplankton concentrations at the surface[23]. Wang Yan [27]found prorocentrum had apparent diel vertical migration accumulating at surface (0-20cm) from 9 Am to 15 Tm. So the endogenous rhythmic migration and attraction to high phytoplankton concentration of zooplankton can explain some irregular data during experiment. Major nutrition and energy source of copepod may come from flagellate and microzooplankton rather than diatom, our result accord with this conclusion which copepod in 1998 P mesocom (mainly flagellate bloom) multiplied more rapidly than that in 1997 P mesocosm (diatom bloom). The abundance peak of copepods was not consistent with that of total zooplankton but ahead of it, and the zooplankton abundance fluctuation was affected by copepodite nauplia , thus it correlate with copepods multiply and growth. Peak time of total zooplankton abundance in P enrichment lag behind that in control indicate the phytoplankton bloom in P enrichment in some degree inhibit the natural depression of zooplankton. Above hypothesis consider no predator because of the significant low abundance.

The high diversity value of 1997 may contribute to the detail classification, regularly, heterogeneity of plankton community in spring is higher than in autumn. Higher abundance of zooplankton was found in P

enrichment enclosure, which is consensus to the result of 1997 experiment, but differ in multiply rate, this lack of consistency led us to make some reservations, taking into consideration the different food supply and predate pressure. The P enrichment in 1998 caused the prorocentrum triestinum(flagellate) and skeletonema costatum (diatom)bloom instead of skeletonema costatum bloom solely in 1997. Traditionally the chained diatom is more easily captured by zooplankton than flagellate, but larger number of zooplankton was found in mesocosm abundant of flagellate indicate flagellate is edible to zooplankton. More N. Scintillans, which may predate some small copepods, emerged in P enclosure than in control enclosure, interpreting less copepods and larvae in P enrichment enclosure. Previous researchers reported diel vertical migration and endogenous rhythm of migration behavior affected the distribution of zooplankton in seawater and copepods congregated where food was most abundant (thin layers), although the consensus of sampling time and locale may diminish these affection. The copepodite nauplius declined progressively indicate the different food supply affect the multiply rate of copepod. The loss of TP was estimated ranged from 1.4% to 14.4% per day which is higher than that estimated about 1.1% by Ann Lyche [25]and found to be caused mainly by sedimentation, mostly due to the loss of DTP which partly transferred to PP. Ann Lyche [25]found the zooplankton community was responsible for almost 60% of the loss of P, also their contribution to total PP contraction was only 20%,in addition, the role of zooplankton in P retention may be important than is suggested from their contribution to total PP and zooplankton biomass. Thus phosphate and zooplankton are interactive directly or indirectly via bacteria and phytoplankton.

The experiments described in this paper (especially 1998 spring experiment) suffer from a common malady of ecological experiments in being of small scale and short duration. In one sense the experimental scale is relatively large, since each enclosure in 1998 spring contained >10E7 phytoplankton and > 10E2 zooplankton. Nevertheless, the most serious potential problems with these kinds of experiments are that the responses may only reflect transient dynamics of zooplankton communities in response to nutrient enrichment, and indirect effects may not be manifested in the time frame of the experiment.

(2) Oil enrichment experiment

The effect of dissolved fraction of No 0 diesel (mainly hydrocarbons) on zooplankton was not significant as that of various crude oil [10],the most evident direct effect of hydrocarbon addition was rapid depression of ciliate and zooflagellate. But stimulation of zooflagellate was found in effects of disperse and oil mixtures[12] , hydrocarbons alone[3] , Ekofisk crude oil[10] . Copepod was also inhibited by addition of hydrocarbon. The different development of protozoans and zooplankton in oil enrichment versus control bag may be explained as an effect of oil. Davies et al[4] found the addition of oil in their bag had a direct inhibitory effect on the development of copepod eggs and naupliae, but Lee et al[3] found no effect of fuel oil addition on naupliar copepods. Hydrocarbon stimulated Copepoda naupalia slightly in our study, but inhibited some carniverous copepod such as corycaeus dahil, corycaeus gibbulus, paracalanus parvus. Phytoplankton bloom and bacteria growth supplied abundant food for zooplankton, and no other physical chemical characters varied apparently between oil and control, thus the zooplankton fluctuation can be contributed to the hydrocarbon addition. The dissolved hydrocarbon reduced from 1870.6ppb to 1287.7ppb during experiment, Dahl et al[10] ascribed it to microbial degradation in combination with sedimentation. Other zooplankton population were largely unaffected by the presence of oil. Total diversity recall the perturbations registered within a single population when the reproduction is affected and the instability is amplified[16], the ecosystem heterogeneity in our study decreased along experiment. It seemed oil do have some effect on the structure of the community, but this conclusion may not be precise not considering other possibility and one week is not long enough to monitor the ecosystem. If the same phenomenon can be found in longer period experiments, the conclusion may be valuable. The effects observed by us somewhat different from previous reports. This may be due to the different concentration and different type of oil applied in our experiment. The use of different pollutants and design of experiment is important to the effects observed, for example, E.Dahl [10]added no nutrients; Davies[10] added nutrients every week, and we added nutrients in initial day solely. The initial concentrations of oil used by us were intermidiate (about 1800ppb) compared with that of crude oil (3000ppb) used by T.R.Parsons [12] and 40ppb by lee et al [3], thus the more significantly zooplankton population decrease can due to different kind and form of oil used . The lag phase emerged on the zooplankton depression indicate that some zooplankton may not be affected by hydrocarbons directly but indirectly via bacteria and phytoplankton. Predator and diet pressure may affect the zooplankton fluctuation in some scale. when oil perturbs one or several components of the test ecosystem, a complex series of interactions occur making it difficult to interpret special result because mesocosm experiments seldom have been replicated, the representativeness of experimental results is uncertain, and few intra- and inter system ecosystem studies

have been conducted. Zooplankton may be more sensitive to stress from toxic substances in winter, when algal standing stocks and primary productivity are low, while in spring when food levels are higher. The experiment was conducted in spring when the organization and complexity of the community reach its high level, which may not protrude the effect of oil on zooplankton population.

5. CONCLUSIONS

Zooplankton communities can be considered within the framework of theory on the regulation of productivity in marine ecosystem. Nutrients appear not to regulate zooplankton directly but via bacteria and phytoplankton indirectly, variation in zooplankton is likely to be related to variability in nutrients and food web structure. When one population becomes absolutely dominant species, the species diversity of zooplankton community was low and low diversity value is due to the absolutely dominant of ciliate. In conclusion, the major phenomenon in both phosphate enrichment experiments (1997 and 1998) was a steadily increase in the abundance of zooplankton in concordance with the increase in abundance of phytoplankton and bacteria. It appears that the petroleum hydrocarbon of No 0 diesel in our experiments behaved similarly to other petroleum hydrocarbons with respect to the decline of zooflagellate and ciliate and some copepod depression.

REFERENCES

1) Heinle,D.R., R.P.Harris, J.F.Ustach & D.A.Flemer: Detritus as food for estuarine copepods, *Mar.Biol.*, Vol 40,pp.341-353,1977.

2) V.R. Gibson and G.D. Grice : Response of macrozooplankton populations to copper: Controlled ecosystem pollution experiment, *Bulletin of Marine Science.*, Vol.27(1),pp.85-91,1977.

3) Lee,R.F, Takahashi, M,Beers,J.R.: *Controlled ecosystems: Their use in the study of effects of petroleum hydrocarbons on plankton in physiological responses of marine biota to pollutants*, Academic press, New York, pp.323-341, 1977.

4) Davies.J.M, Baird,I.E., Massie,l.c., Hay,S.J., Ward,A.P.: Some effects of oil-derived hydrocarbons on a pelagic food web from observations in an enclosed ecosystem and a consideration of their implications for monitoring. *Rapp.P-V. Reum.cons.int. Explor.Mer.*, Vol. 179,pp.201-211,1980.

5) Gu hongzhen et al: The geochemistry of nitrogen and nitrate in sea water near Changjiang estuary, *Journal of Shangdong ocean college.*, Vol.11 (4), pp.37-46, 1981.

6) Reynolds,c.s, and Wiseman,S.W: Sinking losses of phytoplankton in closed limnetic systems, *J Plankton. Res.*,Vol.4, pp.489-522, 1982.

7) A.J.D. Ferguson, J.M. Thompson and C.S. Reynolds: Structure and dynamics of zooplankton communities maintained in systems, with special reference to the algal food supply, *Journal of Plankton Research.*, Vol.4(3), pp.523-542,1982.

8) J.M. Thompson, A.J.D. Ferguson and C.S. Reynolds: Natural filtration rates of zooplankton in a closed system: the derivation of a community grazing index, *Journal of Plankton Research.*, Vol.4(3), pp.545-560,1982.

9)T.L. Hayward, E.L. Venrick and J.A.Mcgowan: Environmental heterogeneity and plankton community structure in the central North Pacific, *Journal of Marine Research.*, Vol. 41,pp.711-729,1983.

10) dahl.E., laake,M., Tjessem,K., Eberlein,k.&Bohle,B: Effects of Ekofisk crude oil on an enclosed planktonic ecosystem, *Mar. Ecol. Prog. Ser.*, Vol.14,pp.81-91,1983.

11)Takeshi HORIE, Yasushi HOSOKAWA et al: Microcosm test for the grasp of nutrient cycle in marine environment., Vol.494, pp.1-28, 1984.

12) T.R parsons, P.J.Harrison. et al: All experimental marine ecosystem response to crude oil and corexit 9527: part 2—Biological effects., *Marine Environmental research.*, Vol.13,pp. 265-275,1984.

13) Edmond,.J.M. et al: Chemical dynamics of changjiang estuary. Continental shelf research., pp.17-36, 1985.

14) Ulrich Sommer: Comparison between steady state and non-steady state competition: Experiments with natural phytoplankton, *Limnol. Oceanogr.*, Vol. 30(2),pp.335-346,1985.

15) Phillip T. Arumugam & Michael C. Geddes: An enclosure for experimental field studies with fish and zooplankton communities, *Hydrobiologia.*, Vol.135,pp.215-221, 1986.

16) S. A. Guzman del proo, E.A. Chavez et al: The impact of the Ixtoc-I oil spill on zooplankton, *Journal of Plankton Research.*, Vol.8(3), pp.557-581,1986.

17) J.J Elser, M.M Elser and S.R. Carpenter: Size fraction of algal chlorophyll, carbon fixation and phosphatase activity: relationships with species-specific size distributions and zooplankton community structure, *Journal of Plankton Research.*, Vol.8(2), pp.365-383,1986

18) Den Oude, P.J. and R.D.Gulati: Phospharous and Ntrogen excretion rates of zooplankton from the eutrophic loosdrecht lakes with notes on other P sources for phytoplankton requirements. *Hydrobiologia.*, Vol.169,pp.179-190,1988.

19) Hu minghui et al: The limiting phosphate to the growth of phytoplankton in Changjiang estuary, *ACTA Oceanologica Sinica.*, Vol.11,pp.439-443, 1989.

20) Michael l. Pace and Elizabeth Funke: Regulation of planktonic Microbial communities by nutrients and herbivores, *Ecology.*, Vol.72(3),pp.904-914, 1991

21) Lin yu, Chen Xiaolin et al: Preliminary study on red tide caused by nutrient enrichment in marine enclosed ecosystem, *OCEANOLOGIA ET LIMNOLOGIA SINICA.*, Vol.23(3), pp.312-317,1992.

22) Lu Douding, Zhang Zhidao, Zhu Genhai, Lou Yi: Distributive pattern of Noctiluca scintillans in the Zhejiang coastal water area,

DONGHAI Marine Science., Vol.12(3), pp.62-69, 1994.
23) Masataka watanabe, Kunio Kohata et al: Generation of a Chattonella antiqua bloom by imposing a shallow nutricline in a mesocosm, *Limnol. Oceanogr.*, Vol.40(8), pp.1447-1460 ,1995.
24) Mats Jansson, Peter Blomqvist et al: Nutrient limitation of bacterioplankton, autotrophic and mixotrophic phytoplankton, and heterotrophic nanoflagellates in lake Ortrasket, *Limnol. Oceanogr.*,Vol.41(7),pp.1552-1559,1996.
25) Anne lyche, Tom Andersen et al: Mesocosm tracer studies. 1. Zooplankton as sources and sinks in the pelagic phosphorus cycle of a mesotrophic lake, *Limnol. Oceanogr.*, Vol.41(3),pp. 460-474,1996.
26) A. D. Mckinnon & D.W. Klumpp: Mangrove zooplankton of North Queensland, Australia, *Hydrobiologia.*, Vol.362,pp.127-143,1998.
27) Wang Yan, Zhang Hongyan et al: Occurence and effects of harmful bloom caused by prorocentrum micans in seawater experimental enclosures. *Journal of fisheries of china.*, Vol.22(3), pp.218-222,1998.

VARIATIONS IN TRACE METAL CONCENTRATIONS IN A PHOSPHATE-ENRICHED CLOSED EXPERIMENTAL ECOSYSTEM

Kazufumi TAKAYANAGI[1], Tomoko SAKAMI[1] and Eiichiro NAKAYAMA[2]

[1] Environmental Management Division, National Research Institute of Aquaculture, Fisheries Agency
(422-1 Nakatsuhamaura, Nansei, Mie 516-0193, Japan)
[2] Department of Ecosystem Studies, School of Environmental Science, The University of Shiga Prefecture
(2500 Hassaka, Hikone, Shiga 522-8533, Japan)

Seawater samples were taken from mesocosms installed near the mouth of the Changjian River in May 1998. Filtered samples were analyzed for Cd, Co, Cu, Fe, Mn, Mo, Ni, Pb, V, Zn, As and Sb. With the exception of Zn and Pb, the concentration levels observed are similar to other coastal waters, implying no significant effect of the Changjian River could be detected. The concentrations of Cd, Cu, Ni, and most prominently As decreased with time in the phosphate-enriched mesocosm. On the other hand, the concentrations of Mn and Sb increased with time. The most likely cause of trace element variations is biological processes including phytoplankton bloom.

Key Words: *Trace Metals, Geochemical Cycling, Biological Activity, Coastal Ecosystem*

1. INTRODUCTION

Chemical and biological processes occurring in coastal waters can modify the riverine input of elements to the ocean. It is essential to understand these processes in order to construct a precise geochemical mass-balance model and also to accurately predict the fate of discharged wastes into coastal water bodies[1, 2].

The concentrations of trace metals are known to fluctuate widely in coastal waters. One of the main causes is biological activity. Organisms can take up trace metals, breakdown organically associated metals, convert dissolved metals into the particulate form or vice versa, and alter the oxidation state of metalloid elements such as As and Sb. Knowing how each process affects metal concentrations can help us understand the geochemical cycling of trace metals in coastal waters. A mesocosm, a closed experimental ecosystem, provides a useful environment for studying these processes. In this study, we installed two mesocosms near the mouth of the Changjian River (**Fig. 1**). In one mesocosm we elevated the phosphate concentration to investigate how trace metals such as As, Sb, Cd, Cu, Co, Ni, Fe, Mo, V, Mn and Pb respond to enhanced biological activity.

2. MATERIALS AND METHODS

During the mesocosm study, surface seawater samples for trace metals were taken daily. The samples were filtered on board through an acid-washed membrane filter (0.4-μm pore size) immediately after sampling and acidified with HCl to a pH of about 1.5 for storage. In our land-based laboratory, the samples were analyzed for As and Sb by hydride-generation AAS methods [3, 4], and for Cd, Cu, Co, Ni, Fe, Mo, V, Mn and Pb by AAS or ICP-AES after preconcentration onto a Kelex-100 XAD-4 column as described by Isshiki *et al.* [5]. Speciation analysis was also done for As, requiring further analysis for both As (III) and As (V).

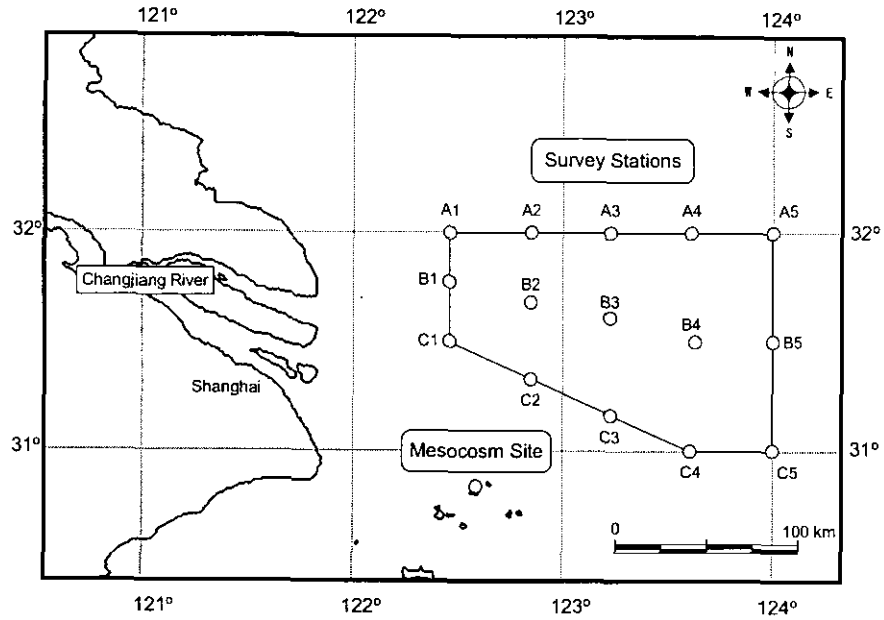

Fig.1 A map of coastal stations and the mesocosm site

For comparison, seawater samples were obtained from two other coastal stations (A1 and C1; see **Fig. 1**). These samples were processed as described above and analyzed for the same 12 trace elements.

3. RESULTS AND DISCUSSION

(1) Mesocosm experiment

Of the 12 trace element analyzed, possible contamination was encountered for Fe and Zn, which was indicated by wide fluctuations in concentration from 20 to 130 nM for Fe and 82 to 312 nM for Zn. For Co, Mo and V, no significant trends were observed, ranging from 1 to 2 nM, from 3 to 6 nM, from 16 to 20 nM, respectively. Therefore, this report focuses only on As, Sb, Cd, Cu, Ni, Mn and Pb. Concentration variations in these metals are plotted in **Fig. 2** together with nutrient data.

In the control (**Fig. 2A**), phosphate (PO_4) was depleted, indicating a PO_4-starved condition. The concentration of silicate (Si) was almost constant at about 26 μM; that of nitrate (NO_3) decreased from 14.5 to 9.9 μM. In the PO_4-enriched mesocosm (**Fig. 2B**), the addition of PO_4 accelerated the decrease of NO_3 and caused depletion of the latter on day 6 of the experiment. It also triggered a slight decline in Si concentration. These results indicate that the addition of PO_4 to the mesocosm stimulated phytoplankton growth. The major species of the phytoplankton bloom was *Prorocentrum cordatum* (H. Koshikawa, personal communication).

Profiles of the As species (**Fig. 2 C & D**) showed that there was a decrease in the concentration of As (III+V) and a concomitant increase in the concentration of As (III) both in the control and PO_4-enriched mesocosms. In the control, under PO_4-starved conditions, the concentration of As (III+V) gradually decreased from 24 to 15.4 nM over 5 days. However, in the PO_4-enriched mesocosm, only a slight decrease in As (III+V) concentration occurred in the first 4 days. On day 5, when PO_4 became depleted, the As (III+V) concentration began to decrease sharply to its minimum value of 14.9 nM. This behavior suggests that As may be actively taken up by phytoplankton under PO_4-starved conditions, but that its uptake under PO_4-rich conditions is minor. The similarity in chemical structure of P and As, both of which belong to the VA group in the periodic table, can cause a co-uptake of these elements and utilization of both by phytoplankton. However, such co-uptake seems to be prevented in PO_4-rich conditions. The progressive As (III+V) decrease corresponded well with an increase of As (III), a minor arsenic species in normal seawater. The concomitant As (III) increase was especially significant in the PO_4-enriched mesocosm during the phytoplankton bloom, implying that it may have been produced by phytoplankton.

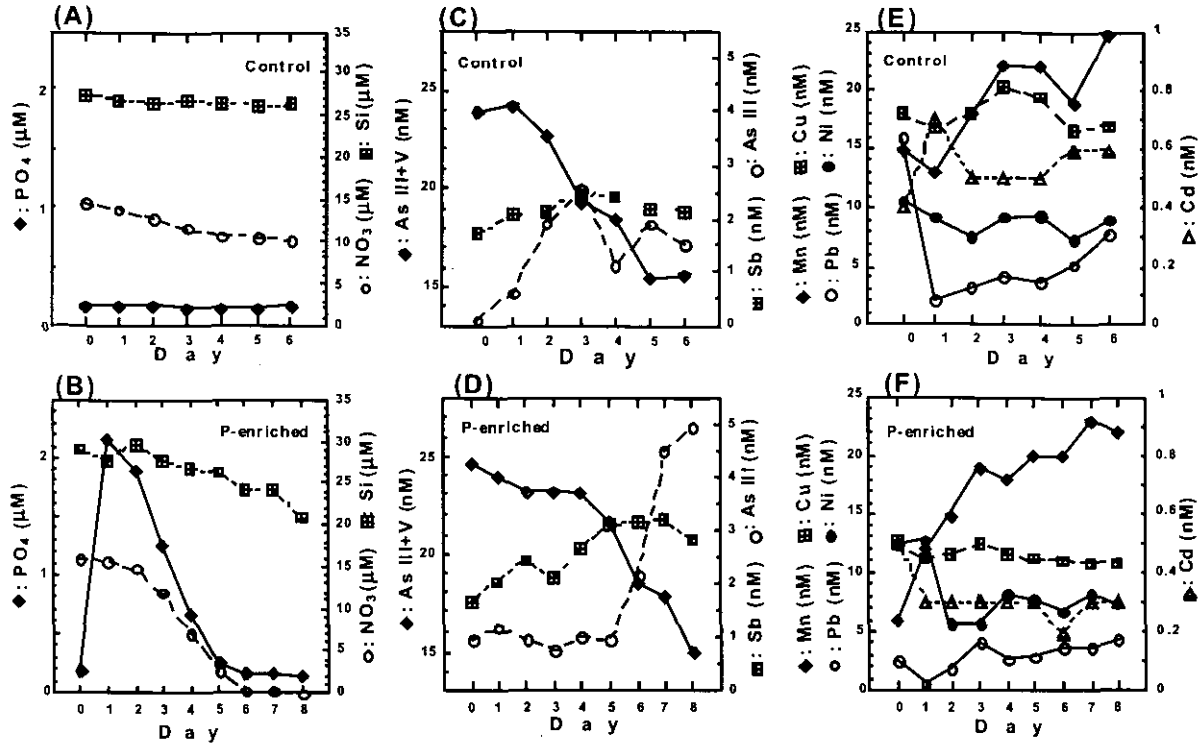

Fig.2 Variations of the metal concentrations in the phosphate enriched mesocosm (D & F) and in the control (C & E). Nutrient Data (A & B) were provided by H. Koshikawa (personal communication).

According to Apte *et al.* [6], changes in the concentration of PO_4 and As follow the following relationship (Equation 1).

$$\Delta[P] / [P] = D \cdot \Delta [As] / [As] \quad (1)$$

In this equation, D is the discrimination factor, Δ [As] is the predicted change in As concentration, Δ [P] is the observed change in PO_4 concentration, [As] is the observed As concentration, and [P] is the observed PO_4 concentration. In plants, Benson *et al.*[7] reported that the discrimination factor D is between 2 and 10. Using our PO_4 and As data, D was calculated to be about 10 in PO_4-rich conditions, implying that the phytoplankton were capable of discriminating between the two elements. However, under PO_4-starved conditions, D was about 3, implying that the discrimination became less efficient and that phytoplankton cells may have actively incorporated As. In contrast with the results of our May 1998, tests performed in October 1997 showed that a discrimination factor of 10 was obtained during the entire period of the PO_4-enriched mesocosm experiment (**Fig. 3**). We suspect that this difference could be attributed to the presence of a different species of predominant phytoplankton in the mesocosms. In October 1997, the dominant species was *Skeletonema costatum*, while in May 1998, it was *P. cordatum*. Our calculations of D suggest that *S. costatum* can discriminate between PO_4 and As but that *P. cordatum* cannot, especially under PO_4-sterved conditions.

The concentration of Sb was almost constant in the control at around 2 nM, but it gradually increased from 1.6 to 3.1 nM in the PO_4-enriched mesocosm (**Fig. 2 C & D**). The increase could be related to the bloom, although there is no known biochemical function of Sb in phytoplankton. The concentration of Mn also increased during the experiment, particularly in the PO_4-enriched mesocosm (**Fig. 2 E & F**). The reason for the Sb and Mn increase is not clear. Further research is necessary to clarify the effects of biological processes on the behavior of Sb and Mn in seawater. Both Cd and Ni tended to decrease during the initial stages of the bloom in the PO_4-enriched mesocosm, while their concentration remained almost constant in the control at 0.5 and 17 nM, respectively (**Fig. 2 E & F**). The phytoplankton bloom was again responsible for the decrease. This behavior is consistent with the biogeochemical cycle of Cd, which is

similar to that of PO_4, and also with the biogeochemical cycle of Ni, which is similar to that of Si in the oceanic environment. There was a little variation in concentration of Cu either in the control or in the PO_4-enriched mesocosm, although Cu is considered to be an essential nutrient for marine organisms (**Fig. 2 E & F**). Pb showed some increase in concentration in the latter stage of the bloom (**Fig. 2 D & F**).

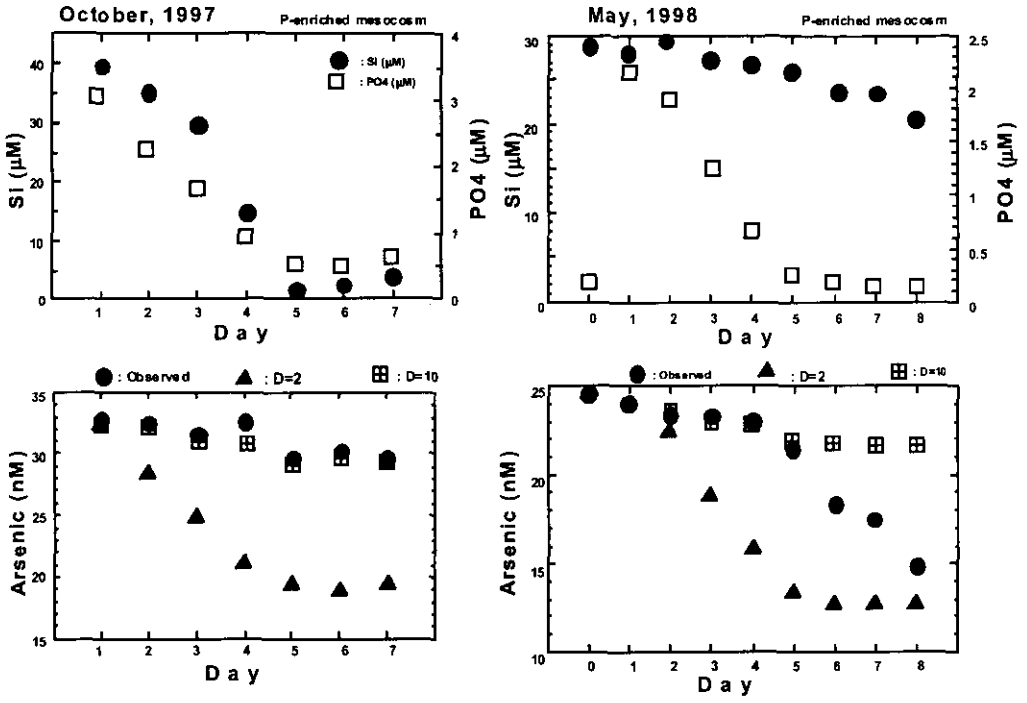

Fig.3 Predicted concentration changes of arsenic in the PO_4-enriched mesocosm according to the equation of Apte *et al.* [6].

(2) Field survey

Excluding As and Sb, trace element concentrations at coastal stations are listed in Table1. The nM concentration ranged from 0.1 to 0.4, from 1 to 13, from 9.1 to 17.3, from 21 to 2631, from 18 to 93, from 3 to 8, 1.5 to 11.8, from 0 to 0.5, from 11 to 19, from 38 to 90, from 22.0 to 25.9 and from 1.19 to 2.07 for Cd, Co, Cu, Fe, Mn, Mo, Ni, Pb, V, Zn, respectively. These concentration levels are similar to those found in other coastal waters [8, 9, 10]. However, a large concentration difference was observed between these two stations. The concentrations at St. A1 were much higher than those observed at St. C1, especially for Co, Fe and Mn. Further research is necessary to clarify the reason for these large concentration fluctuations at relatively close sites.

Table 1 Metal Results from Stations A1 and C1

Station	Depth (m)	Cd (nM)	Co (nM)	Cu (nM)	Fe (nM)	Mn (nM)	Mo (nM)	Ni (nM)	Pb (nM)	V (nM)	Zn (nM)
A1-S	0	0.3	13	16.9	2617	86	8	11.8	1.4	18	77
A1-M	12	0.3	12	15.5	2329	80	8	9.1	0.0	19	69
A1-B	24	0.2	14	15.6	2631	93	8	3.3	0.0	19	90
C1-S	0	0.4	1	17.3	163	18	3	7.6	0.0	11	54
C1-M	13	0.2	2	9.4	358	22	3	1.5	0.5	12	54
C1-B	25	0.1	2	9.1	353	21	3	8.2	0.2	13	38

Vertical profiles of As and Sb are shown in **Fig. 4**. A distinctive trend was observed for Sb. At St. A1,

the concentration at the surface was 1.70 nM and increased with depth to 2.07 nM at the bottom. The opposite trend was observed at St. C1. Our observations clearly demonstrate the dynamic activity of this study area. Clearly, on-going surveys are required to further deepen our understanding of biogeochemical processes taking place in this study area.

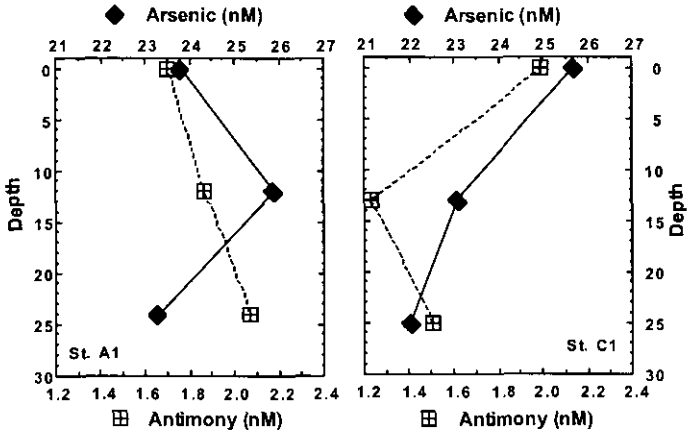

Fig.4 Vertical profiles of As and Sb at Sts A1 and C1.

4. CONCLUSIONS

Several trace metals were found to respond to PO_4 enrichment. The response was greatest for As: a decrease in As (III+V) with concomitant increase in As (III). The speciation study suggests that As (V) is taken up by phytoplankton together with phosphate and As (III) is released from phytoplakton cells. The concentrations of Cd, Cu and Ni also decreased with time in the phosphate enriched mesocosm. On the other hand, the concentrations of Mn and Sb increased with time in the phosphate enriched mesocosm. Biological processes including phytoplankton bloom are suggested as a main cause of the variations of these trace elements. However, no response to the phosphate enrichment was observed for the concentrations of Mo, V, and Co.

The concentration of 12 trace metals from the coastal stations ranged from 0.1 to 0.4 nM, from 1 to 13 nM, from 9.1 to 17.3 nM, from 21 to 2631 nM, from 18 to 93 nM, from 3 to 8 nM, 1.5 to 11.8 nM, from 0 to 0.5 nM, from 11 to 19 nM, from 38 to 90 nM, from 22.0 to 25.9 nM and from 1.19 to 2.07 nM for Cd, Co, Cu, Fe, Mn, Mo, Ni, Pb, V, Zn, respectively. These concentration levels are similar to those found in other coastal waters, implying no significant effect of the Changjian River could be detected at this sampling time.

ACKNOWLEDGEMENTS: We thank Dr. M.-H. Noel for her assistance in water sampling. We also thank for Dr. H. Obata for his laboratory assistance.

REFERENCES

1) Boyle, E., Collier, R., Dangler, A.T., Edmond, J.M., Ng, A.C. and Stallard, R.F.: On the chemical balance in estuaries. *Geochim. Cosmochim. Acta*, Vol. 38, pp. 1719-1728, 1974.
2) Aston, S.R.,: Estuarine chemistry, *Chemical Oceanography*, Vol. 1, 2nd ed, Riley, J.P. and Chester, R. eds., Academic Press, London, pp. 361-440, 1978.
3) Andreae, M.O., Asmond, J.-F., Foster, P. and Van't Dack, L.: Determination of antimony (III), antimony (V), and methylantimony species in natural waters by atomic absorption spectrometry with hydride generation. *Anal. Chem.*, Vol. 53, pp. 1766-1771, 1981.
4) Takayanagi, K. and Michel, P.: Semi-automated determination of dissolved antimony in seawater and sediment pore water. *Bunseki Kagaku*, Vol. 45, pp. 1115-1120. (in Japanese), 1996.
5) Isshiki, K., Tsuji, F. and Nakayama, E.: Preconcentration of trace metals from seawater with 7-dodecenyl-8-quinolinol impregnated macroporous resin. *Anal. Chem.*, Vol. 59, pp. 2491-2495, 1987.
6) Apte, S.C., Howard, A.G., Morris, R.J. and McCartney, M.J.: Arsenic, Antimony and Selenium Speciation during a spring

phytoplankton bloom in a closed experimental ecosystem. *Mar. Chem.*, Vol. 20, pp. 119-130, 1986.
7) Benson, A.A., Cooney, R.V. and Herrera-Lasso, J.M.: Arsenic metabolism in algae and higher plants. *J. Plant Nut.*, Vol. 3, pp. 285-292, 1981.
8) Kremling, K.: The distributions of cadmium, copper, nickel, manganese, and aluminum in surface waters of the open Atlantic and European shelf area. *Deep-Sea Res.*, Vol. 32, pp. 531-555, 1985.
9) Mart, L. and Nurnberg, H.W.: Cd, Pb, Cu, Ni, and Co distribution in the German Bight. *Mar. Chem.*, Vol. 18, pp. 197-213, 1986.
10) Nozaki, Y.: Trace elements in sea water: Their mean concentrations and North Pacific profiles. *Chikyukagaku*, Vol. 26, pp. 25-39 (in Japanese), 1992.

EFFECT OF PHOSPHOROUS ENRICHMENT ON PHYTOPLANKTON BLOOMS AND THE ROLE OF GRAZERS IN MARINE MESOCOSMS IN THE CHANGJIANG ESTUARY

Hiroshi KOSHIKAWA[1], Kai-Qin XU[1], Shogo MURAKAMI[1], Kunio KOHATA[2] and Masataka WATANABE[1]

[1] Soil and Water Environment Division, National Institute for Environmental Studies, Environment Agency (Onogawa 16-2, Tsukuba, Ibaraki 305-0053, Japan)

[2] Regional Environmental Division, National Institute for Environmental Studies, Environment Agency (Onogawa 16-2, Tsukuba, Ibaraki 305-0053, Japan)

To understand the effects of nutrient loading from the Changjiang River on the estuarine plankton ecosystem, phosphate enrichment mesocosm experiments were carried out in the estuary in autumn and spring. The results suggested that phytoplankton blooms could be easily triggered by the addition of only phosphorous to the estuary. The phytoplankton that formed the blooms were diatoms in the autumn and dinoflagellates in the spring. Since silica was rich in both seasons, there seems to be a factor other than silica concentration involved in the regulation of the dominant phytoplankton species. It was also shown that control of phytoplankton blooms through ingestion by zooplankton was more effective for diatoms than for dinoflagellates.

Keywords: *Mesocosm, Macronutrients, Phytoplankton bloom, Predator-prey interaction, and Microbial loop*

1. INTRODUCTION

Freshwater discharge from the Changjiang River, China, to the estuary amounts to about 9.24×10^{11} m^3 $year^{-1}$, ranking it fifth among the world's large rivers. Nutrients carried by fresh river-water provide an essential resource for primary productivity in the marine ecosystems of the Changjiang Estuary and other estuarine systems.[1,2)]

Inorganic nitrogen is considerably richer in the Changjiang estuarine water (e.g. 20 to 50 μM of NO_3^-) than it is in other large rivers such as the Amazon.[3)] However, concentrations of PO_4^{3-} range from 0.2 to 1 μM, which is comparable with those of other rivers, resulting in an environment with a high N/P ratio where phosphate is the limiting nutrient for phytoplankton growth.[4)] One explanation for the high N/P ratio in the estuarine water is that a large quantity of excess nitrogen is discharged from the many large cities in the Changjiang river catchment, and from agricultural lands where much nitrogen but little phosphorous fertilizer is used. In addition, phosphates may be adsorbed by suspended particles that sink to bottom in the river mouth, carrying the phosphates with them.[4)]

It is presumed that the recent rapid growth of the Chinese economy will cause excess nutrient loading through the river. The quality of these nutrients may also change with changes in agricultural practices, people's life-styles, etc. It is a fact that eutrophication, occurrences of harmful algal blooms (HAB) have been becoming a serious problem along the Chinese coastal area.[5)] In the near future, fertilization will be further increased to boost agricultural production and conversion to more phosphorous-rich fertilizers will occur. Furthermore, with development of the catchment area for flood control (e.g. construction of the Three

Gorges Dam), it is presumed that there will be fewer suspended particles reaching the estuary.[6] These factors may cause an increase in the total amount of nutrient loading and/or a change of nutrient quality (e.g. a decrease in the N/P ratio) and will affect the marine ecosystem involving the composition of plankton species, the structure of the food chain, and the elemental cycle in the Changjiang Estuary.

The goal of our research is to understand how the marine ecosystem and its biological carbon cycle will be affected by the nutrient load and the disturbance that will occur in the near future. In the present study, we assumed a situation in which the N/P ratio decreases with an increased supply of phosphate into the estuary through the river. We carried out phosphate enrichment experiments using marine mesocosms in the Changjiang Estuary area about 100 km from the river mouth in October 1997 (autumn) and May 1998 (spring). Mesocosms that capture natural marine environments enable us to investigate the responses of the ecosystem to nutrient disturbance.[7] Our mesocosm experiments focused on how the phytoplankton communities responded to lowering of the N/P ratio in autumn and spring and on how the predator–prey interactions changed following the response of phytoplankton to this nutrient disturbance.

2. MATERIALS AND METHODS

(1) *Marine mesocosms and experimental site*

A pair of bag-type floating mesocosms were deployed twice near Liuhuashan – Huanaoshan (lat 30°50'N, long 122°37'E) in the Changjiang estuarine area for 8 days from 10 October (day 0) to 17 October (day 7), 1997 (autumn) and for 9 days from 18 May (day 0) to 26 May (day 7), 1998 (spring). Each mesocosm (5 m *deep*, 3 m *diameter*, *volume* about 25 m^3) was made of ethylene-vinyl-acetate reinforced with a polyester grid; they were translucent (light transparency about 50%) with no chemical release from the surface. A location map and schematic illustration of the mesocosm are shown in another article contained in these proceedings.[8] On the evening of day 0, in both autumn and spring, seawater was introduced into the pair of mesocosms through the bottom valve almost simultaneously to capture seawater from the same mass to the extent possible. The paired mesocosms filled with seawater were moored to the stern of the anchored research vessel 'Haijian 49' of the State Oceanic Administration, China.

Nutrient concentrations (N, P) of the mesocosms were roughly determined on board the research vessel just after installation of the mesocosms (evening of day 0). Phosphate ($NaH_2PO_4 \cdot 2H_2O$) was then added to one of the paired mesocosms at night, lowering the N/P atomic ratio of the mesocosm seawater to about 10 (P-mesocosm). The mesocosm without added phosphate was a control system (C-mesocosm).

We deployed the autumn mesocosms in the area of sea north of Huanaoshan Island, a site which is more directly influenced by the Changjiang fresh water than is the southern area. However, a storm surge threatened to sink the C-mesocosm and it was salvaged onto the vessel on the evening of day 1 making it impossible to take samples from the C-mesocosm in the autumn experiment. Consequently, in the spring experiment, we deployed both mesocosms in the area of sea south of the island. Conditions in this area were relatively calm, though the ocean current was more likely to be affected by the insular geography (i.e. some small scattered islands) and seawater involving less Changjiang fresh water often flowed into this area. The P-mesocosm could be deployed through the whole spring experimental period (9 days) and the C-mesocosm was done for 7 days.

(2) Sampling and measurements

Seawater temperature and salinity were measured (by Surveyor II, Hydrolab) at depths of 1, 2 and 3 m inside the mesocosms and at depths of 1 to 5 m outside the mesocosms on the evening of day 0 (before phosphate addition) and every morning on days 1 to 7. Seawater samples were collected from both mesocosms at a depth of 1 m, using 10-liter Van-Dorn samplers, on the evening of day 0 and every morning on the other days. In the autumn experiment, seawater was sampled outside of the P-mesocosm. Subsamples of seawater were filtered with pre-combusted (450°C 4 h) Whatman GF/F filters for analysis of nutrients (by Traacs 800, Bran+Luebbe), Chl.*a* (HPLC system[9], Shimadzu), particulate organic carbon (POC, by EA1108, Fisons), and dissolved organic carbon (DOC, by TOC5000A, Shimadzu). The filters and filtrates were stored at –20 °C prior to analysis. A subsample of seawater with HgCl preservative was stored at 5 °C prior to measurement of dissolved inorganic carbon (DIC, by CO_2 Coulometer 5011, UIC Inc.). Phytoplankton samples were fixed with 6% formalin, and the species composition, abundance and greatest axial linear dimension (GALD) were determined by microscopy. A subsample for bacterioplankton was fixed with

glutaraldehyde (final conc. 1%), stained with DAPI[10], and the abundance determined by direct counts under epifluorescence microscopy.[11] A subsample for pico-sized autotrophic plankton (autotrophic picoplankton, APP) was fixed with glutaraldehyde and stored at –20 °C prior to flow cytometric analysis (by FACSCalibur, Becton Dickinson). Samples for micro-sized zooplankton and protists (>20 μm) and metazooplankton (>100 μm) were passed sequentially through 100-μm and 20-μm plankton nets; these samples were fixed with 6% formalin and stored in a cool, dark place. The species composition and abundance were determined by direct counts under light microscopy.

To estimate the transfer of photosynthetic and bacterial production to the grazers, frequent *in situ* batch incubations with dissolved organic and inorganic ^{13}C tracers[12] were conducted most days during the daytime using mesocosm seawater taken from a depth of 1 m. The tracer used to measure the bacterial carbon pathway was D-[U-6-^{13}C]glucose (final conc. ca. 5 mg l^{-1}). For measurement of the photosynthetic carbon pathway, NaH[^{13}C]O_3 (ca. 20 mg l^{-1}) was used. Seawater was transferred to an acid-cleaned 4.5-l clear polycarbonate bottle and the relevant organic or inorganic ^{13}C tracer was added. The bottle was incubated in a seawater bath for 4 h on board the vessel. The *in situ* incubated sample was fractionated by sequential filtration using plankton nets (200-μm, 100-μm, 20-μm, and 10-μm mesh) and a pre-combusted Whatman GF/F (ca. 0.7-μm pore size) filter. The samples on the plankton nets were first washed with filtered seawater (GF/F) to remove particles smaller than the respective mesh sizes and then collected on pre-combusted Whatman GF/C filters. In order to determine the natural isotope ratio of particulate carbon at the beginning of each incubation, the original seawater was also filtered using the same protocol. All filters were stored at -20 °C until analysis. POC and ^{13}C abundance (atom %) were determined using a system comprised of an elemental analyzer (EA1108, Fisons) and an isotope-ratio mass spectrometer (MAT252, Finnigan MAT).[13] The net transformation of the ^{13}C label from dissolved to particulate carbon for each size fraction was calculated as the excess ^{13}C (μg^{13}C l^{-1} 4 h^{-1}) against the natural abundance of the carbon isotope (Equation 1),

$$^{13}C_{ex} = (a_s - a_n) \times POC \quad (1)$$

where a_s is the ^{13}C atom% of a given size fraction in the incubated sample and a_n is the ^{13}C atom% in the natural sample. POC (μg l^{-1}) is the particulate organic carbon in a given size fraction. The >100-μm fraction would comprise mostly the metazooplankton assemblage.

To determine the relative significance of carbon transfer to metazooplankton through bacteria and autotrophs, we calculated the proportion of ^{13}C-label transferred to the >100-μm fraction ($PLT_{>100\mu m}$, %) as the amount transferred to the >100-μm fraction ($^{13}C_{ex,>100\mu m}$) over the total transferred to all fractions ($^{13}C_{ex,all}$) (Equation 2):

$$PLT_{>100\mu m} = \left(\frac{^{13}C_{ex,>100\mu m}}{^{13}C_{ex,all}} \right) \times 100 \quad (2)$$

The PLT represents the proportion of carbon fixed by bacterioplankton or autotrophs and conserved in the particles that may be transferred to metazooplankton by their feeding activities during the 4-h incubation. A proportion of the fixed ^{13}C-label will, however, be respired by the producers themselves and by some intermediaries such as heterotrophic protists. The PLT is an incubation time-dependent value but can be an index of the degree of ease with which carbon passes through the trophic levels to metazooplankton.[12]

The proportion of ^{13}C-label transferred to the 20 to 100-μm fraction ($PLT_{20\mu m}$) was also calculated to consider the transfer of bacterial carbon and photosynthetic carbon to micro-sized grazers when the phytoplankton assemblages were comprised of small autotrophs (<20 μm).

Photosynthetic production was estimated by summation of the rates of carbon transformation from DIC to particles in each size fraction; the calculation was based on the ^{13}C method of Hama et al.[14] Bacterial activity was estimated by total fixation of ^{13}C-glucose into particulate matter.

3. RESULTS

(1) Seawater temperature and salinity in the mesocosms

Daily average of seawater temperatures within the mesocosms were 23.0 °C in the autumn and 19.6 °C in the spring (Fig. 1). The daily changes in seawater temperatures inside and outside the mesocosms were

almost synchronized. Salinity outside the mesocosms varied from 26.4‰ to 30.3‰ in the autumn and from 25.3‰ to 30.6‰ in the spring. Salinity inside the mesocosms ranged from 25.0‰ to 26.5‰ in the autumn and from 28.1‰ to 28.7‰ in the spring. These results indicate that the influence of the Changjiang fresh water on the experimental sea area fluctuated widely according to changes in the tidal current and, in both seasons, the seawater captured in the mesocosms had been influenced relatively strongly by the fresh water.

In the spring, salinity varied by about 0.6‰ within the P-mesocosm and about 0.2‰ within the C-mesocosm, meaning the seawater mass of each mesocosm was almost perfectly isolated. In the autumn mesocosm, however, the salinity increased gradually toward the end of the experimental period. This would be because of the intrusion of the storm surge into the mesocosm in the autumn.

Vertical profiles of seawater temperature and salinity (not shown) were almost the same each day, indicating that the water mass of each mesocosm was almost completely homogeneously mixed.

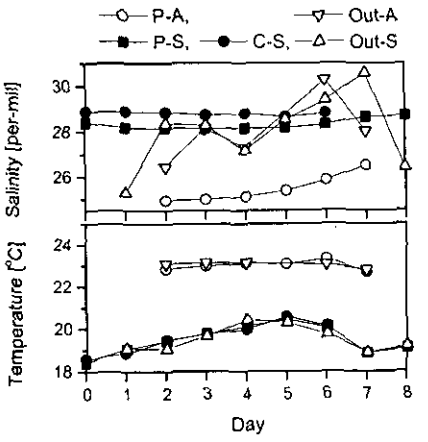

Fig. 1 Temporal changes in salinity and seawater temperatures inside (average values at 1, 2 and 3 m depths) and outside mesocosms (average values at 1 – 5 m depths). P-A: P-mesocosm in autumn; Out-A: outside mesocosm in autumn; P-S: P-mesocosm in spring; C-S: C-mesocosm in spring; and Out-S: outside mesocosm in spring.

(2) Nutrient conditions

Initial N/P atomic ratios of macronutrients in the P-mesocosms (day 0) were about 38 in the autumn ($[NH_4^+]$ = 0.5 μM, $[NO_3^-]$ = 24 μM, and $[PO_4^{3-}]$ = 0.65 μM) and about 94 in the spring ($[NH_4^+]$ = 1.2 μM, $[NO_3^-]$ = 16 μM and $[PO_4^{3-}]$ = 0.18 μM) (Fig. 2). These N/P ratios were considerably higher than the Redfield-Ratio, implying that the mesocosm ecosystems were under P-limited. Initial concentrations of $[Si(OH)_4]$ were 40 μM (autumn) and 29 μM (spring).

After adding PO_4^{3-} to the P-mesocosms on the night of day 0, the phosphate concentrations in the

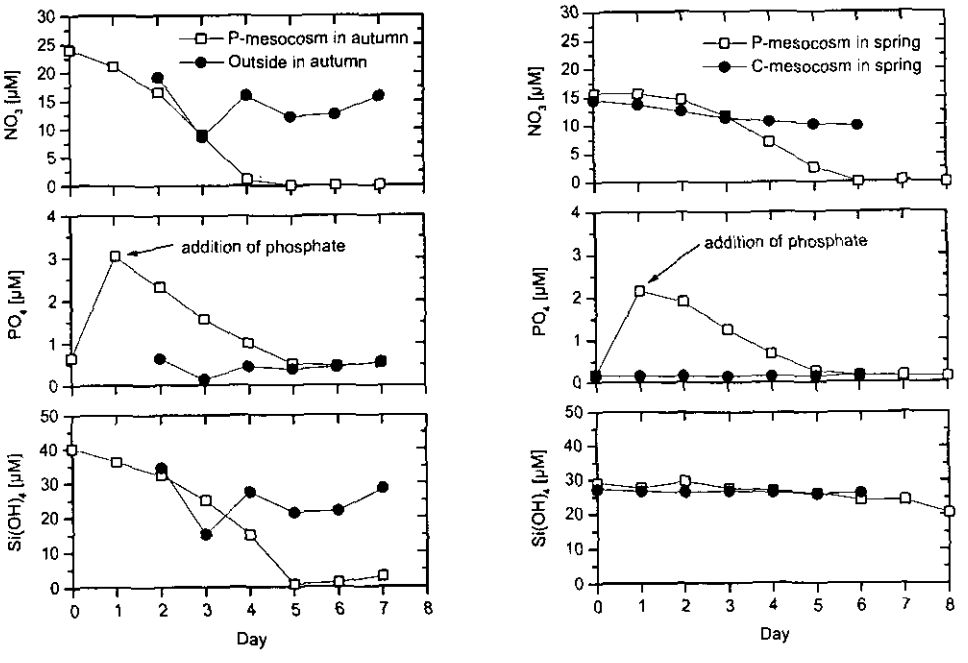

Fig. 2 Temporal changes in concentrations of macronutrients in the autumn and spring experiments.

P-mesocosms increased to 3.1 μM (autumn) and 2.2 μM (spring) by the next morning (day 1). The phosphate concentrations then began to decrease rapidly, reaching 0.51 μM on day 5 (autumn) and 0.16 μM on day 6 (spring)—lower than their initial concentrations. The concentrations of NO_3^- also decreased concomitantly with the phosphate and became < 0.1 μM on day 5 (autumn) and day 6 (spring). The phosphate additions decreased the day 1 N/P atomic ratios to about 7.2 in the autumn and 8.0 in the spring. The N/P ratios continued to decrease and reached minimums of 1.2 in autumn and 6.4 in spring. The concentrations of $Si(OH)_4$ in the autumn mesocosm decreased from 40.2 μM (day 0) to 0.7 μM (day 5) but, in the spring mesocosms, the decrease was only from 29.0 to 20.6 μM. The reduced consumption of silicate in the spring would be caused by the difference in dominant phytoplankton (i.e. diatoms were predominant in the autumn and dinoflagellates predominant in the spring, as described in more detail later).

In the C-mesocosm of the spring experiment, the concentrations of PO_4^{3-} and $Si(OH)_4$ showed little fluctuations with ranges of 0.14 – 0.16 μM and 27.2 – 25.9 μM, respectively. Only the NO_3^- showed a decreasing trend—from 14.5 μM (day 0) to 9.9 μM (day 6). However, the rate of NO_3^- decrease in the C-mesocosm was clearly slower than that in the P-mesocosm, suggesting that NO_3^- uptake by organisms in the C-mesocosm was limited by available phosphate.

In the surface layer outside the autumn mesocosm, the daily concentrations of macronutrients showed large fluctuation. The ranges of $[PO_4^{3-}]$, $[NO_3^-]$ and $[Si(OH)_4]$ were 0.14 – 0.80, 8.6 – 19.1 and 15.2 – 34.5 μM, respectively. However, we found that there was a positive correlation between the NO_3^- and $Si(OH)_4$ concentrations ($r^2 > 0.99$, n=8). We also observed that their concentrations tended to increase as salinity decreased. Considering that the Changjiang water was rich in lithogenous silica, we therefore concluded that the concentration of $Si(OH)_4$ in the area of sea around the mesocosm fluctuated depending on the influence of the Changjiang fresh water. The fact that there was a correlation between NO_3^- and $Si(OH)_4$ may also indicate that phytoplankton around the experiment sea area could not efficiently consume the 2 kinds of nutrients, which might be mainly supplied by the Changjiang River. Turbid water containing much silt sometimes occurred in this area of sea, with transparency and turbidity of about 1 – 2 m and 1.5 – 3 mg l^{-1}, respectively. However, the ordinary transparency was at least several meters (data not shown). Therefore, we considered that nitrate uptake by phytoplankton in this area was mainly suppressed by the limitation of phosphate rather than conditions of light.

(3) Plankton abundance and activity of photosynthetic and bacterial producers

a) P-mesocosm in autumn, 1997

The initial concentration of POC (day 0) in the autumn P-mesocosm was 0.42 mgC l^{-1} (Fig. 3). As the nutrients decreased, POC continually increased and reached 1.78 mgC l^{-1} on day 6. Photosynthetic production was highest on day 1 (39.4 μgC l^{-1} h^{-1}) and continued with relatively large values until day 4. After day 6, however, the production was very low (4.0 – 4.8 μgC l^{-1} h^{-1}). POC also decreased from 1.78 to 1.00 mgC l^{-1} from day 6 to day 7). The tendency of the daily change in DOC concentration was similar to that of POC; it increased from 1.30 mgC l^{-1} (day 2) to 2.22 mgC l^{-1} (day 6) and afterward decreased somewhat.

The initial phytoplankton assemblage in the autumn P-mesocosm was comprised of more than 90% diatoms (the dominant species was *Skeletonema costatum*) (Fig. 4). The cell density of diatoms increased gradually from 1.4×10^2 (day 1) to 1.0×10^4 cells ml^{-1} (day 5). Afterwards, it decreased rapidly and reached 0.5×10^2 cells ml^{-1} on day 7. Chl.*a* increased from 4.8 (day 1) to 18.7 μgChl.*a* l^{-1} (day 4) concomitantly with the abundance peak of dominant diatoms, and decreased rapidly from day 5 to 6 (Fig. 3).

The major zooplankton (>100 μm) groups observed in the P-mesocosm were copepods (mainly *Paracalanus* sp. and *Oithona* sp.) and appendicularians (*Oikopleura* sp.) (Fig. 4). Copepods were observed throughout the whole period. Their abundance showed a tendency of increase from day 1 (11 individuals l^{-1}) to day 7 (72 individuals l^{-1}). Appendicularians were first observed on day 3 and their abundance reached a maximum on day 6 (39 individuals l^{-1}).

Among the micro-sized zooplankton (20 – 100 μm), copepod nauplii, appendicularians, and ciliates were observed in the P-mesocosm. Among them, the appendicularians increased suddenly from day 3 (54 individuals l^{-1}) to day 5 (6.5×10^2 individuals l^{-1}), and became the dominant zooplankton in this size class (Fig. 4).

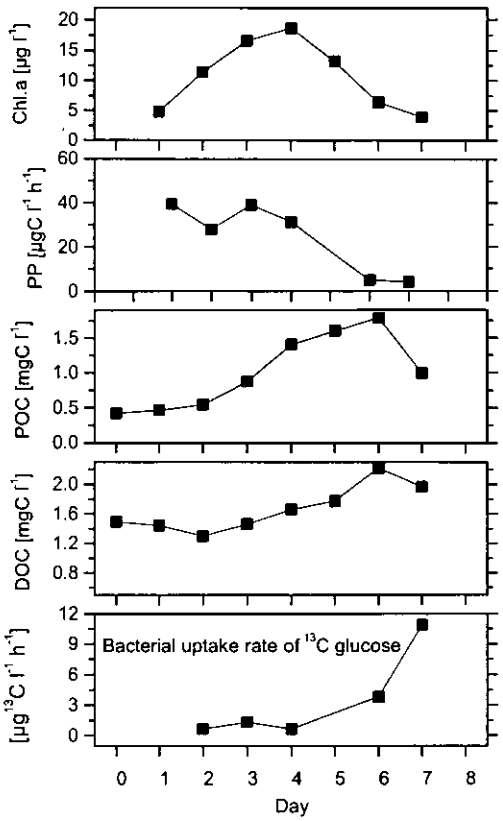

Fig. 3 Daily changes in Chl.*a*, Photosynthetic production (PP), POC, DOC, and bacterial uptake rate of ^{13}C-glucose in the autumn P-mesocosm.

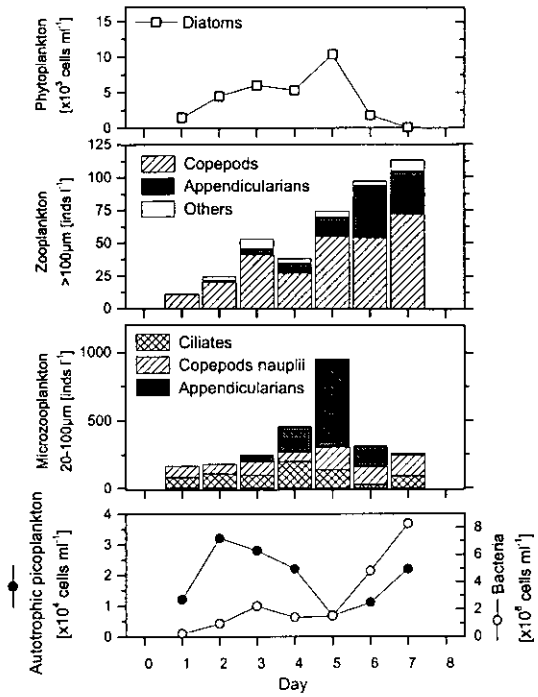

Fig. 4 Daily changes in abundances of organisms in the autumn P-mesocosm.

Bacterioplankton density increased slightly and formed the first peak on day 3 (2.2×10^6 cells ml^{-1}), and subsequently decreased a little from day 3 to 4. Afterwards, it increased dramatically and reached the maximum on day 7 (8.3×10^6 cells ml^{-1}) (Fig. 4). Bacterial activity, determined by ^{13}C-glucose uptake, increased from 0.68 (day 2) to 10.9 µg^{13}C l^{-1} h^{-1} (day 7) (Fig. 3) concomitant with the increase of bacterial abundance (Fig. 4). Abundance of APP (autotrophic picoplankton) increased slightly from day 1 (1.2×10^4 cells ml^{-1}) to day 2 (3.2×10^4 cells ml^{-1}), but subsequently decreased rapidly from day 2 to day 5 (6.8×10^3 cells ml^{-1}). By day 6, APP had reverted to nearly its initial abundance (Fig. 4).

b) P- and C-mesocosms in spring, 1998

Initial concentrations of POC (day 0) were 0.55 mgC l^{-1} and 0.22 mgC l^{-1} in the C- and P-mesocosms, respectively (Fig. 5). Chl.*a* concentrations were 1.8 (C-mesocosm) and 0.8 µgChl.*a* l^{-1} (P-mesocosm). These results revealed that, from the start of the experiment, there was more biomass in the control mesocosm than in the phosphate-enriched mesocosm. This was probably due to the patchiness of the seawater, although the 2 mesocosms were enclosed almost simultaneously.

In the P-mesocosm, POC concentration increased continually with a decrease in nutrients and reached the maximum on day 8 (1.29 mgC l^{-1}). Photosynthetic production also increased gradually from 4.1 µgC l^{-1} h^{-1} (day 1) to 53.5 µgC l^{-1} h^{-1} (day 5) and then decreased to 26.1 µgC l^{-1} h^{-1} (day 8). The trend of daily change in the photosynthetic production in spring was different from that in the autumn P-mesocosm (i.e. in the autumn, the largest value was observed on day 1, and it decreased until the end). An almost continuous increase in DOC concentration was observed in the P-mesocosm but the range and the average of all the concentrations were smaller (i.e. 0.95 – 1.27 mgC l^{-1}, average = 1.13 mgC l^{-1}) than in the autumn mesocosm (average = 1.67 mgC l^{-1}).

In the C-mesocosm, no clear increase of POC concentration was found, but the POC fluctuated (0.39 – 0.72 mgC l^{-1}, average = 0.60 mgC l^{-1}) around the initial value (0.55 mgC l^{-1}). Daily changes in photosynthetic production remained within the range of 3.5 to 12.1 μgC l^{-1} h^{-1} and the average (= 6.8 μgC l^{-1} h^{-1}) was approximately 1/4 of that in the P-mesocosm. Chl.*a* concentration also showed no tendency of increase. DOC concentration showed a slight increase and smaller average than that in the P-mesocosm.

Initially, phytoplankton in both mesocosms consisted almost entirely of dinoflagellates (dominant species was *Prorocentrum dentatum*) (Figs. 6 and 7). In the P-mesocosm, the abundance of dinoflagellates increased gradually from 2×10 cells ml^{-1} (day 1) to 2.7×10^2 cells ml^{-1} (day 6) (Fig. 6). In the C-mesocosm, on the other hand, though the minimum abundance was counted on day 1 (3×10 cells ml^{-1}), only a small daily change was observed with a range of $0.7 - 1.7 \times 10^2$ cells ml^{-1} after day 2 (Fig. 7). In the P-mesocosm, diatoms (*Skeletonema costatum*) began to be observed on day 4 and they increased slightly to reach 0.8×10^2 cells ml^{-1} on day 6.

In both mesocosms, large-sized organisms (>100 μm) consisted of copepods (mainly *Paracalanus* sp., *Oithona* sp. and *Corycaeus* sp.) and *Noctiluca scintillans*, which is a heterotrophic dinoflagellate (Figs. 6 and 7). The abundance of copepods in the P-mesocosm was 0.5 individuals l^{-1} on day 1 which subsequently increased to 31 individuals l^{-1} on day 7 (Fig. 6). *N. scintillans* began to be observed in large numbers on day 3 (36 individuals l^{-1}) and reached a maximum on day 6 (56 individuals l^{-1}). Overall, the abundance of copepods was larger in the C-mesocosm than in the P-mesocosm and increased to 49 individuals l^{-1} on day 6 (Fig. 7). The abundance of *N. scintillans* in the C-mesocosm was comparable with that in the P-mesocosm.

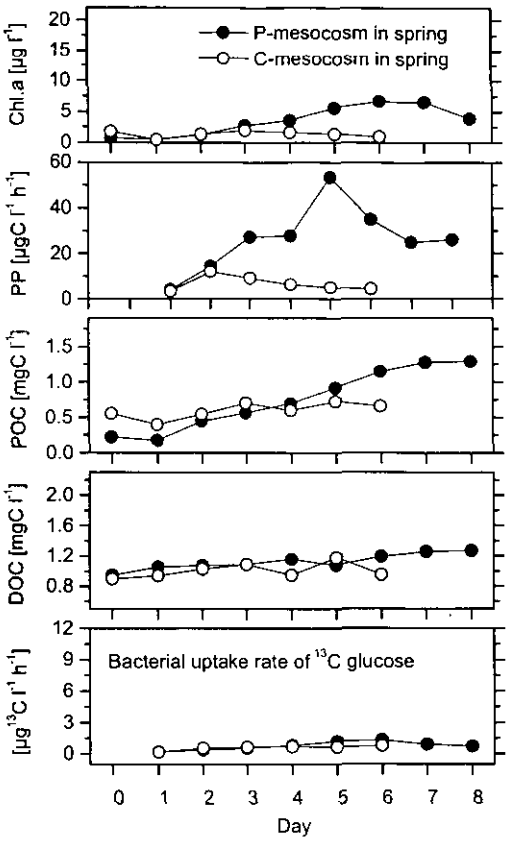

Fig. 5 Daily changes in Chl.*a*, Photosynthetic production (PP), POC, DOC, and bacterial uptake rate of ^{13}C glucose in the spring P- and C-mesocosms.

In the micro-sized (20 – 100 μm) zooplankton samples, we mainly observed copepod nauplii and ciliates (Figs. 6 and 7). In the P-mesocosm, the initial abundance of ciliates (day 1) was very small but they increased rapidly from 4.3×10^2 individuals l^{-1} (day 2) to 1.6×10^3 individuals l^{-1} (day 7). In the C-mesocosm, on the other hand, their abundance changed within only a small range from $1.2 - 3.5 \times 10^2$ individuals l^{-1}.

The initial density of bacterioplankton (day 0) was 8.1×10^5 cells ml^{-1} in the P-mesocosm and 1.1×10^6 cells ml^{-1} in the C-mesocosm. In the P-mesocosm, cell density increased until day 5 (3.6×10^6 cells ml^{-1}) and afterward decreased somewhat (2.9×10^6 cells ml^{-1} on day 8) (Fig. 6). In the C-mesocosm, a slight increase was observed, but the value of 2.2×10^6 cells ml^{-1} (day 4) was the maximum (Fig. 7). The average of the bacterial activity was slightly higher in the P-mesocosm (0.77 μg^{13}C l^{-1} h^{-1}) than in the C-mesocosm (0.58 μg^{13}C l^{-1} h^{-1}) (Fig. 5). However, activities in the spring P- and C-mesocosms did not show any of the conspicuous increases that were observed in the latter period of the autumn P-mesocosm experiment.

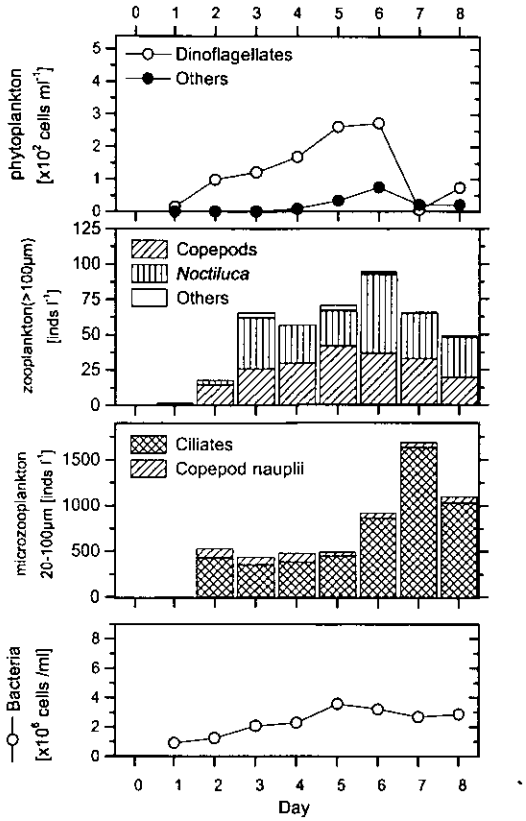

Fig. 6 Daily changes in abundances of organisms in the spring P-mesocosm.

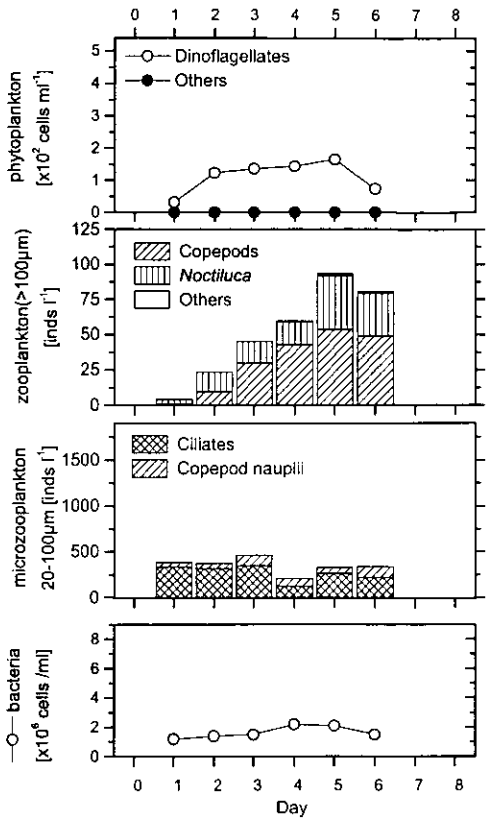

Fig. 7 Daily changes in abundances of organisms in the spring C-mesocosm.

(4) Proportion of ^{13}C-label transfer from producers to grazers

With the ^{13}C tracer experiments, the proportion of the ^{13}C label that was transferred ($PLT_{>100\mu m}$) in the photosynthetic pathway in the autumn P-mesocosm where diatoms were predominant, was initially less than 0.2% (day 1) and subsequently increased to 11% on day 6 (Fig. 8). In the spring P-mesocosm where dinoflagellates were dominant, however, $PLT_{>100\mu m}$ in the photosynthetic pathway remained lower throughout the experiment period (average = 0.5%) and the maximum was only 1.1%. The $PLT_{>100\mu m}$ in the spring C-mesocosm was of almost the same magnitude (average = 0.7%). The $PLT_{20\mu m}$ of the photosynthetic pathway in the spring (Fig. 8) gradually increased in both P- and C-mesocosms but tended to be higher in the P-mesocosm than in the C-mesocosm. The $PLT_{20\mu m}$ in the autumn is not shown here because, according to our microscopic analysis, a significant proportion of the dominant *Skeletonema* would be in the 20 – 100-µm fraction (GALD of a colony for *S. costatum* was about 25 – 50 µm).

The $PLT_{>100\ \mu m}$ values in the bacterial pathway were initially slightly larger in the spring P-mesocosm than in the autumn P-mesocosm, but after day 4 the PLTs in the autumn P-mesocosm rose suddenly (Fig. 9). The $PLT_{20\mu m}$ of the bacterial pathway in the autumn showed a similar tendency of change as the $PLT_{>100\mu m}$ in that season. Consequently, the overall $PLT_{>100\mu m}$ and $PLT_{20\mu m}$ in the bacterial pathway were higher in the autumn than in the spring.

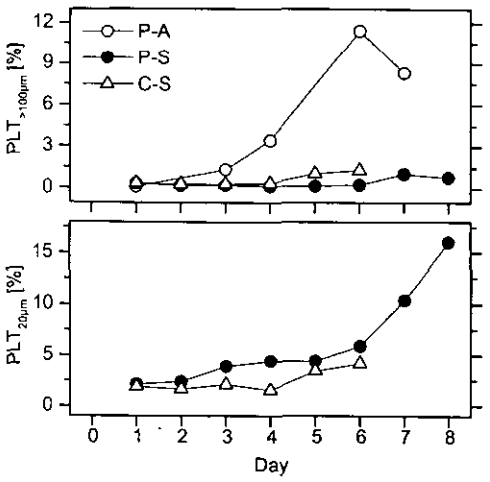

Fig. 8 Daily changes in $PLT_{>100\mu m}$ and $PLT_{20\mu m}$ of the photosynthetic pathway.
P-A: autumn P-mesocosm; P-S: spring P-mesocosm; and C-S: spring C-mesocosm.

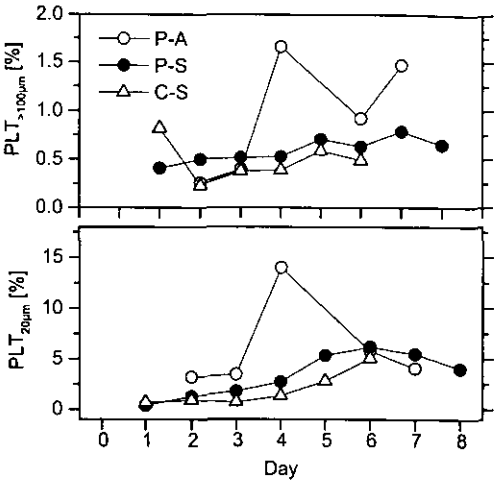

Fig. 9 Daily $PLT_{>100\mu m}$ and $PLT_{20\mu m}$ of the bacterial pathway.
P-A: autumn P-mesocosm; P-S: spring P-mesocosm; and C-S: spring C-mesocosm.

4. DISCUSSION

(1) Effect of phosphate enrichment on productivity in mesocosms

In the phosphate enriched mesocosms where the diatom *S. costatum* and dinoflagellate *P. dentatum* were dominant in the autumn and spring, respectively, both dominant species increased their abundance by about 10-fold within a few days following the addition of phosphate (Figs. 4 and 6). The consumption of nitrate was very fast and by day 5 (autumn) or day 6 (spring) the concentration had fallen to almost a limiting level (Fig. 2). In the autumn mesocosm with diatoms, silicate concentration also decreased and became < 1 μM on day 5. In the control mesocosm, on the other hand, such a marked consumption of nutrients was not observed. This clearly suggests that the captured ecosystems were initially phosphate limited and, consequently, the phytoplankton blooms observed in the P-mesocosms were caused by only the addition of phosphate.

In the seawater outside of the autumn mesocosm, the ratio of nitrate and silicate nutrients remained almost constant, even with large daily fluctuations in their concentrations, and phosphate concentration remained low (average = 0.5 μM) over the whole period of the mesocosm experiment (Fig. 2). These nutrient conditions outside of the mesocosms were similar to those in the initial seawater of the mesocosms. Therefore, we suggest that the phytoplankton were always under phosphate limiting conditions, not only within the mesocosms, but also over this area of sea. We also assumed that the observation was not a result unique to the mesocosm ecosystem, but may enable us to deduce the ecosystem response to phosphate loading in the Changjiang estuarine area.

The P-mesocosm in the autumn initially contained about twice the biomass of the P-mesocosm in the spring; the POC concentrations on day 0 were 0.48 and 0.22 mgC l^{-1} in the autumn and spring, respectively (Figs. 3 and 5). However, the averages of photosynthetic production for each experiment period were almost equivalent (24.4 and 26.6 μgC l^{-1} h^{-1}, respectively). Differences between the initial POC concentration (day 0) and the maximum value (day 6 in the autumn and day 8 in the spring) were 1.36 in the autumn P-mesocosm and 1.07 mgC l^{-1} in the spring P-mesocosm, respectively. These differences were small, as were the difference in photosynthetic production. In the latter periods of the mesocosm experiments in both seasons, there was almost no nitrate or silicate available for phytoplankton growth; it would be impossible to further increase the POC until the nutrients were returned through decomposition of the produced POC. Therefore, it would be suggested that, under conditions where phosphate loading reduces the N/P atomic ratio to approximately 8, the ecosystems in the mesocosms (or in this area of sea) will respond by increasing biomass up to about 1 mg C^{-1} until nitrate or silicate becomes the limiting factor within about a week.

(2) Difference in rate of nutrient uptake by phytoplankton in autumn and spring P-mesocosms

Despite there being a great difference in the initial abundance and species composition of the phytoplankton in the autumn and spring P-mesocosms, the increases of biomass in both mesocosms were almost equivalent. From this observation, we discuss in this subsection the nutrient consumption and manner of growth of the dominant phytoplankton.

Chl.*a*-specific photosynthetic rates on day 1 were quite similar in the 2 seasons (8.2 and 8.8 μgC μgChl.a^{-1} l^{-1} h^{-1} in the autumn and spring P-mesocosms, respectively), but large differences were observed afterward (Fig. 10). In the autumn, 2.4 μgC μgChl.a^{-1} l^{-1} h^{-1} was recorded on day 2 and it continued to decrease, reaching a minimum on day 6 (0.8 μgC μgChl.a^{-1} l^{-1} h^{-1}). In the spring, on the other hand, it increased to 11.1 μgC μgChl.a^{-1} l^{-1} h^{-1} on day 2 and then decreased gradually.

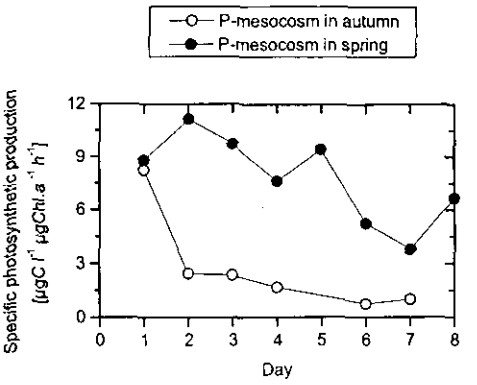

Fig. 10 Daily change in Chl.*a*-specific photosynthetic production rate in the P-mesocosms in autumn (white circles) and spring (black circles).

The rapid decline of the Chl.*a*-specific photosynthetic rate in the autumn might be caused by an environment with an insufficient concentration of nutrients. For example, nitrate concentration decreased more quickly in the autumn than in the spring (Fig. 2), probably because of the larger initial abundance of phytoplankton. In addition to this factor of initial difference in phytoplankton abundance, we expect that *S. costatum,* dominant in the autumn, could respond more sensitively to the phosphate addition than could *P. dentatum,* which was dominant in the spring. *S. costatum* is known as a species that has the ability to respond quickly to nutrient loading and easily forms red-tides in coastal areas. A study in Tokyo Bay, Japan, reported that during the blooming process of *S. costatum*, the cell-volume-specific photosynthetic rate was highest in the initial phase of the bloom and lowest at the peak of bloom.[15] In this study, the highest Chl.*a*-specific photosynthetic rate in the autumn was observed on day 1 and the lowest rate was around day 5 when the abundance of *S costatum* was at its maximum (Fig. 10). Moreover, comparing the Chl.*a*-specific rate of nitrate uptake in the autumn and spring mesocosms, the maximum rate of uptake was observed from day 0 to 1 in the autumn (0.61 μM μgChl.a^{-1} day^{-1}) and from day 3 to 4 in the spring (1.27 μM μgChl.a^{-1} day^{-1}) (Fig. 11). From these observations, we consider that in the autumn, because the dominant *S. costatum* responds quickly to the added phosphate and their initial abundance was relatively large, the other available nutrients were consumed almost entirely by the middle of the experiment period and their growth consequently stagnated in the latter period. In the spring mesocosm, on the other hand, we consider that, because the initial abundance of phytoplankton was relatively small and the dominant *P. dentatum* responds only slowly to the added phosphate, the photosynthetic activity was maintained throughout the whole experiment period without the relatively rapid consumption of the other nutrients.

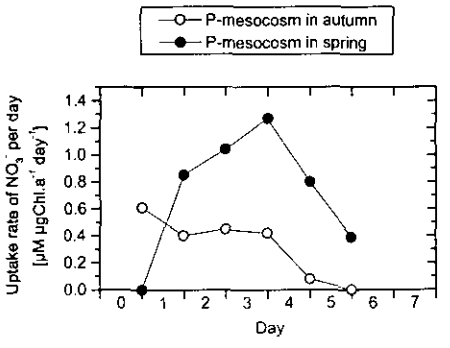

Fig. 11 Chl.*a*-specific nitrate uptake rate in the autumn

The phytoplankton species that formed blooms within the mesocosms were those that were dominant at the beginning of the experiments in both seasons in this area of sea. No succession of dominant species was clearly observed. A major reason would be that the experiment period (about a week) was too short for such a succession to occur. However, the different characteristics of response to phosphate loading may be considered one of the factors regulating the dominant phytoplankton species in this area of sea. Phosphate in the Changjiang Estuary would be supplied by the fresh water from the river and from the seafloor via decomposition of sedimented organic matter. The phosphate loading from the river would be at a relatively stable, low concentration, although it depends on the amounts of the fresh water discharge. The phosphate supplement from the seafloor may usually be maintained at a constant level, but sporadic storms such as typhoons may result in considerable amounts of phosphate being released from the seafloor to the seawater. A sudden increase in phosphate concentration may induce a bloom of *S. costatum,* rather than of *P. dentatum,*

because the former species can respond more sensitively to the change in nutrient conditions. We assume that the dynamics of phosphate supply to the seawater may play a role in the succession of phytoplankton species in the Changjiang Estuary.

(3) Ecosystem structure and carbon cycle in mesocosm food webs

a) Carbon flow from photosynthetic production

In the P-mesocosms of both seasons, the number of zooplankton increased almost concomitantly with the phytoplankton blooms (Figs. 4 and 6). We presumed that the quantity of carbon transfer in the food webs changed according the increased primary production in the ecosystems of the 2 mesocosms. The zooplankton assemblages in the autumn and spring mesocosms were different and, hence, we presumed that there were different pathways of carbon transfer in each ecosystem.

In the autumn P-mesocosm where diatoms were dominant, we observed copepods in the >100-μm fraction as a dominant zooplankton group throughout the whole period of the experiment. In the middle period of the experiment, we observed an increase of appendicularians and they became one of dominant zooplankton groups (Fig. 4). The proportion of ^{13}C-label transferred to the >100-μm fraction ($PLT_{>100\mu m}$) in the photosynthetic pathway was initially less than 0.2% (day 1), but increased gradually to over 11% on day 6 (Fig. 8). Among the dominant zooplankton, appendicularians have only the ability to ingest pico- and nano-sized particles and reject larger particles.[16,17] *S. costatum*, the dominant species in the mesocosm, is a chain-forming species and almost of the *S. costatum* we observed in this study could be grouped with the 20 – 100-μm fraction. The chain-forming diatoms are considered to be rejected by the appendicularians[16] but readily ingested by the copepods[18] which were the other dominant zooplankton. Therefore, we concluded that the higher PLTs in the latter period were due to ingestion of the diatoms, not by the appendicularians but by the copepods. A large decrease in the POC concentration was measured from day 6 to 7 in the autumn (Fig. 3). We concluded that the decrease in the POC was caused not only by stagnation of phytoplankton growth due to the nutrient deficiency, but also by removal through the strong grazing pressure of the copepods.

In the spring P-mesocosm where dinoflagellates were dominant, plankton assemblages in the >100-μm fraction comprised mainly of copepods and *N. scintillans* and the abundances of these grazers increased with an increase in cell density of phytoplankton (Fig. 6). Considering the increase in numbers, we assumed that these large heterotrophic organisms heavily grazed on the phytoplankton. However, compared with those in the autumn mesocosm, the $PLTs_{>100\mu m}$ of the photosynthetic pathway in the spring mesocosm were relatively very low and showed no increasing trend during the experiment period, indicating that the grazing pressure by >100-μm heterotrophs might not be so significant in spring. A marked large abundance of ciliates was also observed in the 20 – 100-μm fraction (Fig. 6). The maximum abundance of the micro-sized ciliates was 1.6×10^3 cells l^{-1} and the average abundance during the experiment (0.6×10^3 cells l^{-1}) was almost 3 times that in the autumn. The $PLT_{20\mu m}$ in the photosynthetic pathway was 2% on day 1, which then increased gradually to 16% on day 8 (Fig. 8). Because almost of the dominant *P. dentatum*, which is responsible for a large proportion of the photosynthesis, could be grouped with the < 20-μm fraction, we suggest that the micro-sized ciliates, rather than the larger zooplankton groups, played an important role in ingestion of the dominant *P. dentatum* in the spring mesocosm.

b) DOC production and consumption

Part of the photosynthetic production is transformed to dissolved organic carbon (DOC) through various processes, which are generally categorized into extracellular release from phytoplankton[19], sloppy feeding and excretion by zooplankton[20,21], and others (e.g. decomposition of particulate matter). Among the various forms of DOC produced through these processes, the DOC produced from extracellular release by phytoplankton, in particular, would be labile and readily used by bacterioplankton.[22] Hence, we assumed that the increase in primary production through the addition of phosphate would induce bacterial activity in the mesocosm.

In the spring, the average DOC concentration and ^{13}C-glucose uptake in the P-mesocosm (1.13 mgC l^{-1} and 0.77 μg^{13}C l^{-1} h^{-1}, respectively) exceeded those in the C-mesocosm (1.00 mgC l^{-1} and 0.58 μg^{13}C l^{-1} h^{-1}, respectively) (Figs. 3 and 5). Although these differences were slight, they indicated the relationship between the increase in primary production by the addition of phosphate and the increase in bacterial activity.

Comparing the autumn and spring P-mesocosms, DOC concentrations in the autumn increased from 1.30 mgC l^{-1} (day 2) to 2.22 mgC l^{-1} (day 6) (Fig 3) whereas, in the spring, DOC only increased from 0.95 mgC l^{-1} (day 0) to 1.27 mgC l^{-1} (day 8) (Fig. 5). Bacterial activity was clearly more enhanced in the autumn than in the spring, particularly in the latter period of the experiment. Because the average photosynthetic rates were

of similar magnitude in both seasons, we concluded that the difference in the amounts of DOC increase and bacterial activity of the 2 mesocosms was caused by differences in species composition and/or the physiological condition of phytoplankton or by differences in the effect of grazing on the phytoplankton by zooplankton assemblages. In the autumn mesocosm, the Chl.*a*-specific photosynthetic rate and Chl.*a*-specific rate of nitrate uptake were higher in the early period of the experiment and decreased remarkably in the latter period (Figs. 10 and 11). In the spring mesocosm, they peaked in the middle period of the experiment, indicating that phytoplankton growth increased more gradually. If photosynthetic production works to produce labile DOC, large quantity of labile DOC would be produced from the former period in the autumn mesocosm. Rapid accumulation of DOC was observed in the latter period (days 4 to 7) of the autumn experiment (Fig. 3). The PLT results at that time (Fig. 8) suggest that ingestion of *S. costatum* by copepods increased significantly and indicated that sloppy feeding by copepods and their excretion produced the DOC. In addition, we concluded that cell activity of the dominant phytoplankton decreased because of the condition of reduced nutrients. A study by Norrman et al.[23] demonstrated that decline of a diatom bloom, when the diatoms were in an unhealthy condition following nutrient depletion, was associated with significant DOC release and the released DOC contained not only labile DOC but also semi-refractory one. We suggest that the large accumulation of DOC in the latter period in the autumn mesocosm was due to the release of such a semi-refractory DOC from the *S. costatum*.

c) Carbon flow from bacterial production

The remarkable increase in bacterial activity in the autumn P-mesocosm would affect the bacterial carbon transfer in the food webs. The average $PLT_{>100\mu m}$ and $PLT_{20\mu m}$ in the bacterial pathway were larger in the autumn (0.94% and 6.1%, respectively) than in the spring (0.59% and 5.7%, respectively) (Fig. 9). In particular, the $PLT_{20\mu m}$ in the autumn increased to 14% on day 4.

From day 4 to 5 in the autumn mesocosm, appendicularians, which were classified into the 20 – 100-μm fraction, increased dramatically (Fig. 4). This implied that bacterial products had been ingested, supporting the increase in the appendicularians. However, a clear decrease in abundance of bacterioplankton was not observed during the same period (Fig. 4). This may have been because enhanced bacterial production almost offset ingestion by bacterivores, including the appendicularians. The abundance of picophytoplankton of similar cell-size to the bacterioplankton declined significantly from day 4 to 5 (Fig. 4), indicating the presence of high grazing pressure on pico-sized particles. The $PLT_{>100\mu m}$ in the bacterial pathway remained relatively high after day 5, whereas the $PLT_{20\mu m}$ decreased, due to the rapid growth of the appendicularians and their size distribution shifting gradually from the 20 – 100-μm fraction to the >100-μm fraction after day 5. Despite the appendicularians remaining until the end (day 7), an extreme increase in bacterial abundance was observed from day 5 onward and the $PLT_{>100\mu m}$ in the bacterial pathway did not exceed the day 4 value. This might be because the ability of the appendicularians to ingest pico-sized particles declined as their body-size enlarged. Deibel and Lee[24] demonstrated using *Oikopleura vanhoeffeni* that retention efficiency of < 1-μm particles was significantly lower for individuals with large body lengths (i.e. > 3.0 mm) in comparison to that of smaller-bodied groups.

In the spring mesocosm, on the other hand, $PLTs_{>100\mu m}$ and $PLTs_{20\mu m}$ did not show large fluctuations such as those observed in the autumn. We attribute the gradual increase in $PLT_{20\mu m}$ in the spring mesocosm to ciliates ingesting bacterial products, either directly or indirectly (i.e. via heterotrophic nanoflagellates etc.). However, we thought that the abundant ciliates in the spring were supported mainly by the abundant dinoflagellates (*P. dentatum* etc.) (see above). In short, the diet of ciliates in the spring was not dependent solely on bacterial production—a different situation to that of the autumn mesocosm where appendicularians are dependent on bacterioplankton.

5. CONCLUSION

To understand how further loading of phosphate into the Changjiang Estuary will affect phytoplankton growth and the carbon cycle in food webs, marine ecosystems in the estuary were enclosed in mesocosms in the autumn of 1997 and spring of 1998. Addition of phosphate reduced the N/P atomic ratios from 38 (autumn) and 94 (spring) to about 8. In the phosphate-enriched mesocosms, abundances of diatoms (*S. costatum*) and dinoflagellates (*P. dentatum*) increased, forming blooms in the autumn and spring, respectively. Such an increase in phytoplankton abundance was not observed in a control mesocosm in the spring. These results suggest that phytoplankton blooms may easily occur at the projected level of

phosphorous loading in the estuarine ecosystem. In addition, such blooms may be not only of diatoms but also of dinoflagellates, despite the existence of high concentrations of silicate in the estuary.

Average rates of photosynthesis in the phosphate-enriched mesocosms in the autumn and spring were almost equivalent. Increments of biomass (POC) were also equivalent; about 1 mgC l^{-1} in both the autumn and spring P-mesocosms. The increase in POC amounted to twice the initial biomass in the mesocosms. We thus conclude that phosphorous loading into this area of sea would cause an upsurge of biomass regardless of the differences in the seasons and/or dominant phytoplankton.

The characteristic response to the phosphate enrichment was different in each dominant phytoplankton. *S. costatum,* which was dominant in the autumn, showed high Chl.*a*-specific photosynthesis activity immediately following the addition of phosphate, whereas the activity of *P. dentatum* in the spring reached its maximum a few days later. Consequently, in the autumn mesocosm, nitrate and silicate were almost completely exhausted within a few days, after which primary production was significantly reduced. On the other hand, primary production in the spring mesocosm increased gradually until the end of the experiment. Considering that there are various types of phosphate loading into the seawater mass (i.e. through rivers or elution from sediment), we assume that such a difference in characteristic response to the nutrient may be a factor regulating the dominant species of phytoplankton in this estuary.

The number of zooplankton increased with the phytoplankton blooms in the mesocosms. The tracer experiment with inorganic ^{13}C-bicarbonate revealed that copepods possessed the ability to ingest a considerable quantity of diatoms in the autumn mesocosm, whereas their ingestion of dinoflagellates was relatively lower. The standing stock of phytoplankton is generally controlled by the growth of the phytoplankton itself and removal of phytoplankton by grazers. Our results indicate that control of phytoplankton blooms through grazing by copepods is more effective for diatoms than for dinoflagellates. In the autumn mesocosm with the diatom bloom, the concentration of DOC increased and bacterial activity was enhanced further than in the spring. The other tracer experiment with ^{13}C-glucose demonstrated that a trophic pathway involving appendicularians as higher order consumers developed in the autumn mesocosm, suggesting that phosphate loading may indirectly affect the carbon cycle in the microbial loop.

Our mesocosm study is the first experiment to demonstrate that the biomass of an ecosystem in the Changjiang Estuary can readily increase with the addition of only phosphate, although previous research[3,5] has discussed nutrient conditions in the Estuary where less phosphate exists and may be a limiting factor for phytoplankton growth. . It is also a fact, however, that this experiment merely simulated one of the scenarios that will occur in the near future in the Changjiang Estuary, and more investigation needs to be done to predict the future change of marine environment in the Estuary and the resulting ecosystem response.

REFERENCES

1) Bennekom, A.J. Van, Berger, G.W., Helder, W. and De Vries, P.T.P.: Nutrient distribution in the Zaire estuary and river plume, *Netherlands J. Sea Res.*, Vol. 12, pp. 296-323, 1978.

2) Edmond, J.M., Boyle, E.A., Grant, B. and Stallard, R.F.: The chemical mass balance in the Amazon plume I: The nutrients, *Deep-Sea Res.*, Vol. 28A, pp. 1339-1374, 1981.

3) Harrison, P.J., Yang, Y.P. and Hu, M.H.: Phosphate limitation of phytoplankton growth in coastal estuarine waters of China and its potential interaction with marine pollutants, In: *Marine ecosystem enclosed experiments* (Eds. Wong, C.S., Harrison, P.J.), pp. 192-202, International Development Research Centre, 1992.

4) Edmond, J.M., Spivack, A., Grant, B.C., Hu, M.H., Chen, Z., Chen, S. and Zeng, X.: Chemical dynamics of the Changjiang estuary, *Continental Shelf Res.*, Vol. 4, pp. 17-36, 1985.

5) Zhu, M., Li, R., Mu, X. and Ji, R.: Harmful algal blooms in China Seas, *Ocean. Research.*, Vol. 19, no. 2, pp. 173-184, 1997.

6) Chinese Academy of Science, Group of Ecological and Environmental Studies on Three Gorges Project (Ed.): *Studies on the ecological and environmental effects of the Changjiang Three Gorges Project and the remedies*, Science Press, China, 1988.

7) Grice, G.D. and Reeve, M.R.: Introduction and description of experimental ecosystems, In: *Marine mesocosms* (Eds. Grice G.D., Reeve M.R.), pp. 1-9, Springer-Verlag, New York, 1982.

8) Xu, K., Koshikawa, H., Murakami, S., Maki, H., Kohata, K. and Watanabe, M.: Impact of discharged fuel oil on plankton ecosystems: a mesocosm study in the Changjiang Estuary, In: this volume.

9) Kohata, K., Watanabe, M. and Yamanaka, K.: Highly sensitive determination of photosynthetic pigments in marine in situ samples by high-performance liquid chromatography, *J. Chromatogr.*, vol. 558, pp. 131-140, 1991.

10) Porter, K.G. and Feig, Y.S.: The use of DAPI for identifying and counting aquatic microflora, *Limnol. Oceanogr.*, Vol. 25, pp. 943-948, 1980.

11) Nakamura, Y., Suzuki, S. and Hiromi, J.: Population dynamics of heterotrophic dinoflagellates during a *Gymnodinium mikimotoi* red tide in the Seto Inland Sea, *Mar. Ecol. Prog. Ser.*, Vol. 125, pp. 269-277, 1995.

12) Koshikawa, H., Harada, S., Watanabe, M., Sato, K. and Akehata, T.: Relative contribution of bacterial and photosynthetic production to metazooplankton as carbon sources, *J. Plankton. Res.*, Vol. 18, pp. 2269-2281, 1996.

13) Thompson, P.A. and Calvert, S.E.: Carbon-isotope fractionation by a marine diatom: the influence of irradiance, daylength, pH and nitrogen source, *Limnol. Oceanogr.*, Vol. 39, pp. 1835-1844, 1994.
14) Hama, T., Miyazaki, T., Ogawa, Y., Iwakuma, T., Takahashi, M., Otsuki, A. and Ichimura, S.: Measurement of photosynthetic production of marine phytoplankton population using a stable ^{13}C isotope, *Mar. Biol.*, Vol. 73, pp. 31-36, 1983.
15) Han, M-S., Furuya, K. and Nemoto, T.: Species-specific productivity of *Skeletonema costatum* (Bacillariophyceae) in the inner part of Tokyo Bay, *Mar. Ecol. Prog. Ser.*, Vol. 79, no. 3, pp. 267-273, 1992.
16) Alldredge, A.L. and Madin, L.P.: Pelagic tunicates: unique herbivores in the marine plankton, *BioScience*, Vol.32, pp. 655-663, 1982.
17) King, K.R.: The population biology of the larvacean *Oikopleura dioica* in enclosed water columns, In: Marine mesocosms, Grice, G.D. and Reeve, M.R. eds., Springer-Verlag, New York, pp. 341-351, 1982.
18) Frost, B.W.: Effect of the size and concentration of food particles on the feeding behavior of the marine planktonic copepod, *Calanus pacificus*, *Limnol. Oceanogr.*, Vol. 17, pp. 805-825. 1972.
19) Williams, P.J.LeB.: The importance of losses during microbial growth: commentary on the physiology, measurement and ecology of the release of dissolved organic material, *Mar. Microb. Food. Webs.*, Vol.4, pp.175-206, 1990.
20) Lampert, W.: Release of dissolved organic carbon by grazing zooplankton, *Limnol. Oceanogr.*, Vol. 23, pp. 831-834, 1978.
21) Copping, A.E. and Lorenzen, C.J.: Carbon budget of a marine phytoplankton-herbivore system with carbon-14 as a tracer, *Limnol. Oceanogr.*, Vol. 25, pp. 873-882, 1980.
22) Kirchman, D.L., Suzuki, Y., Garside, C. and Ducklow, H.W.: High turnover rate of dissolved organic carbon during a spring phytoplankton bloom. *Nature*, Vol. 352, pp. 612-614, 1991.
23) Norrman, B., Zwifel, U.L., Hopkinson, C.S.Jr. and Fry, B.: Production and utilization of dissolved organic carbon during an experimental condition diatom bloom, *Limnol. Oceanogr.*, Vol. 40, pp. 898-907, 1995.
24) Deibel, D. and Lee, S.H.: Retention efficiency of sub-micrometer particles by the pharyngeal filter of the pelagic tunicate *Oikopleura vanhoeffeni*, *Mar. Ecol. Prog.* Ser., Vol.81, pp. 25-30, 1992.

VARIATION OF PARTICULATE ORGANIC CARBON AND PARTICULATE ORGANIC NITROGEN IN PHOSPHATE ENRICHED MESOCOSM EXPERIMENTS AND THEIR SINKING FLUXES

Shang CHEN[1], Mingyuan ZHU[1], Ruixiang LI[1], Xueyuan MU[1], Ruihua LU and Baohua LI[1]

[1]Division of Marine Biology, First Institute of Oceanography, State Oceanic Administration
(3A Hongdaozhi Road, Qingdao, 266003, China)

The phosphate enriched mesocosm experiments were conducted near Yangtze River Estuary during October 1997 and May 1998. After adding phosphate, both particulate organic carbon(POC) and particulate organic nitrogen(PON) gradually increased and reached to the peak at the 4th day in October and at the seventh day in May, then decreased. Compared with October experiment, POC and PON in May were less and the time reaching to peak was longer. In May, the sinking fluxes of POC and PON averaged 0.72 and 0.12 $g.m^{-2}.d^{-1}$ respectively in phosphate enriched mesocosm and were less than in natural seawater.

***Key Words**: Yangtze River Eustary, enclosure experiment, particulate organic carbon, particulate organic nitrogen, sinking flux*

1. INTRODUCTION

Eutrophication is becoming a serious danger to mariculture industry and marine ecosystem in coastal region and river estuary, and one of the main environmental problems too. Eutrophication process provides the material basis for the formation of red tide. To understand the impact of eutrophication on East China Sea ecosystem and estimate the carrying capacity of nutrients in Changjiang River Estuary ecosystem, the Chinese and Japanese scientists jointly conducted the mesocosm experiments and field survey in Changjiang River Estuary during the October 1997 and May 1998. So far, only a few research were focused on the distribution of POC and PON in Changjiang River Estuary and East China Sea[1), 2), 3), 4)], and the sinking of POC and PON are not understood yet. It is very interesting and significant in science to conduct mesocosm experiment at the famous Changjiang River Estuary. The purposes of this paper were to (1). Address the responses of the particulate organic carbon and particulate organic nitrogen in ecosystem after adding phosphate, (2). Distinguish the potential difference of behavior of POC and PON in mesocosm with phosphate and without phosphate enhancement. (3). Understand the sinking flux of POC and PON in mesocosm and in natural seawater.

2. MATERIALS AND METHODS

(1) Site and time of the experiment

The first phosphate enriched mesocosm experiment was conducted for seven days from 10 (day 0) to 17 (day 7) October 1997 at the Huaniaoshan sea region near the Changjiang River Estuary(Fig.1). The second phosphate enriched ecosystem experiments were conducted for 8 days, from 18 (day 0) to 26 (day 8) May in 1998 at the same site.

(2) Brief introduction of mesocosm experiment site

In October, the dominant species of phytoplankton is a diatom, *Skeletonema costatum*, the initial concentration of dissolved inorganic nitrogen (DIN), dissolved inorganic phosphate (DIP), and dissolved inorganic silicate (SiO_3) in mesocosms were 27.27, 0.78 and 34.9 μmol/l respectively. After enriching phosphate (Na_2HPO4), the DIP in P-mesocosm reached 3.25 μmol/l. The water temperature was 23°C and the salinity 25‰(Table 1).

Table 1. Comparison between two phosphate enriched mesocosm Ecosystems in October and in May before enriching phosphate

	DIN μmol/l	DIP μmol/l	SiO_3 μmol/l	Temp °C	Salinity ‰	PP	Chla μg/l	POC μg/l	PON μg/l	Dom. phyto.
Oct.	27.27	0.78	34.90	23.0	25.0	41.70	13.54	744.4	92.0	diatom
May	15.18	0.33	23.15	18.6	28.0	3.82	4.08	370.5	47.0	dinoflagellete

Dom. phyto.: dominant phytoplankton, PP: primary productivity ($mgC/m^3/h$)

In May experiments, the dinoflagellete, *prorocentrum dentatium* was dominant species in marine ecosystem. And the initial concentration of DIN, DIP and SiO_3 were 15.18, 0.33 and 23.15 μmol/l. After enriching phosphate the DIP in P-mesocosm reached 1.723 μmol/l. The water temperature was 18.6 °C and the salinity was 28‰.

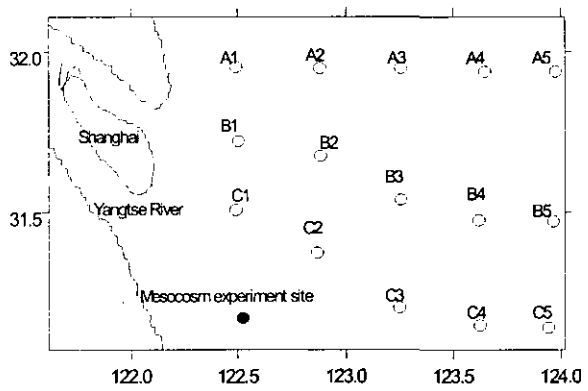

Fig.1 Stations of mesocosm experiments and field survey

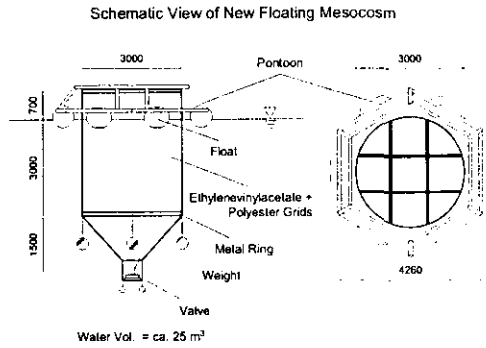

Fig.2 View of mesocosms

(3) Installing of mesocosms

The mesocosm made of the ethylenevinylacetate and polyester grid cloth was provided by National Institute for Environmental Studies, Japan (Fig.2). Two mesocosms were used every experiment, one was enriched with phosphate (Na_2HPO_4), while the other as the control. One mesocosm can fill 21-m^3 seawater (3-m diameter and 4.5-m depth). There is a round opening with 30-cm diameter at the bottom of mesocosm. The seawater entered the mesocosm through this opening by putting down the mesocosm slowly into the seawater. When the water surface in mesocosm reached the same water level as the outside, the opening was closed. This installing process does not significantly destroy the vertical structure of water and does not harm the structure of community.

(4) Sampling and analysis

The seawater was sampled at 1-m depth from 8:30 to 9:30 every morning. About 150-250ml water was filtered through the precombusted (450 °C for 4 hours) ϕ25mm Whatman GF/F glass fibber filter to analyze the concentration of POC and PON in water. Another one piece of GF/F filter was dipped in the just filtered water, as the control. There were two replicates for every sample. The GF/F filters with samples should be fumed for 20 minutes by high-concentration HCl to remove the dissolved inorganic carbon in one close container[6]. Then the filters were stored in a freezer at -18 °C. In laboratory, the filters were dried at 80 °C in electrical oven for two hours and analyzed on C.H.N. element analyzer (PE240C) at 760 °C, The accuracy of

the analyzer was 3.62 μg/l for POC, and 1.14 μg/l for PON [7].

The atomic ratio of POC to PON(C/N) was calculated by the formula:

$f_{C/N}$=(POC μg.l^{-1}/12)/(PON μg.l^{-1}/14)

To measure the sinking flux of POC and PON, two sediment traps were set up in mesocosms. The trap is a plastic cylinder with 50-cm height and 10-cm diameter. The traps were planned to collect for analysis after sampling seawater every morning.

Because of the rough sea condition, during the experiment in October 1997, the control mesocosm was destroyed at the afternoon of the second day. So samples from the natural seawater outside mesocosm were as the control. And the sediment traps in P-mesocosm were collected only one time when finishing the experiment. In May 1998, the control mesocosm was destroyed at the sixth day.

In the paper, the P-mesocosm or P-meso refers to the phosphate-enriched mesocosm, and the C-mesocosm or C-meso refers to the control mesocosm, the ratio of C to N or C/N refers to the atomic ratio of POC to PON.

3. RESULTS

(1) Variation of POC and PON

In October the concentration of POC and PON in mesocosm were 744.4 and 92.0 μg/l respectively before adding phosphate. After adding phosphate, both POC and PON gradually increased and reached the peak at 4th day, with value of 2420.0 and 344.3 μg/l respectively, then decreased to 1434.7 and 210.7 μg/l respectively at 7th day (Fig.3). In natural seawater, POC and PON ranged from 281.4 μg/l to 788.8 μg/l and from 37.0 to 109.0 μg/l respectively and less than P-mesocosm (Fig.4).

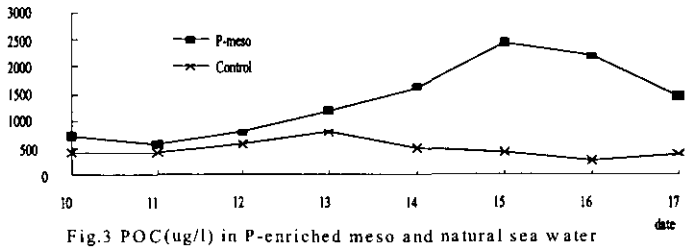

Fig.3 POC(ug/l) in P-enriched meso and natural sea water in Oct.

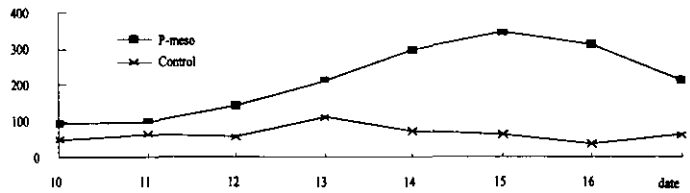

Fig.4 PON(ug/l) in P-enriched meso and natural sea water in Oct.

In May, the beginning concentrations of POC and PON in phosphate enriched mesocosm were 370.5 and 47.0μg/l. Both POC and PON climbed to the maximum value of 1580.0 and 241.0 μg/l until 7th day, then dropped down (Fig.5, 6). Compared with October experiment, POC and PON in May were less and the time was longer to reach the peak. This may be attributed to the low abundance of phytoplankton in May and another reason was that the growth rate of *Prorocentrum dentatium* (dominant species in May) was slower than *Skeletonema costatum* (dominant species in October).

In October, the POC and PON in P-mesocosm was more than May, because the biomass and

photosynthetic ability of phytoplankton were higher in October than in May (Table 1).

(2) The variation of the atomic ratio of POC to PON

During October and May, the atomic ratio of POC to PON in P-mesocosm decreased after adding phosphate, then increased slowly (Fig.8). The average C/N ratio in P-mesocosm was 7.5 in May and 7.8 in October. In May, the ratio of C to N did not show the obvious difference between the P-mesocosm and C-mesocosm (Fig.7).

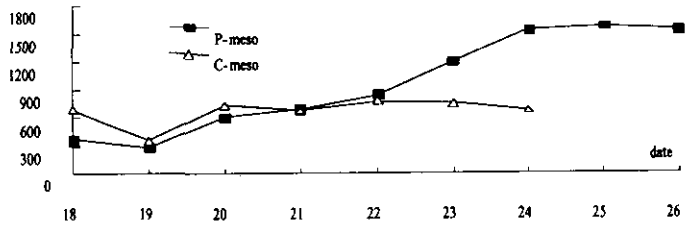

Fig5. POC in P-enriched meso and control in May

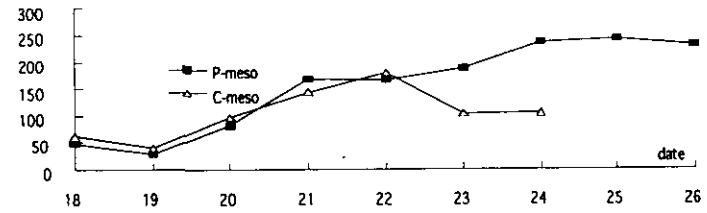

Fig.6 PON in P-enriched meso and control meso in May

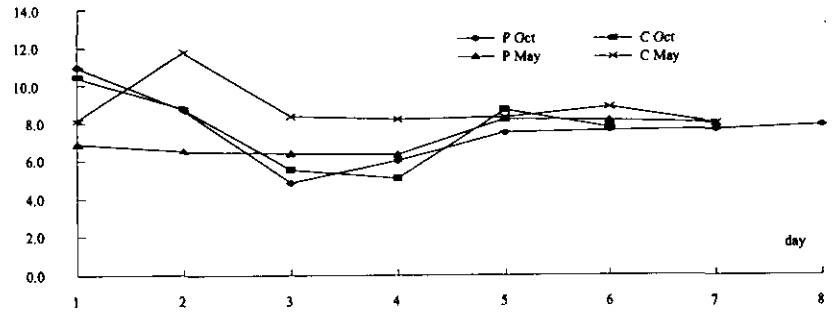

Fig.7 The atomical ratio of POC to PON

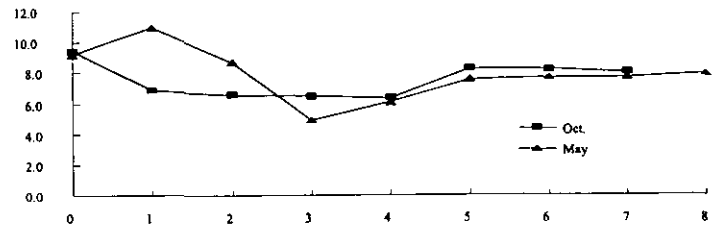

Fig. 8 Atomic ratio of POC to PON in P-meso during October and May

In P-mesocosm, The ratio in P-mesocosm was higher in May than October for the first two days after adding phosphate, but which became less than October from the third day. These were attributed to the different structure of phytoplankton. In October the biomass of phytoplankton was more than in May, so the POC and PON were more than in May. In October, the diatom (*Skeletonema costatum*) was the always the absolutely dominant species during the experiment, but the dominant species in May experiment was dinoflagellete (*Prorocentrum dentatium*) for the first three days and then replaced by the diatom (*Skeletonema costatum*). The dinoflagellete and diatom have the different ratio of C to N. The replace of species composition resulted in the change of the ratio of C to N. In the earlier experiment period, the dissolved inorganic nitrogen was relatively more abundant than in the later period, the phytoplankton cells absorbed relatively more nitrogen so that the ratio of C to N was bigger.

(3)]Sinking fluxes of POC and PON

In October, the average sinking fluxes of POC and PON were 9.50 and 1.20 $g.m^2.d^{-1}$ in P-mesocosm. In May, the sinking flux of POC in P-mesocosm averaged 0.72 $g.m^2.d^{-1}$ and less than C-mesocosm. Meanwhile, the sinking flux of PON averaged 0.12 $g.m^2.d^{-1}$ in P-mesocosm and 0.14 $g.m^2.d^{-1}$ in C-mesocosm. The sinking fluxes of POC and PON were less in May than in October. The daily sinking flux showed the increasing trend both in P-mesocosm and in C-mesocosm (Fig.9). But the sinking flux in C-mesocosm climbed to the maximum value prior to that in P-mesocosm. The sinking flux of POC and PON in P-mesocosm and control were lower than in natural seawater(Table 2). For example, on 30 May, the sinking flux of POC in natural seawater was 3.47 $g.m^2.d^{-1}$, while the value was 2.99 $g.m^2.d^{-1}$ in P-mesocosm and 3.04 $g.m^2.d^{-1}$ in control mesocosm. The values are very higher than offshore ocean[8), 9)] . Smith(1999) conducted a 7-year study and meaured the sinking flux of particulate matter at 600 m above bottom at an abyssal station(4100 m water depth),220 km off the central California coast[10)]. The sinking flux of POC varied from 0.16 to 27.18 $mgC.m^{-2}.d^{-1}$ between October 1989 and October 1996.

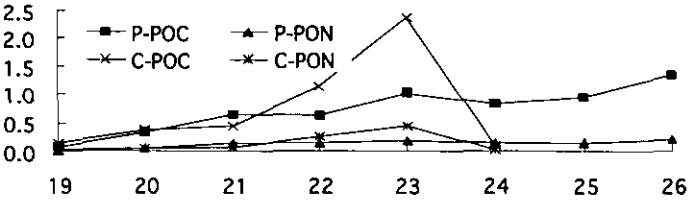

Fig. 9 Sinking fluxes(g/m^2/d) of POC and PON in P-meso and control in May

The daily sinking flux of phytoplankton showed the same trend with the POC and PON (Fig.11). The sinking flux of phytoplankton increased from the initial 0.39 $gChla.m^2.d$ to 24.57 $gChla.m^2.d$ at the fifth day in P-mesocosm then dropped down. Meanwhile, the sinking flux of phytoplankton in C-mesocosm increased from initial 0.56 $gChla.m^2.d$ to the peak, 15.69 $gChla.m^2.d$ at the fifth day, then dropped down. The sink of POC and PON mainly resulted from the death and sink of phytoplankton. In October, the abundance of phytoplankton was high, and the dominant species was big-size diatom, which sink quicker than dinoflagellete. So the average daily sinking fluxes of POC and PON and phytoplankton were higher in October than May

4. DISCUSSIONS

At a certain extent, the results from mesocosm experiment in October reflected the ecosystem behavior in fall in Changjiang River Estuary, and the results in May reflected the change of ecosystem in spring. The two experiment results showed different seasonal response of POC and PON in ecosystem on eutrophication of phosphate. Phytoplankton bloom broke out in the mesocosm experiments by adding phosphate in October and May. They were called as *Skeletonema costatum* bloom in October and *Prorocentrun dentatum* and *Skeletonema costatum* bloom in May. In fall, the shortage of dissolved inorganic silicate and nitrogen caused the disappearance of bloom, but it was the shortage of dissolved inorganic nitrogen caused the disappearance

Table2. Sinking fluxes($g.m^{-2}.d^{-1}$) of suspended particulate matter in mesocosm and in natural sea water

date	P-TPM	C-TPM	OUT-TPM	P-POC	C-POC	OUT-POC	P-PON	C-PON	OUT-PON
5.20	23.2	21.2	43.8	0.32	0.36	0.57	0.04	0.04	0.07
5.22	29.5	49.5	93.52	0.62	1.13	1.74	0.14	0.25	0.24
5.26	28.4		573.69	1.34		4.29	0.20		0.53
5.30	48.5	30.7	295.95	2.99	3.04	3.47	0.418	0.36	0.42

P, C: Phosphate enriched mesocosm and control mesocosm; OUT: natural seawater out mesocosm

Table 3. The some parameters on the particulate organic carbon and bacteria in PE-mesocosm

	Primary productivity $ugC.l^{-1}.d^{-1}$	Daily increasing rate of POC $ug.l^{-1}.d^{-1}$ d	Daily sinking flux of POC $ug.l^{-1}.d^{-1}$	Bacteria abundance 10^5cell/ml	Bacteria productivity $ugC.l^{-1}.h^{-1}$
980519	76.56		0.026	1.9	3.7
980520	297.84	324.0	0.108	2.9	14.4
980521	334.32	91.0	0.214	1.6	7.5
980522	738.72	154.0	0.209	3.8	32.2
980523	1276.32	356.5	0.345	3.3	7.0
980524	1322.64	342.5	0.278	3.4	13.5
980525	1251.36	35.0	0.317	2.1	7.2
980526	1211.52	-28.0	0.451	2.9	20.6

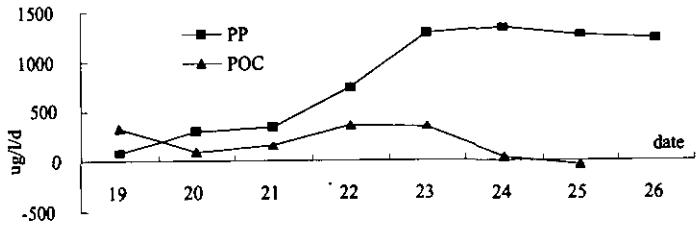

Fig.10 Daily increases of POC and primary production in Phosphorus enriched meso in May

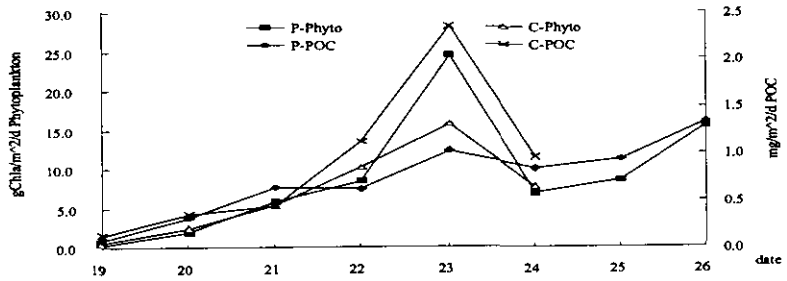

Fig. 11 Sinking fluxex of phytoplankton and POC in P-meso and C-meso in May

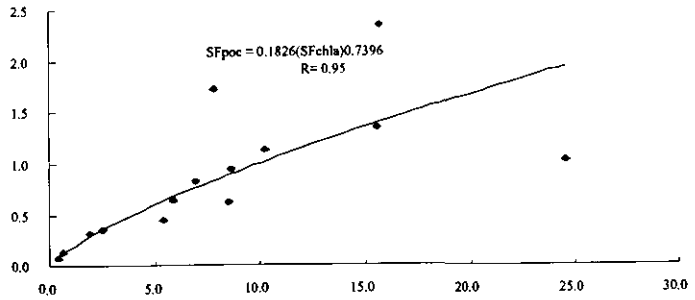

Fig.12 Relationship between the sinking fluxes of phytoplankton and of POC in P-meso in May

of bloom in spring.

In October, the POC and PON were more than those in May, because the phytoplankton was more in October than May. Huang(1997)[2] and Liu(1997)[4] also observed the POC in May was less than in October in Changjiang River Estuary. and After adding phosphate, the POC and PON firstly increase, then dropped down. The increase of POC and PON resulted from the increase of phytoplankton cells; and the decrease of POC and PON were attributed to the decrease of primary production limited by the decreasing nutrients and the bacterial decomposition of detritus. Fig.12 shows the good relationship between the sinking flux of POC with the sinking flux of phytoplankton.

To compare the production of POC with the sinking of POC, we need to transfor the unit of sinking flux($g.m^2.d^{-1}$) into the unit of $ug.l^{-1}.d^{-1}$, The daily sinking flux of POC varied from 0.026 to 0.345 $\mu g.l^{-1}.d^{-1}$, averaged 0.244 $\mu g.l^{-1}.d^{-1}$. It was very smaller than the daily increasing rate of POC (217.17 $\mu g.l^{-1}.d^{-1}$) (Table 3). The daily increasing rate of POC was lower than the primary productivity (813.66 $\mu g.l^{-1}.d^{-1}$) (Table 3), which means only a part of photosynthetic carbon transformed into particulate organic carbon, the other was released through the phytoplankton cell and formed the dissolved organic carbon which was the important bacteria's food. The graze of zooplankton may also explain the low increase of POC [11] . These were proved by the abundance of bacteria and bacterial productivity increased (Table 3). In the late period of mesocosm experiment, the primary productivity kept high increasing rate, while the increasing rate of POC has decreased to a very low level (Fig.10). It showed most of primary product transformed into DOC and went along the microbial loop pathway. This pathway consumes the much of dissolved oxygen and easily caused the red tide disaster.

Unlike the complex behavior of natural marine ecosystem, the mesocosm ecosystem was relatively simple and easy to be studied because of excluding the water exchange, it is a mass-balanced system. In control mesocosm, we may estimate the natural growth rate of plankton and observe the natural behavior of POC

and PON. On the basis of results from the mesocosm experiments we can estimate many ecological parameters, such as, the natural growth rate of phytoplankton. The sinking flux of POC, PON and phytoplankton in Changjiang River Estuary may be estimated on basis of the sinking data in control mesocosm, and they probable are different with the sinking flux in C-mesocosm, Because the nature sinking process was affected by the current and resuspension effect. The mesocosm experiment may determine some important parameters to develop marine ecosystem model and estimate the nutrient load in Changjiang River Estuary.

In Changjiang River Estuary, the sea current flow fast and phytoplankton patchy distribution change quickly, so it is very difficult to obtain the two same mesocosm ecosystems for contrast experiments. Although, the phosphate-enriched mesocosm ecosystem was not thoroughly same as the control, the experiment still provided the useful data, and showed clearly the behavior responses of ecosystem to the eutrophication.

5. CONCLUSIONS

(1). After adding phosphate, both POC and PON in P-mesocosm gradually increased and reached to the peak at the 4th day in October and at the seventh day in May, then decreased. POC and PON in P-mesocosm were less in May than October

(2). In May, the sinking fluxes of POC and PON averaged 0.72 and 0.12 $g.m^{-}2.d^{-1}$ respectively in phosphate enriched mesocosm and were less than in natural seawater.

(3). The variation of POC and PON in mesocosm was mainly attributed to the change of phytoplankton.

ACKNOWLEDGEMENT: Thanks to Drs. J. K. Xu, H. Koshikawa,, Mr. H. Wang, X. Wang and X. Shi for their friendly help. I also thank to Mrs. Fan Xiaoli, Mr. Zhang Youfeng and Mr. Watanabe for their contribution to the mesocosm experiments and field survey. The research project was funded by Natural Science Foundation of China (No. 49876030).

REFERENCES

1) Cai, Delin: Geochemistry of istope carbon in particulate organic carbon in Changjiang River Estuary, *Geochemistry*, Vol. 3: 305-311, 1992.

2) Huang, Zhiqiang, Hu, B. and Zhang, H.: Distribution characteristic of POC in East China Sea, *J. of Oceanography in Taiwan Strait.* 16(2): 145-151, 1997.

3) Ling, Xiureng: Relationship between the respiration rate of microbio with the Chla, POC, bacteria and ATP in Changjiang River Estuary, *Acta Oceanologia Sinica*, 13(6): 831-837, 1991.

4) Liu, Wenchen, Wang. R. and Ji, P.: Study of POC in the East China Sea. *Oceanologia et Liminologa Sinica*, 28(1): 39-43, 1997.

5) Liu, Wenchen, Wang, R. and Li, C.: C/N ratio of particulate organic matter in the East China Sea. *Oceanologia et Liminologa Sinica*, 29(5): 467-470, 1998.

6) Yang, Heming and Liu, Q.: Distribution and variation of POC and PN in seawater of Jiaozhou Bay, *Ecological Research on Jiaozhou Bay*, Jiao, Nianzhu and Dong, Jinhai eds., Science Press, Beijing, pp. 57-61, 1997.

7) Yang, Heming and Liu, Q.: A modified method for determination of POC and PN in seawater, *Ecological Research on Jiaozhou Bay*, Jiao, Nianzhu and Dong, Jinhai eds., Science Press, Beijing, pp. 53-56, 1997.

8) Heiskanen, A. S., Haapala, J. & Cundersen, K.: Sedimentation and Pelagic retention of particulate C, N and P in the Coartal Northern Baltic Sea. *Estuarine, Coastal & Shelf Science* 46: 703-712, 1998.

9) Ellen, R., Druffel, M. & Robison, B. H.: Is the deep sea on a diet? *Science*, 284(5417): 1139-1140, 1999.

10) Kenneth, L., Smith, Jr., Konald, and Kaufmann, S.: Long-term discrepancy between food supply and demand in the deep Eastern North Pacific, *Science*, 284(5417): 1174-1177, 1999.

11) Koshikawa Hiroshi, Harada, S., Watanabe, M., Sato, K. and Akehata, K.: Relative contribution of Bacterial and photosynthetic production to metazooplankton as carbon sources, *J. Plankton Res.*, 18(12): 2269-2281, 1996.

ON SEDIMENTATION OF PHOSPHORUS IN SPECIFIED AREA OUTSIDE OF CHANGJIANG ESTUARY

Huaiyang ZHOU[1], Jiangfang CHENG[1], Jianming PAN[1], Huaizhao WANG[1], Yoshiki SAITO[2], Yutaka KANAI[2] and Mingming JIN [1]

[1] Second Institute of Oceanography, State Oceanic Administration
(Hangzhou 310012, PR China)
[2] Geological Survey of Japan
(1-1-3 Higashi, Tsukuba, Ibaraki, 305-8567 Japan)

Phosphorus content of surface sediments (0-1cm) sampled by multicorer in specified area (122°30'E~124°00'E, 31°00'N~32°00'N) outside of Changjiang estuary respectively in October 1997 and May 1998 is analyzed. Combined with the data of phosphorus concentration in sea waters, grain size and chemical composition as well as the isotopic sedimentary rate of surface sediment and etc., it is recognized that Seasonal variability of different water masses could be sensitively recorded in sediments. Distribution pattern of phosphorous in surface sediment in the area is probably both controlled by the Changjiang River diluted water mass and the Huanghai Sea and East China Sea mixed water mass. Re-transportation and re-sedimentation perhaps do actively happen in the study region that could make re-suspended sediments to release pollutants as phosphorus into seawater and have significant impacts on marine ecosystem, although it is indicated that at least some of phosphorus in sediments exists in forms of immobile or inorganic.

Key Words : *Changjiang Estuary, phosphorus, sediment, seasonal variability, re-sedimentation*

1. INTRODUCTION

Environmental pollution has become a much serious problem with the rapid development of industrialization. The pollution caused by pollutants such as nutrients, heavy metals and organic compounds (including pesticides) etc. could damage the well-balanced circulation of natural ecosystem and induce the negative events such as eutrophication, red tide and poisoning etc. occur frequently. At the same time, it also affects human health and maintainable development of our society. As a result, more attention should be paid to the study and protection of natural environment meanwhile people make use of natural resources on the earth.

Study activities on environment and ecosystem in or near Changjiang Estuary might be traced to 1950's. Especially since the end of 1970's, some characteristics of hydrological, biological, chemical and geological environment of Changjiang Estuary is known through a series of large scale investigations such as Sino-American, Sino-French joint survey, national islands survey and national coastal zone survey etc.. However, probably as the limitation of methods and investigated area at that time, the understanding about some questions and some areas is still not very clear or some work has not even been carried out.

In the framework of joint program "the environment loading in the specified areas of the East China Sea and its effects on the marine ecosystem" between China and Japan government, scientists from both countries carried out two times of survey in aspects of hydrology, biology, chemistry and sedimentation onboard R/V "Hai Jai 49" in the specified area of the East China Sea (122°30'E~124°00'E, 31°00'N~32°00'N) outside of the

Changjiang Estuary in Oct. 1997 and May 1998, respectively. In two cruises, the sediment samples were collected by multiple corer at some stations in specified area and Meso site near Huaniao mountain (30°50.498'N, 122°36.694'E) (Fig.1). Based on the analytical results of concentration of phosphorus in surface sediments, combined with some other parameters, the sedimentation of phosphorus is discussed in this paper.

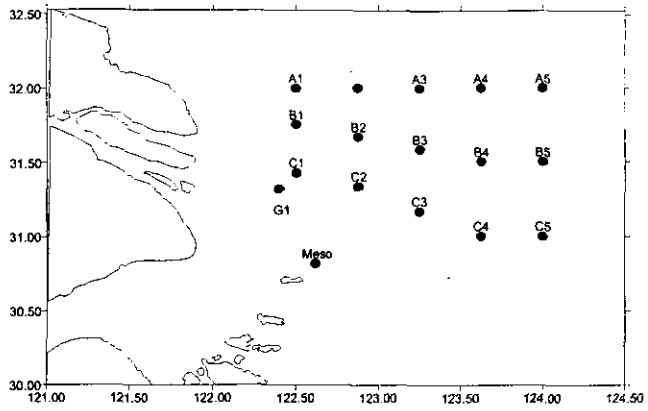

Fig.1 The diagram of sediment sampling station

2. MATERIALS AND METHODS

Sediment samples were collected by the multi-corer which has three tubes (d = 7.1 cm) except of samples at G1 by the gravity-corer. The length of the sediment collected by multi-corer was generally from 20cm to 40cm except of only several samples with a length of several cm. Sediments in some stations could not be collected probably for the reason that sand content is quite high.

After some observing and describing, most of sediment corers were divided into sub-samples with a length of 1~3cm each and frizzed to preserve immediately. Several corers were preserved directly in refrigerator.

3. RESULTS AND DISCUSSION

(1) Distributions of Phosphorus in Surface Sediment

Table 1 shows the content data of phosphorus in surface sediment (0-1 cm in depth) at several stations in specified area and Huaniao mountain meso site. The phosphorous content of the surface sediment in the investigated area varies between 402mg/kg and 734mg/kg. These data are similar to the range of phosphorous content of surface sediment (121°30'E~123°30'E, 30°45'N~32°00'N; sampled in 1985-1986) reported by Yang Guangfu etc., and lower than the data from Huanghe Estuary, Zhujiang Estuary etc. The phosphorous content in surface sediment of the Huaniao mountain meso site ranges from 647mg/kg to 720mg/kg, corresponding approximately to the upper data limitation in the specified area.

According to phosphorous tendency trend-surface analysis, it is concluded that there are obvious characteristics for the variety of phosphorous content in surface sediment in the study area. Among three transects A, B, C, the phosphorous content increases gradually on the A line from west to east (namely A1-A3-A5); but they decrease sequentially from west to east, namely C1(B1)-C3(B3)-C4(B5), on the B, C lines. As a result, two high points in the east-north corner and west-south corner of the study area could be seen on the trend-surface diagram of the phosphorous content in surface sediment.

By Comparing of the phosphorous content in sediment at the same station from two cruises, it is indicated that two sets of phosphorus data in different time keep a resembling distribution pattern mentioned above. However, an interesting phenomena is found that the phosphorous content of May 1998 is higher than that of Oct 1997 on A transect, and lower on C transect.

Table 1 Total phosphorus (TP) content in surface sediment (0-1cm in depth)

STATION	sampled in Oct. 1997	sampled in May 1998	other area	TP(mg/kg)
	TP(mg/kg)	TP(mg/kg)		
A1	517	589	Pearl River Estuary[1)]	699
A3	549	681	Changjiang Estuary[2)]	668
A4		607	Changjiang Estuary[8)]	560(400-860)
A5	609	734	Huanghe Estuary[2),3)]	860
B1	663		Luanhe Estuary[4),5)]	703
B3		655	Sediment of continental China[6)]	651
B5	548		Continental shale[7)]	699
C1	640	611	Brown clay from west pacific[1)]	1572
G1	634			
C3	586	576		
C4		402		
MESO	647	720		

(2) Relationship between Phosphorous Content in Surface Sediment and Water Masses

According to investigated results of two cruises in Oct 1997 and May 1998 and the published data, it is known that there are three kinds of water masses from different directions occur in the survey area. The first one is the Changjiang dilution water mass moved from west to east or southeast. The second one is the Huanghai Sea and East China Sea mixed water mass from north to south. The third is the Taiwan warm current water mass from south to north. These water masses meet each other in this region, although their impacts could be seasonally different.

The impression of the Changjiang River diluted water mass during Oct 1997 in this region was weaker than that during May 1998. Conversely, the Huanghai Sea and East China Sea mixed water mass and the Taiwan warm current water mass were stronger. As a result, the area including station B1, C1, C3 is relatively strongly affected by the Changjiang River dilution water. Impacts of the Huanghai Sea and East China Sea mixed water reduced gradually from station A5, A4 to west and southeast in direction. And station C5, C5 are more influenced by the Taiwan warm current water. The Huaniao mountain meso site and its around areas affected by the water of Chingjiang River and its coastwise current perennially.

Content of phosphorus and its forms in seawater samples from levels of surface, middle and bottom in water column at different station in the specified area are investigated. It is obviously that total phosphorus (TP) in seawater, its concentration in a station is positively relevant to water depth, is mainly controlled by particulate phosphorus (PP). The tendency of dissolved total phosphorus (DTP) is restricted by dissolved organic phosphorus (DOP) which showed an increasing trend from surface, middle to bottom in seawater column generally. It is interesting to notice that concentrations of TP and PP during Oct 1997 were largely higher than that during May 1998, and concentrations of DTP and DOP were a little higher than during May 1998.

According to the tendency surface diagram of phosphorous concentration in seawaters, it is evidently that TP, PP concentration of the Changjiang River diluted water was highest, and that of the Huanghai Sea and the East China Sea mixed water was the next, and that of the Taiwan warm current water was the lowest. The

concentration grads curve of DTP and DOP had also a similar tendency that the concentration of DTP and DOP decreased from the west side and the northeastern to east side or southeastern in the area, which just accorded with the change tendency of phosphorus content in surface sediments. It is also reflected that phosphorous in the surface sediment reasonably derived from two kinds of source: the Changjiang River diluted water and the Huanghai Sea and the East China Sea mixed water. The Changjiang River diluted water carried anthropogenic or natural phosphorus acquired along its long way and deposited them gradually into the sediment which make the sediments containing higher phosphorus content in the area where the Changjiang river diluted water approaches. Higher phosphorus content transported by seawaters from estuary of Huanghe river and Lihe river as well as from Huanghai Sea could also make the Huanghai Sea and East China Sea mixed water deposit corresponding content of phosphorus in the east-north corner of the study area. These two directions' phosphorous sources made the basic pattern come into being that the phosphorous content in surface sediments decreased from east to west on the A line and from west to east on the B, C line.

Kanai et al from Japan Geologic Survey measured the sedimentary rate at several stations in the specific areas by means of Pb^{210}. The tendency figure showed that the deposited rate decreased from the west side C1, B1 and the east-north corner as A5 to the middle in the area. Range of sedimentary rate is about 0.5-2 cm per year, although some phenomena such as strong bioturbation and hydrodynamic disturbation occurred in the region indicate that this isotopic data could be only regarded as a very general and average sedimentary rate.

Combined to consider the characteristics of phosphorus content distribution with the average sedimentary rate, it is reasonable presumed that surface sediment samples collected in May 1998, especially at station A1, A3, A5, C1, C3, are the sediments accumulated from winter, and samples were accumulated from summer are those sampled at the corresponding stations in Oct 1997. These surface sediments sampled in two cruises preserved the different characteristics of phosphorous concentration in the marine seawater in winter and summer, respectively. This is probably the reason why there were evident differences from the phosphorous content in samples of surface sediment collected at several stations during two cruises.

(3) Seasonal variability of grain size of surface sediment and its significance

The systematic measurement of the granularity of surface sediment (0-1cm) from specified area during Oct 1997 shows that the sand content (granularity>0.063mm) varied between 11.3% and 98.4% (Tab.2). Sand contents are >50% at station A1, A3, B5 and C3. The decreasing order of sand content for measured samples at stations is B5>A3>A1>C3>B1>C1>A5. Sand content of surface sediment sample from Huaniao mountain meso site is only 0.19%, and the sediment type is attributed to clay silt.

Probably limited by survey scale and sampling technique, former investigation reported that there is less modern sedimentary deposition in this study area except of certain sedimentation at station B1 and C1. What interesting phenomena discovered in this time is that, besides of nearly lowest sand content at station A5 in study area, grain size of surface sediment collected at station A3 during May 1998 became much finer than that during Oct 1997. It is also comparable in the region including stations B3 and B5. In fact, sediment sample had not been collected by multiple corer during Oct 1997 probably because of its coarse grain size. Evidently, Strong dynamics and rapid movement or variability of sedimentation did occur, not only there is sedimentary activities, in this area.

It is clearly observed that there are some sharp boundary in a depth of about 1-4 cm on some of sediment corer (B3, A3; for example). The sediments above this boundary are much finer than that beneath the boundary and darker in color. It is assumed that sedimentation was not continuous in the region outside of the estuary. It is quite possible that sediments deposited during certain time in this region could more or less be shifted, transported and deposited in some distance. Conclusively, modern sedimentation does happen in the study area, the defined ancient delta. It is considered that the activities of frequent re-transportation and re-deposition could play a great important role in the phosphorous cycling and in the marine ecosystem, because we know that phosphorus content in surface sediment is multiple higher than that in seawaters.

Table 2 Grain size and type of surface sediment

	Surface sediment in 1997				Surface sediment in 1998			
STATION	sand (%)	Silt (%)	Clay (%)	Sediment type	sand (%)	Silt (%)	Clay (%)	Sediment type
A1	65.98	21.14	12.9	Clay-silty sand				
A3	82.66	11.43	5.91	Silty sand	16.24	59.11	24.65	Sand-silt-clay
A5	7.12	70.62	22.6	Sand-silt-clay				
B1	21.2	53.49	25.3	Sand-silt-clay				
B3					8.65	61.15	30.2	Sand-silt-clay
B5	94.05	4.36	1.59	sand				
C1	15.15	54.01	30.8	Sand-silt-clay				
C3	58.78	26.66	14.6	Silty sand				
MESO	0.19	54.5	45.3	Clay silt				

(4) The relationship among phosphorous content, grain size and chemical composition in surface sediment

The orderly geographical distribution pattern of phosphorus content in surface sediment depend not only on the different water masses and their characteristics, but also on the structure, mineral composition and chemical composition in sediments.

It is obviously there is distinct negative relationship between sand content and phosphorous content in the surface sediment. On the contrary, the relationship between silt (d=0.063-0.004mm), clay and phosphorous content is positive. That is, phosphorous is generally enriched in fine sediment. Phosphorus-riched components could exist in a form with a granularity < 0.063mm or be absorbed on/in some particles whose granularity < 0.063mm.

It is also observed on the diagram of tendency surface analysis of grain size grade that the sand content of surface sediment in the investigation area increased from the east-north corner or the west-south side or west to the middle. The high points of clay content are generally also those of the phosphorous content. The phosphorous content became higher while the sediment is finer at the same station in different time. Of course, grain size is not the only factor to control the phosphorous content in surface sediment. For example, there is less sand content in the surface sediment of the Huaniao mountain meso site whose grain size much finer than in the specified areas, however, its phosphorous content is not so proportionally high.

SiO_2, Al_2O_3 and CaO etc are the main oxides in these sediments (Table 3). SiO_2 mainly exists in a form of quite stable quartz or silicate minerals, in addition to minor non-crystallized silicon and biologic activated silicon. In the surface sediment collected during the cruise of Oct 1997, SiO_2 content is very high and reaches 60~72%. Except the samples from station C1 and meso site have a relative higher valuc between 3.08~3.12%, most of sediments contain less biologic activated silicon. The biologic activated silicon content on the A transect seems to increase from west to east. Al_2O_3 is the main component of Al-silicate minerals as feldspar and clay minerals and also the representatives of non-biogenetic composition in the sediment. There is a

distinct inverse relationship between Al_2O_3 and SiO_2 content. The CaO content derived both from organic and inorganic particles ranges 2.48~4.30% in the sediment.

The correlative analysis shows that the correlative coefficients of phosphorus and SiO_2, Al_2O_3, CaO in the surface sediment were -0.75, 0.77 and 0.16 respectively. Actually, those sediments with coarse grain size and lower phosphorous content commonly contain high proportion silicate minerals as quartz that is quite poor in phosphorus. The coarse structure of sediment also does not benefit to the preservation or absorption of phosphorus. In other hand, the sediments have high Al content are generally rich in clay minerals. Clay minerals and fine structure in sediments have advantages of containing or absorbing the phosphorus-rich components.

Table 3 Chemical composition in surface sediment (%)

	surface sediment in Oct. 1997				surface sediment in May 1998			
STATION	SiO_2	TiO_2	Al_2O_3	CaO	SiO_2	TiO_2	Al_2O_3	CaO
A1	70.84	0.58	10.42	2.59	64.33	0.62	9.67	2.90
A3	71.75	0.68	9.58	2.48	54.79	0.75	10.46	4.35
A4					69.30	0.57	10.36	2.04
A5	62.09	0.72	11.17	3.79				
B1	62.09	0.71	11.79	4.30				
B3					55.68	0.85	10.13	3.15
B5	72.54	0.45	9.07	3.18				
C1	60.64	0.71	12.78	3.87	65.63	0.59	9.63	3.67
G1	61.69	0.80	13.13	3.91				
C3	68.60	0.75	10.40	3.81	66.48	0.84	10.67	3.19
C4					63.44	0.56	10.20	2.53
MESO	52.23	0.85	16.34	3.94	57.26	0.82	9.83	4.08

It is interesting to notice that the correlative coefficient between P and TiO_2 could reaches 0.84. TiO_2 commonly occur as fine heavy minerals in the sediments in coastal zone. Combined to consider the coefficients between phosphorus and Al_2O_3 as well as CaO, it could be reasonable assumed that at least some of phosphorus in sediments is inorganic or non-biologic, occur as non-biogenetic apatite for instance. This point is important to recognize because only those organic or mobile forms of phosphorus will have significant impacts in the marine ecosystem when they release into seawater with the changes of environmental condition.

4. PRELIMINARY CONCLUSIONS

Base on the data and discussion, we could have some preliminary conclusions as follows:

1. The distribution pattern of phosphorous in surface sediment in the study area outside of Changjiang Estuary is probably both controlled by the Changjiang River diluted water mass and the Huanghai Sea and East China Sea mixed water mass.

2. Seasonal variability occurs in the sedimentation and phosphorus in surface sediments in the study area. Characteristics of different water masses could be sensitively recorded in sediments.

3. Re-transportation and re-sedimentation perhaps actively happen in the study region that could release pollutants as phosphorus into seawater and have significant impacts on marine ecosystem, although it is indicated that at least some of phosphorus in sediments exists in forms of immobile or inorganic.

REFERENCES

1) Lan, X.: Geochemistry of sediments at Pear estuary, in Zhang Jin (Ed.) *Biogeochemistry of Chinese major estuaries: Chemical material transportation and surroundings,* Oceanography Press, Beijing, pp. 37-53, 1996.
2) Wang, Y., Ren, M., and Zhu, D.: Sediment Supply to the continental shelf by the major rivers of China. *Journal of the Geological Society*, Vol. 143(3), pp.936-944, 1986.
3) Gao, S., et al., Yellow River's delta formation and sedimentary environment, Science Press, Beijing, pp.106-132, 1989.
4) Liu, B., et al., Sedimentary chemistry of current Luanhe estuary, *Acta Oceanologica Sinica*, Vol. 9(3), pp.75-82, 1990.
5) Zhou, F., Elements distribution and their relations with surroundings in sediments at Luanhe estuary, *Acta Oceanologica Sinica,* Vol. 2(2), pp.60-70, 1983.
6) Zhao, Y., et al., Elements abundance in Chinese neritic sediments, Science in China, vol. 23(10), pp.1084-1090, 1993.
7) Liu, Y., *Geochemistry*, Geology department of Nanjing Unveristy (Ed.), Science Press, Beijing, pp. 90-101, 1979.
8) Yang, G., et al., Sanxia Project effects on sedimentary structure and geochemical character at Changjiang estuary, in Oceanographical Collection --Research Special of Sanxia Project ecological and environmental effects on Changjiang estuary, Science Press, Beijing, pp. 69-108, 1992.
9) *Chinese Gulf Annals (Major estuaries, 14th division)*, Chinese gulf annals editorial council (Ed.), China Ocean Press, Beijing, pp. 95-234, 1998.

PRELIMINARY OBSERVATIONS ON THE PHYTOPLANKTON SPECIES AT THE CHANGJIANG ESTUARY MOUTH IN MAY 1998

Masanobu KAWACHI, Mikiya HIROKI and Makoto M. WATANABE

Environmental Biology Division, Environmental Microbiology Laboratory, National Institute for Environmental Studies, Environment Agency
(Onogawa 16-2, Tsukuba, Ibaraki 305-0053, Japan)

Most of the species recognized in this study are well known as cosmopolitan species in coastal areas. A red-tide forming dinoflagellate, *Prorocentrum dentatum*, was widely recognized in this survey. Some fragile species could be detected from the direct observation of fresh samples. Presence of picophytoplankton species were confirmed by enrichment cultures and flow cytometry analysis. A total of 62 species belonging to 10 classes were identified in this investigation.

Key Words : *biodiversity, flora, phytoplankton, picoplankton*

1. INTRODUCTION

The marine phytoplankton of the Chinese coast area has been described in several papers[1) 2)]. Most previous studies were based on observation using light and scanning electron microscope and have targeted dominant taxa like the red-tide forming species and species having a relatively large cell size with distinct cell coverings, such as diatoms and dinoflagellates. While, picophytoplankton and fragile phytoplankton have not received as much attention, probably because of those difficulties of detections and identifications. During the monitoring cruise at the estuary area of Changjiang mouth in May 1998, we collected seawater samples for a floristic investigation on the phytoplankton. The main purpose of this study was to describe in detail the diversity of the phytoplankton of this area. Therefore we used several methods in order to describe the diversity and distribution of the phytoplankton, not only of predominant species, but also some picoplanktonic and naked species which can be easily destroyed during fixation.

2. MATERIALS AND METHODS

Seawater samples were collected during the cruise at stations A1 to A5, B1 to B5 and C1 to C5 (fig. 1) from surface, middle and bottom depths. During mesocosm experiments, seawater samples were also collected from inside and outside the mesocosm. For direct observation by scanning electron microscope (SEM), the seawater was filtered with a polycarbonate filter (Nucleopore, 0.4μm pore size). Size fraction and concentrated samples were also prepared using polycarbonate filters with different pore size (Nucleopore, 8.0, 3.0, 1.0, 0.4μm pore size). Freshly collected samples were also observed directly with a portable light microscope. Both original and treated seawater samples were fixed with glutaraldehyde (2.5% final concentration). Detailed observations were subsequently conducted on fixed samples using a light microscope with differential interference contrast attachments as well as scanning and transmission electron microscopes. In order to detect picophytoplankton, we applied an enrichment technique to the field samples. Seawater samples, filtrated with 3.0μm pore size polycarbonate filter, were inoculated into a culture medium (f/2 medium) and incubated near the windows of the research ship (c. 20°C, sun light with cool-white fluorescent light). For determining the distribution of picophytoplankton, we used a flow

cytometry (FCM) system. Here, seawater samples were fixed with glutaraldehyde (2.5% final concentration) immediately after collection and stored in a freezer at c. -10°C,. Samples were illuminated with an argon laser beam at 488nm, and their green, orange and red fluorescences (FL1, FL2 and FL3), and forward and side-angle light scatters (FSC and SSC) were determined by FCM.

3. RESULTS AND DISCUSSION

During the cruise of Changjiang Estuary, we observed samples with portable light microscope to determine the dominant species and the existence of the fragile species. A red-tide forming dinoflagellate, *Prorocentrum dentatum*, was recognized as the dominant species at the most sites. At stations B3 and C3, visible red-tides formed by this species were observed. Only the dominant species could be detected from the direct observation of seawater samples. And minor species were observed from concentrated samples after filtration at stations C3, C5 and the mesocosm site. Among the phytoplankton, naked phytoflagellates such as haptophytes, prasinophytes and raphidophytes, which are easily broken in fixed preparations, were detected. The number of fragile species identified was 16 (table 1). Most organisms were classified only to the generic level because of the lack of detailed morphological information. Some organisms, however, could be identified to the species level from their characteristic swimming manner and cell appearance, e.g. distinctive cell shape and special appendix. The portable light microscope was a useful tool to confirm the phytoplankton population of fragile species and should be used more widely.

Table 1. Fragile phytoplankton species observed in fresh seawater samples at the Changjiang estuary in May 1998.

Class	Species	Station
Chrysophyceae	*Dinobryon faculiferum*	mesocosm site
	Pseudopedinella sp.	mesocosm site
Dinophyceae	*Lepidodinium* sp.	mesocosm site
	green dinoflagellates (at least 2 speceis)	mesocosm site
Euglenophyceae	*Eutreptiella* sp.	mesocosm site
Haptophyceae	*Chrysochromulina hirta* (or *ericina*)	C3, C5, mesocosm site
	Chrysochromulina spinifera	C3, C5, mesocosm site
	Chrysochromulina quadrikonta	C3, C5, mesocosm site
	Chrysochromulina sp.	mesocosm site
	Halopappus sp.	mesocosm site
	Phaeocystis pouchetii	C3, mesocosm site
Prasinophyceae	*Pyramimonas longicauda*	C3, mesocosm site
	Pyramimonas sp.	mesocosm site
Raphidophyceae	*Fibrocapsa japonica*	C3, mesocosm site
	Heterosigma akashiwo	C3, mesocosm site

Two haptophyte species, *Chrysochromulina quadrikonta* and *C. spinifera*, were commonly observed. *C. spinifera* is known as phagotrophic species[3], and its aggressive uptake of small particles, such as bacteria and detrital material, was observed during the present survey. It is likely that *C. spinifera* plays an ecologically important role as consumer of bacteria in this area.

We also collected seawater samples during two weeks at a fixed site for mesocosm experiments. Pelagic and coastal phytoplankton were detected at this site, and the species composition and cell numbers varied greatly on a daily basis. Although most phytoplankton species observed in this area are well known species having a worldwide distribution, some distinctive taxa including new species were also detected. At least three green colored dinoflagellate species including *Lepidodinium* sp. were regularly observed, and a haptophyte species, *Chrysochromulina quadrikonta* was detected as one of the dominant species. It is known that *C. quadrikonta* is distributed along the coastal areas of Japan, Australia and New Zealand[4], and this study now shows it is dound along the coastal area of the Changjiang estuary.

Species of diatoms and dinoflagellates were identified from SEM observations of the filter samples. However some filters were more or less covered with mud and small particles. Particularly, filters from samples taken at stations B1, C1 and A5 were heavily covered with small particles and mud. Only limited

results, therefore, were obtained for these samples.

The mixing of water from the Changjiang River with seawater occurs at the estuary causes high turbidity. Filters from water taken at the estuary mouth were more easily clogged with mud, thus preventing phytoplankton microscopic observations. True phytoplankton diversity in these case is likely to be inaccurate.

Diatoms and dinoflagellates have been recognized as the most common phytoplankton living in the coastal region. A total of 15 species of diatoms and 20 species of dinoflagellates were identified from the SEM observations (table 2).

Table 2. Phytoplankton species detected by SEM observations of fixed and filtrated samples at the Changjiang estuary in May 1998.

Class	Species	Station
Chrysophyceae	*Meringosphaera mediterranea*	C3, mesocosm site
Diatomophyceae (diatom)	*Actinoptychus senarius*	A1-A5, B1, C1-C5, mesocosm site
	Actinoptychus splendens	A1-A5, B1, C1-C5, mesocosm site
	Adoneis pacifica	C3, C5, mesocosm site
	Chaetoceros atlanticus	A1-A5, B1, C1-C5, mesocosm site
	Chaetoceros debile	A1, A3, C1-C5, mesocosm site
	Chaetoceros sp.	mesocosm site
	Coscinodiscus spp. (at least 2 species)	A1, A3, C1-C5, mesocosm site
	Nitzschia longissima	A3, B3, C3, mesocosm site
	Paralia sulcata	A1, A3, C3, mesocosm site
	Skeletonema costatum	A1-A5, B1, B3, C1-C5, mesocosm site
	Thalassiosira spp. (at least 4 species)	A1-A5, B1, B3, C1-C5, mesocosm site
Dictyochophyceae	*Dictyocha speculum*	B3, C3, mesocosm site
Dinophyceae	*Alexandrium* sp.	B3, C3, mesocosm site
	Ceratium furca	A1-A5, B1, B3, C1-C5, mesocosm site
	Diplopelta parva	A1-A5, B1, B3, C1-C5, mesocosm site
	Dinophysis spp. (at least 2 speceis)	B3, C3, mesocosm site
	Gonyaulax polygramma	B3, C3, mesocosm site
	Gymnodinium spp. (at least 3 speceis)	B3, C3, mesocosm site
	Heterocapsa sp.	B3, C3, mesocosm site
	Noctiluca scintillans	A1-A5, B1, B3, C1-C5, mesocosm site
	Peridinium spp. (at least 3 speceis)	A1-A5, B1, B3, C1-C5, mesocosm site
	Prorocentrum balticum	A3, B3, C3, mesocosm site
	Prorocentrum dentatum	A1-A5, B1, C1-C5, mesocosm site
	Prorocentrum micans	B3, C3, mesocosm site
	Protoperidinium spp. (at least 2 speceis)	B3, C3, mesocosm site
	Scrippsiella sp.	B3, C3, mesocosm site
Haptophyceae	*Emiliania huxleyi*	C5, mesocosm site
	Gephyrocapsa oceanica	A5, C5, mesocosm site
	Syracosphaera sp.	C5
	Umbilicosphaera sibogae	C5
incertae sedis	*Ebria tripartita*	B3, C3, mesocosm site

There were some differences in the frequency of detection and species composition at each site. For example, we could confirm that diatoms were the dominant phytoplankton at stations A1 and A3, but less numerous or even minor species at other stations. On the other hand, the dinoflagellates tended to be more numerous at stations B3, C3 and the mesocosm site. Beside diatoms and dinoflagellates, only a few other taxonomic groups could be detected by SEM observations (table 2). Those groups included Haptophyceae, Chrysophyceae and Dictyochophyceae and constituted a minor component of the phytoplankton community except at station C5. In C5, interestingly, coccolithophorids were recognized as the dominant group, and other organisms were rarely observed. However, considering that the stream tributary from the Kuroshio Current runs near this area, domination of coccolithophorids here is not completely surprising. Since many species of coccolithophorids have been recorded in the Kuroshio Current[5], their presence should be good indicator to identify the water masses from the Kuroshio Current.

Though the investigation area was less than 300 square km, some environmental factors confirmed the

existence of different types of water masses in this complex ecosystem. We could detect easily a water mass originated from the Changjiang River. The horizontal profile of salinity and temperature at the surface showed the existence of low salinity core water, c. 2.7%, located around site C2, while, the surrounding stations, A3-5 and C5, had a salinity range 3.1-3.2%. In the case of seawater temperature, the southeast site, C5, was 18°C, while the north sites, A3 and A5, were 15°C. The complex hydrodynamics of this area come from the existence of the different water masses, being the Kuroshio Current, the Yellow Sea and the Changjiang River. Three phytoplankton assemblages, based on the dominant species, are recognized in this area with diatoms at stations A1 and A3, dinoflagellates at B3, C3 and mesocosm sites and coccolithophorids at C5 (fig. 1). Differences in dominant phytoplankton at each location appear to be related to the corresponding environmental conditions. Therefore the dominant species can be used as indicator of the environmental conditions.

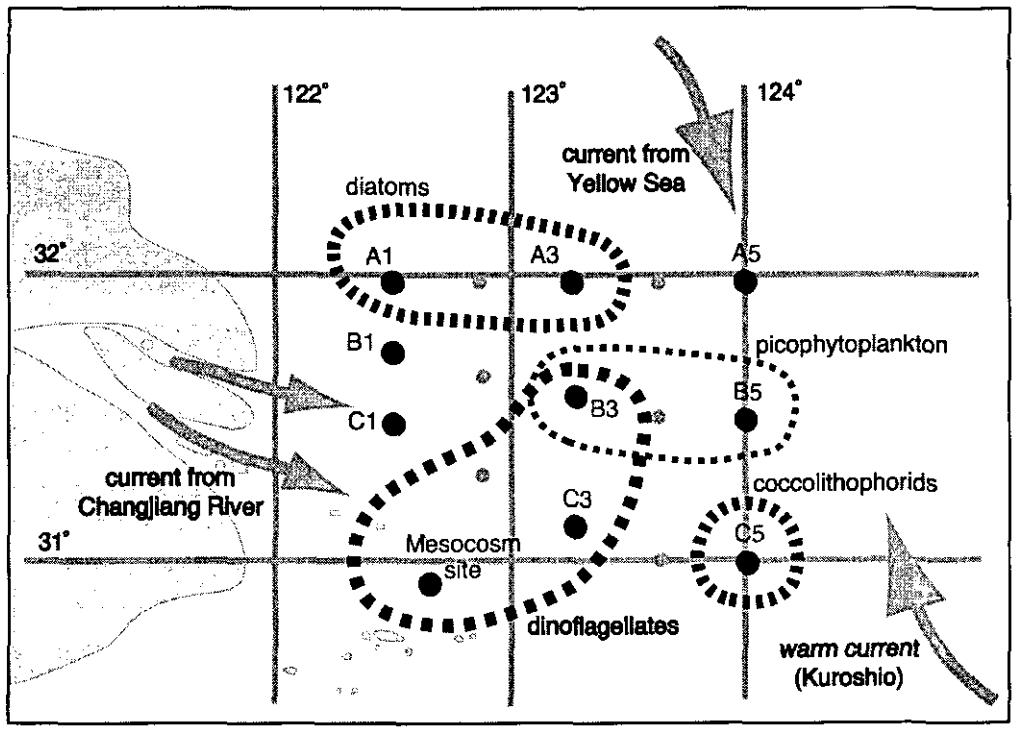

Fig. 1. Distribution of phytoplankton assemblages at the Changjiang estuary in May 1998.

At stations B1, C1 and A5, a high mud content prevented accurate observations and detections of phytoplankton. This may be the primary reason for the low number of species detected at these sites. However, another possibility is that the mud may supply pollutants which affects the phytoplankton cells as well as limiting the light availability. It would be a worthwile study to investigate the effect of mud and small particles on the phytoplankton community.

Prorocentrum dentatum was one of the most dominant dinoflagellate in this survey, because this species showed a wide distribution and was related to the visible red-tide. Interestingly, the cells of *P. dentatum* showed a wide morphological variability. For example, circular-shaped cells were often observed in fixed samples. Some of cells having a circular shape looked like *P. cordatum* or *P. minimum*. We identified most of them as *P. dentatum*, however, since the variability of the cell shape was successive, and cells often formed a linear colony which is a characteristic feature of *P. dentatum*[6]. We caution, however, that further taxonomic investigations, especially using cultured strains, of these species are required to make a conclusive identification.

We targeted picophytoplankton which are normally difficult to detect in field samples because of their small size (around 1μm). In order to detect such species, we applied an enriched culture method and FCM analysis. After 2-3 weeks incubation of enrichment cultures, picoplankton developed. From ultrastructural observation of fixed material, 4 different picophytoplankton were recognized (table 3).

Table 3. Picophytoplankton species observed in enrichment cultures of seawater samples at the Changjiang estuary in May 1998.

Class	Species	Station
Chlorophyceae	*Nannochloris*-like species	mesocosm site
Cyanophyceae	*Synechococcus* spp.	A1-A5, B1, B3, C1-C5, mesocosm site
Haptophyceae	*Imantonia rotunda*	B3, C3, mesocosm site
Prasinophyceae	*Micromonas pussila*	A1-A5, B1, B3, C1-C5, mesocosm site

All of these 4 types are known as cosmopolitan species in coastal and pelagic areas, although further studies for *Nannochloris*-like species and *Synechococcus* species are needed to determine species names. Application of an enriched culture of size fractionated seawater samples seems to be an effective method to detect picophytoplankton.

Distribution of prokaryotic picophytoplankton was revealed from FCM analysis. The results argued the differences of biomass in between sites (table 4). At stations A1, B1 and C1, close to the shore, the cell concentration ranged from 200 to 700 cells/ml, while at stations B3, B5 and C5, furthest from the shore, the maximum number reached was 16,796 cells/ml. Furthermore, the cell concentration in surface water samples tended to be higher than that of middle and bottom samples. Such vertical distribution may indicate some environmental differences in the water column. Generally, prokaryotic picophytoplankton are found in pelagic regions more than coastal areas. Therefore, their high abundance is a good indicator of pelagic environment conditions. Previously published data obtained from pelagic region gave cell concentration of c. 100,000 cells/ml in the West Pacific Ocean in autumn[7] and c. 500000 cells/ml in the Northeast Atlantic Ocean in winter[8]. These figures are an order of magnitude higher than our data, suggesting a lower biomass of picophytoplankton in the Changjiang estuary during the May 1998 survey. It is also possible that mud and small particles originating from the Changjiang River affected the FCM measurements. Furthermore, fixed cells tends to adhere to each other and with other particles decreasing the cell number estimation. Technical improvement may be required before the next survey. A seasonal survey of the picophytoplankton diversity and biomass of the area will help the interpretation of biomass and dominant species data.

Table 4. Cell concentrations of picophytoplankton detected by FCM analysis of the seawater samples at the Changjiang estuary in May 1998.

Station	Depth	Cells/ml	Station	Depth	Cells/ml
A1	surface	269	B5	surface	9726
A1	middle	254	B5	middle	4734
A1	bottom	310	B5	bottom	4038
A3	surface	4471	C1	surface	235
A3	middle	356	C1	middle	320
A3	bottom	489	C1	bottom	745
A5	surface	122	C3	surface	1625
A5	middle	173	C3	middle	189
A5	bottom	270	C3	bottom	249
B1	surface	552	C5	surface	2359
B1	middle	222	C5	middle	1209
B1	bottom	247	C5	bottom	1870
B3	surface	16796	mesocosm site	surface	349-1991
B3	middle	3736			
B3	bottom	2756			

ACKNOWLEDGMENTS

We are grateful to Ms M. Hirabayashi and Ms H. Baba for their assistance with sample preparation, and Ms M. Nakamura for her technical assistance with SEM. We would also like to thank Mr. Hiroshi Kato and Mr. Takahiro Ogawa who kindly helped in sample collection and preparation on the reseach ship.

REFERENCES

1) Furuya, K., Kurita, K. and Odate, T.: Distribution of phytoplankton in the East China Sea in the winter of 1993, *J. Oceanog.*, Vol. 52, pp. 323-333, 1996.
2) Yu, J. and Li, R.: The distribution characteristics of planktonic diatoms in the Kuroshio and its adjacent areas of the East China Sea in spring of 1989. *Essays on the Investigation of Kuroshio.*, Vol. 4, pp. 173-181, 1992.
3) Kawachi, M. and Inouye, I.: Functional roles of the haptonema and the spine scales in the feeding process of *Chrysochromulina spinifera* (Fournier) Pienaar et Norris (Haptophyta = Prymnesiophyta). *Phycologia.*, Vol. 34, pp. 193-200, 1995.
4) Kawachi, M. and Inouye, I.: *Chrysochromulina quadrikonta* sp. nov., a quadriflagellate member of genus *Chrysochromulina* (Prymnesiophyceae = Haptophyceae). *Jpn. J. Phycol.*, Vol. 41, pp. 221-230, 1993.
5) Wang, P. and Samtleben, C.: Calcareous nannoplankton in surface sediments of the East China Sea. *Mar. Micropaleont.*, Vol. 8, pp. 249-259, 1983.
6) Dodge, J.D.: The Prorocentrales (Dinophyceae). II. Revision of the taxonomy within the genus *Prorocentrum*. *Bot. J. Linn. Soc.*, Vol. 71, pp. 103-125, 1975.
7) Shimada, A., Hasegawa, T., Umeda, I., Kadoya, N. and Maruyama, T.: Sparial mesoscale patterns of West Pacific picophytoplankton as analyzed by flow cytometry: their contribution to subsurface chlorophyll maxima. *Mar. Biol.*, Vol. 115, pp. 209-215, 1993.
8) Partensky, F., Blanchot, J., Lantoine, F., Neveux, J. and Marie, D.: Vertical structure of picophytoplankton at different trophic sites of the tropical northeastern Atlantic Ocean. *Deep Sea Res.*, Vol. 43, pp. 1191-1213, 1996.

MODELING OF NUTRIENT DYNAMICS IN THE ESTUARINE SEA OF CHANGJIANG RIVER

Dedi ZHU[1] and Weiyi XU[1]

[1] Second Institute of Oceanography, State Oceanic Administration

(Hangzhou 310012, PR China)

Extensive field observations of nutrient element distributions have been carried out in the Changjiang estuarine sea. However, the knowledge about nutrient dynamics including nitrate and phosphate cycles along with water exchange and circulation in this region is still quite poor. The present report introduce the numerical modeling research which has already been carried out in order to understand the feature of nutrient dynamics in this area., a horizontally two-dimensional numerical model was developed to describe nutrient element dynamics in this estuarine sea. Based on the *in situ* measurements and historical data, we attempted to carry out the research of hydrodynamics· water exchange and transport of nutrient element. The numerical model is the base of the numerical research of red tide, which will be carried out next step in this region.

Key Words : *Changjiang Estuary ,nutrient dynamics ,model, water exchange*

1. INTRODUCTION

The Changjiang estuarine sea covers Hangzhou bay, the Zhoushan Islands areas, the Changjiang estuary and a few area of the East China sea. It locates at the middle of the East China sea, the northern part of which belongs to the Yellow sea and the southern's belongs to the East sea. It is a wide、shallow and open water body , only the western part of which is adjacent to the main land ; it locates at 29.20° -33.00° N and 120.40° -124.00° E(Fig.1). In addition,it is under 15m in depth of the field near Hangzhou bay and Changjiang estuary, and the eastern's is relative deep. The study area of hydrodynamics modeling covers the whole Changjiang estuarine sea ; The study field of water exchange and nutrient dynamics is a square area which is in the middle of the Changjiang estuarine sea, and it locates 31.00° -32.00° N and 122.50° -123.50° E (Fig .1).

The region of Changjiang delta is one of the most important economic centres in China, for the developed production of industry and agriculture, the ecological environment in this area becomes more and more serious. Especially in recent years, as a result of eutrophication, red tide occurs more frequently, so it is quite necessary to understand the environment capacity of the Changjiang estuarine sea.

Environment capacity means the capability of self-purification which includes physical self-purification and biochemical self-purification. In my paper, the water exchange model was employed to understand the physical self-purification of our study area, and the nutrient dynamics model was employed to understand the couple effect of the two self-purifications above.

The essence of water exchange is convection-diffussion of substance in the flow field. Based on HAMSOM (Hamburg Shelf Ocean Model)model, in the present report ,a convection-diffussion model of a conservative substance was developed to understand the feature of water exchange. In the nutrient dynamics model, N-P-Z model is introduced to simulate the biogeochemical effect which means the convection-diffussion of non-conservative substance.

2.NUMERICAL MODEL

HAMSOM (Hamburg Shelf Ocean Model) is a three-dimensional baroclinic primitive equation model, Its general theory was developed by Prof. Backhaus and his colleagues of Hamburg University. Since the model was presented in 1980's, it has been widely applied in shelf oceans of the world, and results of these applications show that HAMSOM model is an advanced model in studying the dynamics of shelf oceans. Based on HAMSOM model, a horizontal and two-dimensional model was developed to describe nutrient element dynamics in the estuarine sea of Changjiang River.

(1) Governnment equation

$$\frac{\partial u}{\partial t}+u\frac{\partial u}{\partial x}+v\frac{\partial u}{\partial y}-fv=-g\frac{\partial z}{\partial x}+A(H)\nabla^2 u \tag{1}$$

$$\frac{\partial v}{\partial t}+u\frac{\partial v}{\partial x}+v\frac{\partial v}{\partial y}+fu=-g\frac{\partial z}{\partial y}+A(H)\nabla^2 v \tag{2}$$

$$\frac{\partial z}{\partial t}+\frac{\partial[(h+z)u]}{\partial x}+\frac{\partial[(h+z)v}{\partial y}=0 \tag{3}$$

$$\frac{\partial \phi}{\partial t}+u\frac{\partial \phi}{\partial x}+v\frac{\partial \phi}{\partial y}=K(H)\nabla^2\phi+R \tag{4}$$

Where

t—time

u,v—components of the depth mean current velocity in the x,y directions respectively

z—elevation of the sea surface

h—undisturbed depth of water

A(H)—horizontal eddy-viscosity coefficient

f—Coriolis parameter

K(H)—horizontal eddy-diffusion coefficient

ϕ—nutrient element concentration

R—biogeochemical reaction

The fraction R can be described as:

$R=R_1+R_2$

Where

$$R_1=K\frac{\partial S}{\partial t}$$

K represents the specific coefficient for nutrients relative to desorption from particles and degradation of organic materials.

S—amount of suspended matter

R2—biochemical factor, in order to give the factor, N-P-Z(Nutrient-Phytoplankton-Zooplankton) model was introduced.

N-P-Z model:

$$\frac{dP}{dt}=uptake-grazing-pm*P \tag{5}$$

$$\frac{dZ}{dt}=ga*grazing-zm*Z \tag{6}$$

$$\frac{dN}{dt} = -uptake + pm * P + (1 - ga) * grazing + zm * Z \quad (7)$$

Where

N—nutrient

P—phytoplankton

Z—zooplankton

Simplified the model as following:

(1) the concentration of zooplankton was certain

Then, the equation (7) can be written:

$$\frac{dN}{dt} = -uptake + pm * P + (1 - ga) * grazing + zm * Z \quad (8)$$

$$\frac{dP}{dt} = +uptake - pm * P - grazing \quad (9)$$

$$uptake = \frac{N}{e + N} * \frac{a}{b + cP} P \quad (10)$$

Units of N、P and Z are gC/m^3,and Time units are days. The conversion equivalence is 1gC≡20mgChl≡10mg at N, where C is carbon, Chl is chlorophyll and N here is nitrogen.

Table 1. Meanings、default values and ranges of the parameters

Parameter	Symbol	Default value	Range
a/b gives maximum P growth rate	a	0.2 $m^{-1} day^{-1}$	0.10-0.60
Light attenuation by water	b	0.2 m^{-1}	0.02-0.20
P self-shading coefficient	c	0.4 $m^2 g^{-1}$	0.30-1.20
Higher predation on Z	d	1 $m^3 g^{-1} day^{-1}$	0.25-2.00
Half-saturation constant for N uptake	e	0.03 g day^{-3}	0.02-0.15
P respiration rate	pm	0.15 day^{-1}	0.05-0.15

(2) Boundary conditions

a) Dynamics boundary condition:

$$\vec{V} \cdot \vec{n} = 0$$

Assuming that the flow velocity at vertical direction of solid boundary was zero.

b) Open boundary condition

At the open sea boundary the water level was prescribed as boundary condition by specifying the tidal constituents M2 and S2 tides.

The flow velocity at open sea boundary was prescribed by the conditions of Orlanski radiation .

For the river boundary conditions, year-averaged fluxes of Changjiang river and Qiangtan river were given.

In the water exchange model, the concentration of inflow conservative matter was zero.In the modeling of water exchange and nutrient dynamics, the nutrient concentration of inflow water was zero at the open boundaries of Changjiang estuarine sea (including sea boundary and river boundary). In the water exchange model, matter concentration inside the square area was set to be 1,and concentration outside the square area is zero. In the nutrient dynamics model, in order to get a initial distribution of variants, a line resource was specified on the west side of the square area. The nutrient concentration of the line resource is 13 gC/m3 Nitrogen and the. Phytoplankton concentration of the line resource is 4 gC/m3 Chl.

3. NUMERICAL SCHEME

A semi-implicit difference scheme was employed to solve barotropic gradient terms in the momentum equations and divergence terms of continuity equations. An explicit central-difference scheme was used to discretized the horizontal diffusion terms of all equations.All horizontally convective terms are discretized with the approach of Eulerian-Lagrangian approximation. The distributions of finite difference grid can be described as following:

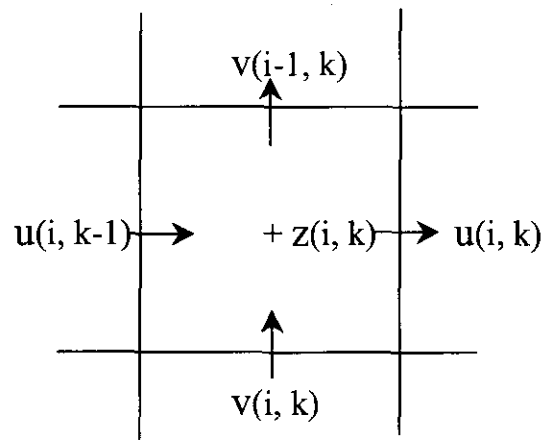

Arakawa-C scheme is adopted in the distribution of variables in grid; the Arakawa-C scheme is a staggered grid in x,y space, u,v locates at different sides of grid, and the other variables such as water level,the concentration of matter locates at the centre of grid.

4. RESULT AND DISCUSSION

In the calculation of hydrodynamics, only two co-tide (M2 and S2) was introduced, the following table is the results of comparison between observed data and that from simulation of the M2 co-tide.

Difference of Amplitude: H=(simulated data-observed data)/observed data*100%.

Difference of Phase: G= simulated data-observed data.

Tidal Station		Shes han	Luhua shan	Lucha ogang	Dajis han	Tanhu	Chang tu	Miaoz ihu	Zhuji ajian	Xiash idao	Damut u
Differe	H (%)	5.3	1.9	-9.3	-4.11	-9.7	4.9	0.7	1.9	-3.7	6.9
nce of M2	G (°)	1.8	-2.0	-0.4	1.1	-4.7	-9.2	0.2	-3.6	-2.2	1.3

The table above shows that the modeling result of M_2-tide is quite well.

When the model of water exchange with annually mean fluxes specified at the river boundaries has been running for 16 days, the concentration of conservative matter in the square field reduced to 0.5(i.e.50% matter was exchanged)(Fig.7) and continued running the model for about 24 days, the value of it reduced to 0.2(i.e.80% matter was exchanged) (Fig.8). The distribution of concentration shows that exchange ratio is

various in different areas; in the square field, water exchange along east-western direction is slower than that along south-northern direction. In addition, there is a relatively high part in the northeast of the square, obviously, the part is the slowest area in the whole square field.

The output results of nutrient dynamics model show that biogeochemical effect plays an important role in determining the environment capacity of the Changjiang estuarine sea. It is quite necessary that biogeochemical effect should be considered when we wants to understand the self-purification capacity of the Changjiang estuarine sea.

5. CONCLUSIONS

Since the tide of Changjiang estuarine sea is the typical semi-diurnal tide, M_2 and S_2 constituent can represent the basic features of tide and tide current. It shows also that the nutrient dynamic model based on above dynamic model could basically represent the basic features of nutrient space and time variation. The main content of present project is the environment capacity. From the typical theory environment capacity is controlled by hydrodynamic factor only. But now the biogeochemical effect has been focused on. It means that environment capacity, self-purification capacity, is controlled not only the hydrodynamic factor such as water exchange but also the biogeochemical effect such as degrade, adsorption and uptake, desorption and mobilization etc. Maybe the biogeochemical effect plays more important role in determination of environment capacity in some cases.

Obviously, the biogeochemical process is complicated process including several factors, it is necessary to make some experiences and field measurement to get those knowledge about this process. In numerical research aspect it is required to determine those parameters that will be used in the couple model. It is difficult to complete whole contents without those parameters. Present report is a trial including some factors only.

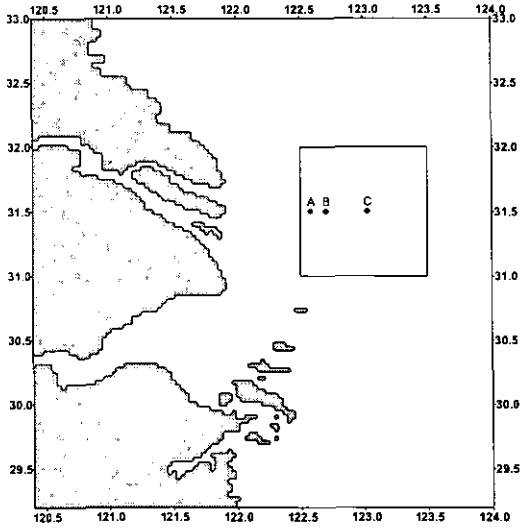

Fig. 1. study field

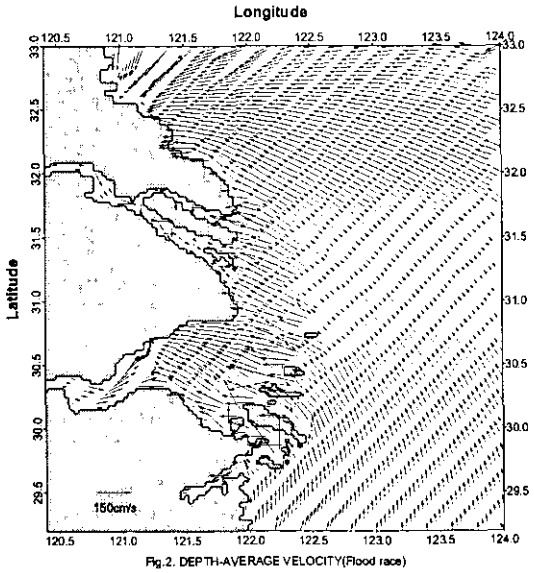

Fig.2. DEPTH-AVERAGE VELOCITY(Flood race)

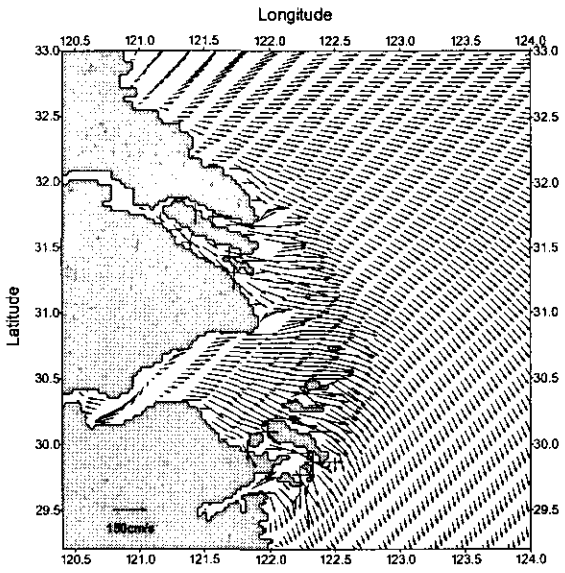

Fig.3. DEPTH-AVEARAGED VELOCITY(Ebb race)

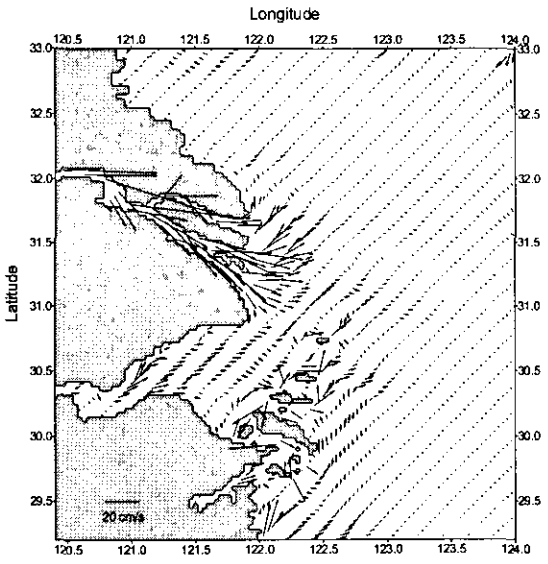

Fig .10. Residual flow velocity in Summer

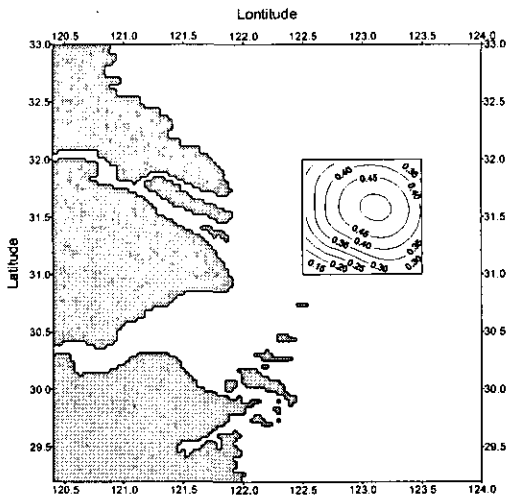

Fig.6. Distribution of conservative matter (runtime=16.27 days)
(water exchange modeling)

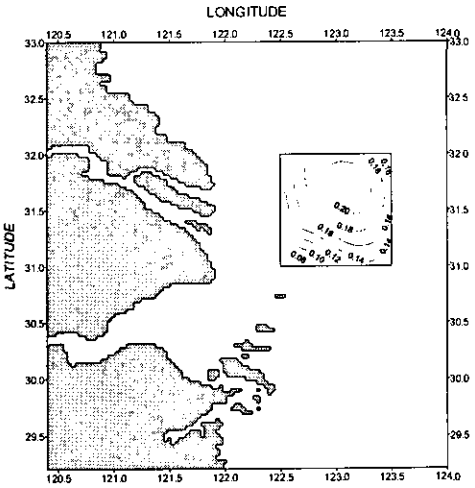

Fig.7. Distribution of conservative matter (runtime=40.08 days)
(water exchange modeling)

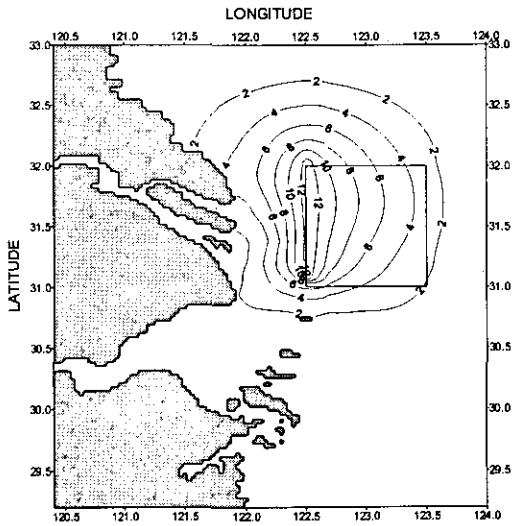

Fig. 8. Initial distribution of nutrient (runtime=50.00 days)
(nutrient dynamics modeling)

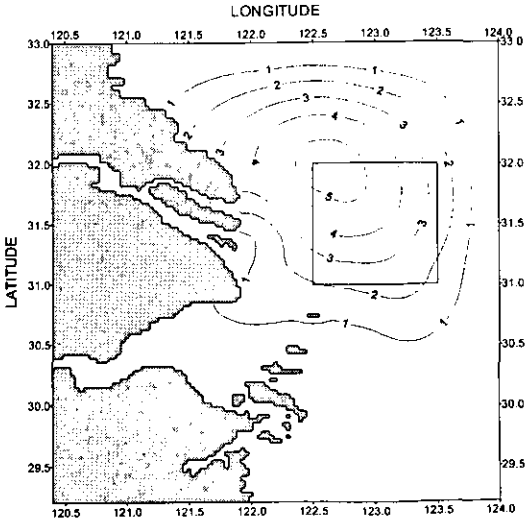

Fig.9. distribution of nutrient(runtime=65.0 days)
(when runtime=50.00 days the line source was sloped)

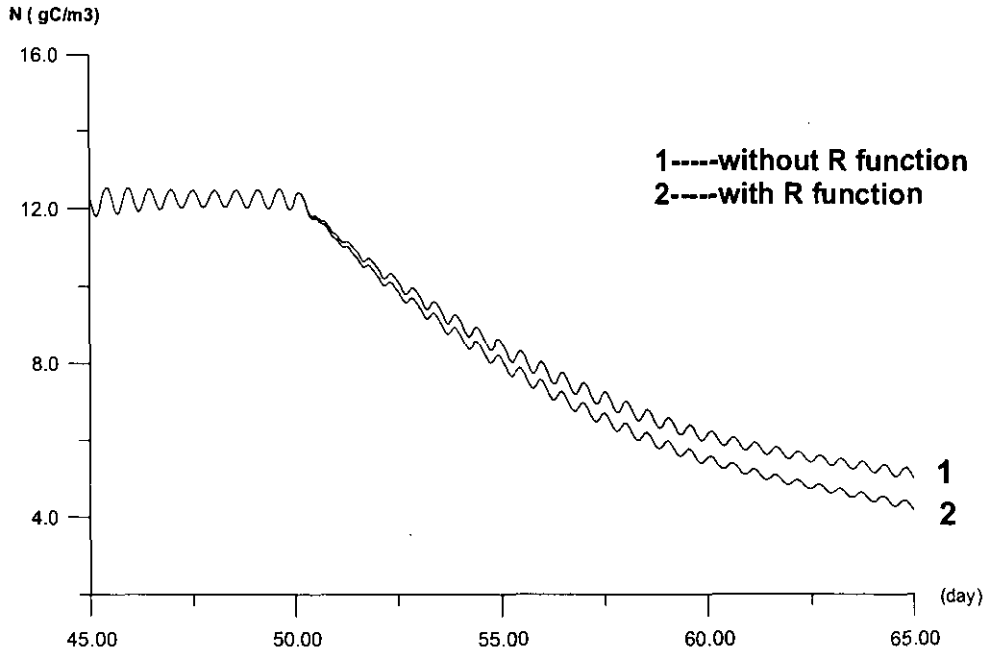

Fig .11. Comparisons between non-conservative model(with R function) and conservative model(without R function) at point A
£¨ when runtime = 50.0 days ,the line source was stoped)

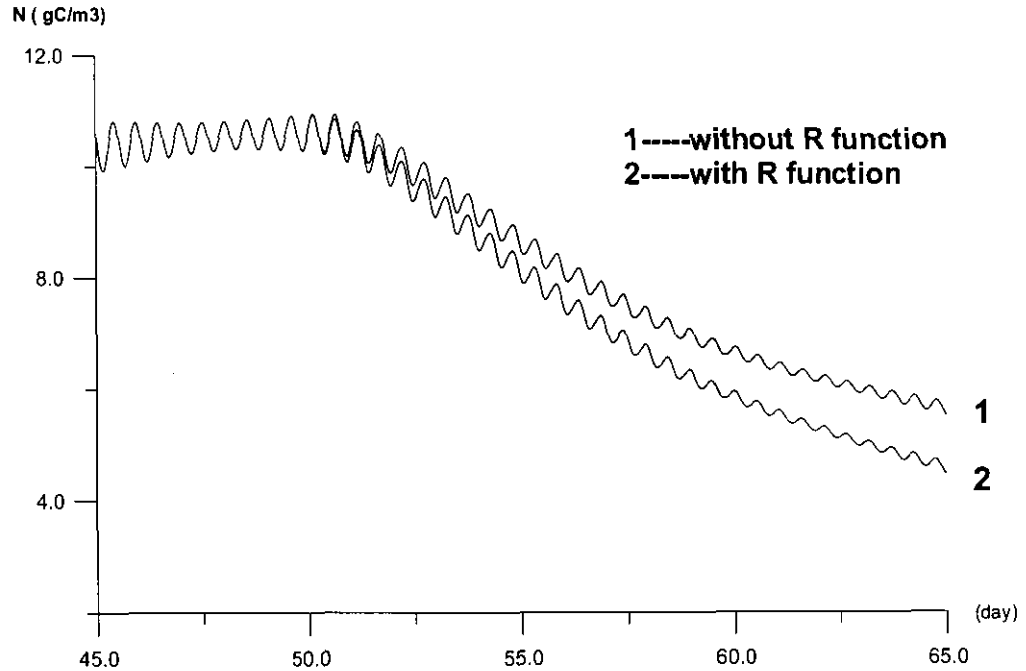

Fig .12. Comparisons between non-conservative model(with R function) and conservative model(without R function) at point B.
£¨ When runtime = 50.0 days, the line source was stopped £©

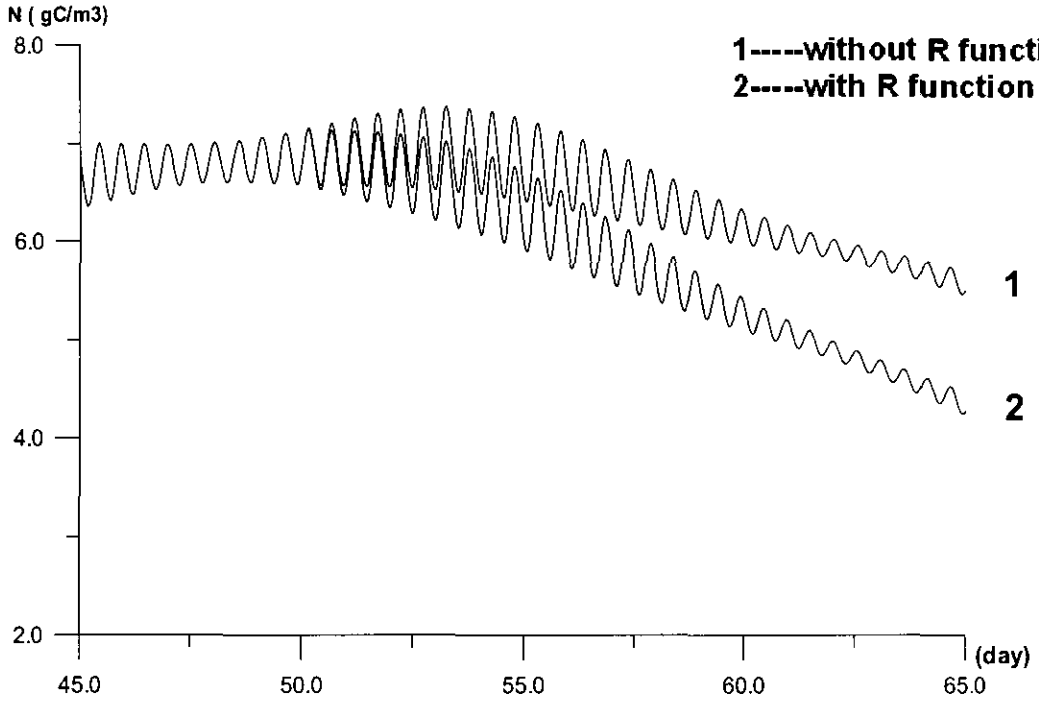

Fig .11 . Comparisons between non-conservative model(with R function) and conservative model(without R function) at point C (when runtime = 50.0 days ,the line source was stoped)

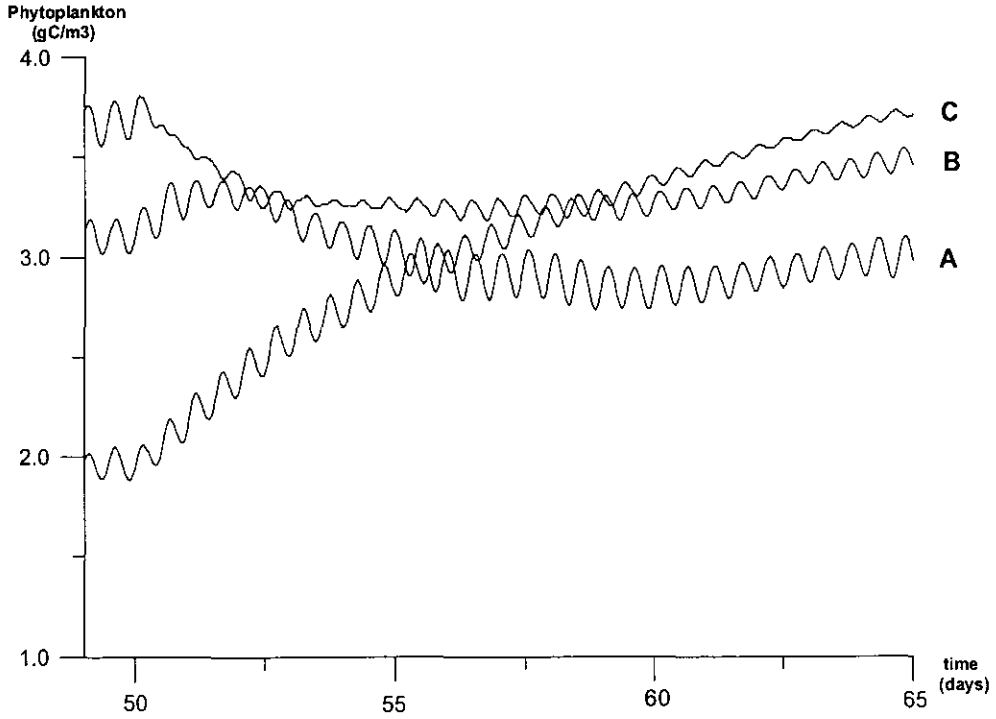

Fig.15. time series of Phytoplankton at points A,B and C respectively.

IMPACT OF DISCHARGED FUEL OIL ON PLANKTON ECOSYSTEMS: A MESOCOSM STUDY IN THE CHANGJIANG ESTUARY

Kai-Qin XU[1], Hiroshi KOSHIKAWA[1], Shogo MURAKAMI[1], Hideaki MAKI[1], Kunio KOHATA[2] and Masataka WATANABE[1]

[1] Soil and Water Environment Division, National Institute for Environmental Studies, Environment Agency (Onogawa 16-2, Tsukuba, Ibaraki 305-0053, Japan)

[2] Regional Environmental Division, National Institute for Environmental Studies, Environment Agency (Onogawa 16-2, Tsukuba, Ibaraki 305-0053, Japan)

An oil enrichment experiment using the water-soluble fraction (WSF) of #0 diesel oil was conducted in mesocosms over a 7-day period to investigate the acute impact of the oil on the plankton ecosystem in the Changjiang Estuary. The dominant grazers (ciliates, noctiluca and copepods) decreased in number after the addition of WSF to the mesocosm. The decline of ciliates was particularly noticeable, suggesting that they were the grazers most sensitive to WSF. The effect on phytoplankton abundance was not clear because macronutrients became limiting in both mesocosms. However, batch experiments with ^{13}C bicarbonate revealed that photosynthetic activity would have been strongly affected. Bacterial activity, determined by ^{13}C D-glucose uptake, was stimulated by WSF. However, the transfer efficiency of bacterial carbon to large grazers (>100 μm) decreased by about 40%, indicating that energy transfer to higher-order organisms in food webs would decline as a result of WSF addition.

Keywords: *Mesocosm, Water Soluble Fraction of Oil, Plankton Ecosystem*

1. INTRODUCTION

The adverse effects of crude and fuel oil on marine organisms have been well documented over the past few decades since large-scale oil-spill accidents began to occur all over the world. Many laboratory studies have indicated that the water-soluble fraction (WSF) of oil is strongly toxic to microorganisms. WSF inhibits growth of phytoplankton[1)] and activity of bacteria[2) 3)]. In the field, experimental ecosystems such as marine mesocosms have been used to investigate the impact of oil on whole planktonic ecosystems[4)]. Mesocosms are useful tools for investigating the response of an ecosystem to pollution loading[5)]. However, major research in whole ecosystems on the effect of WSF alone, which seems to be the most toxic component, has not been done. Although crude and fuel oils contain WSF that would leach from oil slicks or droplets, it is still necessary to assess the impact of WSF alone on whole planktonic ecosystems.

Undoubtedly, large-scale tanker accidents bring about fatalities to marine life through WFS. In addition, frequent small-scale fuel leakage from ships and the discharge of oil into coastal waters from industrial complexes and sewage outfalls may introduce WSF into the marine environment and cause acute and/or chronic impact on marine ecosystems.

The objective of this study was to investigate the acute impact of WSF on the whole planktonic ecosystem in the Changjiang Estuary in the East China Sea. Recently, oil pollution in the estuary has become a serious problem as a result of rapid industrial development of the adjacent coastal zone. The frequency of shipping traffic is increasing in the estuary, which is constantly exposed to pollution crises resulting from nautical accidents. A collaborative research project between Japan and China on 'Environmental loading from river

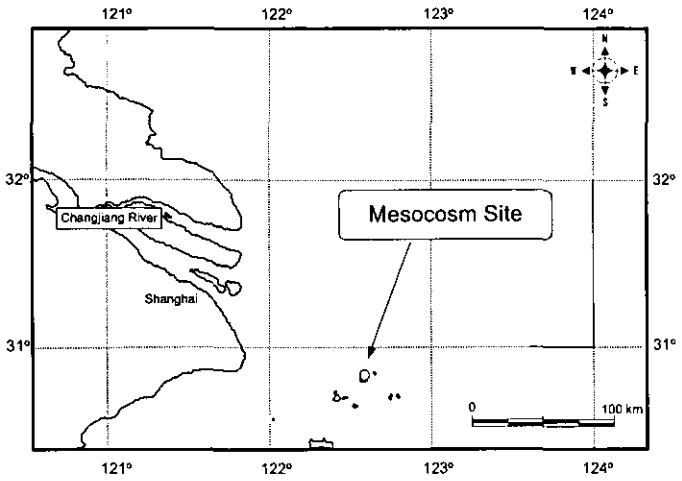

Fig.1 Location of the mesocosm experiments

inputs and their effects on the marine ecosystem in specified areas of the East China Sea' has been operational since 1997. We conducted this experiment on WSF from fuel oil in 1998 as part of the collaborative project, to understand the effect of oil on marine ecosystems.

2. MATERIALS AND METHODS

(1) Marine mesocosm and experimental site

A pair of mesocosms was installed near Liuhuashan – Huanaoshan (lat 30°50'N, long 122°37'E) in the Changjiang estuarine area (Fig. 1) for 7 days from 26 May (day 0) to 1 June (day 6) 1998. This area has a strong tidal current, high waves (over 1 m), and a large tidal exchange (several meters in maximum). We chose a floating mesocosm system, which is best suited to these conditions (Fig. 2). The mesocosms (5 m deep, 3 m diameter, volume about 25 m^3) were made of ethylene-vinyl-acetate reinforced with a polyester grid, and were translucent (light transparency about 50%) with no chemical elution from the surface. On the evening of 26 May, seawater was introduced simultaneously into the mesocosms through the bottom valve. The two mesocosms filled with seawater — one for oil enrichment (OE-mesocosm) and the other the control (OC-mesocosm) — were moored to the stern of the anchored research vessel 'Haijian 49' of the State Oceanic Administration, China.

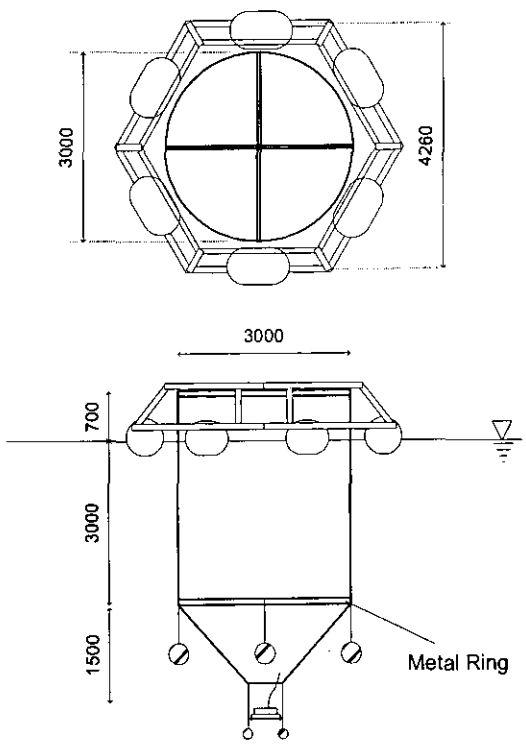

Fig.2 Schematic view of floating mesocosm

(2) Phosphate and oil enrichment

Prior to oil addition, phosphate ($NaH_2PO_4 \cdot 2H_2O$) was added into both mesocosms to a final concentration of ca. 1.5 μM on the night of day 0 when the water masses were isolated, in order to increase the activity of the phytoplankton. Waters in this estuarine area have a high N/P ratio and phytoplankton growth is limited by availability of phosphate[6]. It was presumed that nutrient limitation would complicate evaluation of the effect of oil contamination on biological activity.

Oil was added into the OE-mesocosm at 1200 on day 2 (i.e. between day 2 and day3 samplings). The added oil was the water-soluble fraction (WSF) of #0 diesel oil used as fuel by ships in China. The WSF was prepared by the following procedure. About 0.9 m^3 of seawater taken from the

experimental site and 0.1 m^3 of the diesel oil were mixed well over one day, using a stirrer device within a polyvinyl-chloride tank of volume 1 m^3 on the research vessel. The mixed solution was allowed to stand for almost two days, and then separated into an oil layer and oil-saturated seawater. The oil-saturated seawater was gently drained into the OE-mesocosm using a siphon system. The volume of the oil-saturated seawater added to the mesocosm amounted to about 0.8 m^3.

(3) Sampling and measurements

Seawater samples were collected from both mesocosms at a depth of 1 m, using 10-l Van-Dorn samplers, on the evening of day 0 and every morning on days 1 to 6. Seawater temperature, salinity, pH and dissolved oxygen concentration at depths of 1, 2 and 3 m were measured (Surveyor II, Hydrolab), except in the OE-mesocosm after WSF addition. The concentration and composition of the oil were determined by the TLC-FID method[7] (Iatroscan MK-5, Iatron). Subsamples of seawater were filtered with precombusted Whatman GF/F filters for analysis of nutrients (Traacs 800, Bran & Luebbe), Chl.*a* (HPLC system[8], Shimadzu), particulate organic carbon (EA1108, Fisons), and dissolved organic carbon (DOC, TOC5000A, Shimadzu). The filters and filtrate were stored at –20 °C prior to analysis. Phytoplankton samples were fixed with 6% formalin, and the species composition and abundance were determined by microscopy. Subsamples for bacterial and nano-sized heterotrophic protists were fixed with glutaraldehyde (final conc. 1%) and stained with DAPI[9]; their abundance was determined by epifluorescence microscopy[10]. Samples for micro-sized protists (>20 μm) and metazooplankton (>100 μm) were passed through 100-μm and 20-μm plankton nets sequentially; these samples were fixed with 6% formalin and stored in a cool dark place; species composition and abundance were determined by microscopy. Photosynthetic production and bacterial activity in glucose uptake were determined by 4-h *in situ* incubation using ^{13}C bicarbonate and ^{13}C D-glucose, respectively[11]. Transfer of photosynthetic production and bacterial ^{13}C uptake to large grazers after incubation was estimated by ^{13}C label transfer to >100 μm particles.

(4) Batch experiments for evaluation of WSF impact on photosynthesis

To determine the impact of oil addition on the primary producers more directly, two further batch-incubation experiments (Tests A and B) were performed as follows. Test A started just before WFS enrichment of the OE-mesocosm (day 2). Seawater samples were taken from both mesocosms and incubated with ^{13}C-bicarbonate in a seawater bath on the vessel. After 4 h, the incubated seawater was divided into two 2-l bottles; WSF was added to one at the same concentration as that in the OE-mesocosm. Incubation with and without the oil was continued for 16.5 h. Subsamples were taken after 2, 5.5 and 16.5 h and ^{13}C uptake (atom %) by the particles was determined. Test B was conducted on day 4 to examine the availability of nutrients to phytoplankton in the mesocosms, and consisted of *in situ* incubation with added nutrients (10 μM of nitrate and 1 μM of phosphate) and ^{13}C-bicarbonate. Seawater samples were taken from the two mesocosms; each sample was divided into two 2-l bottles. The nutrients were added to one of the bottles of each pair and incubation continued for 69 h. Subsamples were taken after 6, 21, 45 and 69 h and ^{13}C uptake (atom %) into the particles was determined.

3. RESULTS AND DISCUSSION

(1) Environmental variables

Within the mesocosms, physical and chemical variables (seawater temperature, salinity, pH and dissolved oxygen concentration) were uniform; salinity was almost constant (29.4 – 29.7‰) over the experimental period, while it varied outside the mesocosms (24.8 – 28.4‰). These data indicate that the water columns in the mesocosms were well mixed and conserved in the absence of seawater exchange with the surrounding waters. However, there were diurnal fluctuations in seawater temperature in the mesocosms (19.4 – 21.1°C), similar to those in the surrounding waters.

(2) WSF of #0 diesel oil

The composition of original diesel oil determined by TLC-FID method was 45% saturated hydrocarbons, 11% aromatics, 28% resin and 16% asphaltene. In the oil-saturated seawater prepared on the vessel, however, only fractions of resin and asphaltene were detected. It is presumed that the fraction of 'resin' contained highly polar components that were easy to move from the oil to the seawater phase. The total oil concentration in the

OE-mesocosm remained at ca. 1.6 mg l^{-1} after day 3 (Fig. 3). The DOC concentration increased from 1.1 mgC l^{-1} (day 2) to 3.2 mgC l^{-1} on day 3 and remained at a similar concentration until the end of the experiment (Fig. 3). These unchanging concentrations after WSF addition may indicate that the WSF was dissolved homogeneously in the mesocosm. Because natural seawater was used to prepare the WSF, the indigenous bacteria proliferated and reached 5.7×10^6 cells ml^{-1} in the oil-saturated seawater. The increased bacterioplankton consisted mainly of rod-type cells, which were larger than those in the naturally occurring bacterioplankton. The growing bacterioplankton probably altered the chemical characteristics of the WSF somewhat.

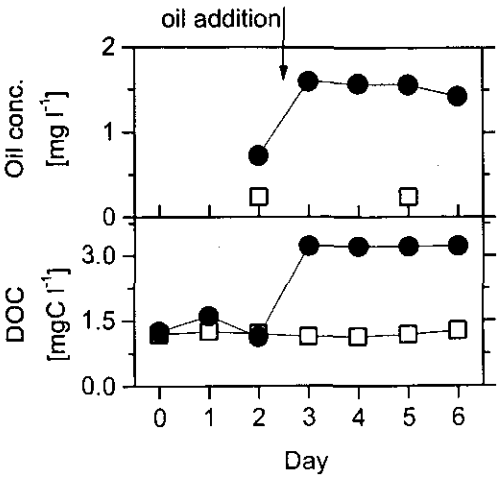

Fig.3 Daily changes in concentration of oil and dissolved organic carbon (DOC).
–□– OC-mesocosm, –●– OE-mesocosm.

(3) WSF impact on phytoplankton abundance

The initial concentrations of macronutrients (day 0) were almost the same in the two mesocosms (phosphate = 0.16 μM, and nitrate + nitrite = 11.6 μM) (Fig. 4). However, on day 1, after the addition of phosphate into the two mesocosms, the concentrations of nutrients were higher in the OE-mesocosm than in the OC-mesocosm. The density of the dominant dinoflagellate, *Prorocentrum dentatum*, in the OC-mesocosm (3.4×10^2 cells ml^{-1}) was about double that in the OE-mesocosm (1.4×10^2 cells ml^{-1}). Plankton abundance in the two mesocosms became different even though the water columns were enclosed almost simultaneously and the same concentration of phosphate was added. This suggests that some slight difference in environmental conditions or in the number of higher-order grazers, etc. can easily cause differences in an ecosystem; hence, differences in abundance of phytoplankton between the OC- and OE-mesocosms cannot be interpreted simply as the impact of oil. The decrease in nutrients was more rapid in the OC-mesocosm and the nitrate + nitrite content was almost consumed by day 2, though it remained until day 4 in the OE-mesocosm.

Net photosynthetic production (PP) in the OC-mesocosm reached a maximum of 164 μgC l^{-1} h^{-1}) on day 2, almost double than that in the OE-mesocosm on the same day (Fig. 5). Afterward, the PP in OC-mesocosm declined and reached a minimum (38 μgC l^{-1} h^{-1}) on day 4. PP in the OE-mesocosm was fairly stable at 64 – 84 μgC l^{-1} h^{-1} during days 2 to 4. The difference in temporal changes of PP between the two mesocosms would

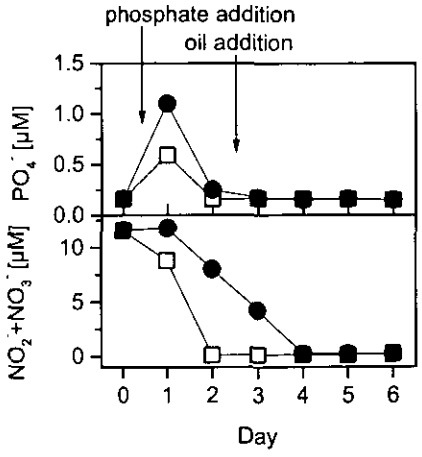

Fig.4 Daily changes in nutrient concentrations.
–□– OC-mesocosm, –●– OE-mesocosm.

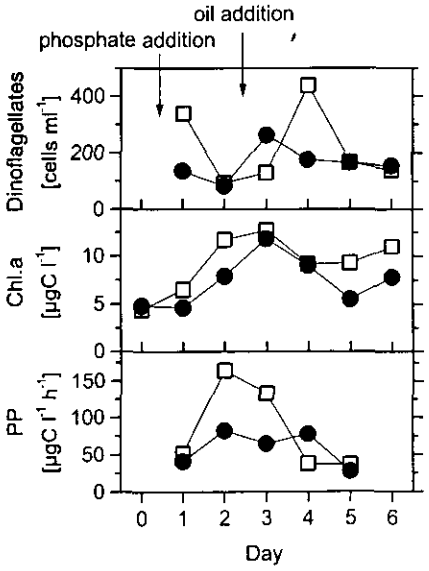

Fig.5 Daily changes in abundance of dominant dinoflagellates, chlorophyll *a* concentration and photosynthetic production (PP).
–□– OC-mesocosm, –●– OE-mesocosm.

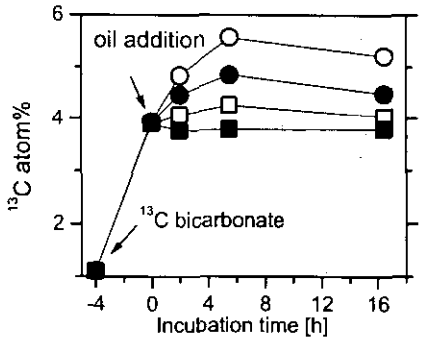

Fig.6 Result of test A: Acute impact of WSF on photosynthetic activity.
-○- OE control, -●- OE with oil-enriched water,
-□- OC control, -■- OC with oil-enriched water.
Dark area indicates night.

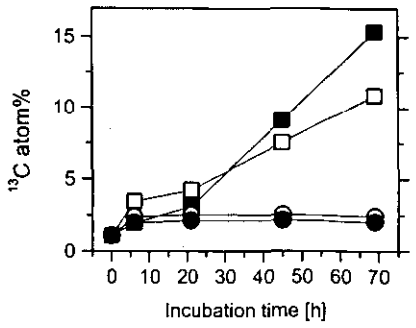

Fig.7 Result of test B: Effect of presence of WSF on nutrient uptake ability of phytoplankton.
-○- OE control, -●- OE with nutrients,
-□- OC control, -■- OC with nutrients.
Dark areas indicate night.

partially reflect the concentrations of available nutrients. The decrease in PP after day 2 in the OC-mesocosm might result from deficiency of nitrate and nitrite. The absence of a similar rapid decrease in the OE-mesocosm would thus be due to a slower rate of nutrient decline there than in the OC-mesocosm. Daily differences and fluctuations in phytoplankton abundance, Chl *a* concentration and PP between the two mesocosms were insufficient to demonstrate an adverse effect of WSF in the OE-mesocosm from day 3.

(4) WSF impact on photosynthesis

The batch incubation experiment with ^{13}C-bicarbonate clearly showed the adverse effect of WSF on photosynthetic activity, although phytoplankton abundance and photosynthetic production alone were insufficient to demonstrate the effect of WSF. In Test A, in incubation experiments using seawater taken from the OC- and OE-mesocosms, it was found that ^{13}C-bicarbonate uptake decreased significantly after WSF addition (Fig. 6). In Test B, nutrient addition was more effective in promoting ^{13}C-bicarbonate uptake in seawater from the OC-mesocosm than in seawater from the OE-mesocosm. These experiments indicate that ^{13}C uptake (photosynthetic activity) was clearly influenced by the addition of WSF, and that uptake in the OC-mesocosm was limited mainly by nutrient concentrations while photosynthetic activity in the OE-mesocosm was inhibited by WSF and/or nutrient concentrations (Fig. 7).

(5) WSF impact on bacterioplankton

Daily changes in abundance of bacterioplankton were similar in the two mesocosms (Fig. 8). The abundances in the OC- and OE-mesocosm on day 1 were 1.3×10^6 and 1.5×10^6 cells ml^{-1}, respectively, increasing gradually to a maximum of 3.8×10^6 and 3.4×10^6 cells ml^{-1}, respectively, on day 3, and afterwards decreasing. However, the average ^{13}C-glucose uptake by particles with larger than the pore size of GF/F filters, comprised of large bacteria, bacterivores, etc., determined by 4-h incubation, was 2.2 times greater in the OE-mesocosm than in the OC-mesocosm after WSF addition (Fig. 8), indicating that bacterial activity was stimulated by the presence of WSF, though some previous studies reported inhibition of bacterial activity by WSF . Bacterivores would then respond rapidly to the increase in bacterioplankton and control abundance.

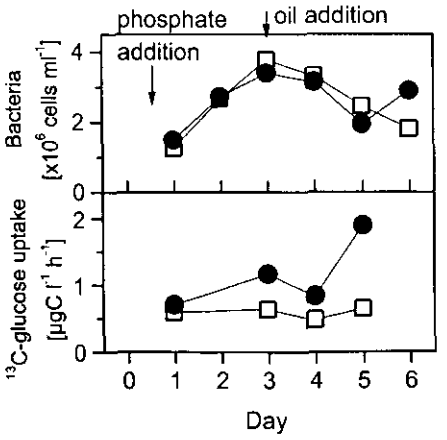

Fig.8 Daily changes in bacterial number and ^{13}C-glucose uptake rate.
-□- OC-mesocosm, -●- OE-mesocosm.

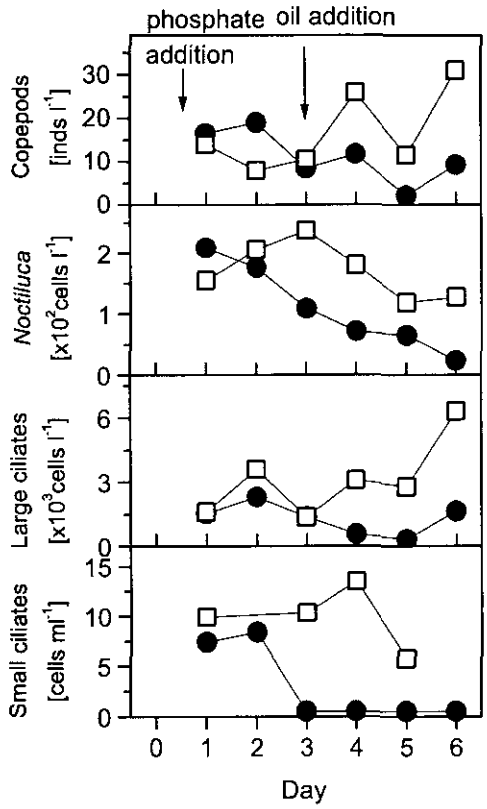

Fig.9 Daily changes in abundance of copepods (>100μm), noctiluca (>100μm), large ciliates (20–100 μm) and small ciliates (<20 μm).
–□– OC-mesocosm, –●– OE-mesocosm.

(6) WSF impact on grazer abundance

Although there were initial differences in abundance of the most dominant phytoplankton organisms between the two mesocosms, the abundance and composition of other plankton were quite similar before the addition of WSF (Fig. 9). Phytoplankton grazers in the two mesocosms included the heterotrophic dinoflagellate *Noctiluca scintillans*, ciliates and copepods. The most abundant grazers before WSF addition were *N. scintillans* ($1.6 \times 10^2 - 2.1 \times 10^2$ inds l^{-1}) in the >100-μm size fraction, tintinnid ciliates ($1.5 \times 10^2 - 3.6 \times 10^2$ inds l^{-1}) in the 20 – 100-μm size fraction, and tintinnid and oligotrich ciliates ($7.4 \times 10^3 - 9.9 \times 10^3$ inds l^{-1}) in the <20-μm size fraction. The average abundance of copepods (>100 μm, mainly *Corycaeus* sp., *Paracalanus* sp. and *Oithona* sp.) on days 1 and 2 was 10 inds l^{-1} in the OC- and 16 inds l^{-1} in the OE-mesocosm.

After addition of WSF into the OE-mesocosm, the total number of *N. scintillans*, nano- and micro-sized ciliates and copepods decreased, while the relative abundance of *P. dentatum* remained similar to that in the OC-mesocosm. The ciliates decreased suddenly and to a large extent with WSF addition. The number of nano-sized ciliates fell from 8.4 cells ml^{-1} on day 2 to <0.5 cells ml^{-1} on day 3. This suggests that ciliates are the most sensitive grazers to WSF at concentrations around 1.6 mg l^{-1}. Other studies have reported the adverse effect of oil on ciliates. Dale (1988)[12] conducted enclosure experiments with oil addition and concluded that loricated choreotrichs are better protected against oil derived material than non-loricated choreotrichs. In this study, oil addition was followed by decreases in both oligotrich ciliates and tintinnids, although only the former disappeared completely; note, however, that abundance data on each type of ciliate were not collected.

The abundance of *N. scintillans* in the OE-mesocosm decreased continually during the experiment period. Using microscopy on fresh samples on board the vessel, the cells of *N. scintillans* after WSF addition were seen to have shrunk and the surface of cells to have lost their turgor. Thus, *N. scintillans*, as well as the ciliates,

was sensitive to WSF. *N. scintillans* in the OC-mesocosm also decreased slightly; however, microscopy showed that the cells seemed to be healthier than those in the OE-mesocosm.

The total abundance of copepods in the OE-mesocosm remained lower than that in the OC-mesocosm after WSF addition, although their numbers fluctuated during the experiment. These daily variations might be caused by the migratory ability of the copepods themselves and/or changes in mixing conditions in the water columns, which would be in proportion to wave height around the mesocosms. The average abundances of copepods before and after WSF addition should show the impact of WSF on them. In the OC-mesocosm, they increased from 10 inds l^{-1} (days 1 and 2) to 19 inds l^{-1} (days 3 to 6), whereas in the OE-mesocosm they decreased from 16 inds l^{-1} to 7.5 inds l^{-1}.

(7) WSF impact on carbon transfer from producers to larger zooplankton (>100μm)

WSF addition caused a decrease in the concentration of some grazers, inhibited photosynthetic activity and enhanced bacterial activity in this experiment. It was presumed that carbon transfer in the planktonic food chain would be correspondingly affected.

After WSF addition, however, the 4-h transfer of photosynthetic production to >100 μm particles (i.e. grazers) was similar in magnitude in the two mesocosms (Table 1). At first glance, the results seem to indicate that WSF had no effect on this carbon transfer, but there are other possible reasons. First, there was a stronger nutrient limitation in the OC-mesocosm, resulting in a similar magnitude of primary production in the two mesocosms. Consequently, transportable primary production to grazers was almost the same in the two mesocosms. Second, primary production by *P. dentatum* can be ingested not only by >100-μm grazers but also by the abundant ciliates, which were <100 μm. Ciliates were more abundant in the OC-mesocosm (Fig. 9) and would have been able to intercept the transfer of primary production between *P. dentatum* and the larger grazers.

The 4-h transfer of ^{13}C from bacteria to >100-μm particles in the OE-mesocosm was about 0.8 times that in the OC-mesocosm after WSF addition (Table 1), even though the total amount of ^{13}C glucose uptake was about 2.2 times higher in the OE-mesocosm than in the OC-mesocosm (Table 1). It was estimated that the efficiency of bacterial carbon transfer in the OE-mesocosm was about 40% of that in OC-mesocosm. The higher activity of bacterioplankton would possibly create carbon transfer pathways in the microbial loop as well as to large zooplankton[13]. The lower transfer efficiency in the OE-mesocosm was likely the result of decreased abundance and activity of higher-order organisms associated with the bacterial carbon pathway in the food web.

Table 1. Comparison of carbon transfer to >100-μm particles between the OC- and OE-mesocosm after addition of WSF (day 3).

Average after WSF addition	OC	OE	OE/OC [b]	$R_{100\mu m}/R_p$ [c]
PP [a] [μgC l^{-1} h^{-1}]	69.3	56.7	0.82	0.96
PP transfer to >100 μm [μg C l^{-1} h^{-1}]	1.2×10^{-1}	9.2×10^{-2}	0.79	
Bacterial ^{13}C uptake [μg ^{13}C l^{-1} h^{-1}]	0.59	1.30	2.2	0.37
Bacterial ^{13}C transfer to >100 μm [μg ^{13}C l^{-1} h^{-1}]	8.9×10^{-3}	7.2×10^{-3}	0.81	

a. PP = photosynthetic production.
b. OE/OC = ratio of each value between OE- and OC-mesocosms.
c. $R_{100\mu m}$ = OE/OC of transfer to >100 μm; R_p = OE/OC of PP or bacterial ^{13}C uptake.

4. CONCLUSIONS

The following results were obtained from our mesocosm study in the Changjiang Estuary.

1) There was little difference in abundance of dominant phytoplankton (*Prorocentrum dentatum*) between the control and oil-enriched mesocosms after WSF addition at a concentration of 1.6 mg l^{-1}, suggesting that WSF did not affect the phytoplankton. However, parallel batch experiments with inorganic ^{13}C revealed clearly that

photosynthetic activity would be affected by WSF addition. We attribute the small differences in abundance between the two mesocosms to greater nutrient limitation in the control mesocosm.

2) Uptake of ^{13}C D-glucose showed that WSF enhanced bacterial production. However, the abundance of bacterioplankton was similar in the two mesocosms. Perhaps, bacterivores responded immediately and removed the increased bacterioplankton.

3) The abundant grazers (*Noctiluca scintillans*, ciliates and copepods) in the mesocosm declined after addition of WSF. Ciliates were the most sensitive organisms to addition of WSF.

4) The 4-h transfer efficiency of ^{13}C from bacteria to large grazers (>100 μm) decreased by about 40% after WSF addition, even though bacterial activity in the oil-enriched mesocosm was 2.2 times higher than that in the control mesocosm. This suggests that carbon transfer in food webs especially to higher-order grazers would decline in the event of WSF pollution.

REFERENCES

1) Siron, R., Giusti, G., Berland, B., Morales-Loo, M.R. and Pelletier, E.: Water-soluble petroleum compounds: chemical aspects and effects on the growth of microalgae, *Sci. Total. Environ.*, Vol. 104, pp. 221-227, 1991.

2) Griffin, L.F. and Calder, J.A.: Toxic effect of water-soluble fraction of crude, refined and weathered oils on the growth of a marine bacterium, *Appl. Environ. Microbiol.*, Vol. 33, pp. 1092-1096, 1977.

3) Henson, J.M. and Hayasaka, S.S.: Effects of the water-soluble fraction of microbiologically or physically altered crude petroleum on the heterotrophic activity of marine bacteria, *Mar. Environ. Res.*, Vol. 6, pp. 205-214, 1982.

4) Parsons, T.R., Harrison, P.J., Acreman, J.C., Dovey, H.M., Thompson, P.A., Lalli, C.M., Lee, K., Li, G. and Chen, X.: An experimental marine ecosystem response to crude oil and Corexit 9527: part 2. Biological effects. *Mar. Envrion. Res.*, Vol. 13, pp. 265-275, 1984

5) Grice, G.D. and Reeve, M.R.: Introduction and description of experimental ecosystems, In: *Marine mesocosms* (Eds. Grice GD, Reeve MR), pp. 1-9, Springer-Verlag, New York, (1982)

6) Harrison, P.J., Yang, Y.P. and Hu, M.H.: Phosphate limitation of phytoplankton growth in coastal estuarine waters of China and its potential interaction with marine pollutants, In: *Marine ecosystem enclosed experiments* (Eds. Wong, CS., Harrison, PJ.), pp.192-202, International Development Research Centre, 1992.

7) Goto. M,. Kato, M., Asaumi, M., Shirai, K. and Venkateswaran, K.: TLC-FID method for evaluation of the crude-oil-degrading capability of marine microorganisms, *J. Mar. Biotechnol.*, Vol. 2, pp. 45-50, 1994.

8) Kohata, K., Watanabe, M. and Yamanaka, K.: Highly sensitive determination of photosynthetic pigments in marine in situ samples by high-performance liquid chromatography, *J. Chromatogr.*, vol. 558, pp. 131-140, 1991.

9) Porter, K.G. and Feig, Y.S.: The use of DAPI for identifying and counting aquatic microflora, *Limnol. Oceanogr.*, Vol. 25, pp. 943-948, 1980.

10) Nakamura, Y., Suzuki, S. and Hiromi, J.: Population dynamics of heterotrophic dinoflagellates during a *Gymnodinium mikimotoi* red tide in the Seto Inland Sea, *Mar. Ecol. Prog. Ser.*, Vol. 125, pp. 269-277, 1995.

11) Koshikawa, H., Harada, S., Watanabe, M., Sato, K. and Akehata, T.: Relative contribution of bacterial and photosynthetic production to metazooplankton as carbon sources, *J. Plankton. Res.*, Vol. 18, pp. 2269-2281, 1996.

12) Dale, T.: Oil pollution and plankton dynamics. 6. Controlled ecosystem experiments in Lindaaspollene, Norway, June 1981: Effects on planktonic ciliates following nutrient addition to natural and oil-polluted enclosed water columns, *Sarsia* Vol. 73, no. 3, pp. 179-191, 1988.

13) Koshikawa, H., Harada, S., Watanabe, M., Kogure, K., Ioriya, T., Kohata, K., Kimura, T., Sato, K. and Akehata, T.: Influence of plankton community structure on the contribution of bacterial production to metazooplankton in a coastal mesocosm, *Mar. Ecol. Prog. Ser.*, Vol. 186, pp. 31-42, 1999.

INFLUENCE AND BIOCONCENTRATION OF PETROLEUM HYDROCARBON ASSOCIATED WITH OIL ON AND BY PLANKTON IN A MESOCOSM EXPERIMENT OF EAST CHINA SEA

Xiaoyong SHI, Xiulin WANG, Yu JIANG and Xiurong HAN

Ocean University of Qingdao
(5 Yushan Road, Qingdao 266003, P.R.China)

A kinetic model was presented to estimate the uptake/release rate constants and thereafter, bioconcentration factor, k_1, k_2 and BCF (bioconcentration factor), for the uptake of PH by plankton were obtained. Implies that PH(petroleum hydrocarbon) caused no significant influence on the uptake of $N\text{-}NO_3$, but significant influence on that of $P\text{-}PO_4$. In addition, the application of kinetic model for the bioconcentration of volatile organic toxic compound by organism suggests that the uptake of PH by plankton was an important process for the environmental capacity of PH.

Keywords: *East China Sea, Mesocosm, Petroleum Hydrocarbon, Nutrient*

1. INTRODUCTION

With economic development and consumer demand, oil pollutants have been one of the main marine pollutants in China' coastal regions. For example, in Changjiang estuary the oil-contaminated area increased sharply to 69% in 1995 and its average criterion index reached up to 2.17[1]. Oil pollutants are generally introduced to marine environment from industrial wastewater, vessel discharge and shipwreck, thus causes a serious marine environment problem. To assess the influences of the oil pollutants on the marine ecosystem, it is necessary to develop a mathematical kinetic model of their transport, distribution and fate in the marine ecosystem, and then especially to estimate environmental capacity.[2, 3] Furthermore, in developing the kinetic model, it is necessary to determine some kinetic parameters required for the model (such as pollutant and nutrient uptake/elimination rate constants) in laboratory and especially in field condition such as in mesocosm. Generally, facts contributed to marine environmental capacity include: 1) hydrodynamic transport self-depuration, 2) sedimentation transport self-depuration, 3) biological self-depuration (such as bioconcentration, biomagnification and biodegradation), and 4) chemical self-depuration.[4,5] However, it is extremely difficult to estimate biological self-depuration.[4] Not only can simple test of acute toxicity mislead indication of toxicity; but also in situ experimental method for determination of some kinetic parameters has not been developed. Therefore, in this paper mesocosm experiment was applied to determine some kinetic parameters for the bioconcentration of petroleum hydrocarbon associated with oil by plankton and to study its influence on the plankton communities and nutrient uptake by phytoplankton.

2. THE KINETIC MODEL FOR THE BIOCONCENTRATION OF VOLATILE ORGANIC TOXIC COMPOUND BY AQUATIC ORGANISM

Bioconcentration of volatile organic toxic compounds (VOTCs) in aquatic organisms (such as phytoplankton, zooplankton, benthos, fish) is predominantly the result of partitioning of VOTC between the

organism and the water.[6,7] As described previously [8], organism growth and its metabolic capability for VOTC can be the factors influencing VOTCs concentration in organisms. Thus, the following model represents this:

$$\frac{dC_A}{dt} = k_1 C_{BT} - (k_1 B + k_2 + k_G + k_M) C_A \tag{1}$$

Where C_A (μg/kg) is concentration of VOTC in the organism and C_{BT} (μg/dm^3) is total (bioavailable) concentration of VOTC, B (kg/dm^3) the biomass of organism. k_1 (h^{-1}) and k_2 (h^{-1}) are the rate constants for, respectively, uptake from the water and elimination to the water. k_G (h^{-1}) is the (average) first order net growth rate constant during the exposure time, k_M (h^{-1}) is metabolic rate constant for VOTC in organism The model has the following steady-state solution:

$$BCF = \frac{C_A}{C_W} = \frac{k_1}{k_2 + k_G + k_M} \tag{2}$$

Where BCF is bioconcentration factor for the uptake of VOTC by organism, C_W (μg/dm^3) is the bioavailable concentration in the water. Organisms generally undergo continuous growth, especially in the field. Most importantly, C_{BT} is a function of time, resulting from abiotic processes (such as volatilization, adsorption by the wall of test container and chemical degradation), and biological processes (such as biodegradation, etc). Supposed that the following equation (3) can be applied to express the time course of C_{BT}:[9]

$$C_{BT} = A + De^{-mt} \tag{3}$$

Where A and D are constants. In addition, the Boltzman equation(4) can be well used to describe the organism growth[10]:

$$B = B_F - \frac{B_F - B_0}{1 + e^{(t-t_o)/\delta}} \tag{4}$$

Where B_F and B_0 are final and initial biomass, respectively, t_0 is the mid-point of the time for organism growth, i.e. is the time when B(t) is equal to $(B_F + B_0)/2$, δ_t is the width of time for organism growth.
Thus, C_A can be obtained by resolving the differential equation (1) and combining equations (3) and (4):

$$\begin{aligned} C_A = {} & e^{-TKt}\left[1 + e^{(t-t_o)/\delta}\right]^{-KBT} \\ & \left\{C + Ak_1 \int e^{TKt}\left[1 + e^{(t-t_o)/\delta}\right]^{KBT} dt + Dk_1 \int e^{(TK-m)t}\left[1 + e^{(t-t_o)/\delta}\right]^{KBT} dt\right\} \end{aligned} \tag{5}$$

If $t \ll t_0$, then equation (5) can be simplified to:

$$C_A = k_1\left[1 + e^{(t-t_o)/\delta}\right]^{-KBT}\left[\frac{A}{TK}\left(1 - e^{-TKt}\right) + \frac{D}{TK - m}\left(e^{-mt} - e^{-TKt}\right)\right] \tag{6}$$

However, if $t \gg t_0$, then equation (5) can be simplified to:

$$C_A = k_1\left[1 + e^{(t-t_o)/\delta}\right]^{-KBT}\left\{\frac{A}{TKK}\left(e^{KBt} - e^{-TK}\right) + \frac{D}{TKK - m}\left[e^{(KB-m)t} - e^{-TKt}\right]\right\} \tag{7}$$

Where

$$TK = k_1 B_0 + k_2 + k_G + k_M \quad (8\text{-}1)$$

$$TKK = k_1 B_F + k_2 + k_G + k_M \quad (8\text{-}2)$$

$$KB = k_1 (B_F - B_o) \quad (8\text{-}3)$$

$$KBT = k_1 (B_F - B_o)\delta t \quad (8\text{-}4)$$

Therefore, from equation (6) or (7) with a limitation of exposure time, k_1 and k_2, and thereafter BCF, can be obtained by fitting the time course of C_A for uptake of VOTC by aquatic organism with a non-linear regression

3. RESULTS AND DISCUSSION

(1) Influence of petroleum hydrocarbon on the growth of phytoplankton and zooplankton

Figure 1 shows the growth of diatom, dinoflagellate, and the total growth of phytoplankton and zooplankton in the O-mesocosm with the addition of PH, and in the C-mesocosm without the addition of PH. As shown in figure 1, the dominant species of phytoplankton was dinoflagellate in the C-mesocosm. But, in the O-mesocosm the dominant species of phytoplankton was changed to diatom after the addition of PH at the second day of the experiment. However, in the last day of the experiment, the dominant species of phytoplankton in the O-mesocosm was re-changed to dinoflagellate, probably due to the significant decrease in the PH concentration in the seawater, as shown in figure 3. Furthermore, during the period of the mesocosm experiment the cell density of diatom in the O-mesocosm was larger than that in the C-mesocosm, but the cell density of dinoflagellate in the O-mesocosm was smaller that that in C-mesocosm.

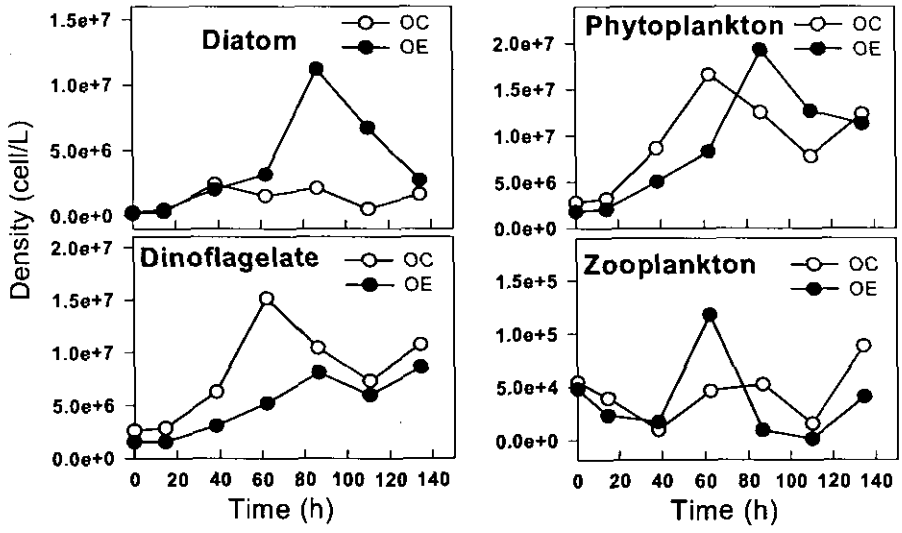

Fig.1 Growth of diatom, dinoflagellate, and total growth of phytoplankton and zooplankton in the O-mesocosm (●) and in the C-mesocosm (○).

This implies that the PH can enhance the growth of diatom, but inhibit the growth of dinoflagellate. The influences of PH on the growth of diatom and dinoflagellate resulted in the total growth of phytoplankton, as shown in figure 1, that in the first two days after the addition of PH the cell density of phytoplankton in O-mesocosm was lower than that in C-mesocosm, but then higher. The total growth of phytoplankton, in some degree, has the same regulation with the time course of PP, for both two mesocosms. Indicate the bio-accumulation of P. In addition, the PH also affected the growth of zooplankton. As shown in figure 1, except the third day, the cell density of zooplankton in O-mesocosm was lower than that in C-mesocosm, implying that the PH inhibited the growth of zooplankton.

In general, in the mesocosm experiment it is difficult to control the same original cell density of

phytoplankton and zooplankton. Thus, to further evaluate the influence of PH on the growth of plankton, the following equation (9) was used to estimate the influence percentage (IP) of PH on phytoplankton[11]:

$$IP\% = \frac{\log CD_{C-M} - \log CD_{O-M}}{\log CD_{C-M} - \log CD_{o(C-M)}} \tag{9}$$

and equation (10) on zooplankton and POC[5]:

$$IP\% = \frac{W_{C-M} - W_{O-M}}{W_{C-M} - W_{o(C-M)}} \tag{10}$$

Where CD and W are, respectively, cell density of phytoplankton and biomass of zooplankton or POC concentration. Subscript "C-M", "O-M" and "o" represent, respectively, C-mesocosm, O-mesocosm and the initial cell density or biomass.

The average values of IP over the experimental period after the addition of PH can be obtained using equation (9) and (10), which are listed in Table 1.

Table 1 The average values of IP over the experimental period after the addition of PH

Diatom	*Dinoflagellate*	*Phytoplankton*	*Zooplankton**
-63%	39%	3%	42%

* the value at third day was not included due to its unusual phenomena

If 0<IP<1, this implies that the PH can inhibit the growth of plankton. However, if IP<0, this implies that the PH can enhance the growth of plankton.

The average values of IP in Table 1 shows that the PH enhanced the growth of diatom, but inhibited the growth of dinoflagellate as well as total growth of phytoplankton and zooplankton, which was consistent with the results directly concluded from figure 1.

Furthermore, as shown in figure 2, the POC concentration in the O-mesocosm was lower than that in the C-mesocosm. Similarly, the average IP value of 48% was estimated from equation (10) for POC. Thus, it may be inferred that the PH inhibited the total growth of plankton (including phytoplankton and zooplankton), because in the short period of mesocosm experiment, the POC can, to some degree, represent the total biomass of plankton.

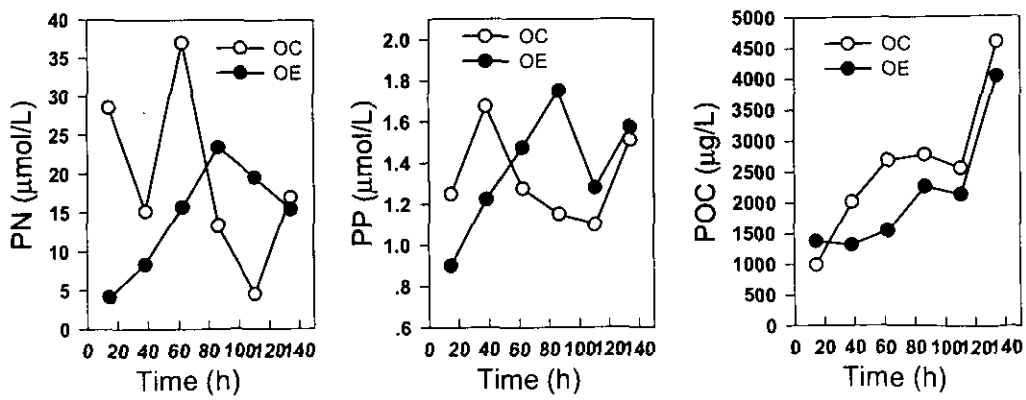

Fig.2 Time course of PN, PP and POC in the O-mesocosm (●) and in the C-mesocosm (O).

4. BIOCONCENTRATION OF PH BY PLANKTON

As shown in figure 3, significant decrease in PH was observed during the experimental period. The decrease was generally resulted from the biological processes (such as bioconcentration and biodegradation), and abiotic processes (such as adsorption by wall of test container, volatilization and chemical degradation).[4, 9] The experimental results showed that no significant adsorption by the wall of mesocosm bag was observed. Thus, to estimate the bioconcentration of PH by plankton, the comprehensive processes, except bioconcentration, of volatilization and (chemical- and/or bio-) degradation of the PH was tested in the laboratory. In the test, the same stock solution of PH associated with No. 0 diesel was used as that in the O-mesocosm. In addition, the test was also conducted 5 days at the same temperature as that in the O-mesocosm.

Figure 3 shows the time course of C_{BT} only resulted from the abiotic processes of volatilization and degradation. As shown in Figure 3, the time courses of C_{BT} as well as B can well defined by the model equation (3) and (4).

Supposed that the abiological processes (such as chemical-degradation and volatilization) and bio-degradation without plankton in the lab test were almost same as those in the O-mesocosm for the same PH stock solution. Consequently, the PH concentration in the plankton, as shown in figure 3, can be estimated by substracting C_{BT} determined in the O-mesocosm (i.e., C_W) from C_{BT} in the laboratory. In the estimating of C_A, the POC concentration was used, for during the short period of the mesocosm experiment the POC concentration can, to some degree, represent the biomass of plankton. Therefore, from equation (6), the uptake and release rate constants, k_1 and k_2, and bioconcentration factor, BCF, can be estimated by fitting the time course of C_A.

As shown in figure 3, the time course for the bioconcentration of PH by plankton was defined well by the model equation (6). The values of k_1, k_2 and BCF are shown in Table 2.

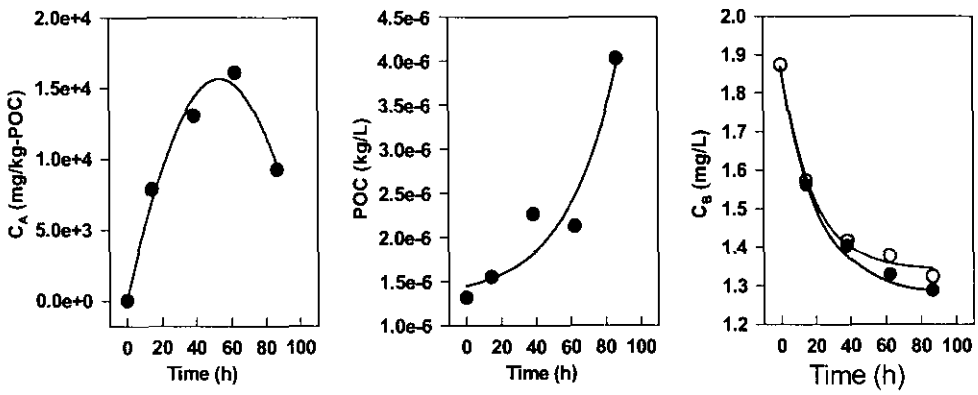

Fig.3 Time course of C_{BT} (o), C_W (•), POC, and C_A for the bioconcentration of petroleum hydrocarbon in the O-mesocosm experiment. The lines, respectively, represent the model fitting shown (3), (4) and (6).

Table 2 The uptake rate(k_1), elimination rate(k_2) and bioconcentration factor(BCF) or O-mesocosm

K_1 (h^{-1})	K_2 (h^{-1})	BCF
754.4	0.061	1.01×10^4

In addition, the results of k_1, k_2 and BCF were based on POC. Although it is difficult to compare the above results directly with data reported in literature, because the differences in plankton communities and test conditions used. In some ceases, however, data on BCF value for the bioconcentration of PH by plankton, as reported in literature, agree well with ours.[6-8, 12]

The major advantages of the proposed kinetic model for the bioconcentration of VOTC (such as PH) over those in current use are economy and available for in situ experiment (such as mesocosm). First, the results for k_1, k_2 and thereafter BCF rely primarily on the difference in VOTC concentration in water between the

experiment with organism sample and that without organism. Second, the results can be determined availably during relatively short exposure periods and significant cost saving can be realized in comparison to use of steady-state partitioning.[13] Most importantly, with the proposed model, it is not necessary to keep VOTC concentration in water (C_W) constant during the test periods, whereas in some current models C_W must be assumed to be constant[14] and/or flow-through systems must be applied[15] . In fact, these are impossible or very difficult for the mesocosm experiment.

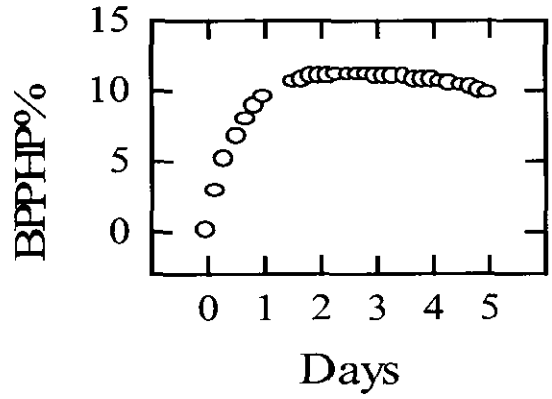

Fig.4 Time course of bioconcentration percentage of petroleum hydrocarbon (BPPHP%) by plankton. C_{BT} was assumed to be 50 □g/l and biomass of plankton to be 1.5 mg-C/l.

To estimate the possible contribution of the bioconcentration of PH to the marine environmental capacity, it is assumed that the average PH concentration for 1997 and 1998 was 50 μg/dm³ and could maintain constant, the biomass of plankton was 1.5 mg-C/dm³ in the given East China Sea. Thus, with the equation (6), the PH concentration in the plankton, C_A, was estimated. Then, the bioconcentration percentage of PH by plankton (BPPHP%) can be estimated. As shown in figure 4, after about 2 days, BPPHP% reached stable. Furthermore, in this case about 11% PH could be uptake by plankton. This implies that the bioconcentration of PH by plankton is an important process to the marine environmental capacity of PH.

5.INFULUENCE OF PH ON THE NUTRIENT UPTAKE AND RELEASE BY PHYTOPLANKTON

Figure 2 shows time course of PN and PP in the O-mesocosm with the addition of to PH, and in the C-mesocosm without the addition of PH. As shown in figure 2, significant differences in PN and PP was observed between O-mesocosm and C-mesocosm. Furthermore, in the first two or three days the concentrations of PN and PP in the O-mesocosm were higher than those in C-mesocosm, but then lower.

To evaluate the influence of PH on the nutrient uptake and release by phytoplankton, the following the equation (11) was applied to estimate the nutrient uptake and release rate constants by phytoplankton:[16]

$$\frac{1}{C_N}=\frac{1}{C_{NO}}+\frac{mk_{n1}e^{ft_o}}{[k_{n1}(C_{WO}+C_{NO}POC_O)-k_{n2}-f]^3}\Big\{e^{-ft}\Big\{[k_{n1}(C_{WO}+C_{NO}POC_O)-k_{n2}-f]^2(t-t_o)^2 - 2[k_{n1}(C_{WO}+C_{NO}POC_O)-k_{n2}-f](t-t_o)+2\Big\}-\Big\{[k_{n1}(C_{WO}+C_{NO}POC_O)-k_{n2}-f]^2t_o^2 + 2[k_{n1}(C_{WO}+C_{NO}POC_O)-k_{n2}-f]t_o+2\Big\}\Big\}+\frac{k_{n1}C_{NS(o)}}{M[k_{n1}(C_{WO}+C_{NO}POC_O)-k_{n2}+k_s]}\left(1-e^{k_s t}\right) \quad (11)$$

Where k_{n1} and k_{n2} are, respectively, nutrient (such as nitrogen, phosphorus) uptake and release rate constant by phytoplankton. C_N is internal phytoplankton nutrient concentration (μmol-N/μmol-C). C_W is nutrient concentration in seawater (μmol/dm³), M is maximal ratio of phytoplankton nutrient to its carbon, and t is time (day). C_{WO} is initial nutrient concentration in seawater. C_{NO} is initial phytoplankton nutrient. POC is

phytoplankton carbon concentration (μmol/dm³). POC_O is initial phytoplankton carbon. C_{NS} is sinking particulate nutrient concentration (μmol/dm³), and $C_{NS(o)}$ is the initial C_{NS}. The k_s, *m*, *n*, *f* and t_0 are constant.

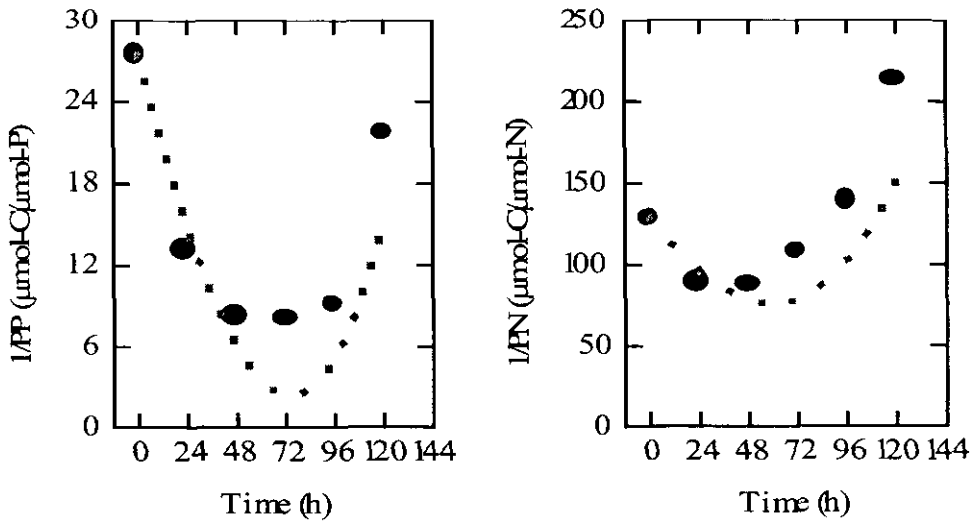

Fig.5 Time course of 1/PP and 1/PN for O-mesocosm experiment.The dash lines represent model fitting shown in equation (11).

Table 3 The $P\text{-}PO_4$ and $N\text{-}NO_3$ uptake and release rete constant(k_{n1}, k_{n2}) by phytoplankton for two mesocosms

O-mesocosm				C-mesocosm			
$P\text{-}PO_4$		$N\text{-}NO_3$		$P\text{-}PO_4$		$N\text{-}NO_3$	
K_{n1} (d^{-1})	K_{n2} (d^{-1})	K_{n1} (d^{-1})	K_{n2} (d^{-1})	K_{n1} (d^{-1})	K_{n2} (d^{-1})	K_{n1} (d^{-1})	K_{n2} (d^{-1})
0.0055	0.0062	0.12	0.012	0.053	0.061	0.053	0.059

As shown in figure 5, the time course of 1/PP and 1/PN for the nutrient uptake by phytoplankton in the O-mesocosm was defined well by the nutrient uptake and release kinetic model equation (11). Thus, the values of the nutrient uptake and release rate constants, k_{n1} and k_{n2}, for $P\text{-}PO_4$ and $N\text{-}NO_3$ were obtained by fitting the time course of $1/C_N$ with a non-linear regression procedure, shown in Table 3.

Furthermore, no significant differences in k_{n1} and k_{n2} for the uptake of $N\text{-}NO_3$ were observed between O-mesocosm and C-mesocosm. But for the uptake of $P\text{-}PO_4$ the values of k_{n1} and k_{n2} in O-mesocosm were far more smaller than those in C-mesocosm. This implies that PH can result in the significant influence on the uptake of $P\text{-}PO_4$ by phytoplankton, but no significant influence on $N\text{-}NO_3$.

These results were well consistent those concluded from influence of PH on the total growth of phytoplankton, especially the growth of dinoflagellate (Figure 1). Furthermore, the results may well demonstrate that the $P\text{-}PO_4$ was a more important environmental factor than $N\text{-}NO_3$ for the growth of phytoplankton in East China Sea .

REFERENCES

1) The National Bureau of Environmental Protection : *Environmental Communications*, 1999.
2) Cohen, Y. : Modeling of pollutant transport and accumulation in a multimedia environment, in the conference on *Geochemical and Hydrologic Processes and Treir Protection*, Council on environmental quality, Washington. D.C., september 25, 1984.
3) Ye, C.M.: Progress of the circling model in multimedia environments , *Env. Sci. Prog.* , Vol.2(1), pp. 9-25, 1994
4) Li Y.Q. : *The Biology of Marine Pollution.* Oceanic Press, Beijing, 1991.
5) Shang, L.S. : The pollution and determination of oil in the sea, *Mar. Env. Sci.*, Vol. 16, pp. 16-20, 1997.
6) Geyer, H., Politzki, G., Freitag, D., : Prediction of ecotoxicological behavior of chemicals: Relationship between n-octanol/water partition coefficient and bioaccumulation of organic chemicals by alga, *Chlorella, Chemosphere*, Vol. 13, pp.269-284, 1984.
7) Gobas, Frank A.C.P., McNeil, E.J., Lovett-Doust, L. and Haffner, G.D. : Bioconcentration of chlorinated aromatic hydrocarbons in aquatic macrophytes. *Environ. Sci. Technol.*, Vol.25, pp924-929, 1991

8) Wang, X.L., Harada, S., Watanabe, M., Koshikawa, H. : Modelling the bioconcentration of hydrophobic organic chemicals in aquatic organisms, *Chemosphere,* Vol. 32, pp1783-1793, 1996
9) Southworth, G.R., Bioaccumulation potential of polycyclic aromatic hydrocarbons in daphnic pulex, *Water Research*, Vol.12, pp.973-977, 1978.
10)Spiegel, M.R. : *Mathematical Handbook*, McGraw-hill Book Company, New York, 1990.
11)Wnag, X.L., Harada, S. Watanabe, M. Koshikawa, H. and Sato, K. : Determination of bioconcentration potential of tetrachloroethylene in marine algae by ^{13}C, *Chemosphere*, Vol.33, pp. 865-877, 1996.
12)Mailhot, H. : Prediction of algal bioaccumulation and uptake rate of nine organic compounds by ten physicochemical properties, *Environ. Sci. Technol.*, vol. 21, pp. 1009-1013, 1987.
13)Lohner, T.W. and Collins, w. J. : Determination of uptake rate constants for six organochlorines in midge larvae, *Environ. Toxi. Chem.*, Vol. 6, pp.137-146, 1987.
14)Mackay, D., Puig, H. and McCarty, L.S. : An equation describing the time course and variability in uptake and toxicity of narcotic chemicals to fish. *Environ. Toxi. Chem.*, Vol.11, pp. 941-951, 1992.
15)Geyer, H.J., Scheunert, I., Bruggemann, R., Matthies, M., Steinberg, E.W., Zitko, V., Kettrup, A. and Garrison, W. : The relevance of aquatic organisms' lipid content to the toxicity of lipophilic chemicals: Toxicity of lindane todifferent fish species. *Ecotoxicology and Environmental Safty,* Vol. 28, pp.53-70, 1994
16) Wang, X. L. : Kinetic model for the determination of nutrient uptake and release rate constants by phytoplankton. In press.

BACTERIAL COMMUNITY STRUCTURE IN THE EAST CHINA SEA

Hiroo UCHIYAMA[1], Hiroyuki SEKIGUCHI[1,2], Mikiya HIROKI[1], Makoto WATANABE[1], Masataka WATANABE[1]

[1] Soil and Water Environment Division, National Institute for Environmental Studies, Environment Agency (Onogawa 16-2, Tsukuba, Ibaraki 305-0053, Japan)

[2] Institute of Applied Biochemistry, University of Tsukuba (1-1-1 Tennoudai, Tsukuba, Ibaraki 305-0006, Japan)

Bacterial community structure in the East China Sea was studied as a baseline for comparison with future changes, in view of the construction of the Three Gorges Dam. We studied bacterial diversity in East China Sea surface water based on phenotypes and genotypes. Bacteria from three common marine groups, *Alpha-proteobacteria, Gamma-proteobacteria* and C/F/B, were dominant. Some other groups, including low G+C Gram positive, high G+C Gram positive and relatives of *Verrucomicrobium* were also observed. The dominant species in phenotype and genotype analyses were close relatives of *Alteromonas macleodii* and close relatives of *Roseobacter* spp.

Keywords : *PCR, bacterial community, phylogenetic tree, diversity*

1. INTRODUCTION

The East China Sea is located offshore from the mouth of the Yangtze River. The huge Three Gorges Dam, height 190 m, width 2 km, being constructed in the middle reaches of the River will create a lake 600 km long, and is expected to lead to changes in river flow that will affect East China Sea water quality (Fig. 1). It is important to evaluate changes in microbial community structure with changes in the environment, since the microbial community functions as the bottom line in marine ecosystems. Our aim in this study was to observe the microbial community structure in the East China Sea as a baseline for comparison with future changes. In the past, detection and analysis of bacteria in the environment have mainly been done by methods based on cultures. However, it is difficult to culture most bacteria in the environment[1]. Recently, bacterial community-structure analyses that do not depend on cultivation have been widely carried out, especially using PCR for targeting 16S rRNA genes for non-culturable bacteria[2-8]. In this study, we used both a culture-dependent method based on the pattern of carbon utilization and a culture-independent method based on the molecular technique of targeting 16S rRNA sequences.

2. MATERIALS AND METHODS

(1) Sampling

Samplings were carried out in October 1997 and May 1998, just before construction began on the Three Gorges Dam. We took 9 samples in total: from the surface (S), midwater (M), and bottom (B) at 3 stations, C1, C3 and C5 (Fig. 1).

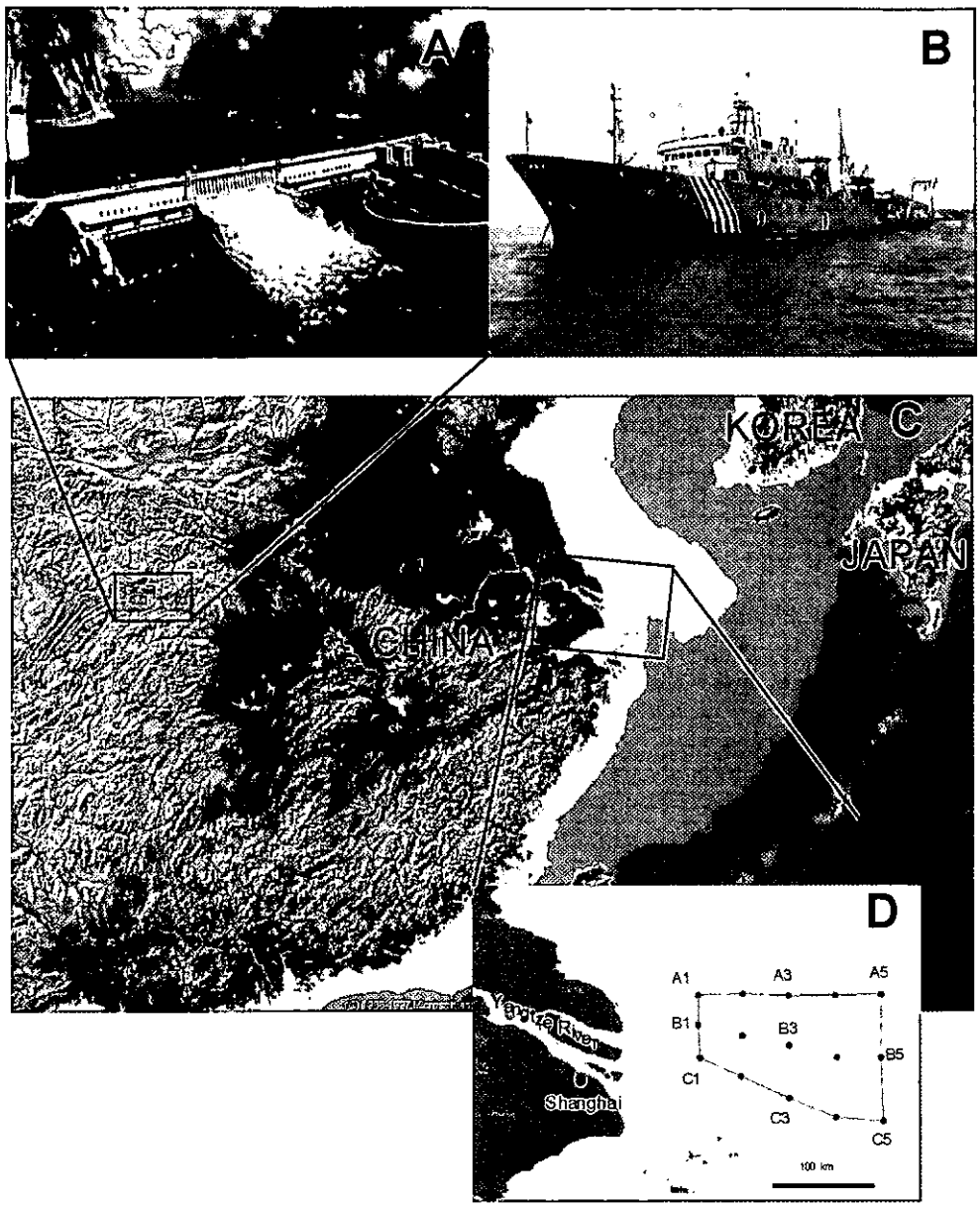

Fig. 1 (A) Conceptual drawing of the Three Gorges Dam at its completion. (B) Kaikan-49, the survey vessel. (C) Map of the area including the Yangtze River. (D) Location of the survey stations.

(2) Comparison of bacterial community based on PCR-RFLP pattern

Bacterial community structures in the 9 samples were compared based on PCR-RFLP patterns. Seawater samples (100 ml) were filtered with a 0.2-μm pore size filter. Total DNA from each filter was extracted with a Fast DNA kit (BIO101 Inc., Vista, CA), the physical extraction method using glass beads, from bacteria cells trapped on the filter. The 16S rRNA genes were amplified by PCR with bacterial universal primer sets[2] and digested with a restriction enzyme. Digested DNAs were separated on 2.5% agarose gel and the patterns were analyzed by the PDI fragment analysis system.

(3) Phenotypic analysis of bacterial clusters

Eighty bacterial clones randomly isolated from marine agar plates on which the surface seawater sample at St. C1 was spread, were applied to Biolog GN plates (Biolog, Hayward, CA), and the utilization patterns were analyzed by the Microlog Mlclust (Biolog) software packages.

(4) Genotypic analysis based on 16S rRNA

Bacterial diversity of the surface seawater at St. C1 was analyzed by comparing the partial sequences of 16S rRNA genes obtained by PCR. Amplified 16S rRNA genes were recovered from agarose gel, and then cloned into pCR. 2.1 vectors using a TA cloning kit (Invitrogen, San Diego, CA). We obtained sequences for 150 clones of 16S rRNA genes with a minimum 400 bp from PCR primer 1494 reverse primer for all clones. All sequences were compared with similar sequences of reference organisms by BLAST search. A phylogenetic tree was constructed by the neighbor-joining method with the CLUSTAL W software package.

3. RESULTS AND DISCUSSION

(1) Comparison of bacterial community structure by PCR-RFLP

The phylogenetic tree constructed from the PCR-RFLP pattern showed that the bacterial community structure at St. C1 was different from that of the other sites; also at all stations the structure at the surface was different from that in midwater and the bottom (Fig. 2). Especially, in May 1998, the bacterial community structure at St. C3 surface resembled to that at St. C1 surface, suggesting that huge amount of freshwater from the Yangtze River reached to St. C3. This suggested that freshwater from the Yangtze River affects the structure of bacterial communities in the East China Sea. We regarded St. C1 as a suitable site for evaluation of changes in the outflow of the Yangtze River.

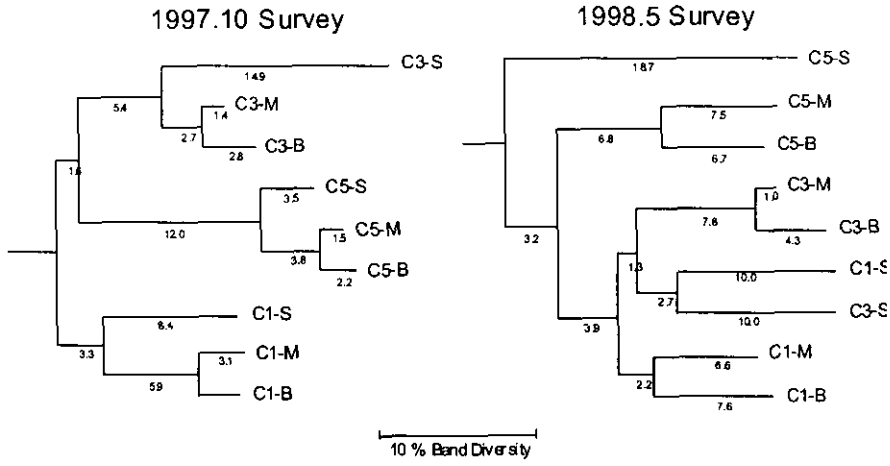

Fig. 2 Seasonal comparison of genetic simirality of microbial communities in C stations based on PCR-RFLP analysis.

(2) Bacterial concentration at St. C1

The density of bacteria at St. C1 as estimated by CFU on Marine agar plates (Difco) and by 4', 6-diamino-2-phenylindol (DAPI) direct count was 2.8×10^4 ml^{-1} and 4.2×10^5 ml^{-1}, respectively, indicating that only some of the bacteria were culturable (Fig. 3).

(3)Phenotypic analysis of bacteria isolated from East China Sea

From phenotypic analysis of 80 isolates using the Biolog test system, we found 4 groups (Fig. 4): relatives of *Alteromonas macleodii*, relatives of *Roseobacter gallaeciensis*, a *Vibrio* group, a Tiny colony group. *Alteromonas macleodii* is distributed in coastal waters and open oceans, utilizing many organic compounds as sole or principal sources of carbon and energy, and has a number of extracellular enzymes including amylase, gelatinase and lipase[9]. Therefore, this bacterium is supposed to have some important role in carbon cycling in oceans, also in East China Sea. The Tiny colony group (Fig. 5), which comprised 70% of the isolates, were close relatives of *Roseobacter litoralis*, which is reported to have photosynthetic ability[10] (Fig. 6). This may be related to the fact that the Tiny colony groups were mainly obtained from surface water, where light is at a maximum (data not shown).

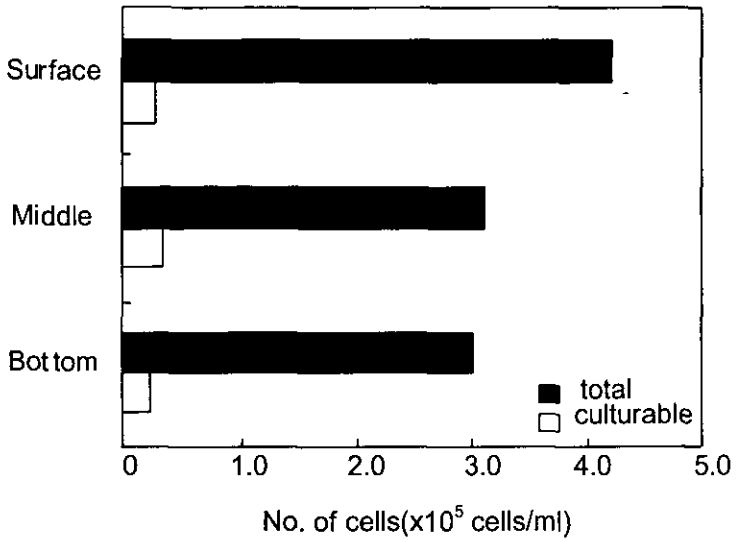

Fig. 3 Comparison of bacterial numbers estimated from CFU on marine agar plates and by DAPI direct counts.

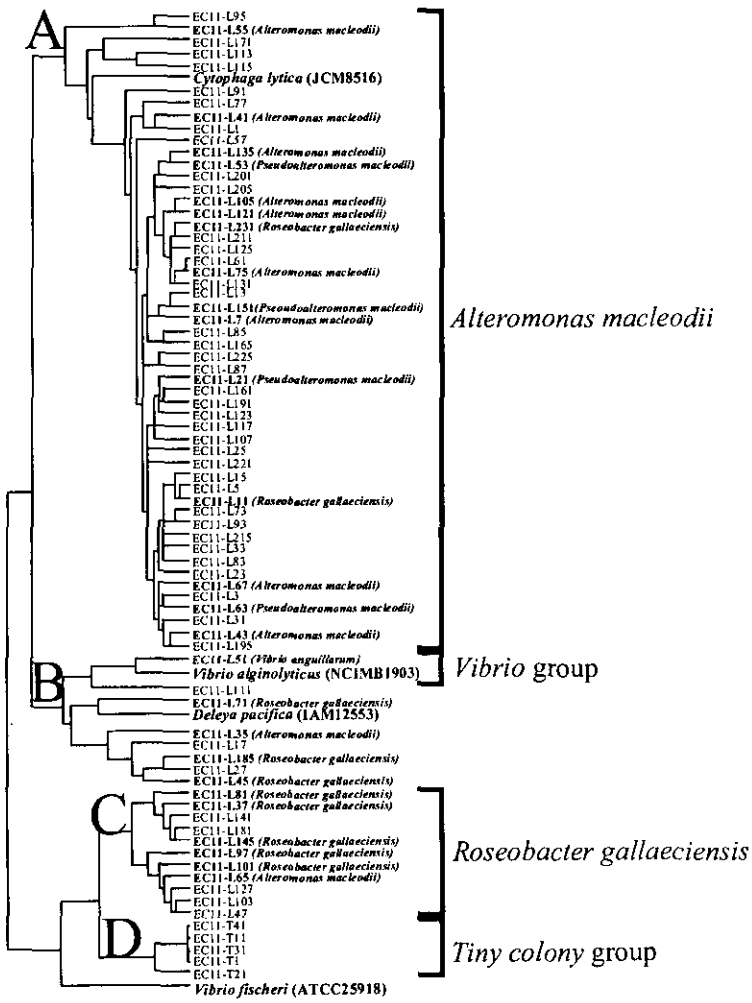

Fig. 4 Phylogenetic tree based on carbon source utilization patterns obtained with the Biolog system for 80 isolates from surface waters at St. C1.

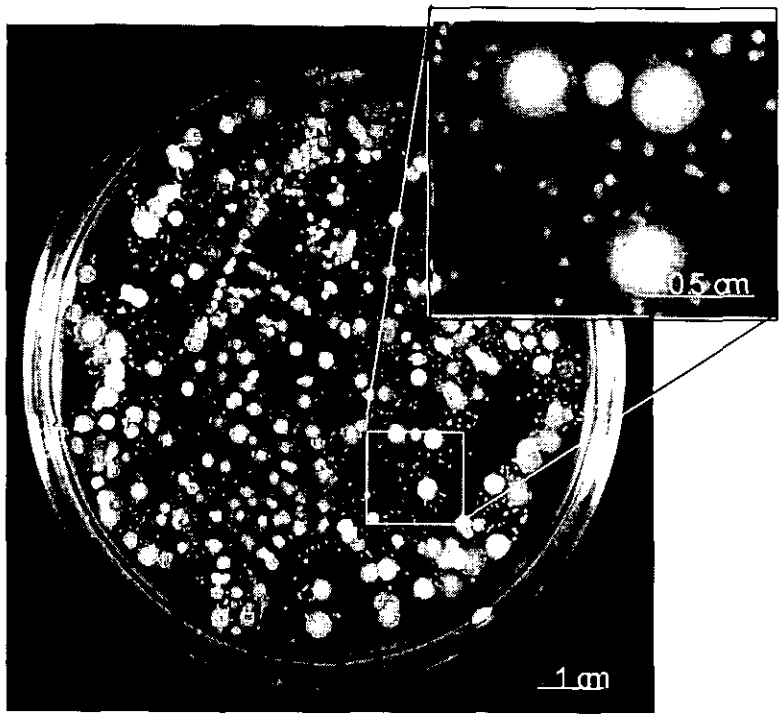

Fig. 5 Bacterial colonies growing on a marine agar plate.

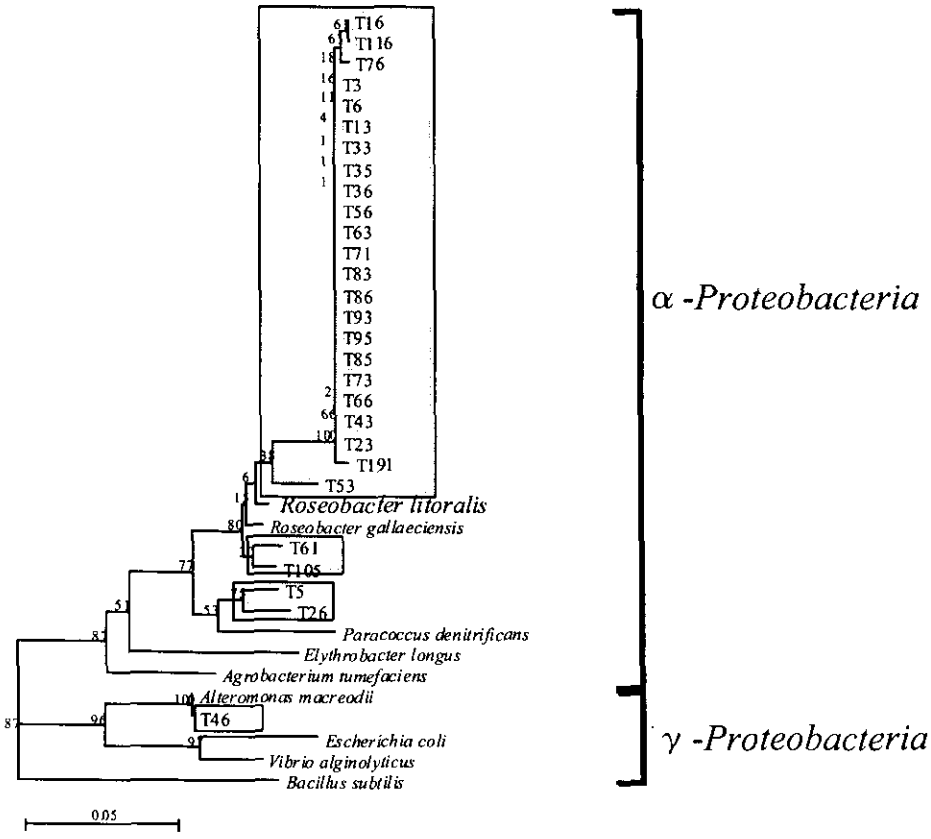

Fig. 6 Phylogenetic tree based on partial sequences of 16S rRNA genes for the Tiny colony group.

(4) Genotypic analysis

From genotypic analysis, bacteria from 3 common marine groups, *Alpha-proteobacteria*, *Gamma-proteobacteria*, and C/F/B, were dominant. Some other groups, including low G+C Gram positive, high G+C Gram positive and relatives of *Verrucomicrobium*, were observed. Further unidentified groups and SAR[11] and OCS clusters (non-culturable groups) were also observed (Fig. 7). These findings suggest that bacterial diversity in the East China Sea is immense.

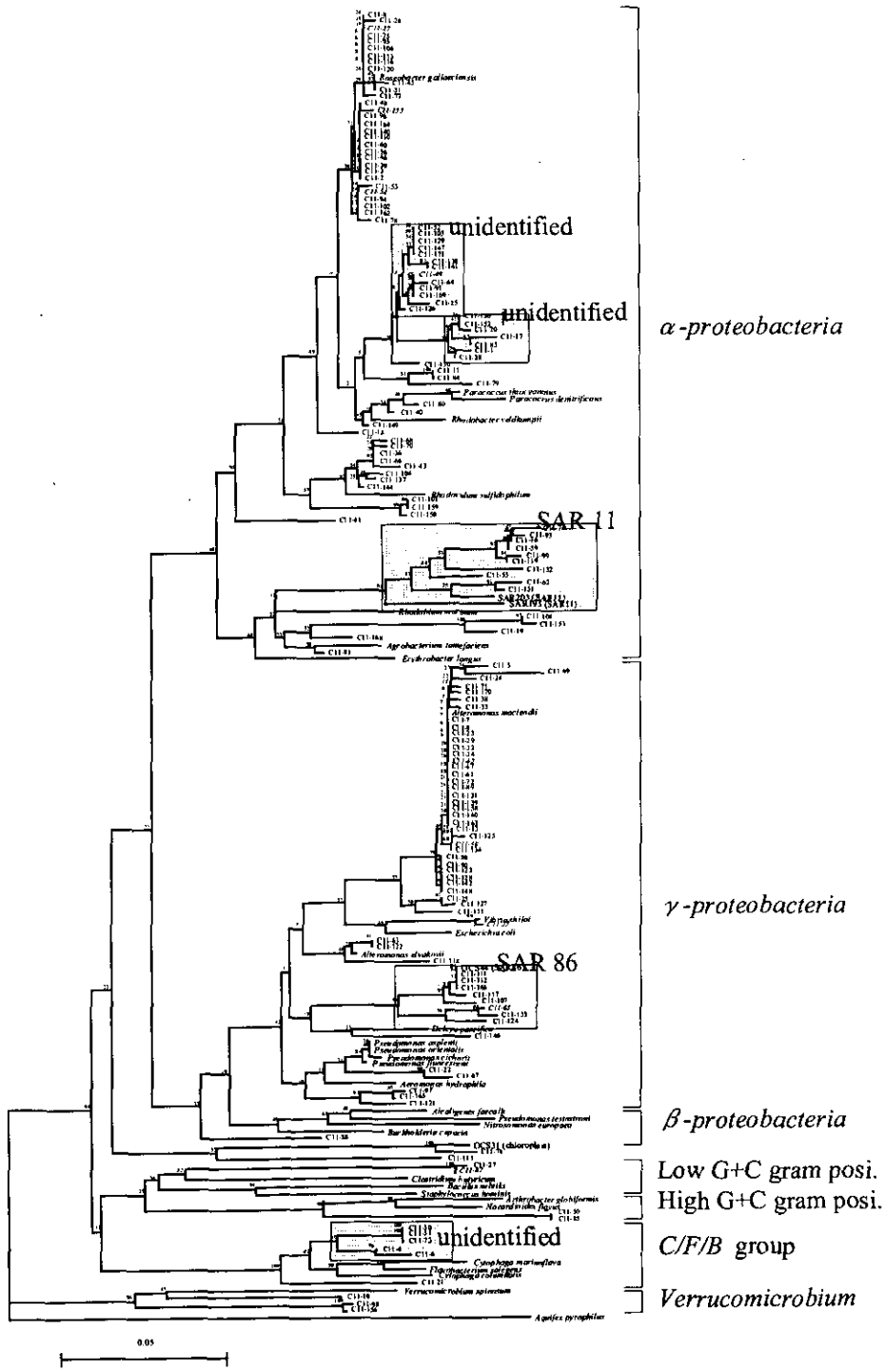

Fig. 7 Phylogenetic tree based on partial sequences of 16S rRNA genes obtained from surface waters at St.C1by PCR with bacterial universal primer sets.

4. CONCLUSIONS

Phenotypic and genotypic analyses revealed that many species of bacteria inhabit in the East China Sea. The knowledge obtained in this study will be an important and valuable baseline for evaluating the effects of environmental change in the area, because the samples were collected just before the start of construction of the Three Gorges Dam.

ACKNOWLEDGMENT: We thank Mrs. Kambe for skilled technical assistance.

REFERENCES

1) M. T. Suzuki, M. S. Rappe, Z. W. Haimberger, H. Winfield, N. Adair, J. Strobel, and S. J. Giovannoni.: Bacterial diversity among Small-Subunit rRNA gene clones and cellular isolates from the same sea water sample. *Appl. Environ. Microbiol.* **63**, 983-989 (1997)

2) R. I. Amann, W. Ludwig, and K-H. Schleifer.: Phylogenetic identification and in situ detection of individual microbial cells without cultivation. *Microbiol. Rev.* **59**, 143-169 (1995)

3) J. Borneman, P. W. Skroch, K. M. O'sullivan, J. A. Palus, N. G. Rumjanek, J. L. Jansen, J. Nienhuis, and E. W. Triplett.: Molecular microbial diversity of agricultural soil in Wisconsin. *Appl. Environ. Microbiol.* **62**, 1935-1943 (1996)

4) W. D. Hirons, B. A. Methe, S. A. Nierzwicki-bauer, and J. P. Zehr.: Bacterial diversity in Adirondack Mountain Lakes as revealed by 16S rRNA gene sequences. *Appl. Environ. Microbiol.* **63**, 2957-2960 (1997)

5) M. G. Wise, J. V. Mcarthur, and L. J. Shimkets.: Bacterial Diversity of a Carolina bay as determined by 16S rRNA gene analysis: Confirmation of novel taxa. *Appl. Environ. Microbiol.* **63**, 1505-1514 (1997)

6) J. A. Fuhrman, and A. A Davis.: Widespread archaea and novel bacteria from the deep sea as shown by 16S rRNA gene sequences. *Mar. Ecol. Plog. Ser.* **150**, 263-274 (1997)

7) J. A. Fuhrman, K. Mccallum, and A. A Davis.: Phylogenetic diversity of subsurface marine microbial communities from the Atlantic and Pacific Oceans. *Appl. Environ. Microbiol.* **59**, 1294-1302 (1993)

8) T. B. Britschgi, and S. J. Giovannoni.: Phylogenetic analysis of a natural marine bacterioplancton population by rRNA gene cloning and sequencing. *Appl. Environ. Microbiol.* **57**, 1707-1713 (1991)

9) P. Baumann, M. J. Gauthier, and L. Baumann.:Genus *Alteromonas*. *Bergey's Manual of Systematic Bacteriology*, vol. 1, ed. By N. R. Krieg and J. G. Holt, Williams & Wilkins Co., Baltimore, 1984, pp. 343-352.

10) B. Lafay, R Ruimy, C. Rausch DE Traubenberg, V. Breittmayer, M. J. Gauthier, and R. Christen.: *Roseobacter algicola* sp. nov., a new marine bacterium isolated from phycosphere of the toxin-producing dinoflagellate *Prorocentrum lima*. *Int. J. Sys. Bacteriol.*, **45**, 290-296 (1995)

11) K. G. Field, D. Gordon, T. Wright, M. RappÈ, E. Urbach, and K. Vergin.: Diversity and depth-specific distribution of SAR11 cluster rRNA genes from marine planctonic bacteria. *Appl. Environ. Microbiol.* **63**, 63-70 (1997)

BACTERIOPLANKTON PRODUCTION IN DILUTION ZONE OF THE CHANGJIANG (YANGTSE RIVER)ESTUARY

Zilin LIU[1], Hiroshi KOSHIKAWA[2], Xiuren NING[1], Junxian SHI[1] and Yuming CAI[1]

1. Second Institute of Oceanography, State Oceanic Administration
(Xixihexia 9, Hangzhou, 310012, China)
2. National Institute for Environmental Studies
(Tsukuba, 305-0053, Japan)

The bacterioplankton production and bacterioplankton number were measured in dilution zone of the Changjiang Estuary and a mesocosm experimental device for enriched phosphate experiment and oil contaminated experiment was placed in the waters nearby Luhua Island during October 1997 and May 1998. The average bacteriaplankton production in spring was higher than that in autumn, the production at the surface water was higher than that at the bottom; the higher production appeared in the middle of the surveyed area. The results from mesocosm experiment with adding phosphate and oil contaminated showed that the bacterioplankton production increased trending rising day by day during the experiment period.

Keywords: *Bacterioplankton production, Estuary, the Changjiang River*

1. INTRODUCTION

Numerous tiny bacteria extensively distribute in the sea. They decompose abundant organic materials and plankton detritus, transforming them into inorganic matters in the seawater. The bacteria utilizing dissolvable organic carbon (DOC) are eaten by protozoan, and the DOC is transformed into particulate organic carbon (POC) which can be utilized by animal, bacteria playing an important role in carbon and nitrogen cycle and energy conversion in the sea and exerting marked influence on marine ecosystem. Therefore, scientists have begun to pay attention to the study of bacterioplankton production (Fuhrman et al., 1980,1982, Kirchman et al., 1985).

The Changjiang River is the largest river in China. Its annual runoff reaches to $9.24\times10^{11}m^3$ with 4.86×10^8t suspended substances (Annals of Chinese Bay, 1998). Except most suspended silts sediment gradually in nearshore zone, a large number of abundant organic substances diffuse in the dilution zone, making there a good environments for bacteria growth. The surveying for the ecological characteristics of marine bacteria were carried out in the Changjiang River Estuary (Zheng Guoxing, et al., 1982, Shi Junxian et al., 1984, 1992), but no data on the bacterioplankton production have been published.

Kirchman et al., (1985) estimated bacterioplankton production with ^3H-leucine method, which consists of measuring the incorporation of radiolabeled leucine into bacterioplankton protein overtime. The physiological basis of the leucine method is protein synthesis. Bacterioplankton production can be calculated from rates of protein synthesis because protein comprises a large, fairly constant fraction (approximately 60%), of bacterioplankton biomass. Through the ratio of protein to total biomass, rates of protein synthesis can be converted to total biomass production. The surveyed of the distribution characteristics of bacterioplankton production in the Changjiang River dilution zone proved basic parameters for the studies on the environmental quality loading of the Changjiang River Estuary and its effect on marine ecosystem and the marine environmental capacity evaluation. And also proved scientific basis for the studies on marine biological productivity processes and resources sustainable development.

2. MATERIALS AND METHODS

(1) Sampling time and station positions

9 and 15 stations were set in the Changjiang River dilution zone (3100'-3200'N, 12230'~12400'E) to survey bacterioplankton production and bacterioplankton number during October 19~20 of 1997 and May 13~16 of 1998 separately. A mesocosm experimental device was placed in the water nearby Luhua Island (30°45.6'N, 122°37.0'E) during October 10~17 of 1997 and May 18~25 of 1998 to conduct the experiment of adding phosphorus (PO_4^{-3}). During May 26 to June 1st of 1998, the oil pollutant experiment (adding No.0 diesel oil) was done to observe the change characteristics of bacterioplankton production and bacterioplankton number in the small ecological environment after adding phosphorus or oil pollutant (Fig 1).

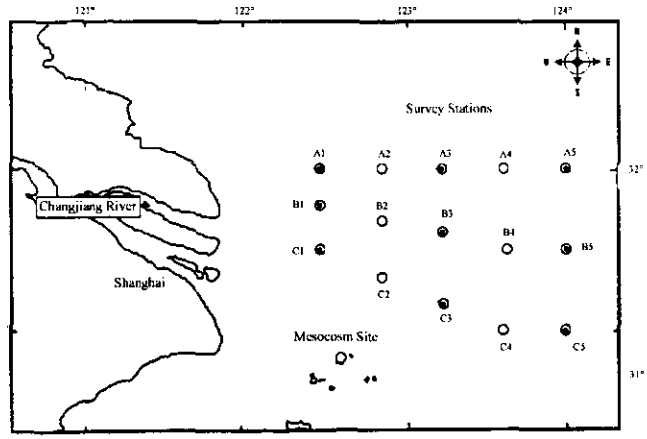

Fig. 1 Sampling station

• stations in October of 1997. o stations in May of 1998.

(2) Bacterioplankton production (BP)

After sterile sampling water, take three parallel test tube of water sample with 10 cm^3, respectively, one of the triplicate samples was added 30% trichloroacetic acid (TCA) solution as a contrast tube. Adding 4.4410^5 Bq ^{3}H-leucine with specific activity of 152mCi/mmol to the triplicate samples and incubate for 60 min; after incubation, adding 30% TCA solution to test tubes separately to kill the incubation and start extraction, then filter them through the 0.2 m Sartorius filter membrane under low vacuum. After filtering, rinse the membranes with 5% TCA solution and 80% alcohol solution respectively; then placed the membranes in scintillation vials and carried them back lab. After adding ethyl acetate to dissolve the membranes, then adding 10cm^3 of Packard Uitima Gold scintillation cocktail. Finally, conduct radioassay with Backman 5801 Liquid Scintillation Analysis device. The bacterioplankton production was calculated according to the formula of Parsons et al. (1984) and Kirchman et al.(1993).

(3) Bacterioplankton number

Bacterioplankton number was enumerated using the acridine orange count method (AODC) by Olympus HB Fluorescence microscopy according to the Specification for Oceanographic Survey, (STSA 1991).

3. RESULTS AND DISCUSSION

(1) Bacterioplankton production in the surveyed area

The bacterioplankton production at the surface water in autumn of 1997 is shown in Table 1. It is 0.22~3.35μgC$dm^{-3}h^{-1}$ with average value of 1.44±1.30μgC$dm^{-3}h^{-1}$. The ratio of this value to the primary

productivity is 0.18, namely, bacteria production is roughly 18% of the primary productivity. It basically coincides with the result that the bacterioplankton production in the southern California bay accounted for 5-25% of the primary productivity (Fuhrman et al., 1982).

Table 1 The comparison of bacterioplankton production (BP), primary productivity (PP) and chlorophyll *a* (Chl *a*) at the surface water of different station in autumn of 1997

	A_1	A_3	A_5	B_1	B_3	B_5	C_1	C_3	C_5	Average
BN ($\times10^8$cell·dm^{-3})	4.4	6.1	5.2	4.3	4.0	6.5	5.9	4.9	5.7	5.2
BP (μgC·dm^{-3}h^{-1})	0.45	3.35	0.64	0.22	3.35	0.42	0.53	2.53	1.49	1.44
PP (μgC·dm^{-3}h^{-1})	4.80	14.00	5.58	4.44	10.42	5.13	3.63	8.25	14.28	7.84
BP : PP (%)	0.09	0.24	0.12	0.05	0.32	0.08	0.15	0.31	0.11	0.18
Chl *a* (μg·dm^{-3})	0.62	3.88	0.88	0.47	2.57	0.83	0.53	1.41	2.55	1.53

From the horizontal distribution of the bacterioplankton production, primary productivity and chlorophyll *a*, it can be seen that their distributing trend is considerably similar to each other (Fig 2a-b). The high values appeared in the middle of the surveyed area. The bacterioplankton production, primary productivity and chlorophyll *a* concentration are more than 3.0μgCdm^{-3}h^{-1}, 10μgCdm^{-3}h^{-1} and 2.5μgdm^{-3} respectively. They all decrease to both sides of the surveyed area. On the southeast of the area, biological parameters are higher and the bacterioplankton production is 1.49μgCdm^{-3}h^{-1} at station C_5. Bacterioplankton production is lower than 0.5μgCdm^{-3}h^{-1} at the stations A_1 and B_1, and B_5.

In May of 1998, Owing to the Changjiang River dilution water increasing and biological metabolism enhancing in waters, the change range of bacterioplankton production at the surface water was 0.56~4.41 μgCdm^{-3} h^{-1} with average value of 2.43±1.22μgCdm^{-3}h^{-1}. They are obviously more than that in autumn. The high production more than 2.0μgCdm^{-3}h^{-1} covered on most of the surveyed area. Especially, the high values more than 4.0gCdm^{-3}h^{-1} appeared at stations B_1 and B_2 in the middle of the area; the low value less than 1.0gCdm^{-3}h^{-1} appeared at station A_1 on the northwest and station A_5 on the northeast of the area (Fig.3).

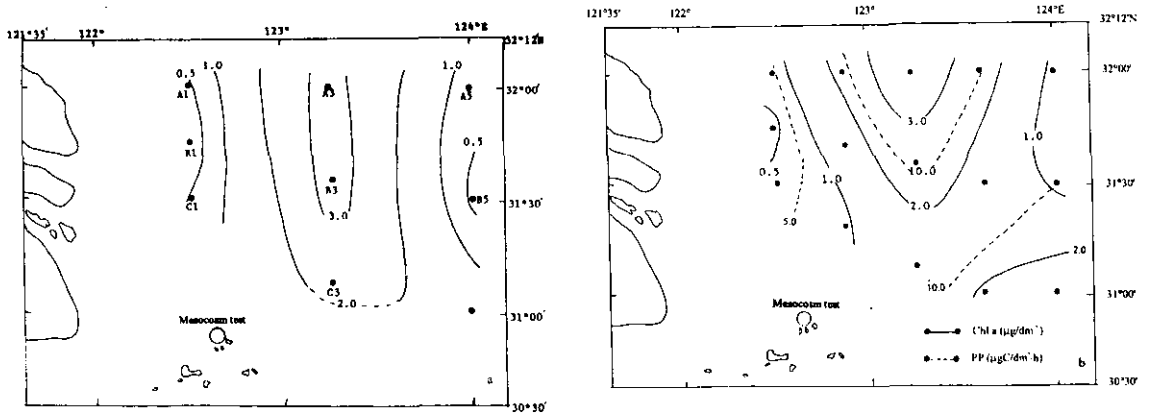

Fig.2 The comparison of horizontal distribution of bacterioplankton production, primary productivity and chlorophyll *a* in October of 1997
a) bacteria. b) chlorophyll *a* and PP.

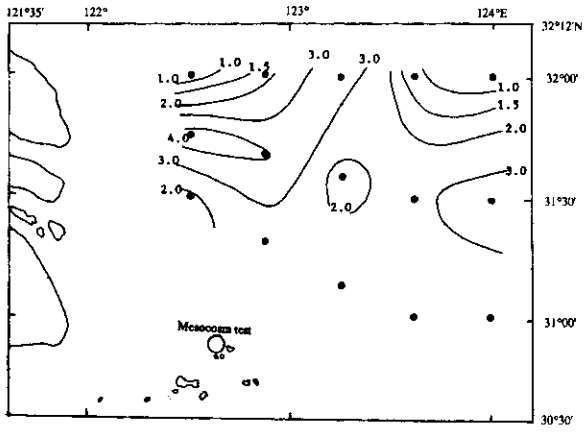

Fig.3 The horizontal distribution of bacterioplankton production ($\mu gC \cdot dm^{-3} \cdot h^{-1}$) at the surface water in May of 1998

Fuhrman et al., (1982) discovered that bacterioplankton production at euphotic zone of waters was the highest. The growth and propagation of bacteria are related unobviously to light except photoautothophy bacteria. The growth of phytoplankton, feeding and excretion of animals and frequent activities of organisms made the POC and DOC concentration increase in seawater, activation of the heterotrophic bacteria utilizing carbon and nitrogen enhanced and bacterioplankton production heightened. In spring, the bacterioplankton production at bottom was $1.01 \pm 0.43 \mu gCdm^{-3}h^{-1}$, only accounting for 42% of that at surface water. For the horizontal distribution, only at the station C_5 on the southeast of the surveyed area appeared the value of $1.77 \mu gCdm^{-3}h^{-1}$, and was lower than $1.0 \mu gCdm^{-3}h^{-1}$ in the west of the surveyed area.

The bacterioplankton production is $0.22 \sim 4.41 \mu gCdm^{-3}h^{-1}$ in autumn and spring in the surveyed area, being lower than the range of $0.83 \sim 11.67 \mu gCdm^{-3}h^{-1}$ in Chesapeake Bay in U.S, and higher than that of $0 \sim 0.5 \mu gCdm^{-3}h^{-1}$ in 3 River plumes of the Georgia Strait in Canada, that of $0.01 \sim 0.3$ $\mu gCdm^{-3}h^{-1}$ in Khone estuary in France, that of $0.21 \sim 1.58 \mu gCdm^{-3}h^{-1}$ in Delaware Bay in U.S, while coinciding with that of $0.21 \sim 3.75 \mu gCdm^{-3}h^{-1}$ in the Mississippi River Plume in U.S.(Gerardo C. L., 1992) and the range $0.08 \sim 6.63 \mu gCdm^{-3}h^{-1}$of annual average value in Jiaozhou Bay of China (Jiao Nianzhi, 1995).

(2) Bacterioplankton number in the surveyed area

The results showed that bacterioplankton number was higher in autumn than that in spring (Table 2), the average at the surface water were$(5.22 \pm 0.88) \times 10^8$ cell$\cdot dm^{-3}$ and $(1.94 \pm 1.10) \times 10^8$ cell$\cdot dm^{-3}$ respectively. In combination with the data in 1986 (Shi Junxian et al., 1992), it can be seen from Table 2, except in winter, bacterioplankton number at the middle layer was higher than that at the surface and bottom. Owing to the middle layer containing many tiny suspended particulate, their specific surface area is greater and liable to store the organic substances, which are utilized by bacteria, being advantageous to be attached for bacteria. Since water temperature at the surface in winter is lower, bacteria number is the least. Water temperature at surface in October of 1997 was higher (23.24 ± 0.69 °C), bacterioplankton number at surface is more than that in summer and spring, water temperature taking an important role for bacteria.

Table 2. The comparison of bacteria number ($\times 10^8$ cell·dm^{-3}) in the dilution water

	October of 1997	May of 1998	July of 1986	January of 1986
Surface	5.22±0.88	1.94±1.10	2.47±1.04	0.32±0.40
Middle	6.46±3.81	2.28±0.77	3.00±1.81	0.27±0.16
Bottom	6.22±2.66	1.74±0.95	2.96±3.65	0.69±0.33
Average	5.97±2.68	1.97±0.96	2.81±1.83	0.41±0.41

The results of continuous observation for six times at anchored station C_1 showed that the range of bacterioplankton production was 1.27~3.63μgCdm^{-3}h^{-1} and bacterioplankton number was 0.53×10^8~2.90×10^8 cell·dm^{-3} (Table 3). High values appeared in 12:00-15:00 at afternoon and low values in 21:00 at night. The organic substances were released to seawater by phytoplankton that possesses obvious light effect promoting the growth of bacteria.

Table 3. The comparison of bacterioplankton production and bacterioplankton number at surface water in an anchored station

Time	0600	0900	1200	1500	1800	2100	Average
BP (μgC·dm^{-3}·h^{-1})	2.47	1.82	2.67	3.63	1.93	1.27	2.30
BN ($\times10^8$·dm^{-3})	1.35	0.93	2.91	1.61	0.63	0.85	1.38

(3) Bacterioplankton production in the seawater outside mesocosm

The sea area of mesocosm experiment is near to seashore and nearby an island. While the experiment of enrichment phosphorus and oil pollutant was done, 15 days' continuous observation for natural seawater outside mesocosm was carried out. The results showed that the bacterioplankton production at surface change ranged from 0.13 ~ 5.79μgCdm^{-3}h^{-1} with average value of 2.47±1.60μgCdm^{-3}h^{-1}. The bacterioplankton number ranged from 0.83×10^8 cell·dm^{-3} to 3.60×10^8cell·dm^{-3} (Fig.4).

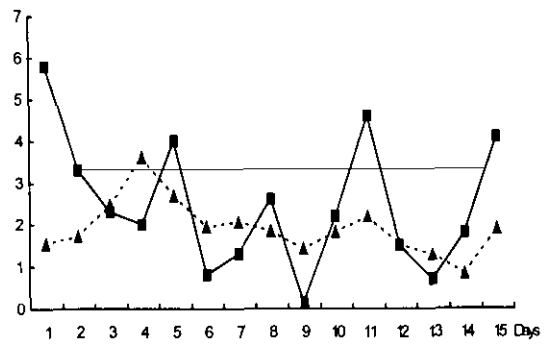

Fig.4 The distribution of bacterioplankton production and bacterioplankton number in seawater outside mesocosm.

—■— S-BP (μg/dm^{-3}·h^{-1}) - -▲- - S-BN ($\times10^8$cell/dm^{-3})

(4) Bacterioplankton production in mesocosm enrichment phosphorus experiment

The enrichment phosphorus experiment adding from 0.78 to 3.25M (PO_4^{-3}) was carried out in October of 1997. It can be seen from Fig.5 that after adding phosphorus in mesocosm, the increasing of nutrients exerts marked effect on the growth of phytoplankton and bacteria. Bacterioplankton production in the experiment increases from 1.43μgCdm^{-3}h^{-1} to 43.47μgCdm^{-3}h^{-1}. The bacterioplankton number increases from 6.24×10^8 cell·dm^{-3} to 18.30×10^8cell·dm^{-3}. Chlorophyll *a*, primary productivity and bacterioplankton production basically trend to rising linearly in the first five day of the experiment. The abundant nutrient and suitable light radiation in water lead to phytoplankton to bloom, and promote rapid increase of bacteria. In the fifth day, phytoplankton transferred into the "cachexia" from blooming, chlorophyll *a* and primary productivity rapidly lower, but bacterioplankton production still increase slowly, because heterotrophic bacteria decompose uninterruptedly numerous detritus of plankton.

Similar adding phosphorus experiment (0.33~2.16M PO_4^{-3}) was done in May of 1998. Bacterioplankton production increasing effect was similar to that of experiment in autumn, but the increasing range was lower than that in autumn. In the second and fourth days after adding phosphorus experiment, the increasing range of bacterioplankton production was the greatest (Fig.6). In the fifth day, bacterioplankton production markedly lowered. Since phosphorus increases in mesocosm ecological environment making the ratio of nitrogen to phosphorus to be adjusted, the bacterioplankton production increased from 2.18 to 32.20μgCdm^{-3}h^{-1} in the four days after adding phosphorus.

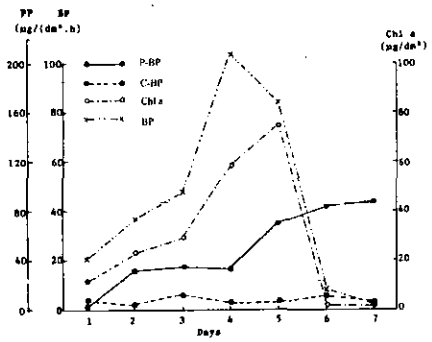

Fig.5 The comparison of bacterioplankton production in mesocosm adding phosphorus experiment in October of 1997.

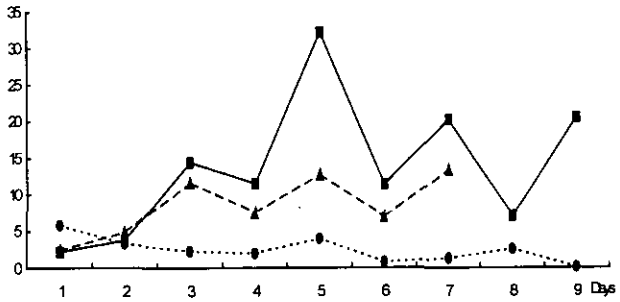

Fig.6 The distribution of bacterioplankton production in mesocosm adding phosphorus experiment in May of 1998.

—■— P-BP (μg·dm^{-3}·h^{-1}) – –▲– – C-BP (μg·dm^{-3}·h^{-1}) – –●– –S-BP (μg·dm^{-3}·h^{-1})

(5) The bacterioplankton production of the oil pollutant experiment in mesocosm

The oil pollutant experiment in mesocosm was conducted by adding No.0 diesel oil (1800μgdm^{-3}) in May of 1998. Generally, petroleum hydrocarbon pollution in the seawater are removed through chemical degradation and biological degradation, but the rate of bacterioplankton degradation is greater than the oxidation-self of petroleum hydrocarbon. Bacteria play an important role in removing petroleum pollutant in the sea water (Shi e'hou, 1988). The production of the experimental group and the contrast group increased simultaneously in the first day. In the second day, the bacterioplankton production of the contrast group lowered, while that of the experimental group increased day by day from 6.61μgCdm^{-3}h^{-1} at the beginning to 37.97μgCdm^{-3}h^{-1} at the ending (Fig.7).

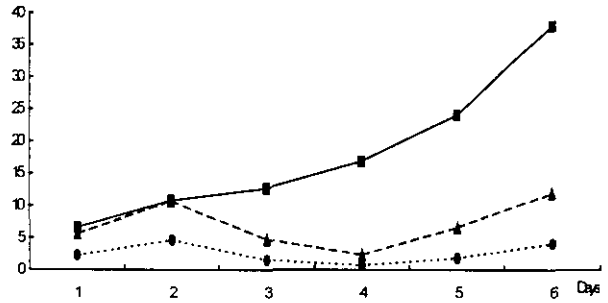

Fig.7 The bacterioplankton production of the oil contaminated experiment in mesocosm

—■— O-BP (μg·dm^{-3}·h^{-1}) - -▲- - C-BP (μg·dm^{-3}·h^{-1}) - -●- -S-BP (μg·dm^{-3}·h^{-1})

4. CONCLUSIONS

In the surveyed area, the bacterioplankton production at surface water ranged from 0.22 to 3.35μgCdm^{-3}h^{-1} with average value of 1.441.30μgCdm^{-3}h^{-1} in autumn, it is roughly 18% of the primary productivity. In spring, bacterioplankton production ranged from 0.56 to 4.41μgCdm^{-3}h^{-1} with average value of 2.431.22μgCdm^{-3}h^{-1}. The high values were in the middle of the surveyed area. Bacteria play an important role in the marine biogeochemistry processes.

In the adding phosphorus experiment, bacterioplankton production increased from 1.43μgCdm^{-3} h^{-1} to 43.47μgCdm^{-3}h^{-1} in autumn and increased from 2.18μgCdm^{-3}h^{-1} to 32.30 μgCdm^{-3} h^{-1} in spring. The increasing of nutrient concentration in the ecosystem exerted marked effect on bacteria and phytoplankton.

In the oil pollutant experiment, bacterioplankton production increased from 6.61μgCdm^{-3}h^{-1} to 37.97 μgCdm^{-3}h^{-1}. Bacterioplankton degradation is one of the effective ways to remove petroleum pollutant of the seawater.

REFERENCES

1) Annals of Chinese Bay compile committee: Annals of Chinese Bay--Estuary fascicle, China Ocean press, Beijin, (in Chinese), pp.105-237, 1998.

2) Chen, Q., Wu ,SH., and Zhuan, L.: Influence of heavy metal on primary productivity in the marine mesocosm ecosystem, *Acta Oceanologica Sinica*,(in Chinese), Vol.11 (2) ,pp.222-227, 1988.

3) Fuhrman,J. A. and F. Azan: Bacterioplankton secondary production estimates for coastal waters of British Columbia, Antarctica, and Califoria, *Appl. Environ. Microbiol,* Vol. 39, pp.1085-1095, 1980.

4) Fuhrman, J.A. and F. Azam: Thymidine incorporation as a measure of heterotrophic bacterioplankton production in marine surface waters: Evaluation and Field Results, *Marine Biology*, Vol. 66, pp.109-120, 1982.

5) Gerardo, C. L. and R. Benner.: Enhanced bacterioplankton production and respiration at intermediate salinity in the Mississippi River Plume, *Mar. Ecol. Prog. Ser.*, Vol. 87, pp. 87-103, 1992.

6) Jiao, N. and Xiao, T.: Bacterioplankton secondary production in Jiaozhou Bay, In *Study on the ecology in Jiaozhou Bay,* Edit, Dong Jinhai et al., Science press, Beijing, (in Chinese) pp. 112-117, 1995.

7) Kirchman, D. L.: Leucine incorporation as a measure of biomass production by heterotrophic bacteria. Edit. Kemp. et al.,

Handbook of method in aquatic microbial ecology, pp. 509-512, 1993.
8) Kirchman, D. L., Kiness, E. and Hodson, R. E.: Leucine incorporation and its potential as a measure of protein synthesis by bacteria in natural aquatic systems, *Appl. Environ. Microbiol.*, Vol. 49, pp. 599-610, 1985.
9) Parsons, T.R., Y. Maita & C.M. Lalli: A Manual of Chemical and Biological Methods for Seawater Analysis, Pergamon press, pp.123-132, 1984.
10)Shi, e': The source of petroleum hydrocarbon in the sea environment, *Marine Environmental Science*, (in Chinese), Vol. 7 (3), pp. 36-47, 1988.
11)Shi, J., Chen, Zh., Ning, X, C. Courties and M. N Hermin: The distribution patterns of bacteria and ATP in the Changjiang River Estuary and its adjacent East China Sea. *Oceanologia et Limnologia Sinica*, (in Chinese), Vol. 23 (3), pp. 288-296, 1992.
12)Shi, J., Zheng, G, Chen, Zh. and Wang, Sh.: Ecological distribution of Heterotrophic bacteria in seawater and sediments of the The Changjiang River Estuary, *Marine Science Bulletin* (in Chinese) Vol. 3 (6), pp. 59-63, 1984.
13)STSA (State Technical Supervision Administration) Marine Biological Survey, *The specification for Oceanographic Survey*, GB 12763.6. (in Chinese), pp. 10-17, 1991.
14)Zhen, G., Shi J., Chen Zh., and Hu X.; Preliminary study on bacteria and sediments interelation in The Changjiang River Estuary and it's adjacent continental shelf, *Oceanologia et Limnologia Sinica*, (in Chinese), vol.4(6), pp.743-753, 1982.

STUDY ON THE HAB DYNAMICAL MODEL AND HAB LIMITATION FACTORS FOR THE SEA AREA ADJACENT YANGTS RIVER ESTUARY

Fangli QIAO, Yeli YUAN, Mingyuan ZHU, Wei ZHAO, Rubao JI,
Zengdi PAN, Shang CHEN and Zhenwen WAN

The First Institute of Oceanography, State Oceanic Administration,
(Hongdao Branch Road 3A, Qingdao, 266003, China)
Key Laboratory of Geophysical Fluid Dynamics and Numerical Modeling, SOA

Based on Sino-Japan cooperative Marine Enclosure mesocosm Experiment (MEE) during October 10 and 17, 1997, a marine Harmful Algal Bloom (HAB) dynamical model is developed in the Yangts River estuary area. The numerical results are consistent with the available data. The threshold values of nitrogen and phosphate concentrations for HAB occurrence are 4.5μmol/l and 1.0μmol/l respectively in this area.

Key Words: *HAB dynamical model, Marine enclosure mesocosm experiment*

1. INTRODUCTION

As the sharp development of coastal industry, HAB often appears in Chinese coastal zone and arrives averagely 50 times per year (Zhu et al., 1996).

HAB damages the local marine ecosystem (Lin et al., 1997). Due to its complication of coupled hydrodynamic-chemical-biological processes, a MEE can remove the hydrodynamic effect and can be used to study marine ecosystem under different conditions.

In Yangts River estuary area, the MME, which located at point (30°50.460' N, 122°36.665' E)(Fig.1), was carried out for the first time during October 10 and 17, 1997. 25m^3 sea water was filled into the two bags separately in the afternoon of Oct. 10, 1997. Samples were get at 9:00 one time per day during the following 7 days. The bag with natural sea water is called control bag, and dissolved inorganic phosphate was added to 3.25μmol/l in the other bag called as P-bag. Due to the strong wave in this area, the outer sea water rushed into the control bag in the next day. A HAB process was successfully induced in the P-bag. The dominant species is *skeletonema costatum.*

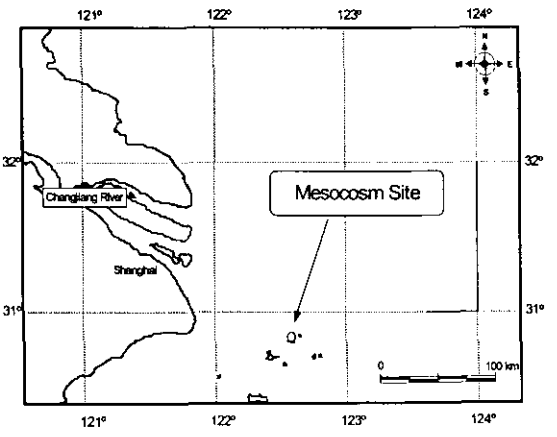

Fig.1 The location of the China-Japan cooperation mesocosm experiment in October, 1997

2. THE HAB DYNAMICAL MODEL AND DATABASE

(1) The HAB dynamical model

Since the tidal current and surface wave are strong in this area, the vertical mixture in the P-bag was well done, so the P-bag can be treated as one layer in vertical direction. Base on Skogen's model (Skogen et al., 1995) and observed data, for the first time in this area a marine HAB dynamical model is developed. The control equations are as follows.

$$\begin{cases} \dfrac{\partial N}{\partial t} = R_{Dia} + R_{Fla} + C_4 Det - (P_{Dia} + P_{Fla}) \\ \dfrac{\partial P}{\partial t} = C_1[R_{Dia} + R_{Fla} + C_4 Det - (P_{Dia} + P_{Fla})] \\ \dfrac{\partial S_i}{\partial t} = -C_2 P_{Dia} \\ \dfrac{\partial Dia}{\partial t} = P_{Dia} - R_{Dia} - C_3 Dia \\ \dfrac{\partial Fla}{\partial t} = P_{Fla} - R_{Fla} - C_3 Fla \\ \dfrac{\partial Det}{\partial t} = C_3(Dia + Fla) - C_4 Det \end{cases}$$

where,

Maximum diatom growth rate at T℃ : $P_{Dia-\max} = a_1 e^{a_2 T}$

Maximum flagellate growth rate at T℃ : $P_{Fla-\max} = a_3 e^{a_4 T}$

Diatom respiration: $R_{Dia} = a_5 \cdot Dia \cdot e^{a_6 T}$

Flagellate respiration: $R_{Fla} = a_5 \cdot Fla \cdot e^{a_6 T}$

Diatom growth rate: $P_{Dia} = P_{Dia-\max} V_{1,Dia} \cdot N_{Lim,Dia} \cdot Dia$

Flagellate growth rate: $P_{Fla} = P_{Fla-\max} \cdot V_{1,Fla} \cdot N_{Lim,Fla} \cdot Fla$

$V_{ij} = \dfrac{S_{ij}}{S_{ij} + Kh_{ij}}$, i=1(light), 2(N); 3(P), 4(Si)

j=1(diatom), 2(flagellate)

Diatom nutrient limitation: $N_{Lim,Dia} = \min(V_{21}, V_{31}, V_{41})$

Flagellate nutrient limitation: $N_{Lim,Fla} = \min(V_{22}, V_{32})$

The concept model is as follows.

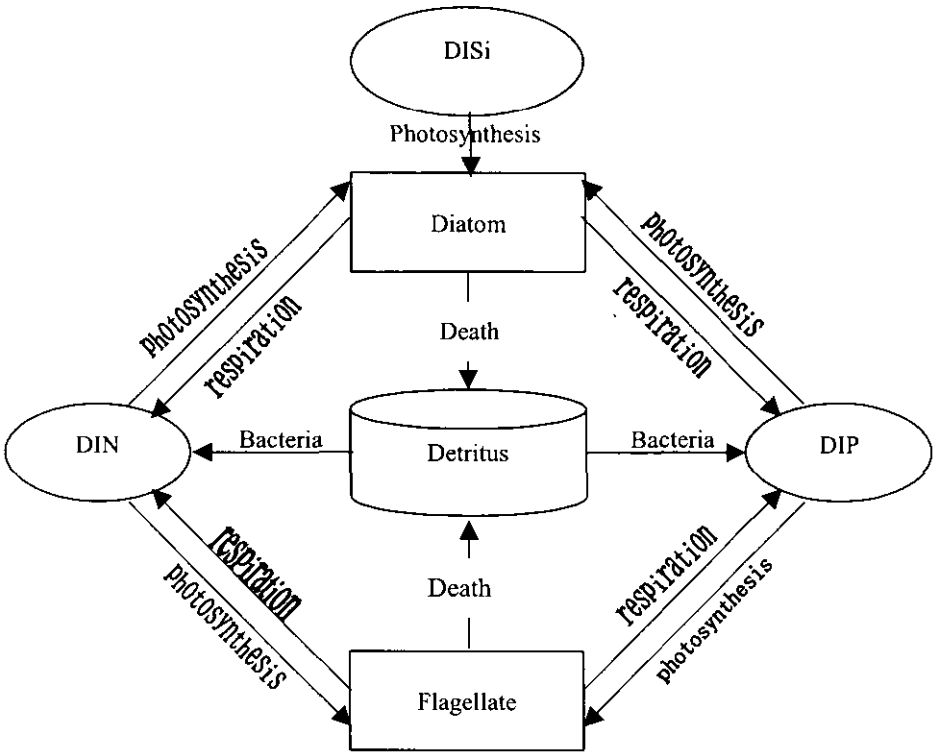

(2) Model parameters

18 parameters are used in the HAB dynamical model and are listed in Table 1.

Table 1 Parameters used in the HAB dynamical model

Parameters	Definition	Value
A_1	Maximum diatom production at 0℃(s^{-1})	1.38×10^{-5}
A_2	Temperature dependence for diatoms(° C^{-1})	0.063
A_3	Maximum flagellate production at 0℃(s^{-1})	1.12×10^{-5}
A_4	Temperature dependence for flagellates (° C^{-1})	0.063
A_5	Respiration rate at 0℃(s^{-1})	12.07×10^{-7}
A_6	Respiration rate temperature dependence (° C^{-1})	0.07
C_1	Fraction of phosphate and nitrate in a cell(mgP/mgN)	0.3
C_2	Fraction of silicate and nitrate in a cell (mgSi/mgN)	1.75
C_3	Phytoplankton death rate(s^{-1})	1.6×10^{-6}
C_4	Decomposition rate for detritus (s^{-1})	1.52×10^{-8}
Kh_{11}	Light half saturation constant of diatom(μ Einstein/m^2/s)	96
Kh_{21}	Nitrogen half saturation constant of diatom(μ molN/l)	1.3
Kh_{31}	Phosphate half saturation constant of diatom(μ molP/l)	0.125
Kh_{41}	Silicate half saturation constant of diatom(μ molSi/l)	1.4
Kh_{12}	Light half saturation constant of flagellate(μ Einstein/m^2/s)	150
Kh_{22}	Nitrogen half saturation constant of flagellate(μ molN/l)	0.25
Kh_{32}	Phosphate half saturation constant of flagellate(μ molP/l)	0.094
PAR	Photosynthetic active irradiance (%)	50

(3) Database

Nutrients: the concentrations of NO_3-N, NO_2-N, NH_4-N,PO_4 and SiO_2 were measured in situ one time per day.

Light intensity: there were two sensors with one at sea surface and the other under sea surface. The later had some wrong and did not get any data. The observed data are listed in Table 2.

Table 2 Observed sea surface light (1h mean μ Einstein/m^2/s) and data number

Date / Hour	13		14		15		16		17		19	
	Light intensity	Data number	Light intensity	Data number	Light intensity	Data number	Light intensity	Data number	Light intensity	Data number	Light intensity	Data number
5											18.0	617
6					151.7	354	552.1	1225	1173.0	591	269.8	3600
7					167.1	3600	1170.8	3600	1283.2	3600	788.9	3600
8					1234.5	3588	1487.2	3600	1457.7	3600	1552.2	3600
9					1815.5	3600	1996.9	3600	2096.3	3588	2234.1	3589
10					1001.3	3600	2629.8	3589	2591.5	3600	2580.7	3600
11	2768.0	524			1218.5	3600	2700.5	3600	2933.8	3589	2657.8	3589
12	2660.6	2980			1721.5	217	2898.3	3600	2921.4	3373	2485.0	3600
13	2285.4	3600	1266.8	3523	913.8	3600	2835.9	2588	2658.9	2929	2604.5	3139
14	1780.3	3600	864.4	3600	448.7	3600	2635.0	3600	2407.3	3600	2303.1	3038
15	1160.1	2863	581.0	3587	227.8	3588	2102.3	3600	1807.6	3600	1775.6	3600
16	418.5	3600	131.6	3600	147.3	3600	893.8	3588	693.1	3589	608.1	3589
17	36.4	1931	12.1	2390	62.6	455	85.0	894	23.7	3600	9.9	3587
18									1.9	3600	0.6	1831
19									1.9	1491		

$$I_z = PAR \cdot I_0 \cdot e^{-Kz}$$

$$K = 0.043 + 0.0545 \cdot TPM$$

Where TPM is the concentration of suspended particle (μg/l) and PAR is photosynthetic active irradiance (%).

The depth of light intensity used in the model for diatom is 1m. For flagellate, the depth is 0.25m, because flagellate can swim up for enough light(Parsons et al., 1997).

Chlorophyll-a and detritus: the concentrations of chlorophyll-a, diatom and flagellate were measured. In this paper, the difference of particle organic nitrogen and chlorophyll-a is regarded as the concentration of detritus.

3. MODEL RESULTS AND DISCUSSION

(1) MEE P-bag simulation

Fig.2 shows the comparison of model results and observations. The fluctuations of nutrients are due to the alternative of day and night. During night, the photosynthetic process is weak, but bacteria discompose detritus and produce nutrients. Because in this experiment, we have only one sample per day, so the simulated fluctuation phenomenon needs more observed data to check. The growth, respiration and limitation factors are shown in Fig.3. The simulation errors are listed in Table 3.

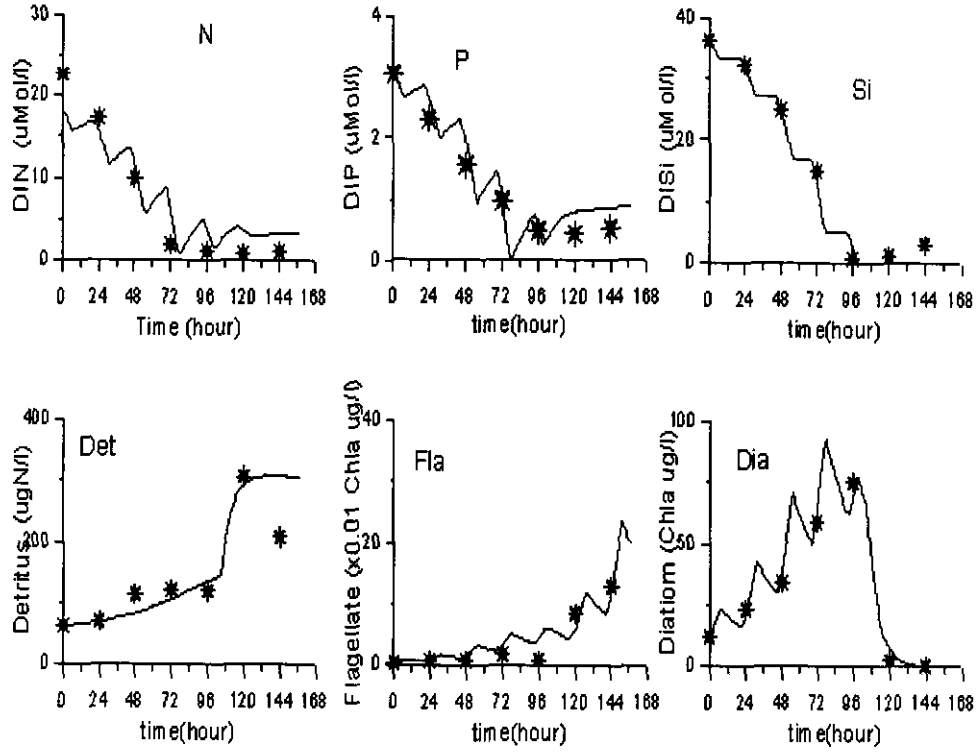

Fig.2 The comparison of model results and observations

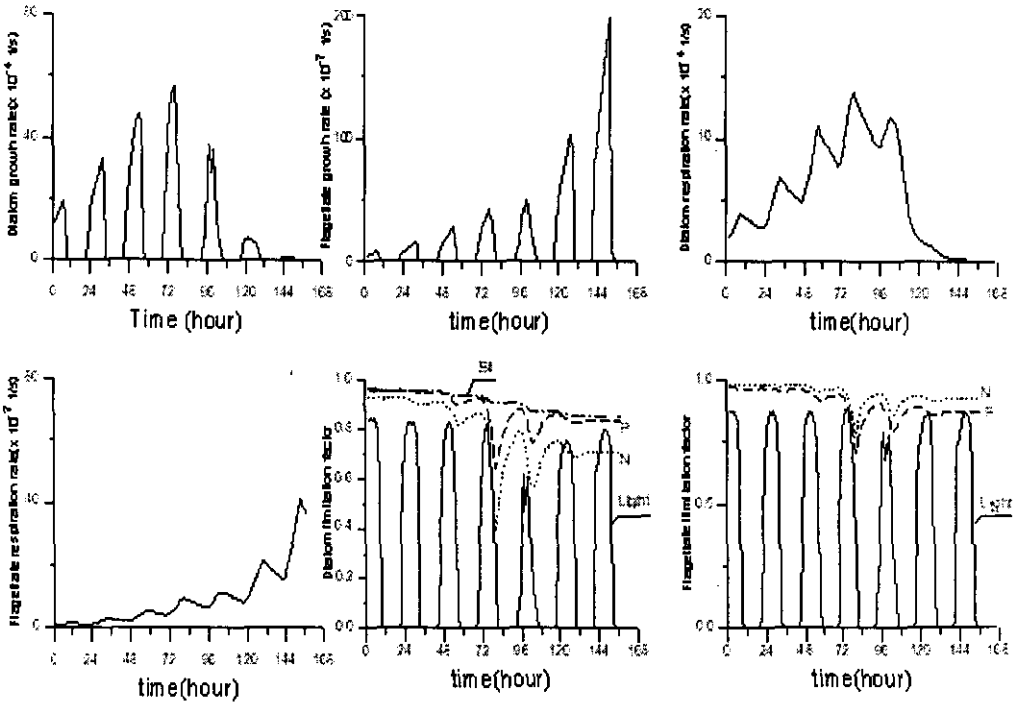

Fig.3 The growth rates, respiration rates and limitation factors of diatom and flagellate

Table 3 Simulation errors

Element / Data	N (μ mol/l)	P (μ mol/l)	Si (μ mol/l)	Flagellate ($\times 10^{-2}$ μ g/l)	Diatom (μ g/l)
12	1.94	0.37	-0.25	0.11	-1.17
13	4.78	0.52	-0.24	0.86	5.01
14	5.88	0.21	-1.55	1.51	3.89
15	3.43	0.21	2.17	3.97	-5.63
16	5.36	0.49	-1.20	-1.54	4.91
17	5.23	0.43	-3.08	1.36	0.15

(2) Numerical experiments

In order to understand the limitation process of HAB, the present work analyses the effect of initial nitrogen, initial phosphate and light intensity. The results of numerical experiments are shown in Fig 4.

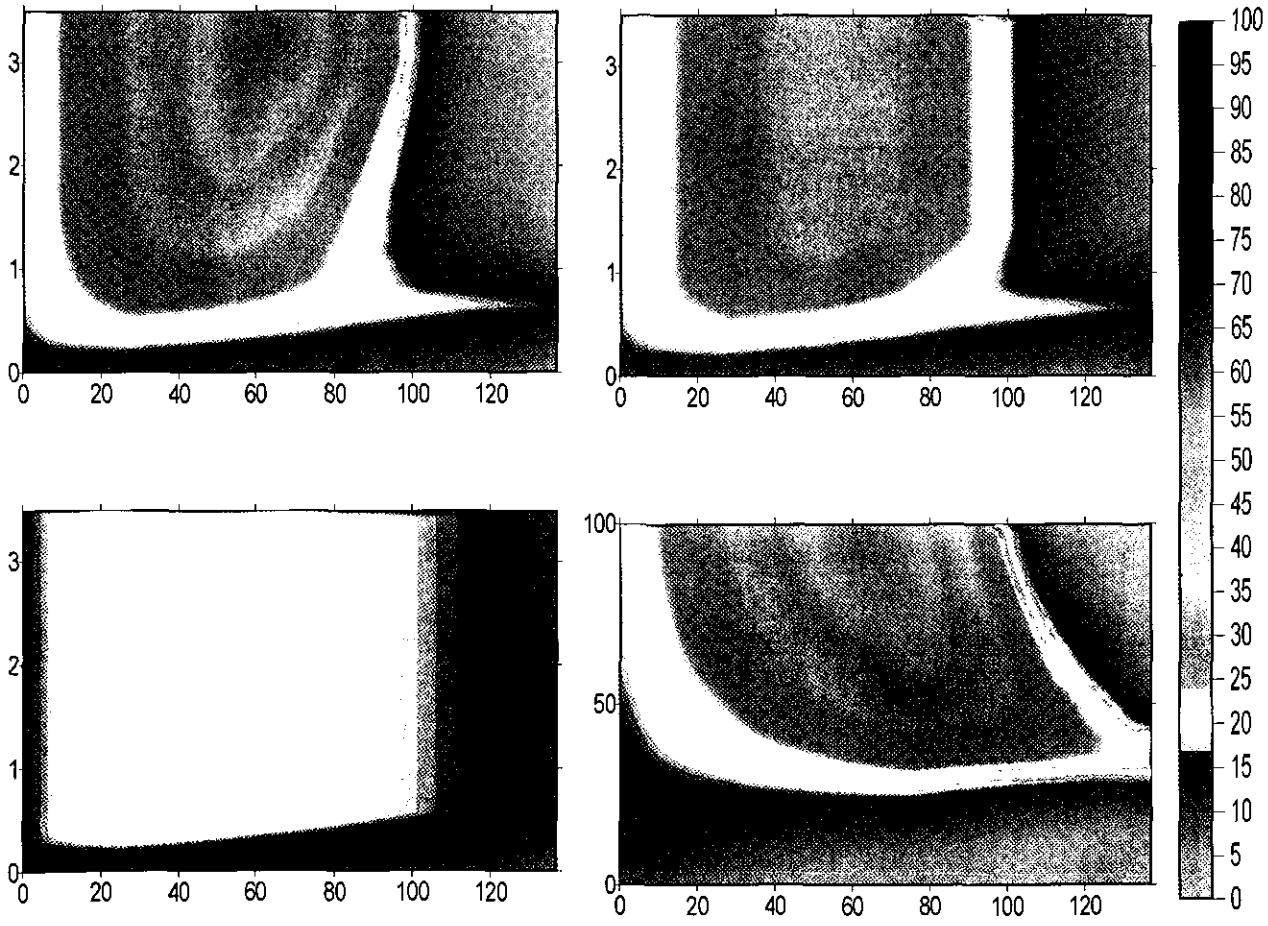

Fig.4 The distributions of simulated chlorophyll concentration with different initial *DIN* concentrations and sunlight a. Initial *DIN*: 18 μ mol/l; b. Initial DIN:9 μ mol/l; c. Initial DIN:4.5 μ mol/l; d. Initial DIN and DIP:18 μ mol/l and 3.25 μ mol/l

The criterion of HAB occurrence is still undefined until now. Xu et.al considers 10 μ g/l of chlorophyll-a concentration as the criterion (Xu et.al, 1996). Here 20 μ g/l is the criterion because HAB will be distinguished easily from sea color with naked eyes in this MEE.

4. CONCLUSIONS

The model results are consistent with available data. The present work analyses the influence of nutrient concentration and light intensity to the formation of HAB. The main results are as follows: (1) The created HAB dynamical model successfully simulates the whole process. The added dissolved phosphate is enough for strengthening the HAB process. (2) The threshold values of nitrogen and phosphate concentration for HAB occurrence are 4.5 μ mol/l and 1.0 μ mol/l respectively for this area. (3) According to the model results, when surface light intensity is half of measured sea surface light intensity, the maximum chlorophyll a concentration is 35 μ mol/l. When the light intensity is 35% or below, HAB will not occur.

ACKNOWLEDGEMENT: I am indebted to all scientists involved in the MEE for supplying observed data. Especial thanks go to professor Guanguo Xu, Ocean University of Qingao for his comments and suggestion. Thanks also go to professor Yongyao Ding and associate professor Ruixiang Li for their helpful discussion.

REFERENCES

Kremer , J.N. and Nixon, S.W.: A coastal marine ecosystem, Spring-verlag Berlin Heidelberg, 37-39, 1978.

Parsons T.R., Takahashi, M. and Hargrave, B.: Biological oceanographic processes, 2nd Ed., Pergamon Press, 37-38, 1977.

Skogen M. D.: Modeling the primary production in the North Sea using a coupled 3 dimensional physical-chemical-biological ocean model. Estuarine, coastal and shelf science, 41, 545-565, 1995.

Wilfried Kuhn and Gunther Radach: A one-dimensional physical-biological model study of the pelagic nitrogen cycling during the spring bloom in he northern North Sea (FLEX'76), *Journal of Marine Research*, 55(4), 687-734, 1997.

Xu Jiashen, Meng Yi, Li Bing and Gao Sulan: The relationship of chlorophyll-a and red tide in Huanghua Shrimp pond. *Huanghai and Bohai Seas,* 14(2),45-51(in Chinese), 1996.

Zhu Mingyuan and Li Ruixiang: The ecological studies in red tide research, In: Proceedings of the second meeting of Chinese committee of SCOR-IOC working group, 121pp, Qingdao press, 1-5 (in Chinese), 1996.

BIOGEOCHEMICAL VARIATIONS OF NUTRIENT ELEMENTS AND ITS EFFECT ON ECOLOGICAL ENVIRONMENTS OFF THE CHANGJIANG ESTUARINE WATERS

Yi-an LIN , Renyou TANG , Jianming PAN , Mingming JIN

Second Institute of Oceanography, State Oceanic Administration

(Hangzhou 310012, P.R.China)

The biogeochemical variation characteristics of nutrient elements and the influence factors on Donhai were studied in this paper. The general trend of nutrient concentration distribution was tended downwards from southwestern to northeastern in horizontal and upwards follow the water depth increase in vertical. But the lower concentrations of the DIN, DIP and SiO_3-Si were appeared at surface layer of stations (A3, B3, C3 and C5,) the species variation of N, P apparent differential respectively due to the plankton absorbing and different biogeochemical mechanism. The special role of frontal area and thermohaline transition layer on species variation and enrich of nutrients have been discovered. The nutrients environmental capacity was primarily estimated.

***Key words**: nutrient elements, biogeochemistry, ecological environmental effect, Donghai*

1.INTRODUCTION

Waters off the Changjiang Estuarine is one of the important areas of land-sea interaction, the current series complex, more water masses just converging here. That admit larger amounts the Changjiang River Diluted Water from west, effected by the Yellow Sea Mixed Water from north and wedged into by the Taiwan Warm Current Water from southeast[1]. The water masses carry in sufficient nutrients for beings growing and reproduction, forming famous the Changjiang Estuary Fishing Field and bringing about the active biogeochemistry actions. But following the economy developing and mankind action increasing, the environmental load of pollutants from land into sea is continuous growth.. For instance, owing to developing agriculture, a vast amount of the chemical fertilizers was applied in the China. According to statistics the using amount of chemical fertilizer have come to 25 $\times 10^6$ t/a during towards the end of 1980s and 1990s early. About 80~90% of total is nitrogenous fertilizer as well as 5 ~ 10% of it is phosphorous fertilizer, and than it is increased with 1.0×10^6 t ~ 1.5×10^6 t/a at late ten years[2]. Thanks to a lot of chemical fertilizer was washed away from the soil into the runoff and the sea. The concentrations of N and P were obviously increase in the Changjiang runoff during last thirty years and nutrition's level was unceasing raise in the Changjiang estuary and its adjacent waters as well. In recent years, the red tide occurred frequently that the eutrophication seems as an important effected factoin this area. Therefor, many scientists have a great interest in variation of the ecological environment and the biogeochemistry of nutrient elements in the Changjiang estuary and its adjacent waters. From 1970s, the researcher of

SOA of China has done some environment investigation in this area.. In 1980s some international co-operation studies have been engaged (for instance, the China – U.S.A joint study in1983, the Sinn – French joint study in 1986 etc.). Scholars have made some thorough study on the nutrients elements[3),4),5),6)]. But the biogeochemical cycle, species variation and environmental capacity of nutrients was less touched on. In order to have a better to understanding of biogeochemistry actions and provide protection of ecological environment and marine resources with scientific basis, the work on this field was carried out in the China –Japan joint study project, during 1997~1998. The research results are reported in this paper.

2.METHODS

(1) Study area and investigation date

The study area spreads region was in a polygon linking up 32.00°N, 122.30°E; 32.00°N, 124.00°E; 31.00°N, 124.00°E; 31.00°N; 123.50°E and 31.50°N, 122.30°E five point (Fig.1). Stations A1, A3, A5, B1, B3, B5, C1, C3 and C5 were for water quality monitoring and sampling station.

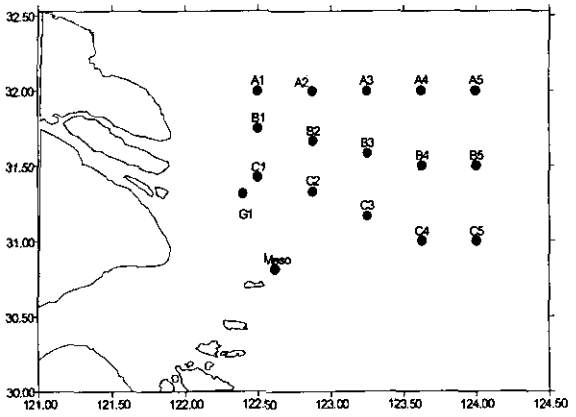

Fig. 1 the location of survey station

The survey has been done in October 1997 and May 1998. In the first cruise, the Changjiang runoff was in medium flow capacity and the plankton was in delay stage. In the second cruise, the Changjiang runoff was abundant and the plankton was growing.

(2) Sampling

The water samples were collected with a Niskin sampler. Water subsample A for DTN, DTP, NO_3^-, NO_2^-, NH_4^+, PO_4^{3-} and SiO_3^{3-} measurement was filtered by 0.45μm millipore filter immediately after sampling. Water subsample B for TN, TP analysis was collected from raw water samples. Samples were stored and kept in – 20°C and afterwards send to laboratory for analysis, except NO_3^-, NO_2^-, NH_4^+, PO_4^{3-} and SiO_3^{3-} were measured in situ.

(3) Methods of measurement

Methods of measurement for nutrients as following:

Species	Analysis methods	Limit of detection
SiO_3^{3-}	Yellow molybdosilicic acid method	0.45μmol/l
PO_4^{3-}	Phosphor-molybdemum blue method	0.02μmol/l

NO_2	Diazo-azo method		0.02μmol/l
NO_3^-	Zinc-cadmium reduction and diazo-azo method	(at in situ)	0.07μmol/l
	Copper-cadmium column and diazo-azo method	(at lab)	0.04μmol/l
NH_4^+	Oxidized hypobromite method		0.03μmol/l

The samples for measured TN, DTN, TP and DTP were pretreated with potassium persulfate oxidation and pressurized decomposition. After adjusted pH, NO_3^- and PO_4^{3-} in the solution was detected separately. The samples for TP measurement were carried out turbidity correction. PN, PP, DON and DOP were calculated as the differential-decrease methods.

Temperature (T), salinity (S), depth (D), dissolved oxygen (DO), and oxidation – reduction potential (ORP) were measured using Hydrolab multiparameter meter in situ.

3. RESULTS AND DISCUSSION

(1) Concentration and distribution of nutrients

Table 1.shows the concentration range and average value of nutrient species that were measured at both survey cruise of October 1997 and May 1998. Comparing the results of two cruises, it is evident which the concentrations of SiO_3^{3-} and NO_3^- in Oct.1997 were higher than that in May 1998. Because the rainfall of the Changjiang basin in spring 1998 was more abundant than former years, following the runoff and the diluted water plume current were increased, and so the output of SiO_3^{3-} and NO_3^- of the Changjiang river were increased. Because there is close relative between flow with output of SiO_3^{3-} and NO_3^- of the Changjiang river[5]. But the concentrations of PO_4^{3-} and TP were not increase in the waters. Owing to one hand the concentrations of PO_3^{3-} and TP were not so difference in both the Changjiang runoff and study area waters and the other hand it is the season of plankton growing and more PO_4^{3-} was grabbed in May.

Table 1. Concentration Range and Average of Various Nutrient Species in Seawater Samples

	Oct. 1997			May 1998		
	Max	**Min**	**Average**	**Max**	**Min**	**Average**
PO_4^{3-}	0.62	0.24	0.45	0.55	0.10	0.26
DOP	0.62	0.01	0.26	0.81	0.08	0.34
DTP	6.24	0.04	0.82	1.11	0.42	0.60
PP	1.10	0.32	0.70	1.98	0.01	0.55
TP	7.25	0.53	1.52	2.70	0.49	1.14
SiO_3^{3-}	44.78	1.66	12.27	50.28	0.66	17.30
NO_3^-	15.97	0.16	5.11	24.93	3.09	16.83
NO_2^-	1.02	0.34	0.67	2.16	0.19	0.71
NH_4^+	1.64	0.14	0.72	4.67	0.38	1.82
DIN	17.32	1.16	6.49	29.65	5.04	19.35
DON	28.28	1.59	9.25			
DTN	19.06	0.22	7.30			
PN	35.00	2.96	15.62			
TN	47.69	6.31	22.92			

Unit:μmol/l

The general tendency of the nutrient distribution was concentrations downward from west to east and from north to south also (Fig.2. a, b, c). Because there are different concentrations in water masses

effected this area, that the higher content was in the Changjiang Diluted water and the yellow sea mixing water mass and the lower content was in the Taiwan Warm Current Water. But the lowest concentration appears at surface layer of A3 – B3 – C3 in autumn. The effect of the Changjiang runoff on distribution of SiO_3^{3-} was fairly obvious in spring. But the concentration of N and P come under the strong influence of the South Yellow Sea water mass, the high

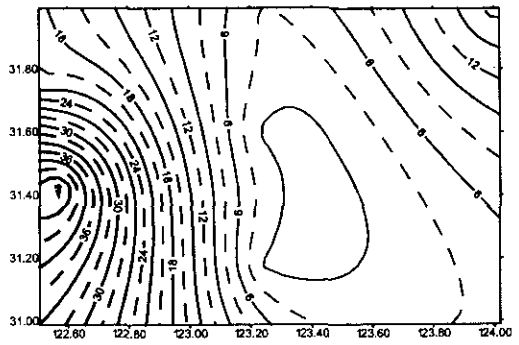

a. SIO3-SI SURFACE CI9710-LT

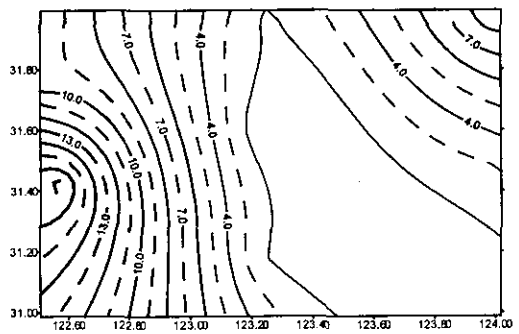

b. DIN SURFACE CI9710-LT

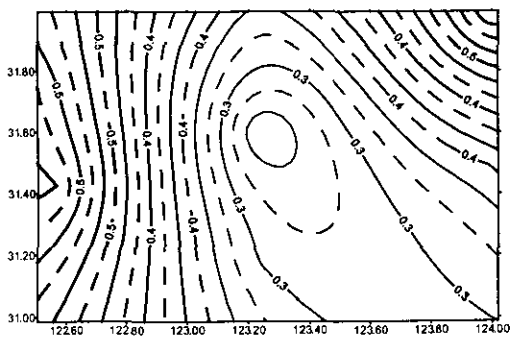

c. PO4-P SURFACE CI9710-LT

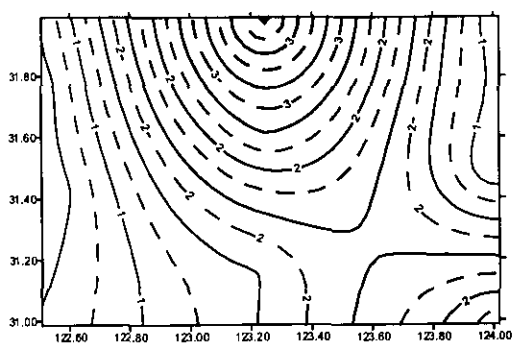

d. Chl a Content Surface (ugC/L) JP9710

Fig. 2 The distribution of Si, N, P andChl. a

(in Oct. 1997)

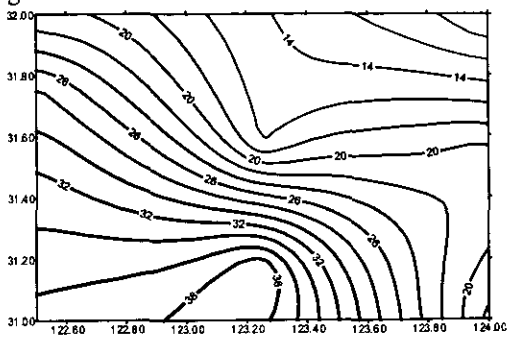

a. SIO3 SURFACE CI99805LP

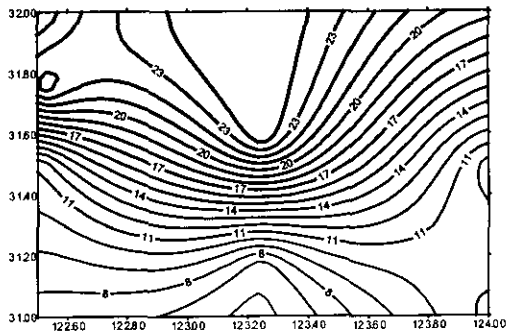

b. NO3-N SURFACE CI9805

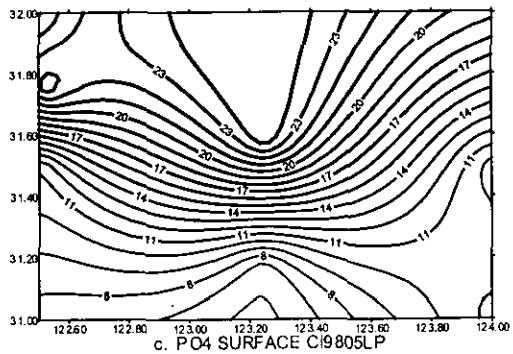

c. PO4 SURFACE CI9805LP

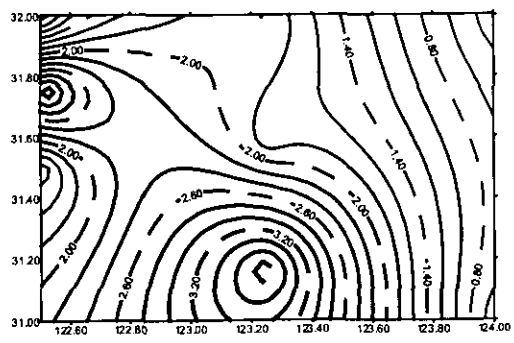

d. Chl a Content Surface (ugC/L) JP9805

Fig. 3 The distribution of Si, N, P andChl. a.

(in May 1998)

concentrationvalue was appeared in the northern (Fig.3. a, b, c). Comparing with the distribution of the chlorophyll a (Fig.2.d and Fig.3.d), it is corresponding between low value area of N and P and high value area of the chlorophyll a on surface layer. This indicated the more nutrients were absorbed for the phytoplankton rapid growing. Among the nutrient element species there is a negative correlation between salinity and SiO_3^{3-} only (Fig.4). This proves that the major factor for controlling the distribution of nutrient elements is not only physical dilution and diffusion, but in a great extent that depends on the biogeochemical variation of every nutrient element species.

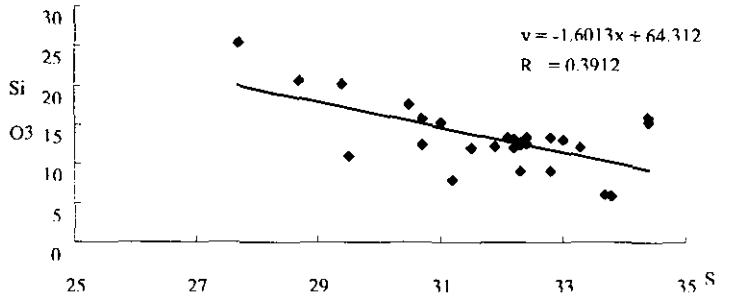

Fig.4 the relation between SiO_3 and salinity

(2) Transform of present form of nutrient elements and its mechanism

The present form of nutrient element is multiple-species. Fig.5 shows the relative rate of present abundant of major nutrient element species in this area. Dissolved inorganic N and P make up 20~30% only, particulate N amount to about 50%, particulate P account for 47~51% of total content, and others was dissolved organic nutrient. These were just some average value. In fact, the nutrient element species were variable along with the environmental condition varying in different parts of the water masses. It is important driving factor of the biogeochemical action, except for the concentration difference and physical mixing of water masses. Fig.6 describes vertical variation of phosphoric species

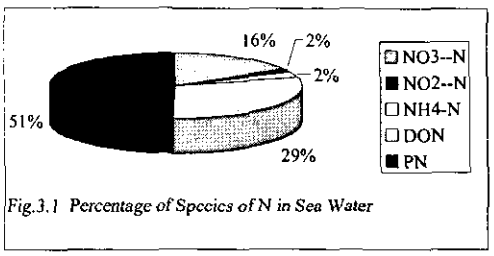

Fig.3.1 Percentage of Species of N in Sea Water

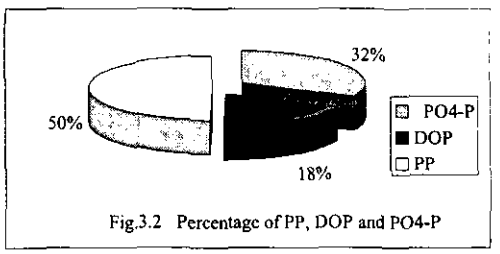

Fig.3.2 Percentage of PP, DOP and PO4-P

Fig. 5 Ratio of concentration of N and P species

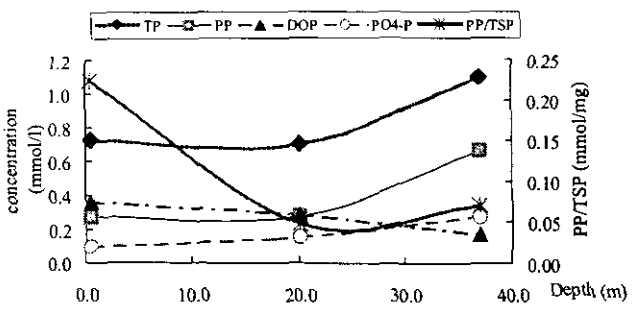

Fig.6 Vertical variation of TP,PP,DOP, PO43- and PP/TSP

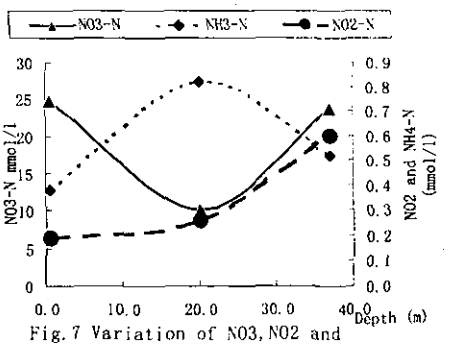

Fig. 7 Variation of NO3, NO2 and NH3-N in St. B3 (May1998)

at station B3. In vertical direction PO_4^{3-}P variation was very little. Although the photosynthesis of plankton has absorbed a lot of PO_4^{3-} from waters, the concentration of PO_4^{3-} was almost kept a stable level state, and did not observed decrease. It indicates that there were some other sources of PO_4^{3-} to add in the first half water column. The concentration of suspended particulate matter (SPM) was raise as depth increase in the water column, but the concentration of PP was not increase and a little decrease opposite. However it is delicate the rate of PP in SPM (PP/SPM) was a great decrease as depth increase in the first half water column, that shows the action process of autolysis, decay decomposition and early mineralization of particulate P (including biodetritus) have been uninterrupted carried on. This is probable as runoff water carries a lot of bacterium and enzyme into the first half water mass and enzyme hydrolyzate phosphate is producing. In other words, the major supplement source of PO_4^{3-} was come from decomposition and release of PP, and the rate of release was almost similar with the settlement rate of SPM. In the second half water column, the concentration of DOP was continually decrease and the decomposition rate speed up. The concentration of PO_4^{3-} was increase while the photosynthesis stopped. The rate of PP/SPM was increase. That shows the particulate surface adsorption have taken place, the higher concentration PO_4^{3-} can combination reaction with Ca^{2+} in the surface of the particle while the concentration of Ca^{2+} increased in the second half water column. In the meantime the PP and TP were increase while the suspended particle concentration increased.

Both of phosphorous and nitrogen in the chemical species converted process are similar for the photosynthesis absorb and respiratory release. The decomposition and early mineralization of organism can release DIN also. However, it is more apparent for the conversion of DIN (including NO_3^-, NO_2^- and NH4+) following the oxidation-reduction reactions occurred. Fig.7 describe the transfer process of NO_3^-, NO_2^- and NH_4^+ in the water column. The high concentration of dissolve oxygen and higher oxidation-reduction potential (ORP) make the higher concentration of NO_3^- and the lower concentration of NO_2^- and NH_4^+ in the surface layer water. But the concentration of NO_3^- was decrease as water depth increase in the first half water column, opposite the concentration of NH_4^+ was increase. This illustrate the ORP was downward, due to decomposition of organism detritus and particles that makes oxidation state (NO_3^-) decrease and reduction state (NH_4^+) increase. In the second half water column, the reaction direction is just opposite so that oxidation state (NO_3^-) increase and reduction state (NH_4^+) decrease as water depth increase. Because the ORP rose as result of the Taiwan Warm Current wedged into bottom and which the concentration of organism was lower than in the first half water column. To sum up, the photosynthesis absorb and respiration release, autolysis, decomposition, enzyme hydrolysis, mineralization of particulate P (including biodetritus), surface adsorption and oxidation-reduction have taken effect in different part of this waters separately, that enhance the biogeochemical cycle of nutrient elements.

(3) Role of frontal area and thermohaline transition layer on the biogeochemical cycle of nutrient elements

During several water masses converging the frontal zone was formed in this area[1]. The frontal zone is the key space for transfer of mass and energy exchange. Fig.2 and Fig.3 shows the frontal zone is most concentrated part of equiscalar line of nutrient element species. That explains these nutrients pass through the frontal zone conducting transfer and diffusion. It is very clear the dissolvable inorganic states of nutrient diffuse across frontal surface from the higher concentration side into lower concentration side. But the concentration of SPM was a great different in both side of frontal surface. A large number of suspended particles in the Changjiang River Diluted Water was concentrated, flocculated and settled to

the west of frontal surface (St. A1) which resulted in transparency increasing in the frontal zone. In fact, the frontal surface seems to provide a screen for the SPM transfer. Abounding in nutrient and light enhance photosynthesis and form a high productivity area in the frontal zone, thus the species converted and biogeochemistry cycled rapidly.

As the Changjiang River Diluted Water plume covered and Taiwan Warm Current Water wedged so the waters exist the thermohaline transition layer. During the investigation an interest phenomenon was discovered the ORP, DO and pH have a delicate variation in the stations appeared thermohaline transition layer (fig.8). It is special the ORP was downward as the water depth increase and lowest value appeared at the upper interface of the themohaline transition layer. Because a large number of organism was produced by photosynthesis in the upper water mass and that was partly concentrated and decomposed on water mass above transition layer, when the transition layer was formed and that can decrease the settling speed of the organism and suspended particles. The water mass under transition layer was wedged the Taiwan Warm Current Water that the concentration of organic matter was lower relatively. This difference cause the ORP appear a sudden rise change from upper interface to down interface of transition layer. Then the

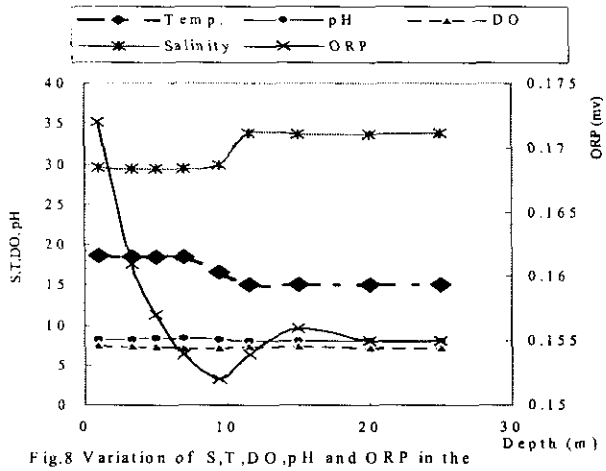

Fig.8 Variation of S,T,DO,pH and ORP in the thermohaline transition layer water column (C5 May,1998)

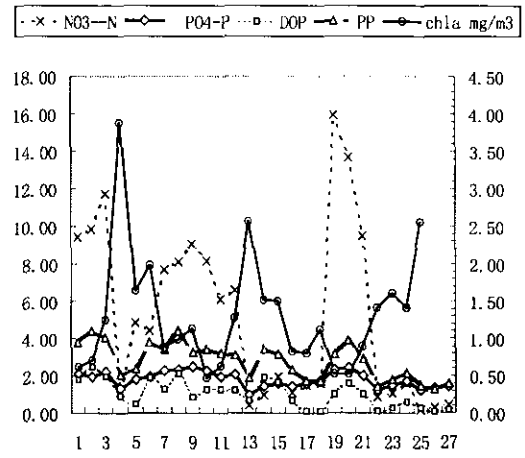

Fig.9 Relation of concentration variation of nutrient species and Chl.a (Oct. 1997)

ORP keep a steady level value. The variation of the ORP is a comprehensive reflex for the photosynthesis, respiratory, autolysis, decomposition, mineralization and oxidation-reduction etc varied action. The difference of ORP variation shows taking place the differentiation of biogeochemical action in the both water masses of up and down the transition layer (as mentioned above). Both series opposite direction reaction process compose a complete nutrient biogeochemical cycle. But it is have to pay attention to that a large number of inorganic nutrient salt absorbed by the photosynthesis will be complement rapidly as the species variance in water mass up the transition layer interface (Fig.9). It will increase dangerous to water environment eutrophication in this area.

(4) Primary estimation of water environmental capacity of nutrient

Owing to biological resource abundant and active in biogeochemical action, this area forms a famous the Changjiang Estuary Fishing Field. In the other side, the environmental pollutant load becomes critical. Protecting ecological environment against pollution is significance. So we attempt to use this investigation result primary estimating the environmental capacity of N and P. It is common knowledge that environmental capacity is a environment can admit most load of pollutant under premise the nature

ecological system is not harmed. As if the dynamic environment capacity was studied, many environmental factors such as migrate, transform and self-purification etc should be considered all-round. But it is limited for this work; here we consider its biogeochemistry action only. Suppose the hydrodynamic factors such as the effect of current, water mass mixing, diffuse, diluted and water mass replace process is as a steady state variation physical process. Then the static capacity was estimated as following:

$$Cwpi = V \times (Csi - Cbi) \quad (1)$$

During considering the purification and regeneration of the biogeochemistry action

$$Cwpi = V \times (Csi - Cbi + Cspi - Cregi) \quad (2)$$

Cwpi -------the environmental capacity of a certain pollutant in waters

V ------- for the volume of environmental waters

$V = A \times D$, (A for area, D for depth)

Csi ------- critical standard concentration here using B category water quality admit concentration of the Chinese sea water quality standard

Cbi ------- background concentration of water environment, here using the average concentration value of this investigation

Cspi ------ decrease concentration value by biogeochemical self-purification

Cregi ------increase concentration value by biogeochemical cycle regeneration

The organism absorption and particulate adsorption is the dominant factors for the biogeochemical purification. Thanks to these action process are very rapidly, the measured concentration background value has considered at present as the concentration while the absorption and adsorption process have reached dynamic balance, as a result the Cspi could consider put off. But the latent increase quantity of DIN and PO_4^{3-} is the regeneration of inorganic N and P by autolysis, decomposition and mineralization process. According the result of release experiment of remineralization during the decomposition of coastal plankton and natural seston by Garber J.H. (1984): there account for about 60% reactive composition of the total N and P in seston and organism and that were released during 30 days. About 20 – 25% of the PP could be converted to dissolve inorganic-P (DIP) fraction after only 7 h[7]. Meanwhile in consideration of the water exchange rate and water mass half residence time: 50% exchange needs 16 days, 80% exchange needs 40 days[8] (Zhu Dedi 1999). As primary estimation it seems to be about 50% of PP, DOP, PN and DON could be decomposed and released into dissolved inorganic state. Therefore

$$Cwpi = A \times D \times [Csi - Cbi + (Cpi - Cdoi) \times 50\%] \quad (3)$$

Taking the following value into equation (3)

$A = 1.30 \times 10^{10}\ m^2$ $D = 38.67$ m

N:	P:	
$C_{SN} = 0.30$ mg/l	$C_{SP} = 0.030$ mg/l	
(Oct. 1997)	(Oct. 1997)	(May 1998)
$C_{bDON} = 6.49$ mol/l	C_{bPO4}-= 0.45 mol/l	C_{bPO4}-= 0.26 mol/l
$C_{PN} = 15.62$ mol/l	$C_{PP} = 0.70$ mol/l	$C_{PP} = 0.55$ mol/l
$C_{DON} = 9.25$ mol/l	$C_{DOP} = 0.26$ mol/l	$C_{DOP} = 0.34$ mol/l

The results are shown as following:

$C_{WP\text{-}DIN} = 1.803 \times 10^4$ t (Oct. 1997)

$C_{WP\text{-}PO4\text{-}} = 6.18 \times 10^2$ t (Oct. 1997)

$C_{W\,P\text{-}PO4\text{-}} = 4.20 \times 10^3$ t (May 1998)

The results have been got only by a relative rough estimate and the distribution unevenness is

unconsidered as yet. In fact, conducting a perfect and accurate estimate of environmental capacity needs getting more data and developing more studies related to the hydrodynamic and biogeochemistry

4.CONCLUSION

The particulate state made up a great ratio among the nutrient species. The particulate N amount to about 50% and particulate P account for 47~51% of total content respectively. The general tendency of the nutrient concentration distribution was downward from west to east and from north to south as well. Among the nutrient element species only there is a negative correlation between salinity and SiO_3^{3-}, the others were different characteristic that depends on the biogeochemical variation of every nutrient element species.

In euphonic layer $PO_4^{3-}$was absorbed and transformed to PP and DOP, but the particulate phosphorus and organic phosphorus took place autolysis, decomposition and mineralization process and regeneration of inorganic P rapidly in the first half water column. The released DIP can join in the photosynthesis again; leading to PO_4^{3-} can keep a rather stable concentration level.

Besides the variation of N species was controlled by solid-liquid and organic-inorganic transform action, the oxidation-reduction for mutual conversion of DIN (including NO_3^-, NO^{2-} and NH_4^+) are quite obvious. NO_3^- was reduced and concentration of NH_4^+ was upward as water depth increase in the first half water column, opposite direction reactions appear in the second half water column.

Different effects of the frontal zone and transition layer on the concentrating and spreading of nutrient element species were discovered. The biogeochemical action was specially active and cycle rapidly. A large amount of particulate of abundant N and P was gathering in upper interface of transition layer. Difference direction of biogeochemical reaction was appeared between up and down of transition layer interface waters that form a special biogeochemical cycle in this waters.

Primary estimated the environmental capacity of DIN and PO_4^{3-}—P was 1.803×10^4 t DIN and 6.18×10^2 t PO_4^{3-} in autumn, and 4.20×10^3 t PO_4^{3-} in spring. But the unevenness of concentration distribution, action of frontal zone and thermohaline transition layer will lead to speed up the eutrophication in partial area. Conducting a perfect and accurate estimate of environmental capacity on this waters needs developing more studies related to the hydrodynamic and biogeochemistry.

ACKNOWLEDGMENTS: We wish to express our gratitude to Prof. Wang Xiulin, Mr. Shi Shao Yong (Qing Dao Ocean University), Professor Zhu Ming Yuan (First Institute of Oceanography, SOA) and KOSHIKAWA Hiroshi (NIES, Japan) for theirs help in providing partial measurement data.

REFERENCES

1) Mao Hanli et al.: Preliminary study of Changjiang diluted water and it's mixing processes. *Oceanologia et Limnologia Sinica*, 5(3): 186~206, 1963.

2) Zhang jing: Nutrient elements from some selected north China estuaries: Huanghe, Luanhe, Daliaohe and Yalujiang. In: *"Biogeochemical study on major estuary in China"*. Zhang Jing editor, China Ocean Press, pp: 205~217,1996. (In Chinese)

3) Hwang Shanggao et al.: Silicon nitrogen and phosphorus in the Changjiang River Mouth Water.*Proceedings of SSCS*, 1: 214~250, 1983.

4) Tang Renyou et al.: *Biogeochemical study of the Changjiang Estuary*. Yu Guohui, J.M.Martin, Zhou Jiayi, editor, China Ocean Press, pp: 322~334, 1990.

5) Shen Zhiliang et al.: Distribution characters of the nutrients in the Changjiang Estuary. *Studia Marina Sinica* No.33, 109~129, 1992. (In Chinese)

6) Lin Yi-An et al.: Relationship between biogeochemical features of biogenic elements and flocculation in the Changjiang Estuary. *Acta Oceanologica Sinica*, 14(2): 225~234, 1995.

7) Garber, J.H.: Laboratory study of nitrogen and phosphorus remineralization during the decomposition of coastal plankton and seston. *Estuarine Coastal and shelf Science*, 10(6): 685~702, 1984.

8) ZHU Dedi, XU Weiyi: Research of environment capacity. In: *The Japan-China joint workshop on the cooperation study of the marine environment.*1999, Tokyo Japan

ELEMENTAL COMPOSITION OF SUSPENDED PARTICLES IN THE CHANGJIANG ESTUARY MOUTH

Masami Kanao KOSHIKAWA[1], Takejiro TAKAMATSU[1], Jitsuya TAKADA[2], Rokuji MATSUSHITA[2], Shogo MURAKAMI[1], Kai-qin XU[1] and Masataka WATANABE[1]

[1] Soil and Water Environment Division, National Institute for Environmental Studies, Environment Agency (Onogawa 16-2, Tsukuba, Ibaraki 305-0053, Japan)

[2]Research Reactor Institute, Kyoto University (Kumatori-cho, Osaka 590-0494 Japan)

Concentrations of 35 elements in suspended particles in the Changjiang estuary mouth in the East China Sea were determined. To examine the possible input of anthropogenic heavy metals from the river, the X/Al ratios (the concentration of the element X as a fraction of Al concentration) in the suspended particles were derived; the main sources of the elements in the suspended particles were natural particles such as soil particles or plankton.

Keywords : *suspended particles, elemental composition, plankton, sediment*

1. INTRODUCTION

Most chemical elements transported by rivers to the sea occur in particulate form. In the sea, these particles from rivers are mixed with sediments from the seabed and organic particles produced by plankton in the surface layers of the sea. Characterization of the origins of suspended particles, and evaluation of their degree of contamination, has been previously done in the Scheldt estuary by analyzing the elemental compositions of the suspended particles[1]. The Changjiang River is the largest source of freshwater flowing into the East China Sea with a discharge about 1×10^{12} m^3/y, and a solid load of about 5×10^8 t/y[2]. Therefore, the river affects not only the estuary but also the marine environment and ecosystem over a wide area of the East China Sea. As part of a US-China cooperative study on sediment dynamics in the Changjiang estuary, Edmond et al.[3] reported the results from field surveys in June 1980 and November 1981, corresponding to the flood season and dry season, respectively. Conservative or non-conservative behaviors of dissolved trace elements were observed during estuarine mixing, and the net flux of dissolved trace elements from the river to the sea was calculated. As part of a France-China cooperative study on the biogeochemistry of the Changjiang estuary, Zhang et al.[4] reported the results from field surveys undertaken in January 1986 and July 1986, corresponding to the dry season and flood season, respectively. The elemental composition of suspended particles, analyzed by instrumental neutron activation analysis, remained almost constant during estuarine mixing. In addition, the "exchangeable" fraction of elements in suspended particles, analyzed according to the method of Tessier[5], was lower in the Changjiang estuary than in the Rhone or Gironde estuaries. Therefore, the pollution from industrialized regions was lower in the Changjiang than in European rivers.

The collaborative research project between Japan and China on 'Environmental loading from river inputs and their effects on the marine ecosystem in specified areas of the East China Sea' has been running since 1997. As part of our research program, field surveys were conducted offshore from the Changjiang River in

October 1997 and May 1998, which corresponded to seasons of plankton blooms. In this study, the distribution and elemental composition of suspended particles were analyzed in order to understand the roles of riverine input and primary production in the mouth of the Changjiang estuary.

2. MATERIALS AND METHODS

(1) Field method

The investigation was carried out between latitudes 31°00'N and 32°00'N and longitudes 122°30'E and 124° 00'E, the area in the East China Sea specified in the agreement of the Japan-China Collaborative Research Project (Fig. 1). Two cruises were conducted from October 19 to 20, 1997 (autumn cruise) and May 14 to 17, 1998 (spring cruise), aboard the research vessel "Haijian 49" of the China State Oceanic Administration. At 15 stations in the specified area (A1 to C5, Fig. 1), vertical profiles of temperature, salinity, pH, dissolved oxygen, and redox potential of water were measured in situ (Surveyor II, Hydrolab). Seawater was collected from the surface layer at 9 stations (C1, B1, A1, C3, B3, A3, C5, B5, and A5) in autumn and spring. At 5 stations (C1, A1, C3, C5, and A5) in autumn and at C1 in spring (14 May), seawater was collected from the surface, middle (according to the water depth), and bottom (a few meters above the sea bed) layers using 20-L Niskin samplers (Table 1). In addition, daily sampling was done in a mesocosm constructed in the Changjiang estuary[6]. Immediately after sampling, the samples were filtered on board the research vessel through Nuclepore® filters (0.4-μm pore size) using a closed system of pressure filtration in a clean box[7]. The filters with the suspended particles were kept below –20°C and delivered to our laboratory in Japan.

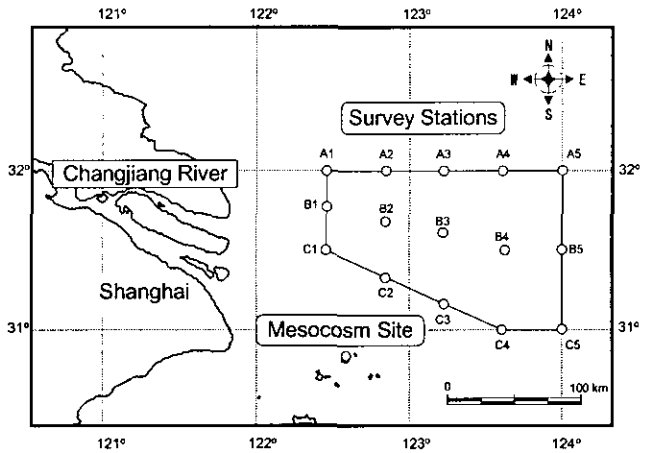

Fig.1 Location of investigation area

(2) Laboratory method

Filters with particles were dried at 60°C and weighed. The concentration of suspended solids (= SS [mg/L]) in each sample was calculated as {[(the weight of filter with particles) – (the weight of blank filter)] / (the volume of the seawater filtrated)}. For each sample, 2 filters with particles were taken; one was subjected to acid digestion followed by inductively coupled plasma atomic emission spectroscopy (ICP-AES) analysis, the other was subjected to instrumental neutron activation analysis (INAA). Acid digestion[8] was done with HNO_3-$HClO_4$-HF at 140°C in airtight Teflon vials. The resulting solution was dried and dissolved in dilute HNO_3, and then subjected to ICP-AES analysis[9] to obtain the concentrations of 18 elements (Al, Ba, Ca, Cr, Cu, Fe, Mg, Mn, Ni, P, S, Sc, Sr, Ti, Pb, V, Y, and Zn). The concentrations of 19 elements (As, Ce, Co, Cs, Eu, Fe, Hf, La, Lu, Nd, Rb, Sb, Sc, Sm, Ta, Tb, Th, U, and Yb) were obtained by INAA according to the method of Koyama and Matsushita[10]. The concentrations of Fe and Sc obtained by both ICP-AES and INAA agreed well; thus concentrations of 35 elements were obtained altogether.

Table 1 Depth and salinity of sampling stations.

a) Autumn cruise (1997)

Sampling date	Station	Sea depth (m)	Sampling depth (m)	Salinity ‰
19 Oct.	C1	29	1	28.0
			12	30.4
			24	33.7
	C3	55	1	33.0
			28	33.9
			50	34.0
	C5	41	1	33.7
			18	33.9
			33	34.0
	B5	43	1	33.8
20 Oct.	A5	42	1	33.4
			18	33.1
			38	33.3
	A3	40	1	29.6
	B3	39	1	30.0
	A1	25	1	31.4
			12	31.5
			22	31.6
	B1	29	1	32.0

b) Spring cruise (1998)

Sampling date	Station	Sea depth (m)	Sampling depth (m)	Salinity ‰
14 May	C1	39	1	28.7
			12	32.5
			24	33.3
15 May	B1	29	1	29.4
	A1	25	1	30.5
	A3	40	1	31.5
16 May	C3	55	1	27.7
	C5	41	1	29.5
	B5	43	1	31.2
	A5	42	1	31.9
	B3	39	1	30.7
17 May	C1	29	1	11.4

3. RESULTS

Because Al content is considered to be a good indicator of the fine-grained clay fraction in suspended particles[11], the elemental composition of the suspended particles was normalized to that of Al content and X/Al ratios (the content of the element X as a fraction of Al content) were derived. Particles from different sources are expected to have different X/Al ratios according to season, station, and sampling depth[1]. SS in surface waters of 9 stations and aluminum contents in those suspended particles are shown in Fig. 2. P/Al, Zn/Al, Mn/Al, Ca/Al, and Fe/Al in suspended particles in surface waters of 9 stations are shown in Fig. 3.

In addition, for the stations where samples were taken from the 3 layers, ratios of [the concentration in bottom waters] / [the concentration in surface waters] were derived (Fig. 4).

(1) Distribution of SS

SS in surface waters at stations A1 and C1 (17 May) were higher than 20 mg/L and were higher than those at other stations (Fig. 2). Except for these 2 stations, SS of surface waters in spring (1.6 ± 0.9 mg/L) were lower than those in autumn (3.2 ± 1.7 mg/L). SS were more than 5 times higher in bottom waters than in surface waters (Fig. 4).

(2) Distribution of Al content

In autumn, Al contents of suspended particles in surface waters at stations A1, C3, B3 and A3 (40 to 60 mg/g) were lower than those at other stations (80 to 100 mg/g; Fig. 2). In spring, Al contents at stations C3, B3, A3, C5 and B5 (7 to 20 mg/g) were lower than those at other stations (45 to 120 mg/g). Compared to surface waters, the Al contents in bottom waters were lower at C1, higher at A1 and C3, and similar at C5 and A5 (Fig. 4).

(3) Distribution of X/Al ratios

P/Al showed large variation, from 0.01 to 0.33 (Fig. 3). Surface water samples showed higher P/Al ratios than did the middle or bottom water samples (Fig. 4); in autumn surface samples at stations C3, B3 and A3 showed higher P/Al ratios than did other stations, and in spring surface samples at stations C3, B3, A3, C5 and B5 showed higher P/Al than did other stations. Zn/Al also showed large variation, from 0.001 to 0.012 (Figs. 3 and 4), and was correlated with that of P/Al ($R = 0.885$). P/Al was also correlated with Sr/Al, Ba/Al, S/Al, and Mg/Al.

The highest Mn/Al ratio (0.012) of surface waters was observed at station A1 in both seasons (Fig. 3). At other stations, Mn/Al of surface waters were almost constant in autumn (0.009 ± 0.001) and in spring

(0.006 ± 0.001); Mn/Al of surface waters were lower in spring than in autumn. Compared with surface waters, Mn/Al of bottom waters were higher at C1, C3, and C5, and similar at A1 and A5 (Fig. 4). Mn/Al of bottom waters at C1 was higher in spring (0.013) than in autumn (0.011).

Ca/Al at stations A1, C5, B5, and A5 in autumn and stations A1 and C5 in spring were higher than 0.30 and higher than at other stations. Ca/Al of surface waters were lower in spring (0.18 ± 0.14) than in autumn (0.27 ± 0.07; Fig. 3). Compared to surface waters, Ca/Al of bottom waters were higher at C1, C3, and C5, and similar at A1 and A5 (Fig. 4). Ca/Al of bottom waters at C1 was higher in spring (0.38) than in autumn (0.30).

X/Al ratios of As, Ce, Co, Cs, Fe, Hf, La, Ni, Pb, Sc, Sm, Th, Ti, V, Y and Yb remained constant regardless of season, station or depth; as an example Fe/Al is shown in Figs. 3 and 4.

The other 10 elements in this study are not discussed here; 6 of them—Cr, Cu, Eu, Lu, Sb, and Ta—were close to the detection limit, and the remaining elements—Nd, Tb, Rb, and U—were detected in a few samples only.

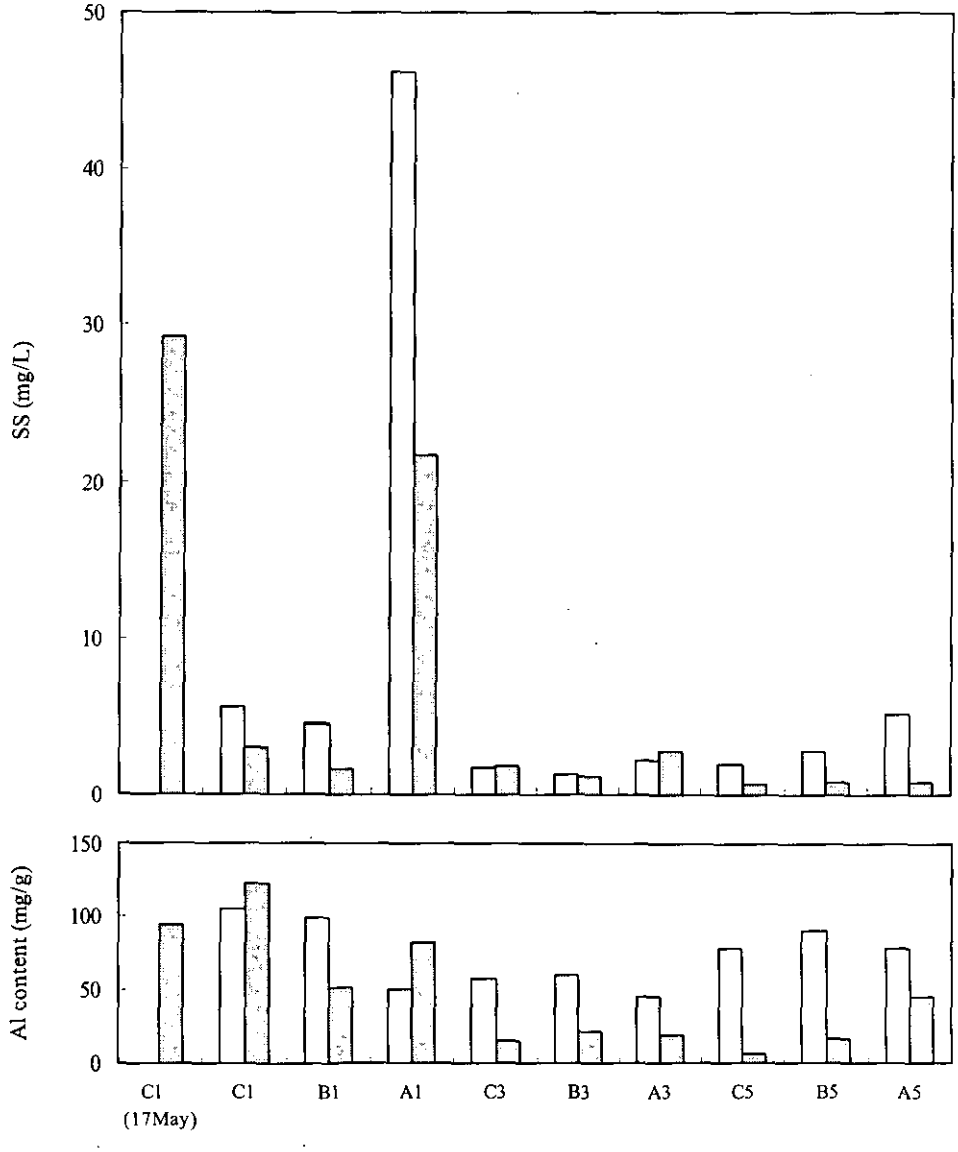

Fig.2 SS and Al content of suspended particles in surface waters; white bar: autumn, shaded bar: spring.

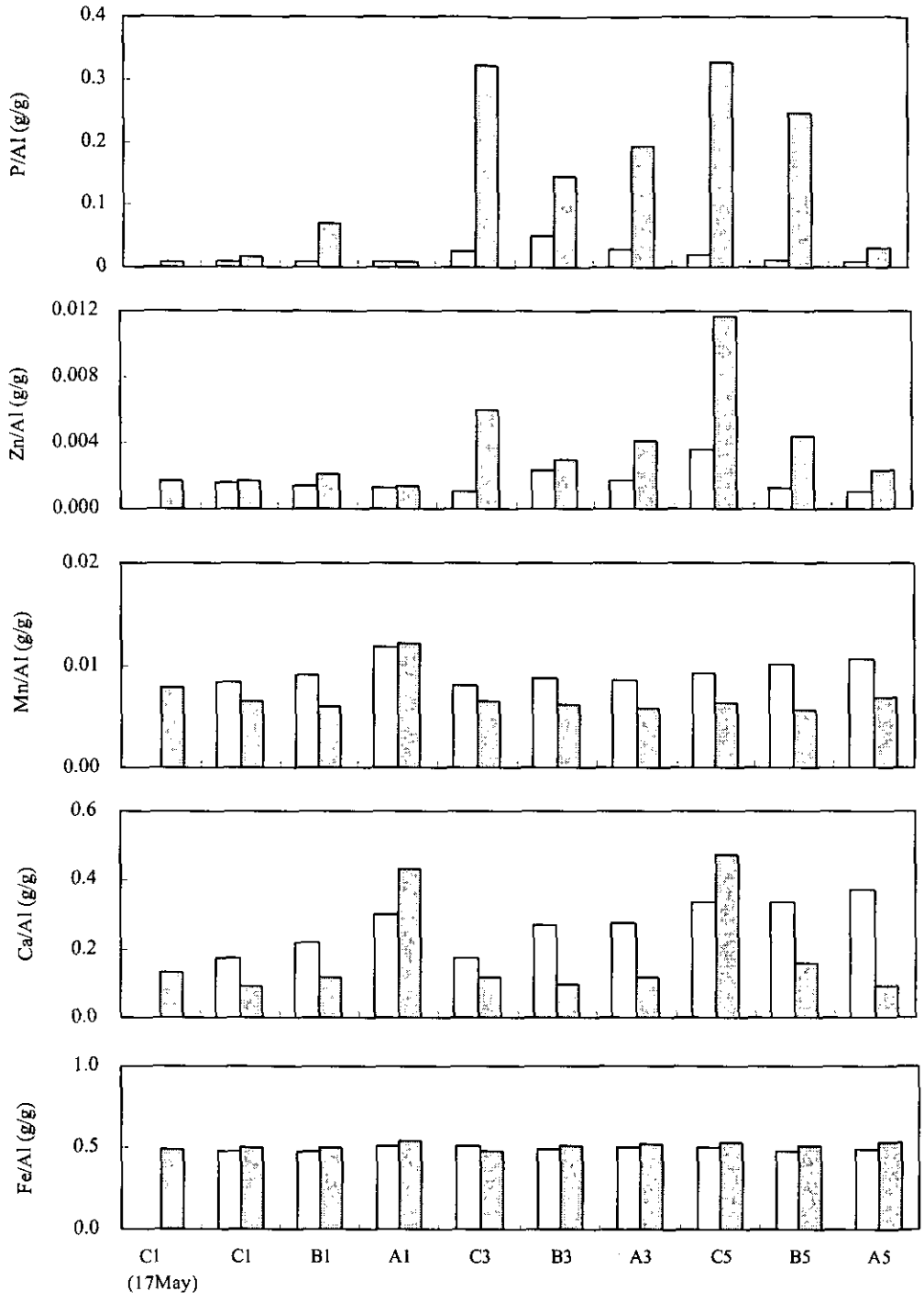

Fig.3 P/Al, Zn/Al, Mn/Al, Ca/Al, and Fe/Al of suspended particles in surface waters; white bar: autumn, shaded bar: spring.

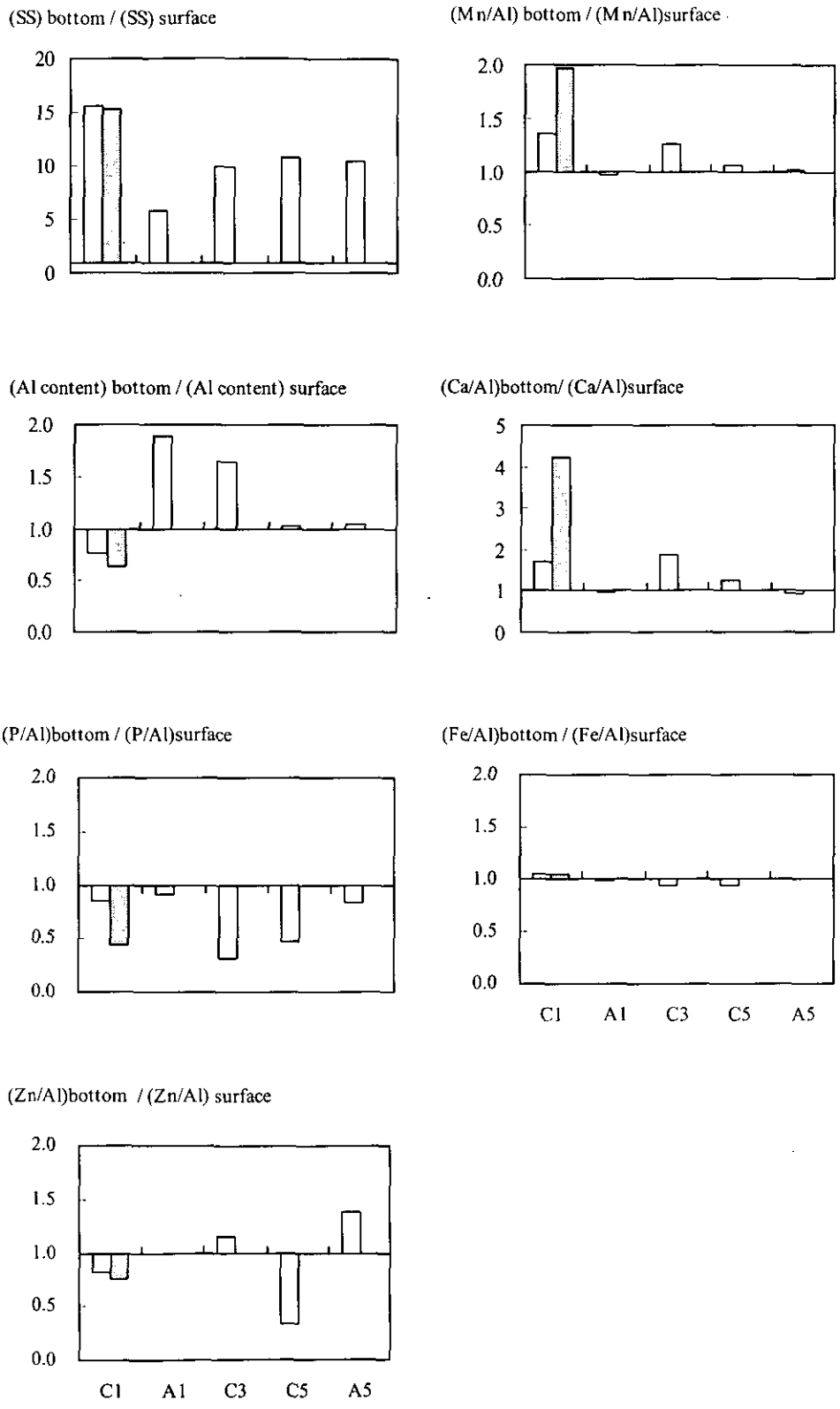

Fig.4 Ratios of bottom/surface levels of SS content, Al content, P/Al, Zn/Al, Mn/Al, Ca/Al, and Fe/Al of suspended particles; *white bar: autumn, shaded bar: spring.*

4. DISCUSSION

(1) Effect of plankton abundance

At stations C3, B3, and A3 in autumn and stations C3, B3, A3, C5, and B5 in spring, P/Al was higher than at other stations. The variation in P/Al was correlated with the organic carbon content of the suspended particles (R = 0.875; Okamura, pers. comm.), and was therefore related to the abundance of plankton.

P/Al was correlated with Zn/Al. The intercept of the regression line [(Zn/Al) = 0.02 (P/Al) + 0.001] was close to the ratio for the earth's crust[12] (Zn/Al = 0.001) and the slope was close to the ratio of Zn/P in plankton[13] (Zn/P = 0.03). P/Al was also correlated with Sr/Al, Ba/Al, S/Al and Mg/Al. These elements have 2 main sources—crustal particles from the river and plankton from the surface layer of the sea—and the contributions of the 2 sources varied at different stations.

Similar elemental compositions were found in the mesocosm samples. As the plankton population in the mesocosm increased, P/Al, Zn/Al, Sr/Al, Ba/Al, S/Al and Mg/Al also increased, while X/Al of other elements, such as Fe and Ti, remained constant.

(2) Effect of bottom sediments

SS, Mn/Al, and Ca/Al were higher in the bottom waters than in surface waters. Higher SS in bottom waters may result from re-suspension of the bottom sediments[14].

Re-suspension of bottom sediments results in higher Mn and Ca concentrations in suspended particles in bottom waters because the bottom sediments contain more Mn and Ca (Mn/Al = 0.013 ± 0.003, Ca/Al = 0.36 ± 0.08; Noel, pers. comm.) than do suspended particles in surface waters. Dissolution of Mn in the sediment and precipitation of Mn in the water column may also results in higher Mn/Al in suspended particles in bottom waters. Reduction of Mn(IV) oxide to dissolved Mn(II) in bottom sediments is reported to begin at a dissolved oxygen concentration of about 2-3 mg/L[15]. Although dissolved oxygen concentrations in bottom sediment was not observed in this study, we observed a decrease in dissolved oxygen from surface water (7 to 8 mg/L) to bottom water (5 to 6 mg/L), which implies consumption of dissolved oxygen in bottom sediments and even lower dissolved oxygen in bottom sediments than in bottom water. Dissolved Mn (II) released from the bottom sediments to the water column would be oxidized and form precipitates with a high Mn/Al ratio that would sink to the bottom[15]. Dissolution of $CaCO_3$ in the sediment and precipitation of Ca in the water will also occur. Mn and Ca in suspended particles may be supplied from the seabed by re-suspension of bottom sediments and/or dissolution of Mn and Ca from bottom sediments.

(3) Effect of density stratification

In spring, SS, Mn/Al, and Ca/Al of surface waters were lower than those in autumn and Mn/Al and Ca/Al of bottom waters were higher than those in autumn. In spring, both the thermocline and halocline were found at a depth of 10 m; temperature (16 to 18°C) was higher and salinity (27 to 31‰) was lower in the surface water than in the bottom water (14 to 15°C, 32 to 34‰), which results in a stable density stratification. Such a stable density stratification was not found in autumn because the temperature of the surface water then (22 to 24°C) was similar to that of the bottom water (23 to 24°C). The density stratification in spring prevented the transport of suspended particles from the bottom to the surface waters, resulting in the lower SS, Mn/Al and Ca/Al of surface waters. In addition, the transport of dissolved Mn and Ca from the bottom to the surface waters may also have been prevented by the density stratification; the formation of Mn and Ca precipitates may have occurred only in the bottom water, resulting in higher Mn/Al and Ca/Al in bottom waters. The density stratification of water could prevent the transport of elements from the bottom to the surface waters. On the other hand, at stations without density stratification, such as at A1 and A5 in autumn, Mn/Al and Ca/Al showed no difference between surface waters and bottom waters.

(4) Effect of Yellow Sea Coastal Current

The levels of SS, Mn/Al, and Ca/Al of surface water were higher at station A1 than at other stations. This may be the result of the hydrodynamic structure in the area studied. In addition to the river discharge, the Changjiang estuary is influenced by the Taiwan Warm Current (salinity about 34 ‰) flowing northwestward from the south and the Yellow Sea Coastal Current (salinity about 31 ‰) flowing southeastward from the north[16]. Because salinity at station A1 was 31‰ and station A1 is located in the northwest corner of the studied area, this was the station most strongly affected by the Yellow Sea Coastal Current (YSCC). The

main source of suspended particles in the YSCC is the Yellow River. Huang et al. reported the Mn/Al and Ca/Al ratios of suspended particles in the Yellow River are 0.011 and 0.50, respectively. Mn/Al of suspended particles in the East China Sea (this study) is similar to those in the Yellow River (Huang et al.), while Ca/Al in the East China Sea (this study) is distinctly lower than those in the Yellow River (Huang et al.). Although it is not clear whether Mn and Ca are delivered by YSCC from the north, or supplied through re-suspension of bottom sediments by the strong current, the higher Mn/Al and Ca/Al ratios at station A1 could be caused by the YSCC.

(5) Effect of Changjiang discharge

The surface water of station C1 (17 May) was strongly affected by Changjiang discharge; it showed the lowest salinity (11‰) and a high concentration of suspended particles. The X/Al ratios of As, Ce, Co, Cs, Fe, Hf, La, Ni, Pb, Sc, Sm, Th, Ti, V, Y and Yb remained constant regardless of season, station or depth, which implies that the sources of these 16 elements do not change. Their X/Al ratios were close to those of either the mean crust or median soil content, except for Cs/Al and As/Al values, which were twice as high as the median soil content (Table 2). It is reported that Ce, Co, Fe, Hf, La, Pb, Sc, Sm, Th and Yb are held in a lattice of minerals and their X/Al ratios remain constant[11]. Although salinity at the surface varied from 11‰ to 32‰ during the spring cruise, the elemental composition of the suspended particles remained constant.

In this preliminary observation, no influence of anthropogenic heavy metal could be detected. However, it does not mean there is no input of pollutants from the river—large amounts of natural particles from the river exist in this area and they can dilute and hide the effects of pollutants. In order to focus on anthropogenic pollutants, more advanced methods for selective detection of anthropogenic matter (such as a sequential extraction of Tessier[5]) should be applied.

Table 2 X/Al ratio of suspended particles (this study) and mean crust and median soil content (Bowen 1979).

Ele.	X/Al (μg/g)		
	Suspended particles	Mean crust	Median soil content
As	170 ± 30	18	85
Ce	830 ± 160	830	700
Co	200 ± 30	240	110
Cs	140 ± 20	37	56
Fe	500000 ± 20000	500000	560000
Hf	52 ± 15	65	85
La	400 ± 70	390	560
Ni	740 ± 500	980	700
Pb	750 ± 450	170	490
Sc	150 ± 20	200	99
Sm	68 ± 13	96	63
Th	170 ± 30	150	130
Ti	49000 ± 3000	68000	70000
V	1400 ± 300	2000	1300
Y	250 ± 70	370	560
Yb	36 ± 9	40	42

5. CONCLUSIONS

The behavior of the elements could be classified into 3 groups. The first group comprised P, Zn, Sr, Ba, S and Mg, which were related to the plankton population; the second group was Mn and Ca, which were affected by re-suspension of bottom sediments; and the third group consisted of the other 16 elements, which showed constant X/Al values and were thus related to crustal particles or soils.

ACKNOWLEDGMENT: We thank Dr. Masataka NISHIKAWA (National Institute for Environmental Studies, Japan) for supervising the ICP-AES analysis.

REFERENCES

1) Regnier, P. and Wollast, R. (1993) Distribution of trace metals in suspended matter of the Scheldt estuary. *Mar. Chem.* 43, 3-19

2) Milliman, J. D., Shen H.-T., Yang, Z.-S., and Meade, R. H. (1985) Transport and deposition of river sediment in the Changjiang estuary and adjacent continental shelf. *Cont. Shelf Res.* 4, 37-45

3) Edmond, J. M., Spivack, A., Grant, B. C., Hu, M.-H., Chen, Z., Chen, S., and Zeng, X. (1985) Chemical dynamics of the Changjiang estuary. *Cont. Shelf Res.* 4,

4) Zhang, J., Martin, J. M., Thomas, A., J., and Nirel, P. (1990) Fate of the particulate elements in the Changjiang estuary and the East China Sea. In: Yu, G., Martin, J. M., Zhou, J., Windom, H., and Dawson, R. (eds) *Biogeochemical Study of the Changjiang Estuary.* China Ocean Press, Beijing, 220-244

5) Tessier, A., Campbell, R. G. C., and Bisson, M. (1979) Sequential extraction procedure for the speciation of particulate trace metals. *Anal. Chem.* 51, 844-851

6) Xu, K., Koshikawa, H., Murakami, S., Maki, H., Kohata, K. and Watanabe, M. (1999) Impact of discharged fuel oil on plankton ecosystems: a mesocosm study in the Changjiang Estuary. (*in this volume*).

7) Nakayama, E. (1997) Pretreatment for trace metal analysis of seawater. In: Umezawa Y. et al. (ed) *New Techniques in Separation, Purification, and Detection*, NTS, Tokyo, 946-948 (in Japanese)

8) Okamoto, K. and Fuwa, K. (1984) Low-concentration digestion bomb method using a teflon double vessel for biological materials. *Anal. Chem.* 56, 1758-1760

9) Nishikawa, M., Ambe, Y., and Chubachi, S. (1986) Concentrations of trace elements in surface snow in the area near Syowa Station, Antarctica. *Mem. Natl. Inst. Polar Res.*, Spec. Issue, 45, 47-55

10) Koyama, M. and Matsushita, R. (1980) Use of neutron spectrum sensitive monitors for instrumental neutron activation analysis. *Bull. Inst. Chem. Res., Kyoto Univ.*, 58, 235-243

11) Thomas, A. J. and Martin, J. M. (1982) Chemical composition of river suspended sediment: Yangtze, Mackenzie, Indus, Orinoco, Parana and French rivers (Seine, Loire, Garonne, Dordogne, Rhone) In: Degens E.T. (ed) *Transport of Carbon and Minerals in Major World Rivers.* Mitt. Geol-Palaont. Inst. Univ. Hamburg, SCOPE/UNEP Sonderband, 52, 555-564

12) Bowen, H. J. M: *Environmental Chemistry of the Elements*, Acad. Press (London), pp. 333, (1979).

13) Morel, F. M. M. and Hudson, R. J. M. (1985) The geological cycle of trace elements in aquatic systems: Redfield revisited. In: Stumm W. (ed) *Chemical Processes in Lakes.* Wiley, New York, 251-281

14) Iseki, K., Okamura, K., and Kiyomoto, Y. (1999) Particle distributions and transport processes from the shelf to the Okinawa Trough in the East China Sea. In: Saito Y. et al. (ed) *Land-Sea Link in Asia "Prof. Kenneth O. Emery Commemorative International Workshop". Proceedings of an international workshop on sediment transport and storage in coastal sea-ocean system.* STA and Geological Survey of Japan, Tsukuba, 13-15

15) Sholkovits, E. R. (1985) Redox-related geochemistry in lakes: Alkali metals alkaline-earth elements, and 137Cs. In: Stumm W. (ed) *Chemical Processes in Lakes.* Wiley, New York, 119-142

16) Beardsley, R. C., Limeburner, R., Yu, H., and Cannon, G. A. (1985) Discharge of the Changjiang (Yangtze River) into the East China Sea. *Cont. Shelf Res.* 4, 57-76

17) Huang, W. W., Zhang, J., and Zhou, Z. H. (1992) Particulate element inventory of the Huanghe (Yellow River): A large high-turbidity river. *Geochim. Cosmochim. Acta* 56, 3669-3680

PRELIMINARY DATA ON FLUX AND DECOMPOSITION RATE OF SINKING PARTICULES IN THE CHANGJIANG ESTUARY

Kazumaro OKAMURA[1] and Yoko KIYOMOTO[1]

[1] Oceanography Division, Seikai National Fisheries Research Institute
(49 Kokubu-machi, Nagasaki 850-0951, Japan)

Experiments using sediment traps were conducted to measure the flux and decomposition rate of sinking particles in the Changjiang Estuary in autumn 1997 and spring 1998. There was a close relationship between the water column conditions, such as stratification and vertical mixing, and the level of particulate flux. The higher C/N ratio of sinking particles in autumn than in spring suggests high biological productivity in autumn and high frequent resuspension events in spring in spite of the high biological productivity. The decomposition rate of sinking particles was low due to the influence of a large amount of lithogenic particles.

Key Words : *East China Sea, Changjiang Estuary, Sediment trap, flux, decomposition rate*

1. INTRODUCTION

The Bohai and East China seas have huge continental shelf areas and high biological productivity due to the large nutrient and suspended sediment inputs from the Huanghe and Changjiang rivers. Excess application of artificial chemicals due to the recent rapid development of agriculture and industry and the population explosion in coastal regions in China has accelerated the increase of riverine pollutants. Further the increased exploitation of water and energy resources and changing land use pattern have also led to changes in the amount and concentration of riverine pollutants. Particulate matter supplied from the river creates high turbidity in the Changjiang Estuary. Heavy metals of Fe, Al, Cu, Pb and Zn in dissolution once entered the estuary environment were absorbed into the particluate matter due to the mixing of fresh and sea water and aggregation has been shown to occur in the area ranging from 15 to 24 of salinity [1]. More than 80% of the hydrophobic organic matter was transferred in a particulate form to the sea, such as PCBs [2]. Various dissolved pollutants are absorbed to the particulate matter in the high turbidity area and transported offshore. It is necessary for evaluating the influence of these pollutants on the marine ecosystem to clarify the transport mechanism of particulate matter in the estuarine and offshore areas.The particles creating high turbidity in the Changjiang Estuary are removed by physical, chemical and biological processes. Little research on the transport of sinking particles in the Changjinag Estuary has been carried out. This study aimed to provide the fundamental data for clarifying the processes of sinking and decomposition of particulate matter in the Changjiang Estuary.

2. SAMPLING AND METHODS

(1) Sampling

Experiments using sediment traps were conducted to measure the flux and decomposition rate of sinking particles in the Changjiang Estuary in autumn, 11 to 13 October 1997, and spring, 20 May to 1 June 1998 (Table 1). Experimental site was at lat 30°52.5'N, long 122°36.5'E, in water depth of about 20m (Fig.1).

Table 1 Time table of the trap experiments

Experiment No.	Experimental date	Duration period (d)	Installed depth (m)	Measurement items
Exp.	11 - 13 October, 1997	2.19	5, 15	Flux, Decomposition rate
Exp. I	20 May, 1998	0.42 (10h)	8	Decomposition rate
Exp. II	22-23 May, 1998	1.15	5, 15	Flux
Exp. III	26 May, 1998	0.42 (10h)	5	Decomposition rate
Exp. IV	30 May - 1 June, 1998	1.97	5, 15	Flux

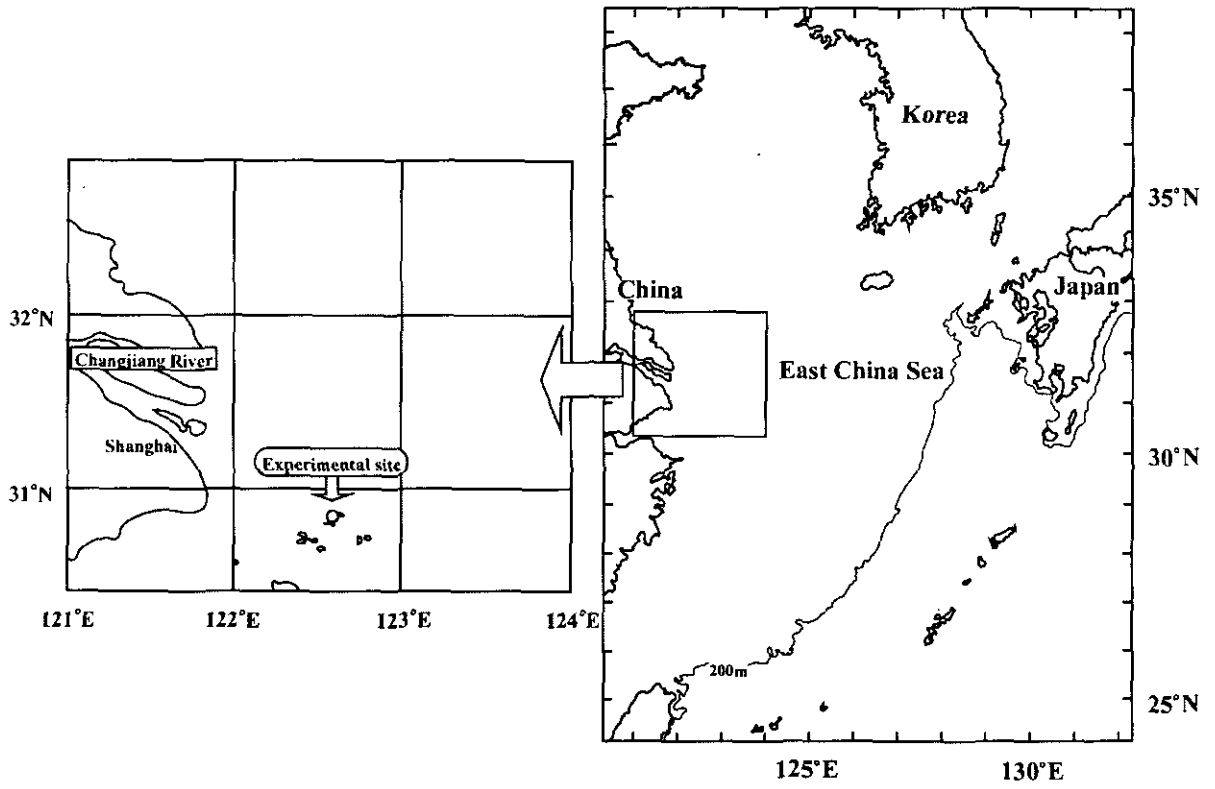

Fig. 1 Location of the study area

In the autumn experiment, two sediment traps (twin-cylinder type) were submerged from the R/V 'Haijian 49' for about 2 d at depths of 5 and 15m, respectively. Formalin (5ml per 500ml-sample bottle) was added in advance to a sample bottle attached to one of the cylinders at each depth. The formalin-containing samples were used for measuring the flux and chemical composition of sinking particles, while the other samples were used for measuring the decomposition rate of the sinking particles.

In spring, four experiments (Exps. I- IV) were conducted to measure the flux and decomposition rate of sinking particles. Exp. I and III were done to measure the flux of sinking particles for 1.15 to 1.97 d and Exp. II and IV were for measuring the decomposition rate of sinking particles for 10 h.

(2) Analysis and measurement

To analyze the flux and chemical composition of sinking particles, after extra large particles (>1000μm) were removed by nylon net, each sample was divided into two size fractions (<100 and 100 to 1000μm) by nylon net and filtering through GF/F and/or Nuclepore (pore size 0.6μm) filters. The samples were weighed before analysis for organic carbon, organic nitrogen, biogenic silica and lithogenic silica content. Organic

carbon and nitrogen were measured using an elemental analyzer (EA1110; CE Instruments). Biogenic and lithogenic silica were measured using a spectrophotometer (UV1600; Simazu).

To measure the decomposition rate of sinking particles, samples were placed in DO bottles on board, packed in a dark bag and incubated at the sea surface. Water temperatures in autumn and spring were 23.1 to 23.8 and 19.2 to 20.7°C, respectively. Subsampling was carried out at intervals of 3hs to 1d and the decomposition rate was determined by two methods in the DO bottles: measurement of oxygen consumption by Winkler method (O_2 method) and the decrease in organic carbon using an elemental analyzer (direct method).

The amount of oxygen consumption is converted to the decreased amount of the organic carbon by the following chemical equation:

$$(CH_2O)_{106}(NH_3)_{16}H_3PO_4+138O_2 \rightleftarrows 106CO_2+16HNO_3+H_3PO_4+122H_2O$$

138 moles of oxygen atoms are necessary to decompose 106 moles of carbon atoms.

Assuming that the decomposition process is logarithmic with time, the decomposition rate (k, d^{-1}) of sinking particles during incubation period (t, day) is approximated as

$$k = -1/t \cdot \ln[(N_0 - \Delta D)/N_0],$$

where N_0 is the initial amount of organic carbon in the sinking particles and ΔD is the decreased amount of the organic carbon during t days [3].

3. RESULTS AND DISCUSSION

(1) Flux and chemical composition of sinking particles

a) Experiment in autumn 1997

In autumn 1997, the water column was stratified. The dry weight flux was 29.6 and 96.5 $g \cdot m^{-2} \cdot d^{-1}$ in the upper (5m) and lower (15m) layer, respectively, and tended to increase in the lower layer (Fig. 2). The organic carbon content was 1.89 and 0.88% in the upper and lower layer, respectively. The biogenic silica content reached 1.98% in the upper layer, while the lithogenic silica content reached 46.6 and 51.5% in the upper and lower layer, respectively (Fig. 3).

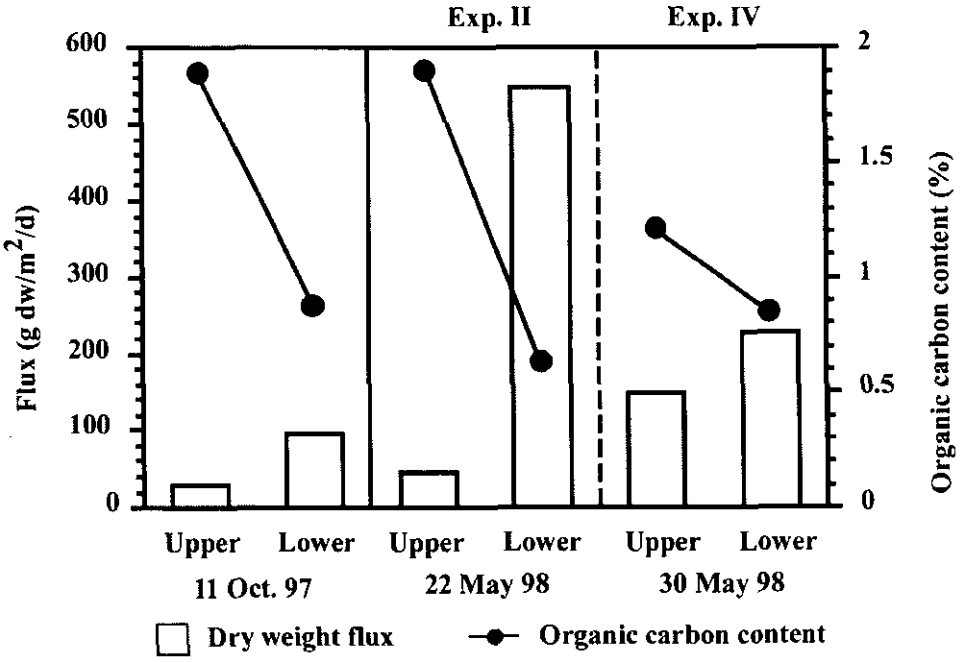

Fig. 2 Dry weight flux and organic carbon content of sinking particles in the upper and lower layer at the experimental site during the autumn and spring experiments.

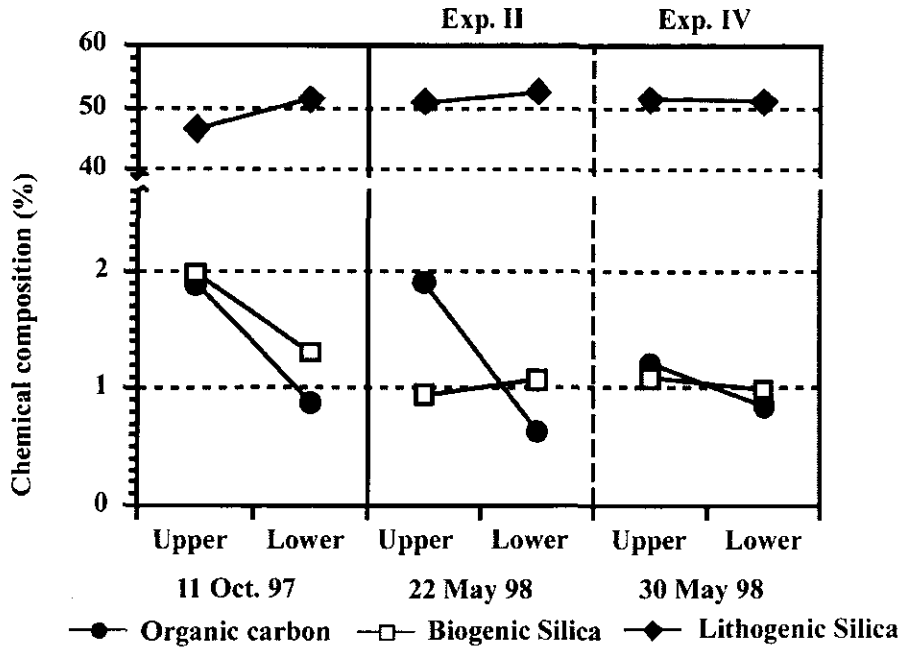

Fig. 3 Organic carbon, biogenic silica and lithogenic silica contents of sinking particles in the upper and lower layers at the experimental site during the autumn and spring experiments.

Small particles (<100μm) constituted over 80% of the sinking particles (Fig. 4). Although the large particles (100-1000μm) constituted 12.4% of the sinking particles in the upper layer, the organic carbon flux of these large particles accounted for 34.9% of the total organic carbon flux (Fig. 5).

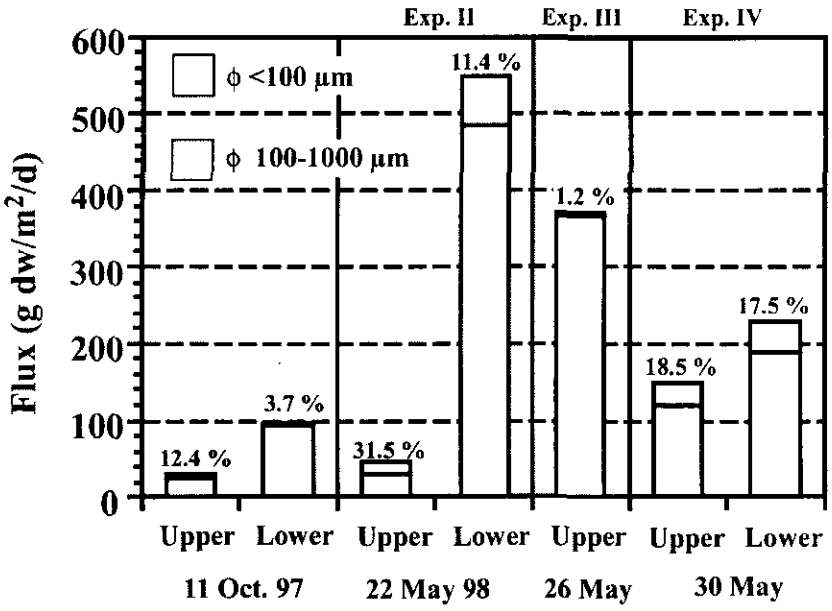

Fig. 4 Fluxes of two-size fractions of sinking particles in the upper and lower layers at the experimental site during the autumn and spring experiments.

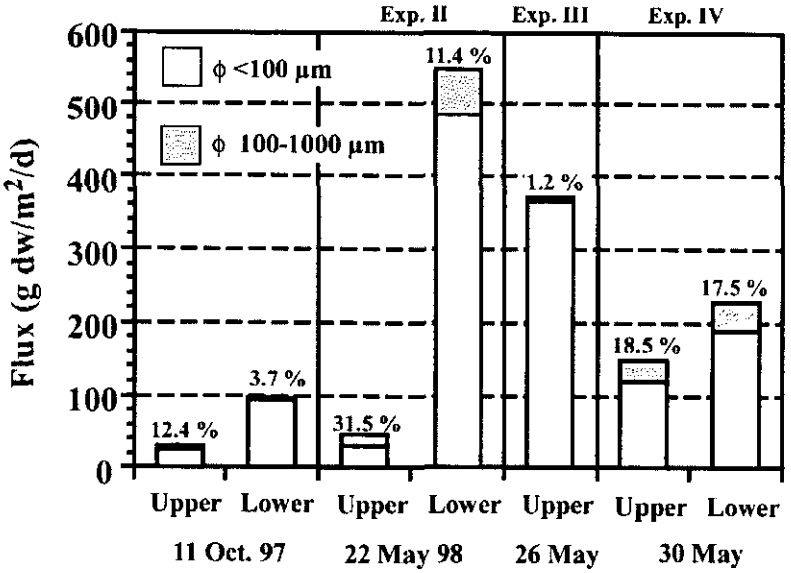

Fig. 4 Fluxes of two-size fractions of sinking particles in the upper and lower layers at the experimental site during the autumn and spring experiments.

From this, it was considered that large particles contribute significantly to the organic matter content in the sinking particles. Cloern [4] repoted that phytoplankton blooms often coincide with stratification events that reduce the mixed detph. In this study also, it is suggested that relatively high biological productivity occurred due to the improvement of light condition and mainly consisted of diatoms in the upper layer. $BSiO_2$/POC ratio (w/w) was 1.05 in the upper layer. Considering a ratio of 0.65±0.20 for live diatoms [5], this suggests that diatoms in the sinking particles were well decomposed so that they became detritus. On the other hand, the high flux and low organic carbon content of the sinking particles in the lower layer is considered to be due to the resuspension of sediments from the sea bottom. The C/N ratio (w/w) of the sinking particles in autumn was about 5.0 in both layers (Fig. 6), which indicates that the organic matter of the sinking particles has a strong influence on the high biological productivity at the experiment site in autumn.

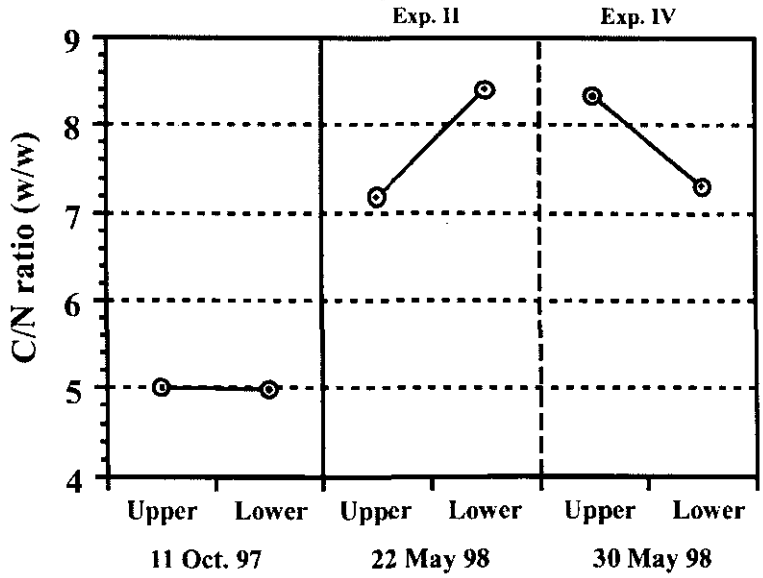

Fig. 6 C/N ratio of sinking particles in the upper and lower layers at the experimental site.during the autumn and spring experiments.

b) Experiment in spring 1998

In spring 1998, the water column was stratified during Exps. I and II; vertical mixing developed during Exp. III under the influence of the spring tide and passage of an atmospheric depression, and this mixing began to weaken during Exp. IV. The dry weight flux varied greatly during the experimental period; at 5m it was 43.8, 45.6, 370.2 and 148.1 $g \cdot m^{-2} \cdot d^{-1}$ in Exps. I, II, III and IV, respectively (Fig. 7). The dry weight flux in the upper layer was higher under the mixing conditions in Exps. III and IV than under the stratified conditions in Exps. I and II. The organic carbon content varied from 0.74 to 1.90% (Fig. 8) and tended to be inversely related to increase in dry weight flux. In Exp. III, the dry weight flux reached 370.2 $g \cdot m^{-2} \cdot d^{-1}$ and the organic carbon content was 0.74, which suggests that the influence of resuspension of the surface sediments from the sea bottom reached to the upper layer.

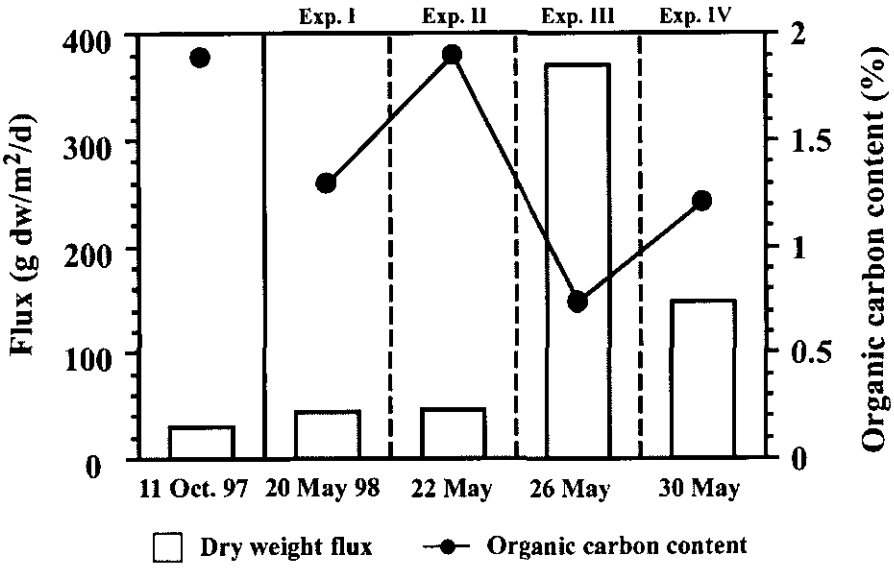

Fig.7 Dry weight flux and organic carbon content of sinking particles in the upper layer at the experimental site during the autumn and spring experiments.

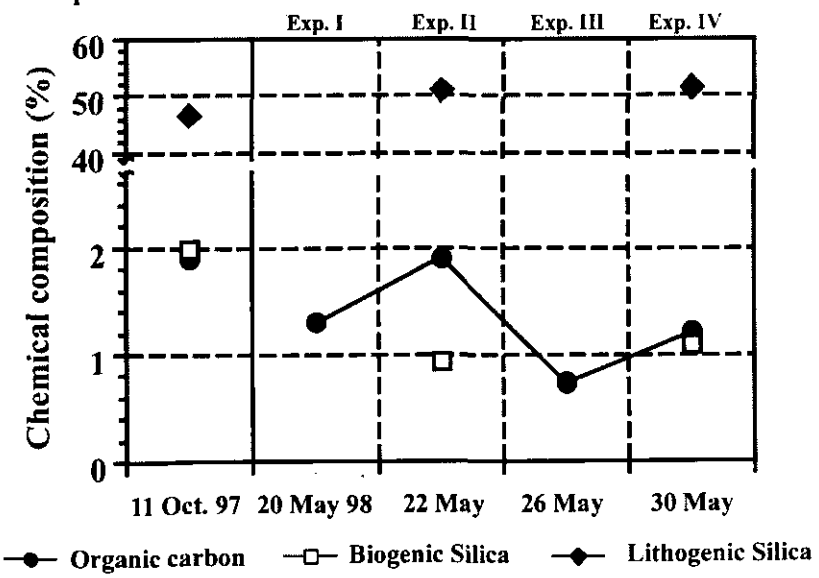

Fig. 8 Organic carbon, biogenic silica and lithogenic silica contents of sinking particles in the upper layer at the experimental site during the autumn and spring experiments.

In Exps. II and IV, sediment traps were also installed at 15m where the dry weight flux was 547.9 and 229.2

$g \cdot m^{-2} \cdot d^{-1}$, respectively (Fig. 2). In Exp. II, the dry weight flux in the lower layer was extremely high and the organic carbon content was 0.63%. Considering 0.47% of organic carbon content of the surface sediment on the sea bottom, the particles resuspended from the sea bottom influenced the composition of the sinking particles in the lower layer below the pycnocline. In Exp. II, the organic carbon content reached 1.9% in the upper layer, but the biogenic silica content was about 1% (Fig. 3), which indicates that the biological productivity in spring was due to other phytoplankton, such as dinoflagellates, while that in autumn was due to diatoms. The lithogenic silica content in spring reached more than 50% (Fig. 3) and the fraction of small particles was more than 80% except for 68.5% in the upper layer during Exp. II (Fig. 4), a tendency similar to that in autumn. In Exp. II, large particles constituted 31.5% of the sinking particles in the upper layer, furthermore, the organic carbon flux of large particles reached 47.1% of the total organic carbon flux (Fig. 5). This indicates that large particles contributed significantly to organic matter content in the sinking particles. However, the C/N ratio (w/w) of sinking particles in spring was 7.2 to 8.4 (Fig. 6), which was higher than that in autumn. This result suggests that the sinking particles had a strong influence due to the large amount of resuspended surface sediment that had already decomposed.

(2) Decomposition rate of sinking particles

In autumn, the decomposition rate of sinking particles sampled for 1.15 to 1.97 d was measured. The results by the O_2 method were 0.026 and 0.022 d^{-1} at 5m and 15m, respectively (Fig. 9).

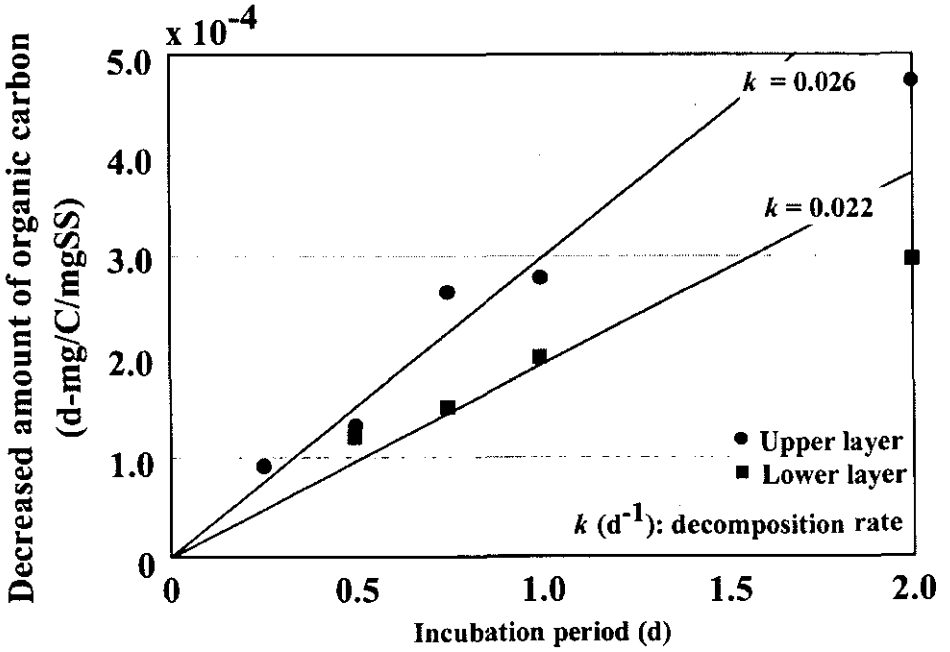

Fig. 9 Decreased amount of organic carbon in the sinking particles measured by the O_2 method in autumn 1997.

Decomposition rate was higher in the upper layer than the lower layer due to the high ratio of organic matter in the upper layer.

In spring, the decomposition rate in sinking particles sampled over 10 h in the upper layer was measured by two methods. The direct method results were 0.223 and 0.035 d^{-1} at 8m in Exp. I and at 5m in Exp. III, respectively. The O_2-method results were 0.053 and 0.024 d^{-1} at 8m in Exp. I and at 5m in Exp. III, respectively (Fig. 10), being directly proportional to the level of organic carbon in the sinking particles. The decomposition rate of the particles measured by the direct method tended to be higher than that by the O_2 method, particularly at higher organic carbon levels in the sinking particles (Fig. 11). However, only when the organic carbon content of sinking particles was more than 5%, the decomposition rate reached more than $0.1 d^{-1}$ [3]. It was considered that the decomposition rate was overestimated by the direct method due to elution of organic carbon from sinking particles during filtration.

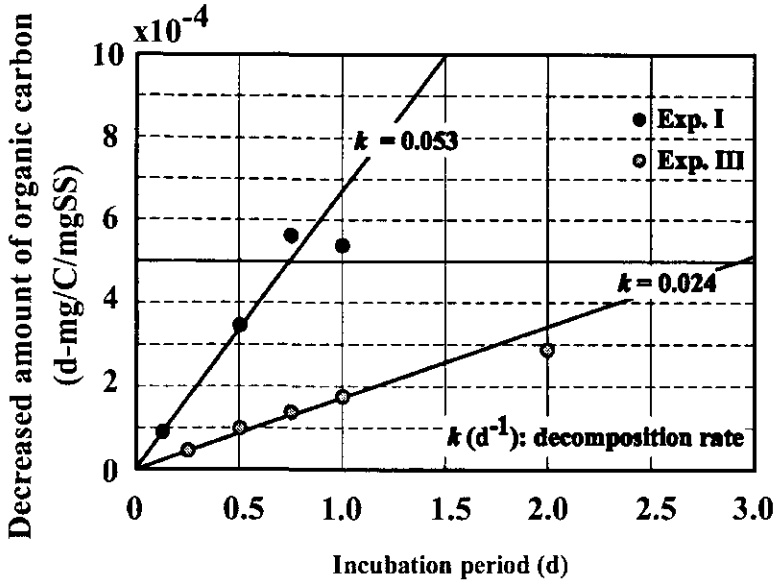

Fig. 10 Decreased amount of organic carbon in the sinking particles measured by the O_2 method during Exps. I and III in spring 1998.

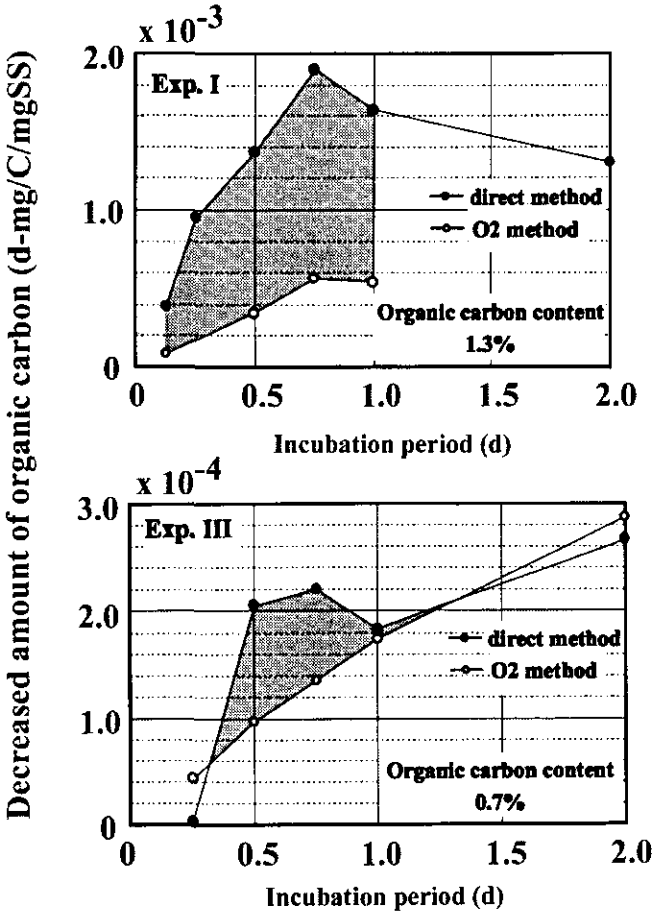

Fig. 11 Decreased amount of organic carbon in the sinking particles measured by the O_2 method and the direct method during Exps. I and III in spring 1998.

Although the organic carbon content of sinking particles in autumn was higher than that in spring, the decomposition rate in autumn was lower than that in spring. It was considered that most of the sinking particles had already decomposed during the 2-d sampling in autumn. Collection of fresh sinking particles during short-term sampling is necessary to determine accurately the decomposition rate.

The decomposition rate of the sinking particles at the experiment site had a low value due to the influence of a large amount of lithogenic particles. For example, in spring, 10% of the organic carbon in the sinking particles decreases for 2 days at a rate of 0.053 d^{-1} and for 4 days at a rate of 0.0024 d^{-1}. At the experiment site, the resuspension of surface sediments from the sea bottom frequently happens due to the strong tidal currents and/or the passage of atmospheric depressions. It is possible that the low decomposition rate of sinking particles and frequent resuspension events supply organic matter to the water column constantly. When these particles containing organic matter are transported offshore, it can be considered that the estuary plays an important role as a source of not only nutrients but also organic matter. To clarify the particulate transport mechanism, a survey from the estuary to the offshore area should be carried out in future.

4. CONCLUSIONS

Experiments using sediment traps were conducted to measure the flux and decomposition rate of the sinking particles in the Changjiang Estuary in autumn 1997 and spring 1998. There was a close relationship between the water column conditions and the level of particulate flux. When the water column was stratified, there was a large difference between the upper (5m depth, in water depth of about 20m) and lower (15m depth) layers in size, type and quantity of particles. When the water column was well mixed, there was little such difference, due to the resuspension of sediments from the seabed. The chemical composition of the sinking particles suggests that biological production was mainly by diatoms in autumn and by other phytoplankton, such as dinoflagellates, in spring. The higher C/N ratio of sinking particles in autumn than in spring suggests high biological productivity in autumn and high frequent resuspension events in spring in spite of the high biological productivity. Our study demonstrates that the decomposition rate of sinking particles measured by the O_2 method should be more accurate than by the direct method and it is better to measure the decomposition rate of fresh sinking particles by short-term sampling than by long-term sampling. The decomposition rate of sinking particles was low due to the influence of a large amount of lithogenic particles.

REFERENCE

1) Lin Z., J. Zheng, J. Chen and R. Huan: Flocculation of Fe, Al, Mn, Cu, Pb and Zn in dissolution with mixing processes in the estuaries. *Acta Oceanological Sinica*, 7, 36-44, 1985.
2) Abaron A., J. Aboine and J. P. Dupont: Role of suspended matter on the distribution of PCB in the Seine estuary (France). *Cont. Shelf Res.*,7, 1345-1350, 1987.
3) Iseki K., F. Whitney and C. S. Wong: Biochemical changes of sedimented matter in sediment trap in shallow coastal waters. *Bull. Plank. Soc.* Japan, 27, 27-36, 1980.
4) Cloern J. E.: Turbidity as a control on phytoplankton biomass and productivity in estuaries. *Cont. Shelf Res.*, 7, 1367-1381, 1987.
5) Brzezinski M. A.: The Si:C:N ratio of marine diatoms: interspecific variability and the effect of some environmental variables. *J. Phycol.*, 21, 347-357, 1985.

GEOCHEMICAL CHARACTERISTICS OF THE ELEMENTS IN THE SEDIMENT OF THE YANGTZE ESTUARY

Aiguo GAO, Deling CAI, and Sulan GAO

First Institute of Oceanography, State Oceanic Administration
(3A, Hongdaozhilu, Qingdao, 266003, China)

The contents of Fe, Al, Ca, Zn, Co, Ni, Cr, Sr, Ba, V, Sc, Hg, As, and Cd in 71 samples in the surface sediments in the Yangtze Estuary were determined. The horizontal and vertical distributions of these compositions were described. The major and minor elements in a cluster diagram constructed from the correlation coefficient between all pairs of elements have been achieved. It can be divided into two groups at 0.232 level. The group 1 contains Al, V, Ni, Sc, Cr, Zn, Ca, Hg, Fe, Co, Ba, Pb, it may be controlled by the aluminosilicates. The group 2 contains Cd, Sr, As. R-mode factor analysis on the geochemistry of the sediments shows that five factors could account for 85.4% of the total variance in the data.

Keywords: *geochemical characteristics, sediment, the Yangtze estuary*

1.INTRODUCTION

The Yangtze (Changjiang) River is the largest river in China and the fourth largest river in the world in terms of runoff. It passes through a densely populated area, and its coastal zone is one of most economically developed and densely populated areas of China. In spite of that a large amount of pollutants discharged into the river, the content of metals in water and sediments of the Yangtze Estuary are close to the natural background. Scientists have noticed its powerful self-purification capacity. In order to evaluate the environment capacity of the Yangtze Estuary, two cruises were carried out during October,1997 and May, 1998, and the geochemistry of elements in the sediment have been studied.

2. MATERIAL AND METHODS

45 surface sediments were collected from 7 stations (Al, A3, A5, B1, B5, C1, and C3) during October 1997, and other 26 surface sediments were sampled from 4 stations (A4, B2, C2, C4) in May, 1998 (Tab 1.). The samples were collected using the multi-tube sampler from vessel "Haijian 47". Subsamples were taken in 2cm interval on board, placed in plastic bags and stored frozen.

Tab.1 Locations of the Stations

Station	Latitude	longitude	Sampling Date
A1	31 ° 59. 786′	122 ° 30. 098′	October,1997
A3	31 ° 59. 775′	123 ° 15. 008′	October,1997
A4	31 ° 59. 771′	123 ° 37. 598′	May,1998
A5	32 ° 00. 179′	123 ° 59. 918′	October,1997
B1	31 ° 45. 137′	122 ° 30. 131′	October,1997
B2	31 ° 39. 964′	122 ° 52. 312′	May,1998
B5	31 ° 30. 040′	124 ° 00. 244′	October,1997
C1	31 ° 29. 600′	122 ° 30. 000′	October,1997
C2	31 ° 20. 951′	122 ° 51. 418′	May,1998
C3	31 ° 10. 080′	123 ° 15. 149′	October,1997
C4	31 ° 01. 086′	123 ° 37. 421′	May,1998

In the laboratory samples were dried in a vacuum desiccator. Representative portions of 42 samples were used for the determination of gravel, sand, silt and mud ratios using wet sieving technique and laser grain size analyzer. A second portion of each sample was finely powdered using an agate mortar, and passed 160-mesh sieve.

Analyses of Fe, Al, Ca, Zn, Cr, Co, Ni, Sr, Ba, Sc, and V were carried out using inductively coupled plasma atomic emission spectrophotometry (ICP/AES), while the measurement of Cd was carried out using an graphite furnace atomic absorption spectrophotometry (GFAAS) after the complete dissolution of the powdered sediment in a mixture of HCl, HNO_3, $HClO_4$, and HF acids. For the analyses of As and Hg, powdered samples were digested with aqua regia, and were analyzed using Atomic Fluorescence Spectrophotometry (AFS).

3. RESULTS AND DISCUSSION

(1) Contents

Data obtained in this study are grouped, together with some of the previous studies, in Table 2. It can be seen that the contents of elements show a wide range of variations; however, the overall average contents are in agreement closely with the Yangtze River sediments for most of the elements, while the contents of elements Ca and Sr are close to Yellow River sediment.

Tab. 2 The Content of major and trace elements

No	Fe	Al	Ca	Zn**	Co	Ni	Cr	Sr	Ba	V	Sc	Hg	As	Cd
1	3.72	5.98	3.26	79	17	33	60	224	530	98	14	0.03	6.93	0.15
2	5.51	7.39	4.74	130	23	56	82	283	726	150	18	0.06	19	0.25
3	2.62	4.91	1.91	55	12	15	35	187	439	76	10	0.01	4.2	0.12
4*	3.15	5.82	2.22	66	13	28	70	200	510	80	11	0.03	8.5	0.1
5*	2.2	4.87	3.29	40	9	20	60	220	540	60	8.8	0.015	7.5	0.077
6*	3.85	6.51	2.86	78	17	33	82	150	512	97	13	0.08	9.6	0.25
7*	2.6	3.92	4.93	50	10	19	48	330	375	55	7	0.017	7	0.06
8*	3.08	5.72	3.86	68	12	26	67	227	425	76	9	0.021	6.5	0.068
9*	4.4	8.15	2.57	99	16	38	85	153	430	103	15	0.045	10.7	0.087
10*	3.15	5.31	4.15	66	12	25	61	269	396	71	10	0.025	8	0.068

Note: the unit of Fe, Al, Ca was in wt%, others in $\times 10^{-6}$; *:Zhao Yiyang and Yan Mingcai(1994); **Zn was adjusted according to the result of standard material analyses; 1.Average in this study; 2. Maximum in this study; 3. Minimum in this study; 4. Sediment in China continent; 5. Sediment in Yellow River; 6. Sediment in Yangtze River; 7. Sands in sediment of the East China Sea ; 8. Silts in sediment of the East China Sea; 9. Clays in sediment of the East China Sea; 10. Sediment in East China Sea

(2) Comparing with other sediments

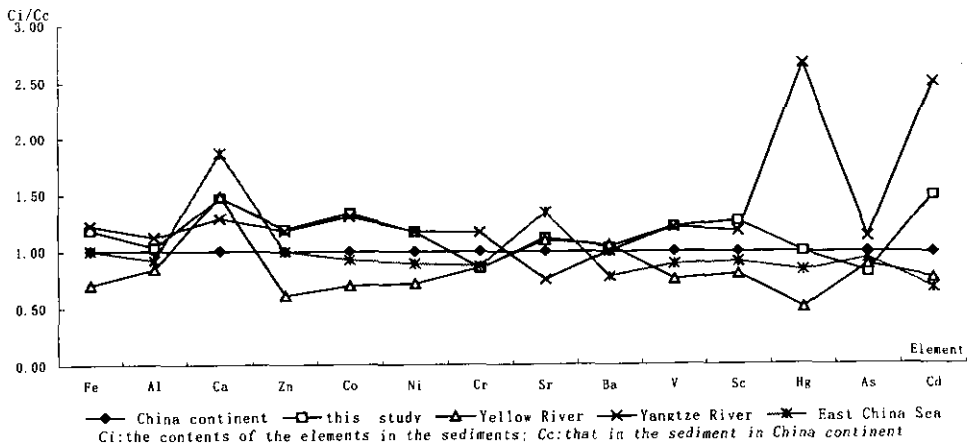

Fig. 1 Contents of elements normalized by China continental sediment

To compare the contents of the elements among different sediments, the contents of the elements in the sediments in this study, Yangtze Rive, Yellow River, and the East China Sea are normalized by that in the

sediment in China Continent. (Fig1). Fig.1 shows that most elements have a content close to the Yangtze River.

1. Contents of Fe, Al, Zn, V, and Sc in this study area are close to that in the Yangtze River, the average contents of Co and Ni are equal to that in the Yangtze River, and both of them are higher than that in the East China Sea.
2. The contents of Ba in the study area, Yangtze Rive, Yellow River, and China continental sediment are at the same level and higher than that in the East China Sea
3. Calcium, Cr, Sr and As are close to that in the Yellow River, lower than the East China Sea and higher than the Yangtze River.
4. Mercury content is close to that in continental sediment, and is lower than Yangtze River, higher than Yellow River, and the East China Sea.
5. Cadmium is higher than that in the Yellow River and East China Sea, lower than the Yangtze River.

It shows, from Tab.2, that the contents of Fe, Al, Ca, Cr, Sr, Zn, and As are close to that in silts in East China Sea. Co, Ni, V, and Sc are close to that in clays in sediment of the East China Sea. In general, the contents of element in this study area are basically background value, it means that in the study area sediment was unpolluted.

(3) Horizontal distribution of Elements

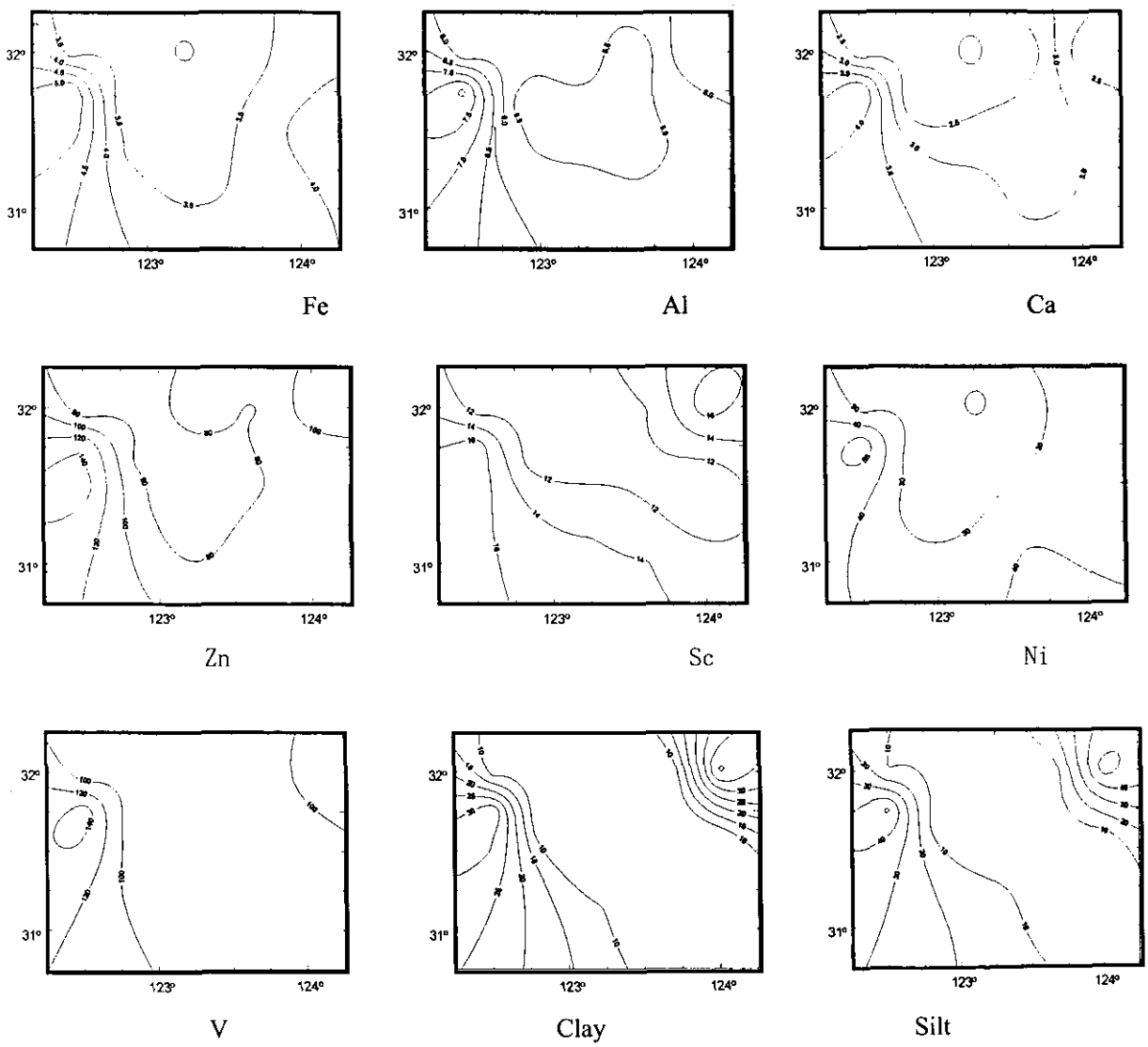

Fig2-1. Distribution of Fe, Al, Ca, Zn, Sc, Ni, V, Clay and Silt

There are four elements distribution patterns in this area. Iron, Al, Ca, Zn, Ni, Cr, Sc, Cd and V have a similar distribution to clay and silt (Fig2.--1); these may be controlled by grain size. Mercury and Co have higher value in the west part of the area, and decrease seaward; they may be affected by the Yangtze River dilute water (Fig2.-- 2). The distribution of Ba is similar to that of sand, comparing its content with soil or continental sediment in China (Tab.2, Fig2.--3), it may be controlled by continental material. From B5 to A1 the distributions of As and Sr show a tendency of decrease (Fig2.--4).

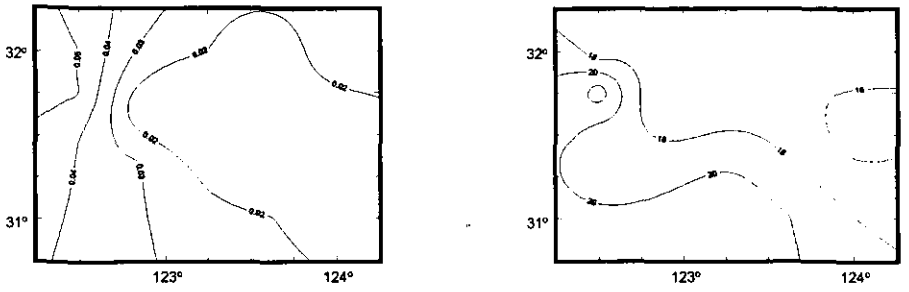

Fig2-2. Distribution of Hg and Co

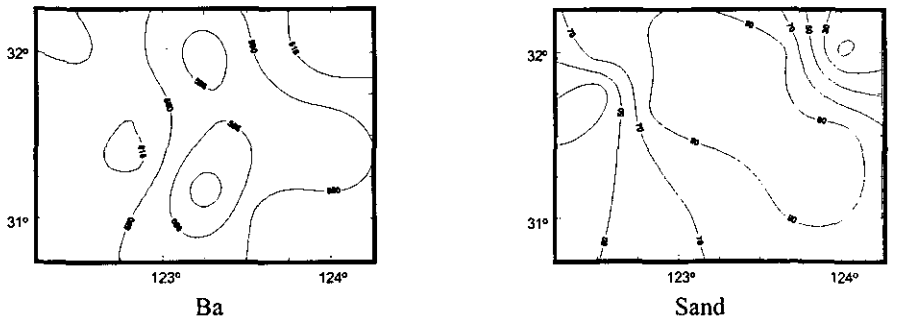

Fig2-3. Distribution of Ba and Sand

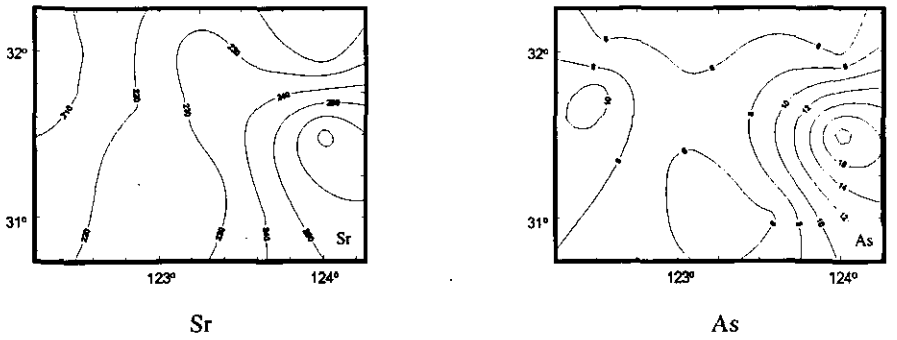

Fig2-4. Distribution of Sr and As

(4) Vertical distribution of elements

Fig.3 are vertical distributions of elements and clay of sediment in station A1, C1, and C4. The vertical distributions of most elements are stable. Some elements increase with depth from bottom to surface. It may be influenced by the fine sediment, Fe-hydroxide, or Al-hydroxide, such as station C1. In the surface of station A1 and C4, the sediment is dominated by coarse sand, so the contents of element decrease. It should be pointed out that:

1.Mercury in station Al increase from bottom to surface. In spite of its content is lower than 0.06×10^{-6}, attention should be paid to the fact, since the sediments in Yangtze River had a high background value, the environmental capacity is small. There is potential possibility for environmental pollution.

2.Zinc is high in the surface of station C1. This may relate to the increase of the amount of fine sediment and organism. According to the result of Zheng Guoxing (1983) ,in the adjacent area of C1 ,the amount of bacteria was very high. Zinc is influenced by the factors of biogeochemistry (Wang et al., 1990). The Distribution of elements is controlled by organism. It may result in enhanced contents of Zn.

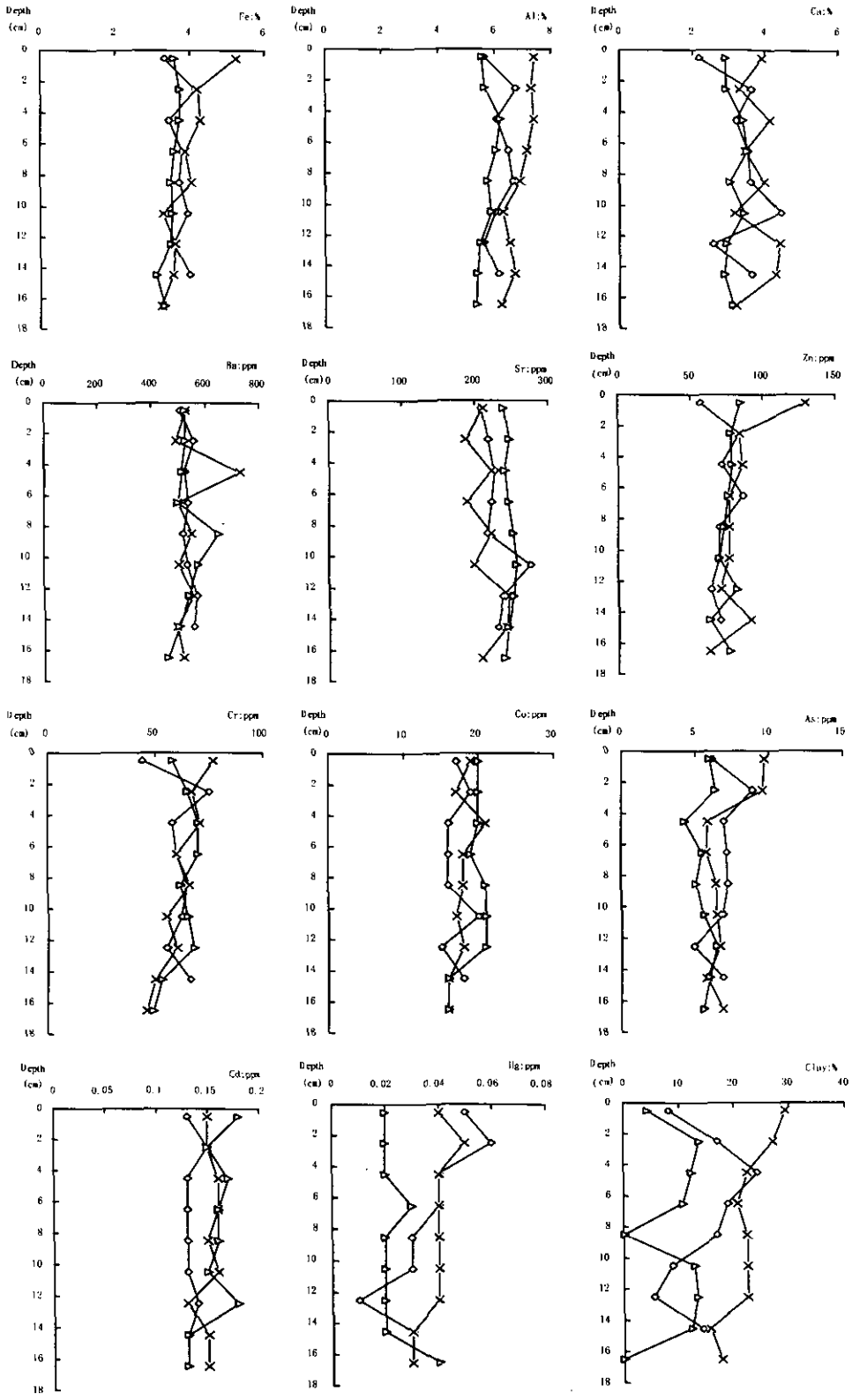

Fig.3 Vertical distribution of elements and clay

3.The vertical distribution of most elements in station Cl are very typical. It may reflect the seasonal variation of sedimentation.

(5) Factor analysis

Correlation analysis shows that positive correlation exists between most element pairs, i.e. Fe, Al, Ca, Zn, Co, Ni, Cr; Ba, V, Sc, Hg and As; but Sr is negatively correlated to Al.(Tab.3)

R-mode factor analyses on the geochemistry of the sediments show that five factors could account for 85.42% of the total variance in the data (Tab.4). Factor 1 is related to Fe, Al, Ca, Zn, Co, Ni, Cr, V, Sc, and Hg; it may be controlled by the aluminosilicates. Factor 2 is related to Sr and Ba; they are related to orthoclase, anorthite, mica, and heavy mineral. It may be heavy mineral factor. Factor 3 is positively related to As, negatively related to Co. In the study area, the contents of As increase, but that of Co decreases rapidly seawards. Cobalt comes from Yangtze River water; it is more stable and not influenced by biological, chemical or physics action. Cobalt is stable in biogeochemical cycle (Wang Zhengfang, 1990). Arsenic is effected by the diatoms, which play an important role in biogeochemical cycle of As (Gao Shengquan,1990). So factor 3 may be affected by marine organism. Factor 4 was related to Cd. The main transfer species of Cd is in carbonate-combined state and Fe-Mn oxide combined state (Zhou Jiayi, 1990). Cadmium was highly complexed by chlorine ions in seawater, and complexed to some extend by organic matter, too. (Mouchel et al.,1990). It was related to marine autogenetic material. Factor 5 was related positively to Ba (Tab.5), it may be related to feldspar and mica.

Tab.3 Correlation coefficients matrix for the elements of surficial sediments of the Yangtze estuary

Elements	Fe	Al	Ca	Zn	Co	Ni	Cr	Sr	Ba	V	Sc	Hg	As
Al	0.853												
Ca	0.688	0.701											
Zn	0.815	0.734	0.515										
Co	0.480	0.348	0.359	0.388									
Ni	0.792	0.790	0.637	0.678	0.557								
Cr	0.757	0.735	0.587	0.692	0.621	0.694							
Sr	-0.042	-0.385	0.179	-0.136	0.219	-0.168	-0.119						
Ba	0.320	0.216	0.134	0.221	0.524	0.274	0.304	0.213					
V	0.943	0.910	0.706	0.782	0.472	0.793	0.785	-0.176	0.314				
Sc	0.717	0.807	0.699	0.640	0.370	0.670	0.679	-0.260	0.131	0.764			
Hg	0.481	0.650	0.492	0.439	0.235	0.535	0.528	-0.401	0.051	0.549	0.529		
As	0.390	0.087	0.224	0.211	-0.110	0.158	-0.066	0.349	0.051	0.202	0.016	-0.046	
Cd	0.131	0.118	0.053	0.292	0.174	0.170	0.221	-0.062	0.098	0.123	0.137	0.011	-0.097

n=71 $\alpha_{0.05}$=0.232 $\alpha_{0.01}$=0.302

Tab.4 Percentage of eigenvalue

N0	Eigenvalue	Proportion value	Accumulative total
1	7.0317	0.5023	0.5023
2	1.7890	0.1278	0.6301
3	1.4061	0.1004	0.7305
4	0.9859	0.0704	0.8009
5	0.7462	0.0533	0.8542
6	0.4943	0.0353	0.8895
7	0.4461	0.0319	0.9214
8	0.3396	0.0243	0.9456
9	0.2312	0.0165	0.9621
10	0.2191	0.0157	0.9778
11	0.1470	0.0105	0.9883
12	0.0917	0.0066	0.9949
13	0.0458	0.0033	0.9981
14	0.0262	0.0019	1.0000

Tab.5 Factor load matrix of each element

Element Factor	1	2	3	4	5
Fe	0.9299	0.1638	0.1873	0.0792	0.1262
Al	0.9260	-0.2321	0.1020	-0.0247	0.0847
Ca	0.7641	0.1565	0.2583	-0.1087	-0.4396
Zn	0.8267	0.0186	0.0415	0.2914	0.1186
Co	0.5715	0.4056	-0.5361	-0.2225	-0.1010
Ni	0.8729	0.0178	-0.0121	-0.0092	0.0342
Cr	0.8579	-0.0002	-0.2418	-0.0490	-0.1068
Sr	-0.1698	0.8832	0.0899	-0.0437	-0.3651
Ba	0.3339	0.5259	-0.4464	-0.1986	0.4827
V	0.9489	0.0098	0.0925	-0.0030	0.0957
Sc	0.8356	-0.1932	0.0543	-0.0259	-0.1784
Hg	0.6442	-0.4177	0.0594	-0.2346	-0.0237
As	0.1526	0.5001	0.7173	0.2483	0.2580
Cd	0.2019	-0.0010	-0.4574	0.8194	-0.1363

(6) Hierarchical cluster

The major and minor elements in a cluster diagram constructed from the correlation coefficient between all pairs of elements have been achieved. It can be divided into two groups at 0.232 level. Group 1 contains Fe, V, Al, Ni, Zn, Cr, Sc, Ca, Hg, Co, and Ba; it may be controlled by the aluminosilicates. Group 2 includes Cd, Sr and As. (Fig.4)

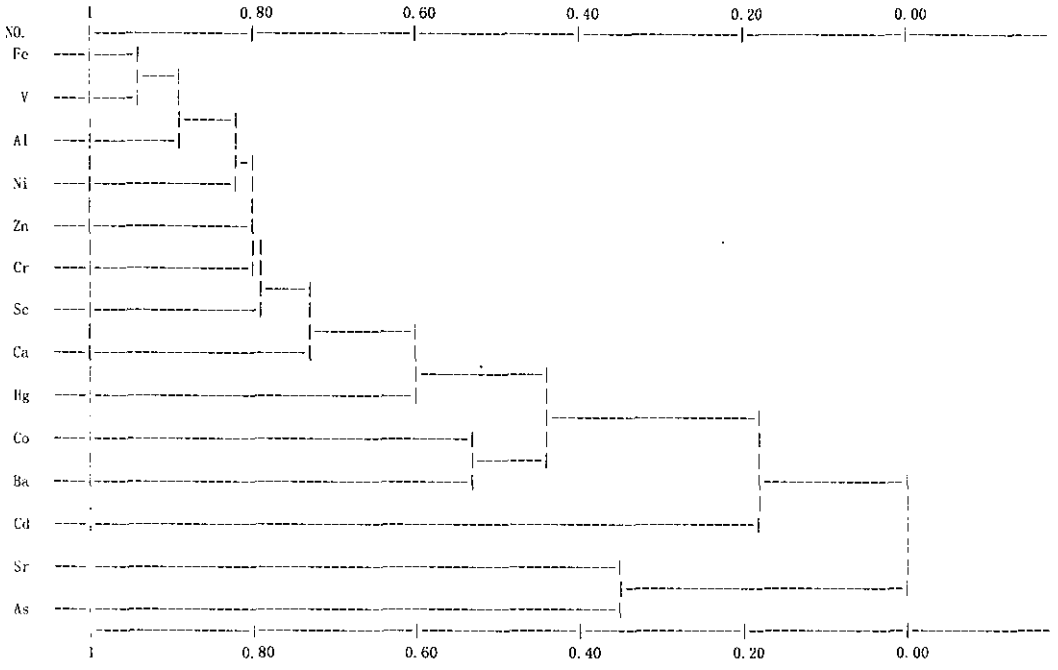

Fig.4 Hierarchical clustering diagram of R—model

(7) Discussion

It is known that the geochemistry of element in sediment is controlled by material sources, amounts of material, grain size and sedimentary environment.

In the study area, from the contents and distribution of the elements in the sediment, the material are mainly terrigenous, with most of them come from the Yangtze River, some from the ancient Yellow River or the Yellow Sea, and some representing relict sediment. There is some marine organisms and /or authigenic material too.

Tidal currents, waves and currents are the major agents to affect the distribution of the sediment. In study area, the hydrodynamic conditions are complicated. There were Yangtze River diluted water, Taiwan warm current, Subei longshore current, eddy diffusion or upwelling, etc. The seasonal variations in the strength and the route of the above-mentioned dynamic regime directly influence the sedimentation. They affect the primary productivity of marine organism as well.

Tab.6 Correlation Coefficient between elements and grain size

Element	Fe	Al	Ca	Co	Ni	Cr	Sr	Ba	V	Sc	Hg	As	Cd
Md Φ	0.6466	0.7818	0.6399	0.11	0.6751	0.5771	-0.564	0.0303	0.7306	0.6702	0.6202	0.1361	0.1955
sand	-0.64	-0.82	-0.705	-0.132	-0.67	-0.631	0.535	0.0783	-0.711	-0.74	-0.659	-0.06	-0.21
silt	0.6091	0.7936	0.7234	0.104	0.6435	0.5993	-0.501	-0.089	0.6819	0.7074	0.6338	0.0555	0.1692
clay	0.6672	0.8326	0.6524	0.1732	0.6887	0.6591	-0.57	-0.056	0.7327	0.7645	0.677	0.0654	0.2659

n=42 $\alpha_{0.05}$=0.304 $\alpha_{0.01}$=0.393

The sediment coverage of the Yangtze Estuary was the result of the interplay of riverine and marine influx of sedimentary material. The influence of each of these sources was more or less localized resulting in a

particular textural and compositional distribution. According to the result of grain size analysis, sandy size sediments were more abundant in the middle part of the survey area. In the 1~2cm layer, Sandy samples occupy 72.7% of 11 station, and stations B1. C1 and A5 were dominated by clayey silt. A close correlation appears between grain size and the contents of Fe, Al, Ca, Zn, Ni, Cr, V, Sc and Hg. These elements were positively correlated to the content of clay or silt size sediments and negatively correlated to the contents of sand size sediments. Contrary to these elements, Sr was positively correlated to grain size (Tab. 6).

4.CONCLUSION

Most elements, in the study area, have a content close to the Yangtze river, and a similar distribution to clay or silt. They are correlated to the contents of clay or silt; and negatively correlated to the contents of sand. It may be influenced by the fine sediment, Fe-hydroxide, or Al-hydroxide. Material sources are mainly terrigenous, with most of them coming from Yangtze River, some from the ancient Yellow River or the Yellow Sea. Their distribution is controlled by the terrigenous material provided by the Yangtze River and the grain size, which was affected by the hydrodynamic condition. Anthropogenic heavy metals have a little effect on this area, and it had a large environment capacity.

REFERENCES

1)Gao Shengquan, Geochemical characteristic of Arsenic in sediments of the Changjiang Estuary and its adjacent areas, *Proceedings of the International Symposium on Biogeochemical Study of the Changjiang Estuary and Its Adjacent Coastal Waters of the East China Sea.* China Ocean Press,496-507,1990.

2)Mouchel, J.M., Adsorption behavior of several trace metal in the Changjiang Plume, *Proceedings of the International Symposium on Biogeochemical Study of the Changjiang Estuary and Its Adjacent Coastal Waters of the East China Sea.* China Ocean Press,263-279,1990.

3)Wang Zhengfang et al., Biogeochemical Behaviors of dissolved trace metal in the Changjiang Estuary and its adjacent sea area, *Proceedings of the International Symposium on Biogeochemical Study of the Changjiang Estuary and Its Adjacent Coastal Waters of the East China Sea.* China Ocean Press,280-292,1990.

4)Zhao Yiyang and Yan Mingcai, *Geochemistry of sediments of the china shelf sea,* Science Press. 1-203,1994.

5)Zhou Jiayi et al., Role of suspended particulate matter in transfer of trace metals in the Changjiang Estuarine Area, *Proceedings of the International Symposium on Biogeochemical Study of the Changjiang Estuary and Its Adjacent Coastal Waters of the East China Sea.* China Ocean Press, 203-219, 1990.

6)Zheng Guoxing et al., Relationship between Heterotrophic bacteria and sediments in the Changjiang delta and its adjacent sea regions. Sedimentation on the continental shelf, with special reference to the East China sea. China Ocean Press. 858-867,1983.

IMPORTANCE OF THE SEDIMENT INTERFACE IN THE NUTRIENT STATUS OF THE EAST CHINA SEA AT THE MOUTH OF THE CHANGJIANG RIVER

Mary-Hélène NOËL and Masataka WATANABE

Water and Soil Environment Division, National Institute for Environmental Studies, Environment Agency
(Onogawa 16-2, Tsukuba, Ibaraki 305-0053, Japan)

Modifications in the Changjiang River supply are expected in the future when the Three Gorges Dam is completed, together with land-use and industrial development in the catchment area. Resuspension experiment, vertical profile of nutrients in the sediment, and interstitial water content argued for a phosphorus release from the sediment to the water column. Concentration measured in the interstitial water of the sediment are potentially able to induce phytoplankton growth or even a bloom formation.

The Changjiang River supply influenced mainly the area including the stations B1, C1 and C3 in autumn 1997 while in spring 1998 the influenced area also included the mesocosm site and the station A1.

Key Words : *nutrient status, ecosystem response, phosphorus release*

1. INTRODUCTION

Coastal ecosystems are controlled by complex and dynamic equilibria between physical and biogeochemical factors. They are altered by nutrient imbalance, which affects algal growth, the microbial community, fish resources and aquaculture production. The consequences on the ecosystem and resource quality include red tides and associated shellfish poisoning, changes in environmental capacity to biodegrade pollutants, and human health.

In the East China Sea ecosystem, most nutrients are supplied by the Changjiang River, although marine currents greatly influence the region. The Changjiang flow shows a high seasonal variability with low inter-annual variation. The construction of the Three Gorges Dam may lead to a drastic change in the river flow in the near future. It is essential to determine the present state of the marine ecosystem in order to forecast the response of the East China Sea ecosystem to changes.

In marine ecosystems, the phosphorus (P) cycle includes benthic processes in addition to those in the water column. The aim of this study was to investigate the importance of the processes and exchanges at the sediment–water interface for the nutrient status of the East China Sea ecosystem. Special focus was given to P because of its role in the control of eutrophication and red tides in coastal waters of the East China Sea Wu *et al.*, 1992[1]. The second reason is that the behavior of P is closely linked with that of exchangeable pollutants like Fe, Cu, Zn, Mn, Pb and As. Using knowledge of such exchanges, the flux and fate of P can help us estimate exchanges in those pollutants.

Storms resuspend sediment particles, particularly in winter Xie and Li, 1990[2] in this shallow area (lat 31° to 32°N, long 122° to 124°E), which has depths of 20 to 60 m. Hydrodynamic conditions, oxygenation, composition of the water column and biological activity affect the equilibria at the sediment–water interface. The role of sediment as a sink or source of nutrients and pollutants varies with these conditions. Therefore, to study the sediment–water interface, it is necessary to investigate the conditions in the water masses above the sediment as well as the hydrodynamic and biological features.

2. MATERIALS AND METHODS

The water column was sampled with Go-Flo bottles and the samples were immediately filtered (Nucleopore 0.4-μm pore size; 47 mm) and frozen until analyzed in the laboratory.

The sediment was investigated in two ways. For bulk sediment at stations A1, A3, B1, C1 and C3 and the mesocosm area, gravity cores were sliced directly after sampling and frozen. For interstitial water in the sediment at stations B1, C1 and C3 and the mesocosm area, a specially designed system was used (Fig. 1). By compressing the core without contact with air, interstitial water was filtered through a Millipore Millex FG PTFE 0.2-μm filter, and samples were frozen. The compressed sediment was then sliced and frozen.

Gravity core sampler

Special tube designed for interstitial water sampling without contact with air

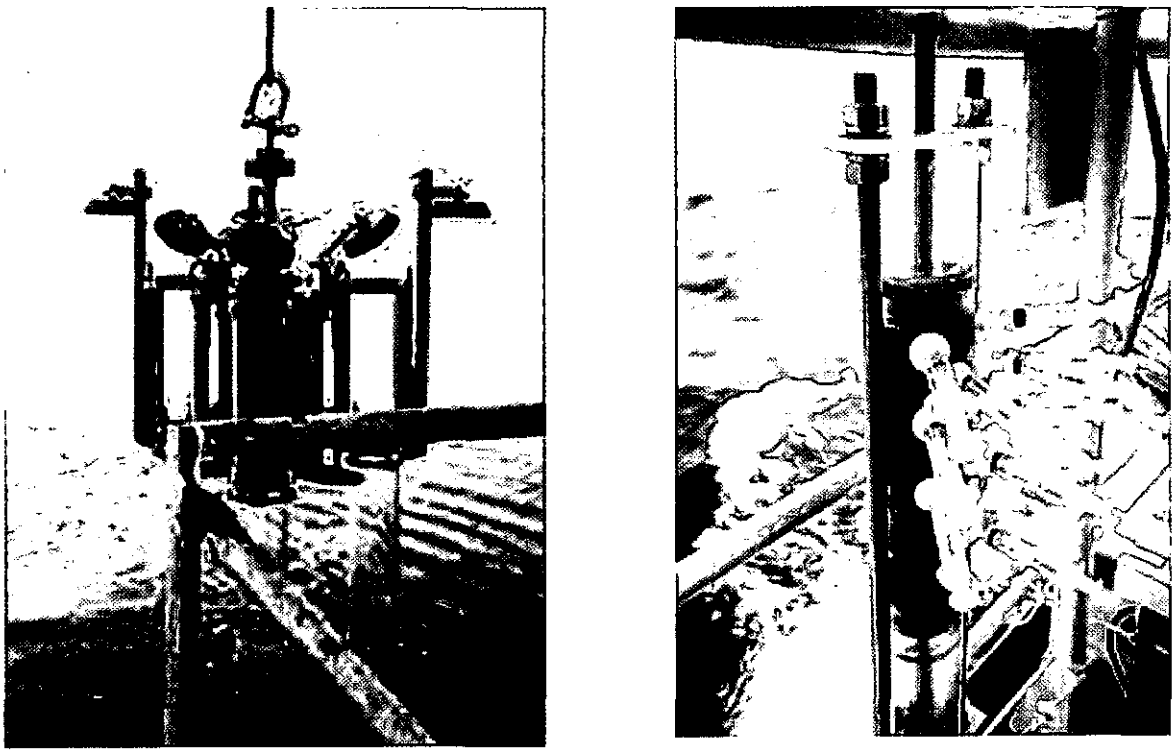

Fig. 1 Gravity core sampler and interstitial water sampling system

In addition to sampling, on–board experiments to simulate sediment–water resuspension were run (Table 1). The first 2 cm of the sediment were homogenized. A few grams were placed in a dark bottle (to avoid light effects) in contact with samples of water from different depths and stirred with a Teflon bar magnet. The aim was to simulate the impact of the water on the bottom on windy days and to simulate new conditions of concentration and physico-chemical properties that might occur in the future at the sediment–water interface in addition to simple resuspension with the existing water above the sediment. For steady equilibration of concentration between the water and the sediment, the suspension was incubated at the in-situ temperature for at least 15 h Andrieux-Loyer, 1997[3]. Three sediment were investigated one in autumn 1997 and the other two in spring 1998 (Table 1). The investigation was done in such a way as to separate the total processes occurring during physical resuspension and, by lysing the cells with ultrasound, those processes that do not require complete biological activity.

Table 1 Characteristics of the bottom resuspension simulations

	Sediment characteristics		Inorganic P	Dissolved inorganic P		Experimental conditions
	Element	%	$\mu mol \cdot g^{-1}$	Sample	$\mu mol \cdot L^{-1}$	
Mesocosm area October 1997 (muddy)	Al Ca Fe	8.2 1.9 4	13.3	Surface water Above sediment (20 m)	0.78 0.78	20 g of wet sediment 250 ml of water sample total incubation 18 h one set with ultrasound
Mesocosm area May 1998 (mixed)	Al Ca Fe	6.4 2.9 7	15.5	Surface water Control mesocosm Enriched mesocosm Above the sediment (28 m) + surface water at 50%	0.09 0.03 1.28 0.11	5.5 g of wet sediment 200 ml of water samples total incubation 38 h
Station A1 May 1998 (sandy)	Al Ca Fe	5.5 2.4 5.5	14.5	Surface water Bottom water (24 m) Above sediment (26 m)	0.25 0.18 0.15	6.5 g of wet sediment 200 ml of water samples total incubation 24 h one set with ultrasound

In the laboratory, analysis of dissolved inorganic N and P (DIP) was done using an auto-analyzer. Subsamples of sediment were dried (to determine water content and sediment density) and ground until homogeneous. Extraction of inorganic and organic P from the sediment was done according to Slomp *et al.*, 1993[4]. The sediment matrix composition was analyzed by flame atomic absorption spectrometry. To check the extractions and accuracy of analysis, a certified reference sediment (MESS-2 from the Beaufort Sea provided by National Research Council of Canada) was treated in the same way as the other samples. For the water samples, blank samples were also run on-board to check background levels and contamination.

3. RESULTS AND DISCUSSION

(1) P content of the surface sediment

The phosphorus content (Table 2) in the surface sediment was investigated with regard to the effective resuspension depth of sediment, i.e. the top 2 cm.

Table 2 Phosphorus and aluminum content in the top 2 cm of the sediments

	October 1997			May 1998		
	Al %	inorganic P $\mu mol \cdot g^{-1}$	organic P $\mu mol \cdot g^{-1}$	Al %	inorganic P $\mu mol \cdot g^{-1}$	organic P $\mu mol \cdot g^{-1}$
Station A1	6.9	12.4	2.1	5.4	14.8 (2 cores)	2.6 (2 cores)
Station A3	6.0	14.1	0	not sampled	not sampled	not sampled
Station B1	7.3	15.8	1.5	6.6	15.2	2.1
Station C1	7.6	15.0	1.3	6.5	13.1 (5 cores)	4.0 (5 cores)
Station C3	6.6	15.8	0.6	4.8	15.8 (2 cores)	2.0 (2 cores)
Mesocosm area	8.2	13.3	3.3	6.0	15.2 (7 cores)	2.2 (7 cores)

Inorganic P (IP) was the major component (70 to 99%) of the total sedimentary phosphorus stock. The concentration range was 12.4 to 15.8 $\mu mol \cdot g^{-1}$. Such concentrations are in the same order as eutrophic areas like the Long Island Sound (USA), the Seto Inland Sea (Japan) and Xiamen Bay (South China, Wu, Y. *et al.*, 1992[1]).

The organic P (OP) content varied from 0 to 4 $\mu mol \cdot g^{-1}$ and exhibited larger spatial variability in autumn than in spring. At the same location, the OP content of spring samples was up to 3 times higher than that of autumn samples. This feature was most likely due to fresh particulate organic matter settling on the bottom in spring. Seasonal variations can therefore be shown as different proportions of the different P forms stored in the sediment.

Since the concentration of P in the sediment is function of sediment type (e.g. sandy-muddy), normalization with aluminum content (Table 2) was calculated in order to eliminate the preferential adsorption effect. The inorganic P content at the surface of the sediment exhibited an homogenous distribution at the estuary mouth with a greater accumulation at the deepest station C3 (depth 58 m). The IP content normalized to aluminum at this station was 1.3 to 1.7 times higher than at all other stations measured. Moreover, IP concentration in interstitial water at station C3 was higher than at the other stations by a factor of 2 to 4 (Table 3). The bottom morphology may favor higher accumulation/sedimentation of river inputs at this location.

Table 3 Characteristics of the bottom resuspension simulations

	Autumn 1997 Dissolved inorganic P, $\mu mol \cdot L^{-1}$				Spring 1998 Dissolved inorganic P, $\mu mol \cdot L^{-1}$			
	Water column		Sediment intersititial water		Water column		Sediment intersititial water	
	Depth (m)	$\mu mol \cdot L^{-1}$	Depth (cm)	$\mu mol \cdot L^{-1}$	Depth (m)	$\mu mol \cdot L^{-1}$	Depth (cm)	$\mu mol \cdot L^{-1}$
Station B1	0	0.42	3-4	2.62				
	12	0.40	4-6	0.37				
	24	0.45	8-12	1.31				
Station C1	0	0.47	1-2	3.0	0	0.16	1-2	1.10
	12	0.65	2-3	2.6	25	0.18	6-8	2.40
	25	0.45	3-4	4.1	28*	0.10	8-10	2.10
	30*	1.1	4-6	2.5				
Station C3	0	0.05	0-1	3.9	0	0.29	0-0.5	2.73
	28	0.19	1-2	3.9	26	0.47	0.5-1	2.96
	55	0.25	2-3	4.0	52	0.36	1-2	3.94
	58*	0.50	3-4	5.3	55*	0.35	3-4	4.74
			4-6	7.1			4-6	10.87
			8-12	7.8			6-8	8.73
			14-18	12.6				
			18-22	8.2				
			20-24	7.2				
Mesocosm area					0	0.03	0-0.5	0.51
					28*	0.43	0.5-1	0.53
							1-2	0.15
							2-3	0.16
							3-4	0.54
							4-6	0.23
							6-8	0.20
							8-10	0.68
							10-12	0.11
							12-14	0.70
							14-16	1.39
							16-19	1.27

* water sample just above the sediment (overlying water)

The seasonal feature in P content of the sediment was observed even after normalization to aluminum content. Also, the IP content of spring samples revealed that there was a wider area of accumulation in that season than in autumn. This would be connected with the seasonal variation of the Changjiang River flow: 70% of the annual runoff occurs during spring-summer.

(2) Potential of P release from the sediment to the water column

Because the IP content of interstitial water in the sediment at station C3 was much higher than in the water column (Fig. 2 and Table 3), the potential P that could be released from the sediment to the adjacent water was correspondingly high.

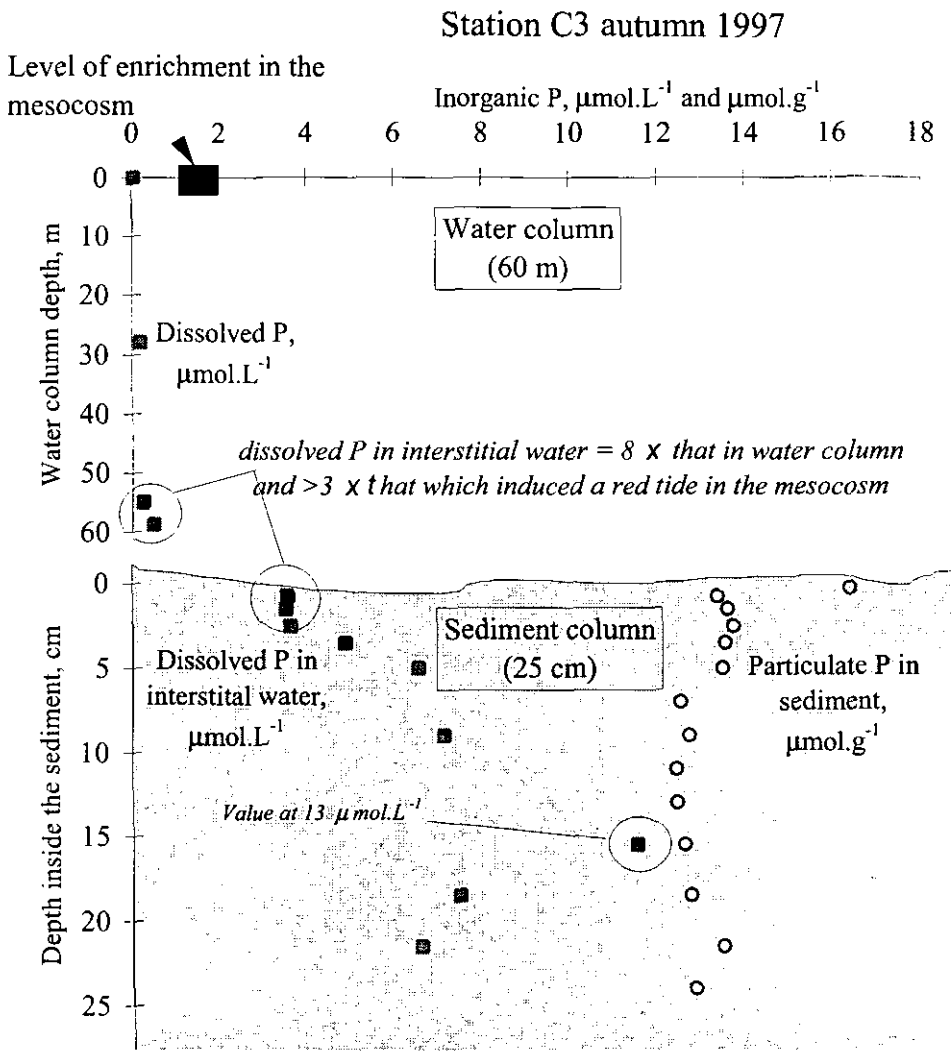

Fig. 2 Dissolved, interstitial and particulate inorganic P at Station C3 in autumn 1997

The sediment would apparently be more a sink than a source of P for phytoplankton growth. The concentration of IP dissolved in interstitial water of the sediment was higher than the IP concentration in the water column by a factor of 1.4 to 65 (according to the location and sediment layers). The maximum interstitial concentration found during the two surveys was 13 $\mu mol \cdot L^{-1}$ at station C3 in autumn (Fig. 2). An in-situ mesocosm experiment was also conducted in autumn and spring. Phytoplankton blooms in the mesocosm were successfully induced in the mesocosm after P enrichment of 1.5–2 and 3 $\mu mol \cdot L^{-1}$, respectively, in the three experiments done. In the sediment, the range of IP concentrations in the interstitial water was 1 to 13 $\mu mol \cdot L^{-1}$, high enough to induce phytoplankton growth.

Depending on local conditions (bottom resuspension, bioturbation, concentration in the water column, etc.) the sediment would be both a sink and a source of P. However, the flux of nutrients released to the water column would be high enough to induce a phytoplankton bloom.

(3) Simulation of the bottom resuspension effect on P release from the sediment

Experiments were conducted on-board to estimate the release of nutrients from the sediment to the water column when sediment was resuspended. Only physical resuspension was simulated, not deep bioturbation as made by worms and shellfish. In the field, exchanges might be enhanced or lowered when all such processes are taken into account.

Experiments were conducted immediately after core sampling. Three sediments were investigated and seasonal effects were incorporated by carrying out experiments in both autumn and spring (Table 1). The DIP content was measured in the initial water samples and in the water after the resuspension experiment (Table 4).

Table 4 Dissolved inorganic P content after the resuspension experiments

	Without ultrasound Dissolved inorganic P		**With ultrasound** Dissolved inorganic P	
	Sample	μmol·L^{-1}	Sample	μmol·L^{-1}
Mesocosm area October 1997	Surface water	1.35	Surface water	1.40
	Above sediment (20 m)	1.34	Above sediment (20 m)	1.24
Mesocosm area May 1998	Surface water	0.76		
	Control mesocosm	0.59		
	Enriched mesocosm	0.94		
	Above sediment (28 m) + surface water at 50%	0.57		
Station A1 May 1998	Surface water	0.34	Surface water	0.64
	Bottom water (24 m)	0.39	Bottom water (24 m)	0.27
	Above sediment (26 m)	0.56	Above sediment (26 m)	0.30

The DIP content after the resuspension simulation was compared with the initial content (Tables 1 and 4), from which the corresponding IP release from or fixation in the sediment was calculated (Table 5).

Table 5 Calculation of inorganic P exchanges after the resuspension experiments

	Without ultrasound Loss-gain in inorganic P			**With ultrasound** Loss-gain in inorganic P		
	Sample	μmol·L^{-1}	%	Sample	μmol·L^{-1}	%
Mesocosm area October 1997	Surface water	+0.57	73	Surface water	+0.62	79
	Above sediment (20 m)	+0.56	72	Above sediment (20 m)	+0.46	59.
Mesocosm area May 1998	Surface water	+0.66	>100			
	Control mesocosm	+0.56	>100			
	Enriched mesocosm	-0.34	-26			
	Above sediment (28 m) + surface water at 50%	+0.46	>100			
Station A1 May 1998	Surface water	+0.09	37	Surface water	+0.39	>100
	Bottom water (24 m)	+0.21	>100	Bottom water (24 m)	+0.09	50
	Above sediment (26 m)	+.041	>100	Above sediment (26 m)	+0.15	96

a) Discussion on the mesocosm-area sediment experiment in autumn

Resuspension simulation of a muddy sediment in autumn gave a similar DIP content from experiments with and without ultrasound treatment. In the case of this sediment in autumn, the release of P seems to be governed only by physical processes. The calculated percentage of IP removed from the sediment was small, less than 0.1%, but the increases in the water in contact with the sediment were 59 to 80% (Table 5). The IP was also measured in the interstitial water of the sediment after the resuspension experiment (Table 6).

Table 6 Interstitial water inorganic P of the mesocosm-area sediment after the resuspension experiments in autumn 1997

	Sample	Dissolved inorganic P		
		Water column $\mu mol \cdot L^{-1}$	Interstitial water $\mu mol \cdot L^{-1}$	
			With ultrasound	Without ultrasound
Mesocosm area October 1997	Surface water	0.78	1.11	1.19
	Above sediment (20 m)	0.78	1.16	1.13

The average ratio between the interstitial DIP of the sediment and the water column above the sediment (Table 6) for all results on the mesocosm-area sediment in autumn was 0.85. Because of the uniformity of this ratio in the bottle experiments, it should be useful as a predictive model of sediment–water interface exchanges. However, its extrapolation to other seasons and sediment types needs to be verified with complementary experiments. The present results on equilibration of the concentration at the sediment–water interface emphasize the quick and reversible response of the sediment to the water column changes. Therefore, the sediment should be considered as a buffer able to both store and release P according to environmental conditions.

b) Discussion on the mesocosm-area sediment experiment in spring

In this set of experiments, biological effects in the exchanges cannot be ditinguished since not test was done for cells lyse. The dissolved P in the seawater sampled from the enriched mesocosm was high at 1.28 $\mu mol \cdot L^{-1}$, while the initial condition above the sediment during sampling was 0.43 $\mu mol \cdot L^{-1}$. In all other cases of mixing for this sediment, the water in contact during the experiments had a lower initial concentration of DIP than did the initial water above the sediment in field conditions (Table 1). After the mixing experiments, the water increased in DIP except for the enriched mesocosm water, in which DIP decreased (Table 4). Loss and gain in inorganic P of the water in contact with the sediment seems to be gouverned by an equilibration of the concentrations initially present in the water and sediment. Results of equilibration of the concentrations in the water and the sediment showed that no steady ratio was reached in these experiments, unlike the case in autumn. Either physico–chemical reactions in the different sets of water samples or variability in biological activity could explain the varying exchanges obtained in the spring experiments.

c) Discussion on the Station A1 sediment experiment in spring

The DIP concentration in the water after stirring with the sediment from A1, which was sandy and slightly muddy, was highly variable (Tables 4 and 5). After resuspension, DIP increased by 40% to more than 100% with large differences between experiments with and without ultrasound treatment. No real trend can be drawn from the results, in contrast with the experiments on muddy sediment in autumn and spring. Exchange of P at the interface of this sandy, slightly muddy sediment in spring was highly reversible, rapid and variable.

In conclusion, when the bottom particles are resuspended by storms (as simulated on–board), active or passive exchange occurs at the sediment interface. The DIP in the water above the sediment is highly influenced by both the exchange and the DIP content of the sediment.

(4) Release of other nutrients from the sediment

The release of other nutrients was also analyzed (Table 7) in the on-board experiments (Table 1). Concentrations of NO_3^-, NO_2^-, NH_4^+, and PO_4^{3-} were higher in the interstitial water than in the water column, except sometimes for NO_2^-. The NH_4^+ concentrations in the sediment were 50 to 190 times higher than in the water column. Sediment content mineralization and organic matter degradation were likely causes. These results suggest active processes in the sediment and explain the changes in stocks of organic versus inorganic forms of P from spring to autumn. The concentrations of NO_2^- in the water column at mid-depth and above the sediment were higher than at the sea surface, suggesting nitrification or release from the sediment. Simulation of bottom resuspension (Table 7) also suggests nutrient release from the sediment to the water column.

Therefore, the sediment is not a simple receptacle of particles settling from the water column. The sediment compartment has to be included in models that forecast the ecosystem response to changes in the water column composition and quality. Results from this preliminary study can be used in such models.

Table 7 Concentration of different nitrogen forms in the interstitial water of the sediment after the resuspension experiments

	Dissolved content, µmol·L^{-1}	NO_2-	NO_3-	NH_4+
Mesocosm area	*Initial conditions, surface water*			
October 1997	Surface water	0.21	26.5	0.6
	Above sediment (20 m)	0.19	26.0	1.0
	Interstitial waters after experiment			
	Surface water without ultrasound; (with ultrasound)	0.26 ; (0.24)	34.6 ; (36.3)	1.2 ; (1.4)
	Above sediment (20 m) without ultrasound; (with ultrasound)	0.23 ; (0.28)	20.4 ; (21.8)	1.0 ; (1.3)
Mesocosm area	*Initial conditions*			
May 1998	Surface water	0.37	6.6	0.5
	Control mesocosm water	0.28	6.1	0.6
	Enriched mesocosm water	0.38	8.8	0.8
	Above sediment (28 m) + surface water at 50%	0.42	7.1	2.7
	Interstitial waters after experiment			
	Surface water	0.17	11.7	0.8
	Control mesocosm water	0.07	12.8	0.6
	Enriched mesocosm water	0.11	13.2	0.7
	Above sediment (28 m) + surface water at 50%	0.12	12.8	0.9
Station A1	*Initial conditions*			
May 1998	Surface water	0.32	8.8	0.7
	Bottom water (24 m)	0.22	4.6	1.4
	Above the sediment (26 m)	0.25	4.5	1.3
	Interstitial waters after experiment			
	Surface water	0.26 ; (0.33)	11.2 ; (10.4)	1.9 ; (1.1)
	Bottom water (24 m)	0.13 ; (0.59)	8.8 ; (10.6)	1.1 ; (11.9)
	Above the sediment (26 m)	0.23 ; (0.23)	8.8 ; (10.9)	5.5 ; (3.4)

4. CONCLUSIONS

The issues addressed in this work were the role and importance of the sediment compartment in the nutrient status of the East China Sea, close to the mouth of the Changjiang River. Because the flux and quality of nutrient supply are expected to change in the near future, this work was also oriented toward forecasting the ecosystem response and future nutrient status of the area.

Is the sediment able to provide P for primary production ?

The majority of P stored in sediments in the study area is in the inorganic form. P concentration in the interstitial water of the sediment was higher than in the water column. The potential release of P is supported by the resuspension simulation experiment, vertical profile of nutrients in the sediment, and interstitial water content. The release is likely to involve migration and equilibration exchanges between the interstitial water of the sediment and the water column. The sediment compartment would therefore become a source of P instead of a sink. The concentration of IP in the interstitial water of the sediment varied from <1 to 13 µmol·L^{-1}. A phytoplankton bloom was induced after P enrichment of less than 3 µmol·L^{-1}. Therefore, the sediment could induce a bloom if the flux of P released from the sediment were sufficient.

Does the sediment indicate the area that is strongly influenced by the Changjiang River supplies ?

From north to south, there was a difference in the source of nutrients according to the forms (organic versus inorganic) accumulated in or processed within the sediment. This feature can be attributed to the influence of supply from the Changjiang Estuary in addition to that from the Taiwan and Yellow Sea coastal

currents.

From the results, the area that is strongly influenced by the Changjiang River can be approximated, which will help future investigations seeking to forecast the effect of changes in supply. In autumn, the area under strong river influence included station C3 and to a lesser extent B1 and C1. In spring, the area was wider and included station A1 and the mesocosm area in addition to C3, B1 and C1.

Does the sediment–water interface influence the water column composition?

From this study, we confirm that the sediment appears to be in continuous dynamic exchange with the water column and affecting its composition. The water column composition is therefore related to that of the sediment compartment. Exchanges processes differ according to the sediment type and season. Biological activity in the sediment, in addition to purely physical processes, is of great importance in exchanges at the sediment–water interface. According to the water column concentration and characteristics coupled with the local hydrodynamic conditions and biological activity, exchanges at the sediment–water interface will occur to a greater or lesser extent. Further investigation is required to determine to what extent a release from the sediment will modify the concentration of a nutrient in the whole overlying water column. We should be able to estimate better the exchanges and flux by taking representative cores of the different sediment types and conducting benthic chamber measurements. Key parameters for a predictive model of the nutrient state of the area would help our understanding of this complex ecosystem.

This study is a first step in this approach. A seasonal effect was clear and will have to be taken into account in predictive models. An equilibrium ratio of 0.85 for IP was found between the interstitial water and water in contact with muddy sediment in autumn. The study has highlighted the physical processes involved in exchanges at the sediment–water interface.

Exchangeable pollutants like Fe, Cu, Zn, Mn, Pb and As are likely to follow the same trend as that found for P. To assess their exchanges at the sediment–water interface, a special focus should be given to studying their behavior in relation to that of P.

ACKNOWLEDGMENTS: Thanks to Dr. Masuzawa for great help and advice in designing the core compressing system. Thanks also to Miss Kato who kindly helped in the auto-analyzer measurements. Mary-Hélène NOËL's post-doctorate is funded by EU-STA and EU-STF fellowships.

REFERENCES

1) Wu, Y., Lin, Y., Guo, T., Wang, L., Zheng, Z.: Mechanisms of phosphorus released from the sediment-water interface in Xiamen Bay, Fujian, China, pp. 1087-1097, *in Marine Coastal Eutrophication, Proceedings International Conference*, Bologna, Italy, 21-24 March 1990, Ed: Vollenweider, R.A., Marchetti, R., Viviani, R., Elsevier, p. 1310, 1992.

2) Xie Qinchunn and Li Yan.: Behaviors of suspended matter in the Changjiang estuary, pp. 88-98, *Biogeochemical study of the Changjiang estuary, Proceedings of the International Symposium on Biogeochemical Study of the Changjiang Estuary and Its Adjacent Coastal Waters of the East China Sea*, March 21-25, 1988, Hangzhou, China, Ed. Yu Guohui, J-M Martin, Zhou Jiayi, SOA-CNRS, China Ocean Press, 898 p., 1990.

3) Andrieux-Loyer, F.: Les formes de phosphates particulaire et sédimentaire en environnement côtier. Méthodes d'analyse, biodisponibilité, échange. *Ph.D. thesis, University of Brest*, France, pp. 329, 1997.

4) C.P. Slomp, W.Van Raaphorst, J.F.P. Malschaert, A. Kok, A.J.J. Sandee.: The effect of deposition of organic matter on phosphorus dynamics in experimental marine sediment systems, *Hydrobiologia*, 253: 83-98, 1993.

DECADAL TO MILLENNIAL ENVIRONMENT CHANGES OF THE CHANGJIANG DELTA RECORDED IN SEDIMENT CORES

Yoshiki SAITO[1], Hajime KATAYAMA[1], Yutaka KANAI[2], Akira NISHIMURA[1], Setsuya YOKOTA[3] and Kazumi MATSUOKA[4]

[1] Marine Geology Department, Geological Survey of Japan, AIST, MITI
[2] Geochemistry Department, Geological Survey of Japan, AIST, MITI
(Higashi 1-1-3, Tsukuba, Ibaraki 305-8567, Japan)
[3] Hokkaido Branch, Geological Survey of Japan, AIST, MITI
(Sapporo Godo-Chosya No.1 Bldg, Kita-ku, Sapporo 060-0808, Japan)
[4] Faculty of Fisheries, Nagasaki University
(1-14, Bunkyo-machi, Nagasaki 852-8521, Japan)

Sediment cores taken from the delta plain and delta-front to prodelta areas of the Changjiang Delta were analyzed for studies on natural and anthropogenic changes of the coastal environment of theChangjiang Delta on decadal and millennial time scales. Borehole samples showed recent increase of delta progradation rate. It means the increase of sediment discharge for the last one to two thousand years. Though its reason is not clear, human impacts on the river and its drainage area are not negligible. Surface sediments and core sediments deposited in the neashore area of the Changjiang after about 1970 contain some cysts of red-tides causative dinoflagellates such as *Lingulodinium polyedrum*, *Scrippsiella trochoidea* and *Polykrikos kofoidii/schwartzii* complex. These sediments also yield ellipsoidal and ovoidal cysts, which are probably identical to toxic species such as *Alexandrium catenella/tamarense* and *A. minutum*, respectively.

Keywords *: Changjiang, Yangtze, human impact, marine palynomoph, dinoflagellate, sediment load, sediment discharge*

1. INTRODUCTION

The Changjiang River, which is one of largest rivers in the world in terms of sediment and water discharge, is the major nutrient, water and sedinent supplier to the East China Sea. The drainage area of the river has approximately 400 million population presently, where is one of old civilization areas for human beings with long history of more than ten thousand years. The river has received influences of human activities on millennial time scale. At the present time, the river is forming a large delta at its mouth. Since the Holocene maximum inundation of about 6000 to 7000 years ago, the Changjiang Delta has prograded seaward. A huge funnel-shaped delta plain, approximately 200 km by 100 km, has formed from riverine sediments during the late Holocene. In this paper we discuss recent changes in the Changjiang Delta on decadal and millennial time scales, based on analyses of sediment cores taken from the delta plain and delta-front to prodelta areasof the Changjiang Delta.

2. MATERIALS AND METHODS

Two kinds of sediment cores were collected from the Changjiang Delta: core samples from the sea bottom of delta-front to prodelta areas and borehole samples from the delta plain (Tables 1, 2, Fig. 1). The core samples were taken using a simple multicore sampler (three simultaneous cores, each 60 cm long) and a gravity corer. These cores were split, described, and photographed. X-ray photographs were taken using slab samples from all split cores. Sand and mud content, water content, and magnetic susceptibility were measured

every about 2cm. Mineralogical analyses were done by X-ray diffraction method (XRD). Accumulation rates were measured by the Pb-210 and Cs-137 methods. Marine palynomorph analysis was conducted under the light microscope and SEM. Heavy-metal contents (Zn, Cu, Pb, Ni, Co, Cr, Mn, Fe) was measured by atomic absorption every one cm. The borehole samples (CM-97) were taken on Chongming Island in 1997. The length of the CM-97 core is about 70 m, and core recovery was over 90%. Other two borehole samples were taken in 1998 (JS-98, HQ-98). These cores were also split, described, and photographed. X-ray photographs were taken using slab samples from the split core. Sand and mud content was measured from 5-cm thick samples taken every 20 cm. Wet bulk density was measured every 2.2 cm. Approximately fifty radiocarbon dates were obtained from mollusc shells and organic matter for CM-97 core using Accelerator Mass Spectrometry by Beta Analytic Inc. Only CM-97 core is dealt with for borehole core analyses in this paper.

Table 1. Sampling location of surface sediments taken from the offshore of the Changjiang.

Site	Latitude	Longitude	water depth	core length
Meso-1	30-50.5N	122-36.6E	20.5 m	31 cm
A-1	31-59.8N	122-30.3E	25.5 m	24 cm
A-3	31-59.5N	123-14.8E	42.0 m	8 cm
A-5	32-00.1N	123.59.9E	39.8 m	20 cm
B-1	31-45.4N	122-30.4E	27.2 m	26 cm
B-3	31-35.6N	123-14.9E	42.0 m	14 cm
B-5	31-29.8N	123-59.8E	41.5 m	12 cm
C-1	31-25.5N	122-34.7E	35.3 m	28 cm
C-3	31-10.5N	123-14.7E	58.7 m	31 cm
C-5	30-59.8N	124-00.0E	39.0 m	no sample
G-1 Core	31-27.1N	122-23.4E	16.0 m	88 cm
B-1 Core	31-45.2N	122-31.1E	28.5 m	160 cm

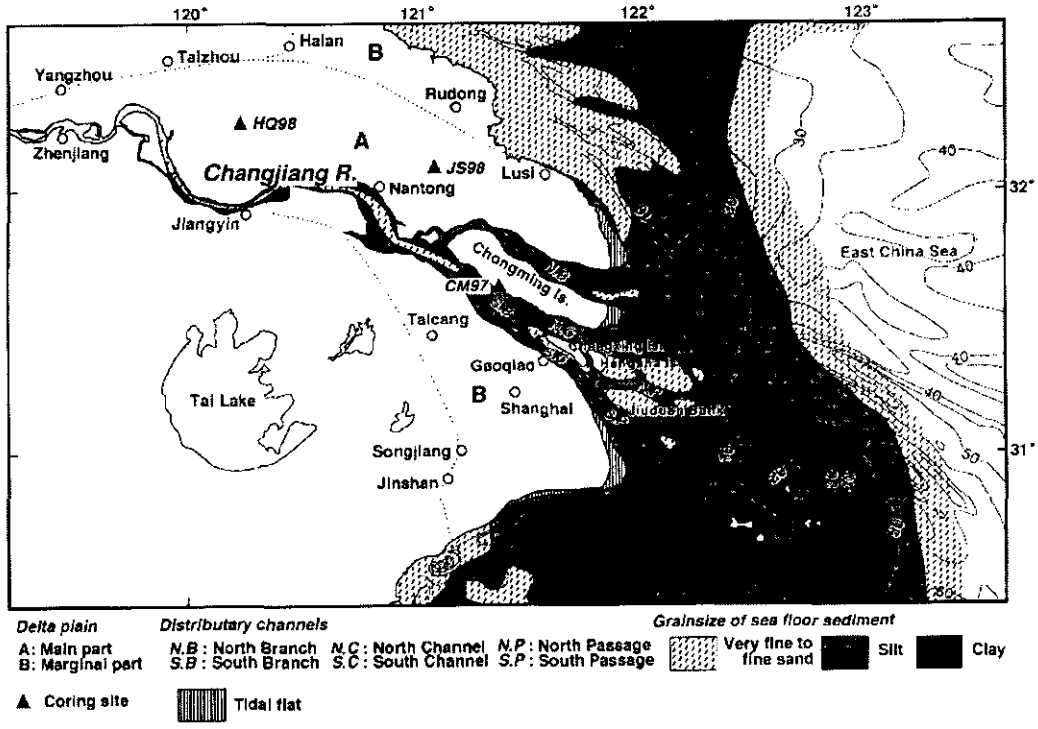

Fig. 1. Borehole locations and sediment distribution offshore of the Changjiang. Sediment distribution is after Department of Marine Geology (1975)[1].

Table 2. Sampling location of borehole sediments taken from the Changjiang Delta.

Site	Hole	Latitude	Longitude	Altitude		Depth	
CM-97	A,B,C	31-37.5N	121-23.6E	2.48	m	70.50	m
JS-98	A,B,C	32-05.0N	121-05.0E	4.20	m	61.50	m
HQ-98	A,B	32-15.0N	120-14.0E	5.91	m	60.55	m

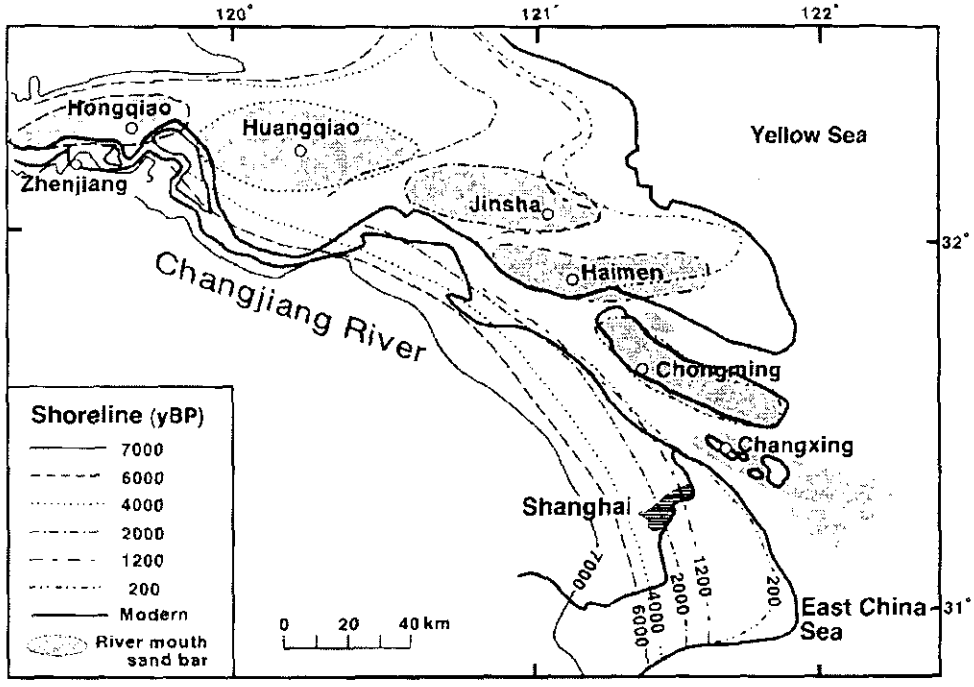

Fig. 2 Shoreline and river-mouth bar migration in the Changjiang Delta during the last 6 ka. After Li and Li (1983)[2].

3. RESULTS AND DISCUSSION

(1) Millennial scale changes

Lithologically, the borehole samples exhibited an upward-fining succession from 70 m to ca. 25 m, an upward-coarsening succession from 25 m to 11 m, and an upward-fining succession from 11 m to the ground surface. Based on sediment facies and foraminifera/mollusc analyses, these successions were interpreted as fluvial, through estuary, to neritic environments for the lower succession, prodelta to delta-front environments for the middle succession, and tidal flat to delta plain for the upper succession, in ascending order. Radiocarbon ages of these successions were from 12 000 to 6000 years BP for the lower succession and 6000 to 1000 years BP for the middle to upper successions (Fig. 3). The high accumulation rate from 2000 to 1000 years BP and the sediment facies from this time period indicate that the paleo-delta front of the Changjiang Delta passed the CM-97 site at this time. Since the present delta front is located about 100 km east of this site, the average progradation rate of the delta front for the last 1000 to 2000 years was 60 to 70 m/yr. This is a slightly higher than the average migration rate of 40 to 50 m/yr for river-mouth bars during the last 6000 years. Considering the funnel-shape of the Holocene delta plain and prodelta depth, the annual sediment volume deposited in the

delta-front and prodelta areas must have been increasing over the last 1000 to 2000 years. A similar result has been reported for the shoreline migration rate in the southern delta plain of the Changjiang by Chen and Zong (1998)[3]. They report an abrupt increase in the shoreline migration rate 2000 years ago, from ca. 2 m/yr to between 6 and 35 m/yr. This increase is thought to have been caused by a depocenter change from the fluvial plain to the delta area of the Changjiang (Chen, 1996)[4]. Other possible reasons are the increase of sediment discharge and sediment yield due to soil erosion, and additional sediment supply from the Huanghe (Yellow River) during 1128-1855, when the Huanghe emptied into the Yellow Sea at Jiangsu about 350km north of the Changjiang mouth.

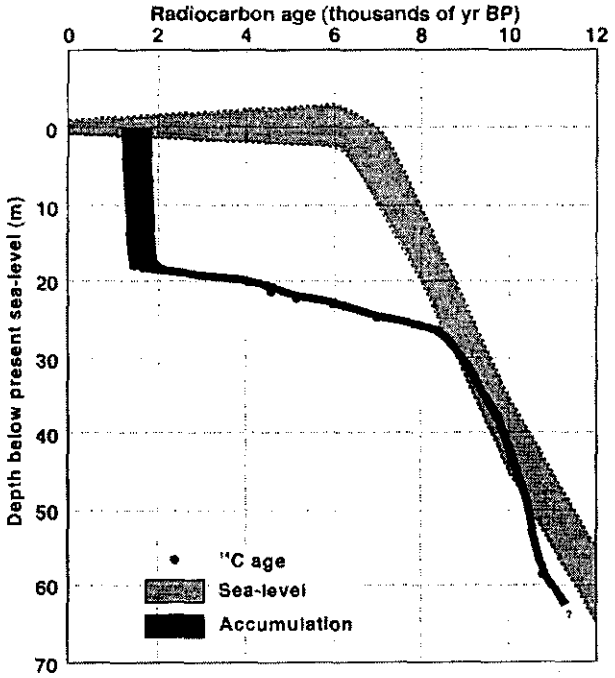

Fig. 3. Accumulation curve and age-depth plots for CM-97 core, and Holocene sea-level curve in the East China Sea. After Hori et al. (1999)[5]

(2) Decadal scale changes

Surface sediments were taken from the lower part of the delta front, prodelta, and inner-shelf areas. These sediments consisted of alternating sand and mud in the delta-front area, silty clay in the prodelta area, and muddy sand to sand in the inner-shelf area. Downcore variation in grain size was large in the delta-front area. The grain-size distribution in surface sediment samples did not show large differences compared with that of samples collected 20 to 25 years before (Department of Marine Geology, 1975)[1]. In muddy sediments taken from the prodelta area, a slight upward increase of about 10 to 20% is recognized for heavy metal content such as Zn, Cu, Pb, Ni, and Cr (Fig. 4). This change occurred over the last 10 to 20 years. Though sediments from the delta-front area indicate some downcore changes in heavy metal content and mineralogical assemblage, they are thought to be due to mainly variations in grain size. The maximum concentrations of heavy metals were 115 ppm (Zn), 43 ppm (Cu), 34 ppm (Pb), 49 ppm (Ni), 19 ppm (Co), 145 ppm (Cr), 1.4% (Mn), and 4.7% (Fe). Most of heavy metal contents do not reach a level of polluted sediments. This is thought to be the effect of dilution by huge sediment supply from the Changjinag.

A palynological study was carried out on 9 surface sediments and G-1 core. Palynomorphs found in these samples consisted of various taxonomic groups such as dinoflagellate cysts, *Prasinophycean phycoma*, freshwater *Chlorophycean Pediastrum*, *Chrisophycean archeomonads*, tintinnid lorica, microforaminiferal linings, resting eggs and bodies of copepods, and acritarchs. The results are summarized as follows;

1. The occurrence of *Pediastrum* suggests that freshwater plum derived from the Changjiang River is extending to around 100 km off from the mouth.
2. In the surface sediments, dinoflagellate cyst concentration, 10 to 10^2 cysts in 1ml sediment, is approximately one-tenth of that in coastal areas and inner bays of Korean Peninsula and west Kyushu.
3. As autotrophic dinoflagellate cysts are dominated in all surface sediments, eutrophication does not extensively progress off the Changjiang River. However, in the G-1 core samples increase of hetrotrophic dinoflagellate cysts upward probably reflects the development of gradual eutrophication since the last three or two decades (Fig. 5).
4. Some cysts of red-tides causative dinoflagellates such as *Lingulodinium polyedrum*, *Scrippsiella trochoidea* and *Polykrikos kofoidii/schwartzii* complex occurred in the surface sediments and also in the core samples.
5. Ellipsoidal and ovoidal cysts are probably identical to toxic species such as *Alexandrium catenella/tamarense* and *A. minutum*. respectively. These are found in the upper part of the gravity core G-1, which dates to after about 1970.

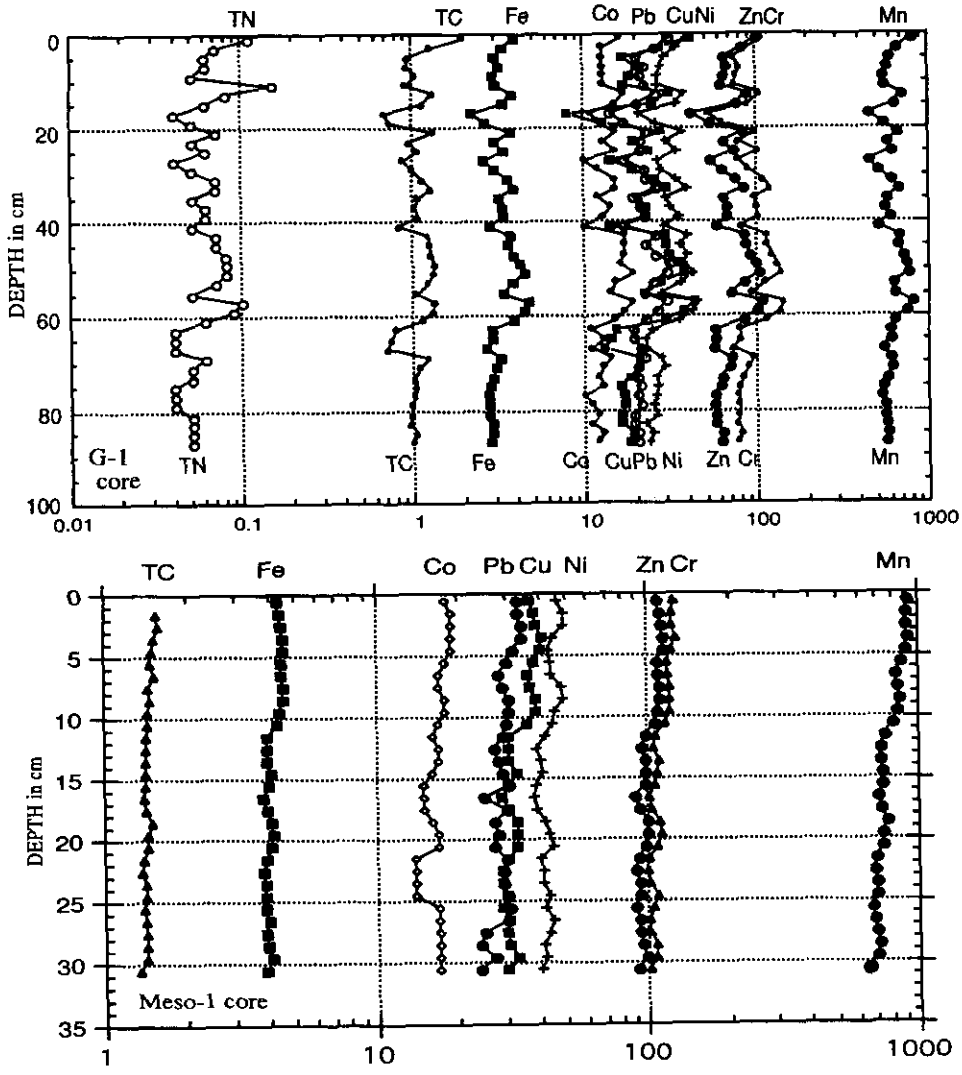

Fig. 4. Downcore analysis of heavy metals for G-1 core (above) and Meso-1 core (below). TN (total nitrogen), TC (Total carbon), and Fe: %, Co, Pb, Cu, Ni, Zn, Cr, and Mn: ppm Accumulation rates are estimated to be 1.5 cm/yr by Cs-137 method for G-1 core and 1.5 cm/yr by Pb-210 method for Meso-1 core.

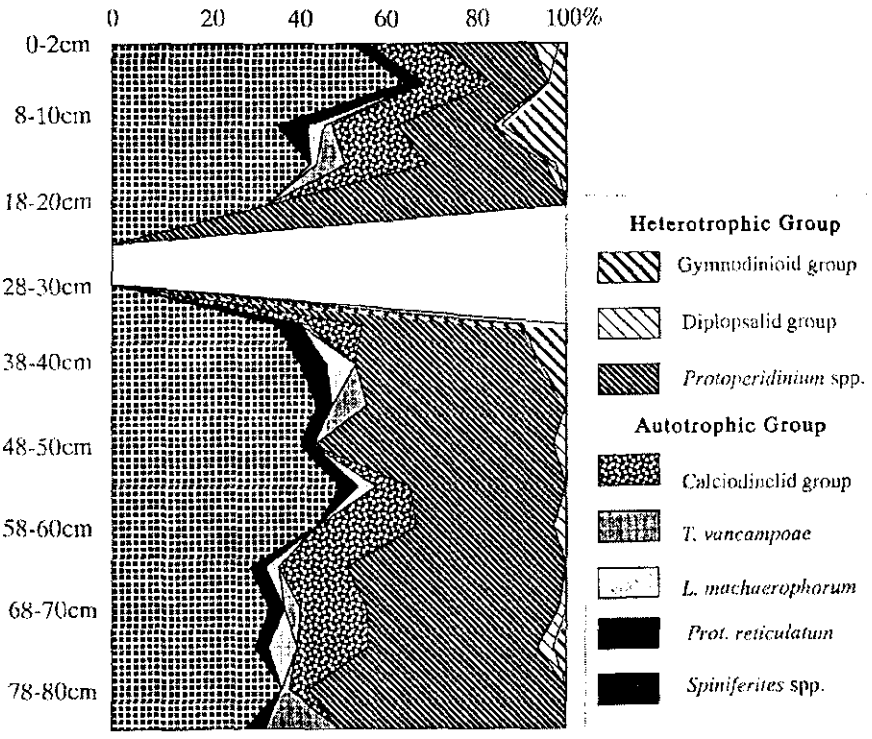

Fig. 5. Change of dinoflagellate cyst assemblage in G-1 Core.

4. CONCLUDING REMARKS

Sediment cores taken from the delta plain and delta-front to prodelta areas of the Changjiang Delta have recorded natural and anthropogenic changes of the coastal environment of the Changjiang. Land use and human activities in the drainage area of the Changjiang rapidly have been changing for the last hundred years and impacted on coastal ecosystem. For the evaluation of past human activities and their influences on coastal environments, more detailed analyses of past environmental changes should be done using sediment cores from the two viewpoints of natural and anthropogenic changes.

ACKNOWLEDGMENT: We are very grateful to Drs. Zhou Huaiyang and Chen Jianfang of the Second Institute of Oceanography, SOA for collaborative work on sediment cores and crew of Haijian No. 49. We also thank prof. Wang Pinxian and Zhao Quanhong of Tongji University for their kind support for the joint borehole study on the Changjiang Delta.

REFERENCES

1) Department of Marine Geology: Basic characteristics of modern sedimentation in the Changjiang Delta. Tongji University, 61p. (in Chinese), 1975.

2) Li, C. and Li, P.: The characteristics and distribution of Holocene sand dodies in the Changjiang delta area. Acta Oceanologica Sinica, 2, 54-66, 1983.

3) Chen, X. and Zong, Y.: Coastal erosion along the Changjiang deltaic shoreline, China: History and Perspective. Estuarine, Coastal and Shelf Science, 46, 733-742, 1998.

4) Chen, X.: An integrated study of sediment discharge from the Changjiang River, China, and the delta development since the Mid-Holocene. *Journal of Coastal Research*, 12, 26-37, 1996.

5) Hori, H., Saito, Y., Zhao, Q., Cheng, X., Wang, P. and Li, C.: Sedimentary characteristics of post-glacial deposits beneath the Changjiang River Delta. In Land-Sea Link in Asia "Prof. Kenneth O. Emery Commemorative International Workshop". Proceedings of an international workshop on sediment transport and storage in coastal sea-ocean system. Edited by Yoshiki Saito, Ken Ikehara and Hajime Katayama, STA (JISTEC) & Geological Survey of Japan, Tsukuba, Japan, 140-144, 1999.

Appendix

Programme

Participants List

PROGRAMME

Thursday 18 March

Opening Addresses	(Chairman: Dr. WATANABE Masataka, NIES)
10:00 – 10:15	**Mr. ENDO Yasuo** Director-General, Water Quality Bureau, Environment Agency, Japan
10:15 – 10:30	**Mr. WANG Fei** Director-General, Department of Marine Environmental Protection, SOA, China
10:30 – 10:45	**Dr. OHI Gen** Director-General, NIES, Japan
10:45 – 11:00	**Mr. ZHANG Youfen** Deputy Director, East China Sea Branch, SOA, China

Keynote Addresses	
11:00 – 11:30	**Dr. WATANABE Masataka** Director, Water & Soil Environment Div., NIES, Japan "Interaction between the Changjiang River and the East China Sea Ecosystem"
11:30 – 12:00	**Prof. ZHU Mingyuan** Director, Div. Of Marine Biology, First Institute of Oceanography, SOA "Project Summary Report From Chinese Side"

12:00 – 12:15	**Group Photograph**
12:15 – 14:00	**Lunch**

General Session	
14:00 – 14:20	**1. Effect of Phosphate Enrichment on Phytoplankton by Mesocosm Experiments** LI Ruixiang, ZHU Mingyuan, CHEN Shang, MU Xueyuan, LU Ruihua, LI Baohua First Institute of Oceanography, SOA
14:20 – 14:40	**2. Response of Zooplankton Populations to Dissolved Fraction of Oil and Phosphate Enrichment in Mesocosm** WANG Jinhui, WANG Weifei, WU Zhengnan, ZHANG Youfen East China Sea Branch, SOA

14:40 – 15:00 **3. Variations in Trace Metal Concentrations in a Phosphate-Enriched Closed Experimental Ecosystem**

TAKAYANAGI Kazufumi[1], SAKAMI Tomoko[1], NAKAYAMA Eiichiro[2]
1. National Research Institute of Aquaculture, Japan, 2. Shiga Prefectural University, Japan

15:00 – 15:20 **4. Effect of Phosphorous Enrichment on Phytoplankton Blooms and the Role of Grazers in Marine Mesocosm in the Changjiang Estuary**

KOSHIKAWA Hiroshi, XU Kaiqin, MURAKAMI Shogo, KOHATA Kunio, WATANABE Masataka
National Institute for Environmental Studies

15:20 – 15:40 **5. Change of POC and PON in Phosphate Enriched Mesocosms and Their Sinking Fluxes**

CHEN Shang, ZHU Mingyuan, LI Ruixiang, MU Xueyuan, LU Ruihua, LI Baohua
First Institute of Oceanography, SOA

15:40 – 16:00 **Coffee Break**

General Session

16:00 – 16:20 **6. On the Sedimentation of Phosphorus, BHC and DDT in Specified Area outside of Changjiang Estuary**

ZHOU Huaiyang, CHEN Jiangfan, PAN Jiangming, WANG Huaizhao JIN Mingming
Second Institute of Oceanography, SOA

16:20 – 16:40 **7. Preliminary Observations on the Phytoplankton Species at the Changjiang Estuary Mouth in May 1998**

KAWACHI Masanobu, HIROKI Mikiya, WATANABE Makoto
National Institute for Environmental Studies

16:40 – 17:00 **8. Research of Environment Capacity**

ZHU Dedi, XU Weiyi
Second Institute of Oceanography, SOA

18:00 – 20:00 **Reception**

Friday 19 March

General Session

10:30 - 10:50 **9. Impact of Discharged Fuel Oil on Plankton Ecosystems: A Mesocosm Study in the Changjiang Estuary**

XU Kaiqin, KOSHIKAWA Hiroshi, MURAKAMI Shogo, MAKI Hideaki, KOHATA Kunio, WATANABE Masataka
National Institute for Environmental Studies

10:50 - 11:10 **10. Preliminary Investigation to the Distribution, Influence and Bioconcentration of Petroleum Hydrocarbon Associated with Oil on and by Plankton in a Given East China Sea**

SHI Xiaoyong, WANG Xiulin, JIANG Yu, HAN Xiurong
Ocean University of Qingdao

11:10 - 11:30 **11. Phylogenetic Analysis of Bacterial Community Structure in the East China Sea**

UCHIYAMA Hiroo[1], SEKIGUCHI Hiroyuki[2], NAKAHARA Tadaatsu[2]
1. National Institute for Environmental Studies, 2. University of Tsukuba

11:30 - 11:50 **12. Bacterioplankton Production in Dilution Zone of the Changjiang (Yangtze River) Estuary**

LIU Zilin[1], KOSHIKAWA Hiroshi[2], NING Xiuren[1], SHI Junxian[1], CAI Yuming[1]
1. Second Institute of Oceanography, SOA, 2. National Institute for Environmental Studies

11:50 - 13:30 **Lunch**

General Session

13:30 - 13:50 **13. A Marine Redtide Phytoplankton Dynamical Model for the Sea Area Adjacent Yangze River Estuary**

QIAO Fangli, YUAN Yeli, ZHU Mingyuan, ZHAO Wei, JI Rubao, PAN Zengdi, CHEN Shang, WAN Zhenwen
First Institute of Oceanography, SOA

13:50 - 14:10 **14. Biogeochemical Variations of Nutrient Elements and Its Effect on Ecological Environments off the Changjiang Estuarine Waters**

LIN Yian, TANG Renyou, PAN Jianming
Second Institute of Oceanography, SOA

14:10 - 14:30 **15. Elemental Composition of Suspended Particles in the Changjiang Estuary Mouth**

KOSHIKAWA Kanao-Masami[1], TAKAMATSU Takejiro[1], MATSUSHITA Rokuji[2], TAKADA Jitsuya[2], MURAKAMI Shogo[1], XU Kaiqin[1], WANATABE

Masataka[1]
1. National Institute for Environmental Studies, 2. Kyoto University

14:30 – 14:50 **16. Preliminary Data on Flux and Decomposition Rate of Sinking Particle in the Changjiang Estuary**

OKAMURA Kazumaro, KIYOMOTO Yoko
Seikai National Fisheries Research Institute, Japan

14:50 – 15:10 **Coffee Break**

General Session

15:10 – 15:30 **17. Geochemical Characteristics of the Elements in the Sediment of the Changjiang Estuarine Area**

GAO Aiguo, CAI Delin, GAO Sulan
First Institute of Oceanography, SOA

15:30 – 15:50 **18. Importance of the Sediment-Water Interface in the Nutrient Status of the East China Sea at the Mouth of the Changjiang Estuary**

NOËL Mary-Hélène, WATANABE Masataka
National Institute for Environmental Studies

15:50 – 16:10 **19. Decadal to Millennial Environment Changes of the Changjiang Delta Recorded in Sediment Cores**

SAITOH Yoshiki[1], KATAYAMA Hajime[1], YOKOTA Setsuya[1], KANAI Yutaka[1], NISHIMURA Akira[1], MATSUOKA Kazumi[2]
1. Geological Survey of Japan, 2. Nagasaki University

Guest Remarks

16:10 – 16:25 **Mr. NAKAMURA Takehiro**
Programme Officer, UNEP

Closing Address

16:25 – 16:40 **Dr. WATANABE Masataka**
Director, Water & Soil Environment Div., NIES

PARTICIPANTS LIST

CHINA

WANG Fei
Director-General,
Department of Marine Environmental Protection,
SOA
1 Fuxingmenwei Ave, Beijing
100860 P.R.China

FAN *Xiaoli*
Deputy Director-General,
Department of International Cooperation, SOA
1 Fuxingmenwei Ave, Beijing
100860 P.R.China

ZHANG Youfen
Deputy Director-General
East China Sea Branch, SOA
630 Dongtang Rd, Pudonog, Shnghai
200137 P.R.China

ZHU Mingyuan
Director, Professor
Division of Marine Biology
First Institute of Oceanography, SOA
3A Hongdao, Branch Road,
P.O.Box 98, Qingdao
266003 P.R.China
TEL:+86-532-2896972
FAX:+86-532-2879562
E-mail: myzhu@public.qd.sd.cn

ZHOU Huaiyang,
Second Institute of Oceanography, SOA
P.O.Box 1207, Hangzhou
310012 P.R.China

QIAO Fangli
Key Laboratory of Geophysical Fluid Dynamics
and Numerical Modelling, SOA
3A Hongdao, Branch Road,
P.O.Box 98, Qingdao
266003 P.R.China

LIN Yian
Second Institute of Oceanography, SOA
P.O.Box 1207, Hangzhou
310012 P.R.China

LIU Zilin
Second Institute of Oceanography, SOA
P.O.Box 1207, Hangzhou
310012 P.R.China

LI Ruixiang
First Institute of Oceanography, SOA
3A Hongdao, Branch Road,
P.O.Box 98, Qingdao
266003 P.R.China

GAO Aiguo
First Institute of Oceanography, SOA
3A Hongdao, Branch Road,
P.O.Box 98, Qingdao
266003 P.R.China

SHI Xiaoyong
Ocean University of Qingdao
5 Yushan Road, Qingdao
266003 P.R.China

CHEN Shang
Division of Marine Biology
First Institute of Oceanography, SOA

3A Hongdao, Branch Road,
P.O.Box 98, Qingdao
266003 P.R.China

ZHU Dedi
Marine Numerical Modeling Laboratory
Second Institute of Oceanography, SOA
P.O.Box 1207, Hangzhou
310012 P.R.China

WANG Jinhui
Marine Environmental Protection Division
East China Sea Branch, SOA
630 Dongtang Rd, Pudonog, Shnghai
200137 P. R. China

GONG Genlin
East China Sea Branch, SOA
630 Dongtang Rd, Pudonog, Shnghai
200137 P. R. China

PAN Jiangming
Second Institute of Oceanography, SOA
P.O.Box 1207, Hangzhou
310012 P.R.China

JAPAN

Gen OHI
Director-General,
National Institute for Environmental Studies
16-2 Onogawa, Tsukuba, Ibaraki
305-0053 Japan

Masataka WATANABE
Director,
Water & Soil Environment Division
National Institute for Environmental Studies
16-2 Onogawa, Tsukuba, Ibaraki
305-0053 Japan
TEL:+81-298-50-2338
FAX:+81-298-50-2576
E-mail:masawata@nies.go.jp

Hiroo UCHIYAMA
Water & Soil Environment Division
National Institute for Environmental Studies
16-2 Onogawa, Tsukuba, Ibaraki
305-0053 Japan
TEL:+81-298-50-2412
FAX:+81-298-50-2576
E-mail:huchiyam@nies.go.jp

XU Kaiqin
Water & Soil Environment Division
National Institute for Environmental Studies
16-2 Onogawa, Tsukuba, Ibaraki
305-0053 Japan
TEL:+81-298-50-2339
FAX:+81-298-50-2584
E-mail:joexu@nies.go.jp

Hiroshi KOSHIKAWA
Water & Soil Environment Division
National Institute for Environmental Studies
16-2 Onogawa, Tsukuba, Ibaraki
305-0053 Japan
TEL:+81-298-50-2505
FAX:+81-298-50-2584
E-mail:koshikaw@nies.go.jp

Shogo MURAKAMI
Water & Soil Environment Division
National Institute for Environmental Studies
16-2 Onogawa, Tsukuba, Ibaraki
305-0053 Japan
TEL:+81-298-50-2388
FAX:+81-298-50-2576
E-mail: murakami@nies.go.jp

Hideaki MAKI
Water & Soil Environment Division
National Institute for Environmental Studies
16-2 Onogawa, Tsukuba, Ibaraki
305-0053 Japan
TEL:+81-298-50-2394
FAX:+81-298-50-2576
E-mail: hidemaki@nies.go.jp

Masami KOSHIKAWA
Water & Soil Environment Division
National Institute for Environmental Studies
16-2 Onogawa, Tsukuba, Ibaraki
305-0053 Japan
TEL:+81-298-50-2440
FAX:+81-298-50-2584
E-mail:mkanao@nies.go.jp

Mikiya HIROKI
Environmental Biology Division
National Institute for Environmental Studies
16-2 Onogawa, Tsukuba, Ibaraki
305-0053 Japan
TEL:+81-298-50-2513
FAX:+81-298-50-2577
E-mail:hiroki-m@nies.go.jp

Masanobu KAWACHI
Environmental Biology Division
National Institute for Environmental Studies
16-2 Onogawa, Tsukuba, Ibaraki
305-0053 Japan
TEL:+81-298-50-2345
FAX:+81-298-50-2577
E-mail:kawachi@nies.go.jp

NOËL Mary-Hélène
Water & Soil Environment Division
National Institute for Environmental Studies
16-2 Onogawa, Tsukuba, Ibaraki
305-0053 Japan
TEL:+81-298-50-2440
FAX:+81-298-50-2584
E-mail:noel@nies.go.jp

Yoshiki SAITO
Marine Geology Department
Geological Survey of Japan
1-1-3 Higashi , Tsukuba, Ibaraki
305-0046 Japan
TEL: +81-298-54-3772
FAX: +81-298-54-3533
E-mail: yoshi@gsj.go.jp

Hajime KATAYAMA
Marine Geology Department
Geological Survey of Japan
1-1-3 Higashi, Tsukuba, Ibaraki
305-0046 Japan
TEL:+81-298-54-3677/3722
FAX:+81-298-54-3666/3589
E-mail:katayama@gsj.go.jp

Kazufumi TAKAYANAGI
Environmental Management Division
National Research Institute of Aquaculture
Nansei, Mie
516-0193 Japan
TEL:+81-5996-6-1830
FAX: +81-5996-6-1962
E-mail: kazufumi@nria.affrc.go.jp

Kazumaro OKAMURA
Seikai National Fisheries Reserch Institute
49 Kokubu-machi, Nagasaki
850-0951 Japan
TEL:+81-5996-6-1830
FAX: +81-5996-6-1962
E-mail: kazufumi@nria.affrc.go.jp

OBSERVERS

Kunihiko AMANO
Public Works Research Institute
Ministry of Construction
1 Asahi, Tsukuba, Ibaraki
305-0804 Japan
TEL:+81-298-64-2269
FAX: +81-298-64-7221
E-mail:amano@pwri.go.jp

Abdulla BABA
Marine Geology Department
Geological Survey of Japan,
1-1-3 Higashi, TSUKUBA, 305-8567
TEL: +81-298-54-3627
FAX: +81-298-54-3533
E-mail: Bava@gsj.go.jp

BAI Hong
Institute of Oceanology,
Chinese Academy of Sciences,
7 Nanhai Road, Qingdao Shandong
266071, P. R. China
TEL:+86-532-2860099
E-mail: goalis@ms.qdio.ac.cn

Lallan P. GUPTA
Marine Geology Department
Geological Survey of Japan,
1-1-3 Higashi, TSUKUBA, 305-8567
E-mail: gupta@gsj.go.jp

Toshiyuki HIRANO
Chairman, Tokiwamatsu Gakuen
4-17-16, Hibumiya Meguro
Tokyo 152-0003
TEL:+81-3-3713-8161
FAX:+81-3-3793-2562

HU Dunxin
Institute of Oceanology,
Chinese Academy of Sciences
7 Nanhai Road, Qingdao Shandong
266071, P. R. China
3663N. Zhongshan Road,
Shanghai, 200063, P. R. China
TEL:+86-532-2879062
FAX:+86-532-2860099, 532-2870882
E-mail: dxhu@ms.qdio.ac.cn

Tomohisa IRINO
Geological Survey of Japan,
Tsukuba, Ibaraki, JAPAN
Higashi 1-1-3, Tsukuba
305-8567 Japan
TEL: +81-298-54-3772
FAX: +81-298-54-3533
E-mail: irino@gsj.go.jp

Kazuo ISEKI
National Research Institute of Fisheries Science,
2-12-4, Fukuura, Kanazawa-ku,
Yokohama, 236-8648 JAPAN
E-mail: kiseki@ss.nrifs.affrc.go.jp

Yoshihisa KATO
School of Marine Science and Technology
Tokai University
Shimizu, Shizuoka 424-8610
JAPAN
E-mail: ykato@scc.u-tokai.ac.jp

Philippe KERHERVE
Graduate School of Environmental and
Earth Sciences,
Hokkaido University
Sapporo
E-mail: philippe@ees.hokudai.ac.jp

Yutaka KOBORI
International Emecs Center
1-5-1,Wakihamakaigandouri,chuou-ku
Koube 651-0073
TEL:+81-78-252-0234
FAX:+81-78-252-0404
E-mail:kobori@emece.or.jp

KHIM Boo Keun
Research Institute of Oceanography,
Seoul National University
151-742, Seoul, Korea
TEL: +82-2-880-6469
FAX: +82-2-872-0311
E-mail: bkkocean@plaza1.s.nu.ac.kr

Jingpu LIU
School of Marine Science,
Virginia Institute of Marine Science
The College of William & Mary
Gloucester Point, Virginia 23062
USA
TEL:+1-804-684-7739
FAX:+1-804-684-7195
E-mail: jpliu@vims.edu

Masamitsu ORITANI
Northwest Pacific Region Environmental Cooperation Center
7-18 Azumi-cho, Toyama-shi
Toyama 930-0094
TEL: +81-764-45-1571
FAX: +81-764-45-1581

SHEN Huanting
Institute of Estuarine and Coastal Research,
East China Normal University
3663 N. Zhongshan Road
Shanghai, 200063, P. R. China
TEL:+86-21-6223-2842
FAX:+86-21-6254-6441
E-mail: htshen@sklec.ecnu.edu.cn

Prabhaker Shirodkar
National Institute of Oceanography
Dona Paula, Goa, 403-004, India
TEL:+91-832-226253
FAX:+91-832-223340
E-mail: shirod@darya.nio.org, shirod@csnio.ren.nic.in

Vaidyanatha Subramanian
School of Environmental Sciences
Jawaharlal Nehru University
New Delhi, 110067, India
TEL:
FAX: +91-11-6106501
E-mail: subra@jnuniv.ernet.in

Shunji TAKESHITA
National Institute of Environmental Research
Ministry of Environment
613-2 Bulkwang-dong, Eunpyung-ku
Seoul, KOREA
TEL: +82-351-4038
FAX: +82-351-4038

Hi-Il YI
Korean Ocean Research & Development Institute (KORDI)
P.O.Box 29, Ansan, 425-600,
Korea
TEL:+82-345-408-5822
FAX:+82-345-400-6263
E-mail: hilee@sari.kordi.re.kr

Schexnayder Margaret
National Oceanographic Office
Stenis Space Center,
MS 39522-5001, USA
TEL:+1-228-689-8004
FAX:+1-228-689-8053
E-mail: kevin@fastband.com

YANG Zuosheng
Institute of Estuarine and Coastal Studies,
Ocean University of Qingdao
5 Yushan Road, Qingdao, 266003,
P. R. China
TEL:+86-532-2860620
FAX:+86-532-2032799
E-mail: Zshyang@mail.ouqd.edu.cn

Environment Agency of Japan

Yasuo ENDO
Director-General
Water Quality Bureau
Environment Agency
1-2-2 Kasumigaseki, Chiyoda-ku
Tokyo

Susumu OHTA
Water Quality Bureau
Environment Agency
1-2-2 Kasumigaseki, Chiyoda-ku
Tokyo

Masahiro SHISHIME
Water Quality Bureau
1-2-2 Kasumigaseki, Chiyoda-ku
Tokyo

Kazuaki MURAMATSU
Water Quality Bureau
1-2-2 Kasumigaseki, Chiyoda-ku
Tokyo

Mugen YAKUBO
Water Quality Bureau
1-2-2 Kasumigaseki, Chiyoda-ku
Tokyo

UNEP

Takehiro NAKAMURA
Programme Officer (Water)
Technical Cooperation Unit
P.O.Box 30552, Nairobi, Kenya
TEL: +254-2-623886
FAX: +254-2-624249
E-mail: Takehiro.Nakamura@unep.org

RESEARCH REPORT FROM
THE NATIONAL INSTITUTE FOR ENVIRONMENTAL STUDIES, JAPAN

No. 151

国立環境研究所研究報告　第151号
(R-151-2000)

【平成11年12月1日編集委員会受付】
【平成11年12月20日編集委員会受理】
平成12年1月31日発行

発　行　環境庁 国立環境研究所
〒305－0053 茨城県つくば市小野川16番2
電話　0298－50－2343（ダイヤルイン）

印　刷　株式会社　イ　セ　ブ
〒305－0005 茨城県つくば市天久保2－11－20

Published by the National Institute for Environmental Studies
16-2 Onogawa, Tsukuba, Ibaraki 305-0053 Japan
JAN 2000

本報告書は再生紙を使用しています。